Imperial College
London

Centre for Petroleum Studies
Department of Earth Science
and Engineering

Well Test Analysis of Infrequent Flow Behaviour of Fractured Wells in Oil and Gas Reservoirs

Aram Amin

A Dissertation Submitted in Fulfilment of the Requirements for the Degree of Doctor of Philosophy of the University of London and the Diploma of Imperial College London, 2012

COPYRIGHT DECLARATION

'The copyright of this thesis rests with the author and is made available under a Creative Commons Attribution Non-Commercial No Derivatives licence. Researchers are free to copy, distribute or transmit the thesis on the condition that they attribute it, that they do not use it for commercial purposes and that they do not alter, transform or build upon it. For any reuse or redistribution, researchers must make clear to others the licence terms of this work'

DECLARATION OF ORIGINALITY

The author declares that the work contained within this thesis is entirely his own, and all the referenced works in this document have been duly cited to the best of his knowledge.

ACKNOWLEDGEMENT

I would like to express my profound gratitude to my supervisor Professor Alain C. Gringarten, Director of the Centre for Petroleum Studies at Imperial College, London. His guidance, assistance and review at all stages of this project are very much appreciated indeed.

I am very thankful to my late mother Fatima Amin for her love, patience, support and encouragement in my life. I would like to express my gratitude to my son Hauras for his understanding and patience.

I would also like to thank my work and research colleagues: Irinel Gabriel Marcu, Alex Assaf, Manijeh Bozorgzadeh, Lekan Aluko, Moshood Sanni, Thomas von Schroeter and Thabo Kgogo for their comments and valuable assistance during this work.

I would like to take this opportunity to thank the excellent people in the Department of Earth Science and Engineering that I have had the honour of knowing them, especially the department support staff for their assistance and friendship.

Finally, I wish to thank everyone who added to the value of the work described in this thesis.

DEDICATION

To Fatima Amin (1949-2007), my beloved mother who always supported and believed in me, but sadly is no longer with me.

To Hauras Amin, my beloved great son, thank you for your patience and understanding to make this work.

ABSTRACT

The purpose of hydraulic fracturing is to increase the contact area of the wellbore in the reservoir to maximise production rates. For modelling purposes, the induced fracture is assumed to be of infinite or finite conductivity. The modelled fracture tends to show either features of infinite conductivity with half slope or finite conductivity with quarter slope at early time. These flow behaviours are clear indications of a stimulated well. However, observations in some post-frac well tests report a single unit slope in early time, which indicates non-fractured well response.

The objective of this study is to investigate the unusual flow behaviour associated with the testing of fractured wells following a proppant frac job and address reasons for this behaviour assuming the frac job has targeted the reservoir interval of interest. This infrequent behaviour is referred to briefly in a limited number of publications but with no clear explanation. Study suggests that the controlling factors are fracture length, fracture conductivity, non-Darcy flow in the case of gas wells and the damage caused by the fracture operation including choked fracture effect and less importantly fracture face skin.

This study utilizes 3-D numerical black oil and compositional simulation in single and multi-layered reservoirs containing different fluid types. A range of factors are examined that may impact the introduced fracture flow behaviour based on actual fractured well flow features found in the literature. The main fracture and reservoir parameters investigated include: fracture half-length (x_f), fracture conductivity ($k_f w_f$), fracture damage including fracture choke (S_{fc}) and fracture face skin (S_{ff}), non-Darcy effect, formation permeability and many others. The study also examines fractured well behaviour in naturally fractured reservoirs and gas-condensate (lean and rich) reservoirs to investigate liquid drop out effect on the induced fracture flow behaviour.

It is concluded that the investigated fracture behaviour is likely to be associated with damaged fractures of short lengths and low fracture conductivity values, which often result from poorly executed frac job on the well. Knowledge obtained from the study is applied to the analysis of well tests from actual fractured wells. Understanding the flow behaviour of fractured wells is crucial to operators and service companies in evaluating the effectiveness of stimulation work performed on the well.

CONTENTS

ABSTRACT ii
LIST OF FIGURES iiv
LIST OF TABLES vii
NOMENCLATURE AND ABBREVIATIONS viii
CHAPTER I 1
BACKGROUND AND MOTIVATION 1
1.1 Introduction 1
1.2 Problem Recognition 2
1.3 Methodology 3
1.4 Objectives 4
1.5 Project outline 5
1.6 Publication 5
CHAPTER II 6
FRACTURED WELL: CONCEPT and FLOW PATTERENS 6
2.1 Introduction 6
2.2 Wellbore storage 7
2.3 Skin 11
2.4 Fractured Well Flow Patterns 16
2.4.1 Linear Flow - Infinite Conductivity Fracture 17
2.4.2 Bilinear Flow - Finite Conductivity Fracture 18
2.4.3 Pseudo Radial Flow 19
2.5 Research Problem Review 21
2.6 Conclusions 26
CHAPTER III 27
FRACTURED WELL NUMERICAL MODELLING 27
3.1 Introduction 27
3.2 Fracture Modelling 28
3.3 Model Description 31
3.4 Relative Permeability Modelling 33
3.5 Model Verification 34
3.6 Conclusions 38
CHAPTER IV 39
FRACTURED WELLS FLOW BEHAVIOUR ANALYSIS 39
4.1 Introduction 39
4.2 Fracture and Formation Parameters Sensitivities 43
4.2.1 Effect of Fracture Half-Length, X_f 44
4.2.2 Effect of Fracture Permeability, K_f 48
4.2.3 Effect of Formation Permeability, K 51
4.2.4 Effect of Fracture Fluid Leak-off 52
4.2.5 Effect of Fracture Choke and Face skin 55
4.2.6 Effect of Un-equal Fracture Half-length 63
4.2.7 Effect of Fracture Width, w_f 64
4.2.8 Effect of Fracture Conductivity, $K_f w_f$ 65
4.2.9 Effect of Formation Fractured Interval 66
4.2.10 Effect of Non-Darcy in Gas Reservoirs 68
4.2.11 Effect of Proppant Agent Type 69
4.2.12 Effect of Multi-layered (Two Layers) 70
4.2.13 Effect of Multi-layered (Three layers) 76
4.2.14 Effect of Fractured Layer Position in Multi-layered System 81

4.3 Discussions 82
4.4 Conclusions 84
CHAPTER V 85
FRACTURED WELL IN NATURALLY FRACTURED RESERVOIRS 85
5.1 Introduction 85
5.2 Fractured Well in Naturally Fractured Reservoirs 86
5.3 Numerical Simulation of Fractured Well in Naturally Fractured Reservoirs 88
5.4 Conclusions 93
CHAPTER VI 94
FRACTURED WELL IN LEAN AND RICH GAS-CONDENSATE RESERVOIRS 94
6.1 Introduction 94
6.2 Fractured Well in Gas-condensate Reservoirs 95
6.3 PVT Analysis 98
6.4 Relative Permeability Modelling 99
6.5 Near Wellbore Effects 100
6.5.1 Effect of Condensate Banking 101
6.5.2 Effect of Velocity stripping 102
6.5.3 Effect of Non-Darcy Skin 102
6.5.4 Effect of Miscibility 103
6.6 Well Productivity 106
6.7 Conclusions 115
CHAPTER VII 116
FIELD APPLICATIONS OF FRACTURED WELL 116
7.1 Introduction 116
7.2 Case (I): Fractured Gas Well_ (Fracture damage) 117
7.3 Case (II): Fractured Gas Well_ (Low Fracture Conductivity) 124
7.4 Case (III): Fractured Gas-condensate Well 129
7.5 Conclusions 133
CHAPTER VIII 134
CONCLUSIONS AND RECOMMENDATIONS 134
8.1 Summary 134
8.2 Conclusions 135
8.3 Recommendations 137
REFERENCES 138
APPENDIX A 155
I. Eclipse Black Oil Input File_ Single Layer Oil Model 155
II. Eclipse Compositional Input File_ Single Layer Gas-condensate Model 163
APPENDIX B 170
I. Oil Sample PVT Modelling 170
II. Gas Sample PVT Modelling 171
III. Lean Gas Condensate Sample PVT Modelling 172
IV. Moderate Gas Condensate Sample PVT Modelling 173
V. Rich Gas Condensate Sample PVT Modelling 174
APPENDIX C 175
I. Fractured Choke Effect 175
II. Fractured Face Effect 176
APPENDIX D 177
I Gas-condensate Saturation Change Profiles 177
II Well Productivity in Lean and Rich Gas-condensate 182

LIST OF FIGURES

FIGURE 1- 1: SCHEMATIC OF FRACTURED WELL WITH DAMAGED ZONE 1
FIGURE 1- 2: POST-FRAC INFREQUENT FRACTURE BEHAVIOUR INDICATING NON-STIMULATED WELL 2

FIGURE 2- 1: WELLBORE STORAGE EFFECT ON FRACTURED WELL FLOW BEHAVIOUR (RAMEY, 1970) 8
FIGURE 2- 2: WELLBORE STORAGE AND SKIN FEATURES ON LOG-LOG PLOT (GRINGARTEN, 2002) 10
FIGURE 2- 3: PRESSURE PROFILES FOR DAMAGED AND STIMULATED WELL 13
FIGURE 2- 4: FRACTURE CHOKE DAMAGE (TOP) AND FACE SKIN (BELOW) 14
FIGURE 2- 5: FRACTURE FLOW PATTERNS: 16
FIGURE 2- 6: FIELD CASE WITH SIMILAR PRE AND POST-FRAC BEHAVIOURS (ROBINSON *ET AL*. 1991) 21
FIGURE 2- 7: PRE AND POST-FRAC IDENTICAL FLOW BEHAVIOURS (CHU, 1996) 23
FIGURE 2- 8: LOG –LOG PLOT OF PRE-FRAC (YELLOW) & POST-FRAC (GREEN) INFREQUENT BEHAVIOURS 25
FIGURE 2- 9: UNUSUAL FLOW BEHAVIOUR OF A STIMULATED WELL WITH IMPROVED SKIN & KH 26

FIGURE 3- 1: SCHEMATIC OF TYPICAL FRACTURED WELL DESIGN AND PARAMETERS 27
FIGURE 3- 2: RADIAL GRID MODEL FOR FRACTURE MODELLING 28
FIGURE 3- 3: CARTESIAN GRID USED FOR FRACTURE MODELLING IN THE STUDY 29
FIGURE 3- 4: RESERVOIR PROPERTIES INPUT INTO FRACPROPT FRACTURE DESIGN 30
FIGURE 3- 5: INDUCED FRACTURE DESIGN IN TWO LAYERS COMMINGLED MODEL 30
FIGURE 3- 6: SINGLE LAYER INDUCED FRACTURE MODEL 31
FIGURE 3- 7: FRACTURED WELL DESIGN IN TWO LAYERS COMMINGLED MODEL 32
FIGURE 3- 8: FRACTURED WELL PROFILE IN TWO LAYERS CROSS FLOW MODEL 32
FIGURE 3- 9: FRACTURED WELL IN MULTI-LAYERED COMMINGLED MODEL 32
FIGURE 3- 10: HETEROGENEITY EFFECT ON OIL AND WATER RELATIVE PERMEABILITY CURVES 33
FIGURE 3- 11: VERIFICATION OF THE NUMERICAL MODEL WITH ANALYTICAL SOLUTION FOR *FCD* OF 1.6 . 36
FIGURE 3- 12: VERIFICATION OF THE NUMERICAL MODEL VERSUS ANALYTICAL SOLUTION VARIOUS *FCD* 36
FIGURE 3- 13: ANALYTICALLY VERIFIED INFINITE VERSUS FINITE CONDUCTIVITY FRACTURE MODELS 37

FIGURE 4- 1: EFFECTIVE WELLBORE RADIUS VERSUS *FCD* (PRATS *ET AL.* 1962) 39
FIGURE 4- 2: COMPARISON OF FRACTURE HALF-LENGTHS OF 10 AND 100FT WITH FCD OF ONE 44
FIGURE 4- 3: COMPARISON OF FRACTURE HALF-LENGTHS OF 10 AND 100FT WITH FCD OF 10 45
FIGURE 4- 4: FRACTURED WELL PRESSURE BEHAVIOUR WITH FCD OF 1 &10 AND X_F OF 10FT 45
FIGURE 4- 5: FRACTURED WELL PRESSURE FEATURE WITH FCD OF 1 &10 & HALF-LENGTH, X_F OF 100FT... 46
FIGURE 4- 6: FRACTURED WELL PRESSURE BEHAVIOUR WITH FCD OF 1 &10 AND X_F OF 1000FT 46
FIGURE 4- 7: LOG-LOG PLOT OF FRACTURED WELL WITH FCD OF 0.25, 1, 5 & 10, HALF-LENGTH OF 10 FT . 47
FIGURE 4- 8: LOG-LOG PLOT OF FRACTURED WELL WITH FCD OF 0.25, 1, 5 &10, HALF-LENGTH OF 100 FT 47
FIGURE 4- 9: LOG-LOG PLOT OF FRACTURED WELL WITH FCD OF 0.25, 1, 5 & 10, HALF-LENGTH 1000 FT .. 47
FIGURE 4- 10: PRESSURE BEHAVIOUR OF 100FT X_F AND FRACTURE PERMEABILITY OF 10, 40 AND 400D .. 48
FIGURE 4- 11 : FRACTURED WELL OF 1 MD MODEL WITH FCD OF 1, 3, 5, 10, 50 AND 100 AND X_F=100FT . 49
FIGURE 4- 12: FRACTURED WELL IN 10 MD MODEL WITH FCD 0.1, 0.3, 0.5, 1, 5 & 10 AND, X_F=100FT 49
FIGURE 4- 13: FRACTURED WELL IN 100 MD WITH FCD OF 0.01, 0.03, 0.05, 0.1, 0.5 AND 1 X_F=100FT..... 50
FIGURE 4- 14: LOG-LOG PLOT OF FRACTURE PERMEABILITY OF 50D & FRACTURE HALF-LENGTH OF100FT 51
FIGURE 4- 15: TWO MODELS WITH FORMATION PERMEABILITIES OF 1 AND 100MD AND X_F OF 100FT 52
FIGURE 4- 16: CROSS SECTION SHOWING EFFECT OF FACTURE FLUID LEAK-OFF EFFECT 53
FIGURE 4- 17: WATER PRODUCTION RATE DURING CLEAN-UP PERIOD FOLLOWING WELL STIMULATION . 54
FIGURE 4- 18: FRACTURE LEAK-OFF EFFECT IN 10 MD FORMATION WITH *FCD* OF 4 AND X_F OF 100FT..... 54
FIGURE 4- 19: FRACTURE CHOKE EFFECT ON THE PRESSURE PROFILE OF FRACTURE HALF-LENGTH 100FT 55
FIGURE 4- 20: FRACTURE FACE SKIN PRESSURE PROFILE OF FRACTURE HALF-LENGTH OF 100FT 56
FIGURE 4- 21: FRACTURE FACE AND CHOKE EFFECTS IN LOW PERMEABILITY RESERVOIR OF 1MD..... 57
FIGURE 4- 22: FRACTURE FACE & CHOKE EFFECTS IN MODERATE PERMEABILITY RESERVOIR OF 100MD .. 57
FIGURE 4- 23: FRACTURE CHOKE EFFECT ON THE PRESSURE PROFILE OF FRACTURE HALF-LENGTH 500FT 58
FIGURE 4- 24: FRACTURE FACE SKIN ON THE PRESSURE PROFILE OF FRACTURE HALF-LENGTH OF 500FT .. 58
FIGURE 4- 25: FRACTURE CHOKE AND FACE SKIN EFFECT IN 1MD & FRACTURE HALF-LENGTH OF 500FT... 59
FIGURE 4- 26: FRACTURE CHOKE AND FACE SKIN EFFECT IN 100MD AND FRACTURE HALF-LENGTH 500FT 59

FIGURE 4- 27: FRACTURE CHOKE EFFECT ON THE PRESSURE PROFILE OF FRACTURES HALF-LENGTH 10FT 60
FIGURE 4- 28: FRACTURE CHOKE EFFECT ON THE PRESSURE PROFILE OF FRACTURES HALF-LENGTH100FT 60
FIGURE 4- 29: FRACTURE FACE SKIN EFFECT ON THE PRESSURE PROFILE OF FRACTURE HALF-LENGTH 10. 61
FIGURE 4- 30: FRACTURE FACE SKIN EFFECT ON THE PRESSURE PROFILE OF X_F OF 100FT 61
FIGURE 4- 31: FRACTURE CHOKE EFFECT COMPARISON ON THE PRESSURE PROFILE OF FRACTURES HALF-LENGTHS OF 10FT AND 100 FT..... 62
FIGURE 4- 32: UN-EQUAL FRACTURE HALF-LENGTH EFFECT IN COMMINGLED LAYERS CASE..... 63
FIGURE 4- 33: UN-EQUAL FRACTURE HALF-LENGTH EFFECT IN CROSS-FLOW SCENARIO 64
FIGURE 4- 34: FRACTURE WIDTH EFFECT ON THE PRESSURE RESPONSE..... 64
FIGURE 4- 35: FRACTURE CONDUCTIVITY VALUE EFFECT ON THE WELL FLOW BEHAVIOUR..... 65
FIGURE 4- 36: PARTIALLY FRACTURED FORMATION EFFECT WITH X_F=100FT AND 10MD FORMATION 66
FIGURE 4- 37: COMPLETED FRACTURED INTERVAL EFFECT ON THE FRACTURED WELL FLOW BEHAVIOUR 67
FIGURE 4- 38: COMPLETED FRACTURED INTERVAL EFFECT ON THE FRACTURED WELL FLOW BEHAVIOUR 67
FIGURE 4- 39: EFFECTS OF NON-DARCY (RED) AND CAPILLARY NUMBER (PURPLE) ON THE PRESSURE 68
FIGURE 4- 40: NON-DARCY EFFECT ON THE GENERATED PRESSURE BEHAVIOUR OF FRACTURED WELLS... 68
FIGURE 4- 41: RCP AS FRACTURING PROPPANT AGENT WITH DIFFERENT DAMAGE EFFECTS 69
FIGURE 4- 42: TWO LAYERS OF 0.1 BY 10 MD WITH FRACTURE PERMEABILITY OF 0.1, 0.5, 1 AND 1.5D AND FRACTURE HALF-LENGTHS OF 10, 25, 50 AND 100FT 70
FIGURE 4- 43: TWO LAYERS OF 10 BY 100 MD WITH FRACTURE HALF-LENGTHS OF 10, 25, 50 AND 100FT 71
FIGURE 4- 44: TWO LAYERS OF 0.1 BY 10MD AND FRACTURE HALF-LENGTHS OF 10, 25, 50,100 & 500FT . 71
FIGURE 4- 45: TWO LAYERS OF 0.1 BY 10MD AND FRACTURE HALF-LENGTHS OF 10, 25, 50,100 & 500FT . 72
FIGURE 4- 46: TWO LAYERS WITH TOP LAYER (0.01MD) FRACTURED ONLY..... 73
FIGURE 4- 47: DOUBLE LAYERS WITH LOWER LAYER (100MD) FRACTURED ONLY 73
FIGURE 4- 48: TWO LAYERS OF 0.1 BY 10MD & 0.01 BY 10MD, CLEAR FRACTURE FLOW BEHAVIOUR 74
FIGURE 4- 49: TWO LAYERS OF 0.1 BY 100MD AND 0.01 BY 100MD, NO FRACTURE FLOW..... 74
FIGURE 4- 50: TWO LAYERS OF 0.01 BY 100MD PERM WITH FRACTURED PERMEABILITIES OF 1 AND 10D. 75
FIGURE 4- 51: TWO LAYERS OF 0.001. 0.01. 0.1 AND 1D BY 100MD PERM WITH FRACTURED PERMEABILITIES OF 1 AND 10D 75
FIGURE 4- 52: MULTI-LAYERED SYSTEM (THREE LAYERS) WITH TOP LAYER (0.1MD) FRACTURED ONLY 77
FIGURE 4- 53: MULTI-LAYERED SYSTEM (THREE LAYERS) WITH MIDDLE LAYER (10MD) FRACTURED ONLY 77
FIGURE 4- 54: MULTI-LAYERED SYSTEM(THREE LAYERS)WITH BOTTOM LAYER (100MD) FRACTURED..... 78
FIGURE 4- 55: MULTI-LAYERED WITH THREE LAYERS (0.1-10-100MD) FRACTURED STIMULATINGLY..... 78
FIGURE 4- 56: THREE LAYERS WITH TOP LAYER (0.1MD) FRACTURED ONLY. & X_F = 1000FT 79
FIGURE 4- 57: THREE LAYERS WITH MIDDLE LAYER OF10MD FRACTURED ONLY AND X_F = 1000FT..... 80
FIGURE 4- 58: THREE LAYERS WITH BOTTOM LAYER OF100MD FRACTURED ONLY AND X_F = 1000FT..... 80
FIGURE 4- 59: THREE LAYERS OF 0.1-10-100MD FRACTURED STIMULATINGLY WITH X_F = 1000FT 80
FIGURE 4- 60: THREE LAYERS FRACTURED WITH DIFFERENT LAYER POSITIONS AND K_F OF 1D 81
FIGURE 4- 61: THREE LAYERS WITH ALL LAYERS FRACTURED STIMULATINGLY AND DIFFERENT LAYER POSITIONS AND FRACTURE PERMEABILITY OF 1D..... 81

FIGURE 5- 1: VERIFICATION OF NUMERICAL AND ANALYTICAL MODELS FOR A FRACTURED WELL..... 88
FIGURE 5- 2: VERIFICATION OF NUMERICAL VS. ANALYTICAL SOLUTION OF VARIOUS FRACTURE PERMEABILITY IN SINGLE LAYER FRACTURED FORMATION..... 89
FIGURE 5- 3: DIMENSIONLESS PRESSURE BEHAVIOURS OF VARIOUS FRACTURE PERMEABILITY IN SINGLE LAYER FRACTURED FORMATION..... 89
FIGURE 5- 4: PRE FRAC PRESSURE BEHAVIOUR OF LEAN GAS-CONDENSATE OF VARIOUS RATES 90
FIGURE 5- 5: POST-FRAC PRESSURE BEHAVIOUR OF LEAN GAS-CONDENSATE OF VARIOUS RATES..... 90
FIGURE 5- 6: PRE FRAC PRESSURE BEHAVIOUR OF RICH GAS-CONDENSATE OF VARIOUS RATES..... 91
FIGURE 5- 7: POST-FRAC PRESSURE BEHAVIOUR OF RICH GAS-CONDENSATE OF VARIOUS RATES 92
FIGURE 5- 8: PRE & POST-FRAC PRESSURE BEHAVIOUR OF RICH GAS-CONDENSATE FRACTURED WELL.... 92
FIGURE 5- 9: POST-FRAC PRESSURE RESPONSE OF FRACTURED WELL AFFECTED BY FRACTURE DAMAGES 93

FIGURE 6- 1: SHOWS NEAR WELLBORE LIQUID DROP OUT END OF 5DAYS BU FOLLOWING 180 DAYS DD 101
FIGURE 6- 2: RELATIVE PERMEABILITY CURVES FOR MISCIBLE, LESS, BASE AND HIGH MISCIBLE 104
FIGURE 6- 3: CASES WITH/OUT FRACTURE OF MISCIBLE, AND BASE, HIGH AND LOW MISCIBILITY FLUIDS104
FIGURE 6- 4: LOG-LOG OF NON-FRACTURED WELL OF MIS. LESS MISCIBLE. BASE & MORE MISCIBLE. 105

FIGURE 6- 5: LOG-LOG PLOT OF FRACTURED WELL OF MIS.LESS MISCIBLE. BASE AND MORE MISCIBLE... 105
FIGURE 6- 6: COMPARISON OF FLOW BEHAVIOUR OF LEAN AND RICH GAS-CONDENSATE FLUID 106
FIGURE 6- 7: FLOW BEHAVIOUR OF FRACTURED WELL IN LEAN & RICH MODELS..... 107
FIGURE 6- 8: IMPACT OF SHORT FRACTURE HALF-LENGTH IN LEAN CASE MODEL..... 107
FIGURE 6- 9: EFFECT OF SHORT FRACTURE HALF-LENGTH IN THE RICH CASE 108
FIGURE 6- 10: FRACTURE CHOKE DAMAGE EFFECT ON WELL BEHAVIOUR IN LEAN & RICH CONDENSATE 108
FIGURE 6- 11: PRODUCTION TIME EFFECT ON CONDENSATE BANK DEVELOPMENT AFTER 1, 2, 3, 6, 12, 24 AND 36 MONTHS WITH CASE A & H SHOWING END OF DD AND REST SHOWS SATURATION AT END OF BU PERIOD FOLLOWING DD END..... 109
FIGURE 6- 12: FRACTURED WELL BEHAVIOUR OF VARIOUS LENGTHS AT END OF 30DAYS DD 110
FIGURE 6- 13: FRACTURED WELL BEHAVIOUR OF VARIOUS LENGTHS AT END OF 30DAYS DD 110
FIGURE 6- 14: FRACTURED WELL BEHAVIOUR OF VARIOUS LENGTHS AT END OF 180DAYS DD 111
FIGURE 6- 15: FRACTURED WELL BEHAVIOUR OF VARIOUS LENGTHS AT END OF 180DAYS DD 111
FIGURE 6- 16: FLOW BEHAVIOUR COMPARISON IN LEAN FLUID OF 30D&180D PRODUCTION PERIODS .. 112
FIGURE 6- 17: FLOW BEHAVIOUR COMPARISON IN RICH FLUID OF 30D&180D PRODUCTION PERIODS ... 112
FIGURE 6- 18: FLOW BEHAVIOUR OF LEAN FLUID FOR FRACTURED WELL DURING FOUR LOW PERIODS . 113
FIGURE 6- 19: FLOW BEHAVIOUR COMPARISON IN RICH FLUID OF FOUR FLOW PERIODS 113
FIGURE 6- 20 : FLOW BEHAVIOUR COMPARISON OF MULTILAYERED MODEL OF LEAN & RICH FLUID 114

FIGURE 7- 1: MAIN FRAC JOB TREATMENT RESULTS OF THE STIMULATED WELL..... 118
FIGURE 7- 2: INDUCED FRACTURE CONDUCTIVITY WITH PERFORATED INTERVAL LOCATION 118
FIGURE 7- 3: CREATED FRACTURE WIDTH, LENGTH AND CONDUCTIVITY OF THE FRACTURED WELL..... 119
FIGURE 7- 4: ANALYTICAL WELL TEST INTERPRETATION RESULT OF THE ACTUAL DATA (FP#4)..... 120
FIGURE 7- 5: LOG-LOG DIAGNOSTIC ANALYTICAL SOLUTION MATCH AGAINST NUMERICAL RESULT FP#4 120
FIGURE 7- 6: SHOWING TOTAL PRODUCTION HISTORY OF THE DST RUN OVERTHEFRACTUREDINTERVAL 121
FIGURE 7- 7: ANALYTICAL WELL TEST INTERPRETATION OF THE NUMERICAL MODEL RESULTS (FP # 4) ... 121
FIGURE 7- 8: LOG-LOG PRESSURE MATCH FOR THE MAIN BUILD-UP FLOW PERIOD..... 122
FIGURE 7- 9: VERIFICATION OF THE NUMERICAL MODEL AGAINST THE ANALYTICAL SOLUTION 122
FIGURE 7- 10: NUMERICAL MODEL VERSUS ANALYTICAL SOLUTION RESULTS OF THE FRACTURED WELL 123
FIGURE 7- 11: LOG-LOG DIAGNOSTIC WITH WBS & RADIAL FLOW FEATURES AS PRESENTED..... 125
FIGURE 7- 12: LOG-LOG PLOT OF THE MEASURED DATA AGAINST ANALYTICAL SOLUTION 125
FIGURE 7- 13: MEASURED DATA VERSUS ANALYTICAL MATCH FOR ALL FLOW PERIODS..... 125
FIGURE 7- 14: WELL TEST ANALYSIS RESULTS OF THE ACTUAL MEASURED DATA..... 126
FIGURE 7- 15: LOG-LOG PRESSURE MATCH FOR THE MAIN BUILD-UP OF THE NUMERICAL MODEL 126
FIGURE 7- 16: MEASURED DATA VERSUS ANALYTICAL MATCH FOR ALL FLOW PERIODS..... 127
FIGURE 7- 17: GRAPHS SHOWING WELL TEST ANALYSIS RESULTS OF THE NUMERICAL MODEL..... 127
FIGURE 7- 18: GRAPH SHOWS LOG-LOG PLOT OF THE NUMERICAL MODEL WITH ANALYTICALSOLUTION 128
FIGURE 7- 19: WELLBORE STORAGE AND SKIN WITH NO INDICATION OF FRACTURED FLOW IN 130
FIGURE 7- 20: PRESSURE AND FLOW BEHAVIOURS FOR PRE-FRAC FLOW PERIODS (FP15, FP28 AND FP54) AND POST-FRAC FLOW PERIODS INCLUDE (FP59, FP66, FP70 AND FP79)..... 131
FIGURE 7- 21: LOG-LOG PLOT OF PRE-FRAC FP#15INDICATING WELLBORE STORAGE AND SKIN 131
FIGURE 7- 22: LOG-LOG PLOT OF PRE-FRAC FP#28 INDICATING WELLBORE STORAGE & SKIN FEATURES. 132
FIGURE 7- 23: LOG-LOG PLOT OF POST-FRAC FP #59INDICATING WELLBORE STORAGE AND SKIN 132

FIGURE B- 1: PVT PROPERTIES ANALYSED IN PVTI FOR THE USED OIL SAMPLE..... 170
FIGURE B- 2: PVT PROPERTIES ANALYSED IN PVTI FOR THE USED GAS SAMPLE IN THE STUDY 171
FIGURE B- 3: PVT PROPERTIES ANALYSED IN PVTI FOR THE LEAN GAS CONDENSATE SAMPLE..... 172
FIGURE B- 4: PVT PROPERTIES ANALYSED IN PVTI FOR THE MODERATE GAS CONDENSATE SAMPLE 173
FIGURE B- 5: PVT PROPERTIES ANALYSED IN PVTI FOR THE RICH GAS CONDENSATE SAMPLE 174

FIGURE C- 1: FRACTURE FLOW BEHAVIOUR OF 10, 30, 50 AND 100FT WITH CHOKED DAMAGE EFFECT .. 175
FIGURE C- 2: FRACTURE FLOW BEHAVIOUR OF 300, 500, 1000 AND 1500FT WITH CHOKED DAMAGE..... 175
FIGURE C- 3: FRACTURE FLOW BEHAVIOUR OF 10, 30, 50 AND 100FT WITH FRACTURE FACE SKIN..... 176
FIGURE C- 4: FRACTURE FLOW BEHAVIOUR OF 300, 500, 1000 AND 1500FT WITH FACE SKIN EFFECT 176

FIGURE D- 1: GRAPH A: SHOWS 10FT FRACTURE HALF-LENGTH BEFORE PRODUCTION 177
FIGURE D- 2: GRAPH A: SHOWS 50FT FRACTURE HALF-LENGTH BEFORE PRODUCTION 177
FIGURE D- 3: GRAPH A: SHOWS 100FT FRACTURE HALF-LENGTH BEFORE PRODUCTION 178
FIGURE D- 4: GRAPH A: SHOWS 300FT FRACTURE HALF-LENGTH BEFORE PRODUCTION 178
FIGURE D- 5: GRAPH A: SHOWS 500FT FRACTURE HALF-LENGTH BEFORE PRODUCTION 179
FIGURE D- 6: GRAPH A: SHOWS 1000FT FRACTURE HALF-LENGTH BEFORE PRODUCTION 179
FIGURE D- 7: LIQUID SATURATION DISTRIBUTION AT THE END OF 30DAYS DD FOR FRACTURE HALF-LENGTH OF 10-50-100-200-300-400FT 180
FIGURE D- 8: LIQUID SATURATION DISTRIBUTION AT THE END OF 50DAYS BU FOLLOWING PRECEDING 30DAYS OF DD FOR FRACTURE HALF-LENGTH OF 10-50-100-200-300-400FT 180
FIGURE D- 9: LIQUID SATURATION DISTRIBUTION FOR A 100FT FRACTURE HALF-LENGTH AT THE END: .. 181
FIGURE D- 10: LIQUID SATURATION DISTRIBUTION FOR A 100FT FRACTURE HALF-LENGTH AT THE END OF 5 DAYS BU FOLLOWING: 181
FIGURE D- 11: PRODUCTION GAS RATE, CUMULATIVE GAS AND LIQUID PLUS WBHP COMPARISON FOR FRACTURE HALF-LENGTH OF 10, 50, 100, 200, 300, 500, 1000 AND NO FRAC IN LEAN GAS-CONDENSATE 182
FIGURE D- 12: PRODUCTION GAS RATE, CUMULATIVE GAS AND LIQUID PLUS WBHP COMPARISON FOR FRACTURE HALF-LENGTH OF 10, 50, 100, 200, 300, 500, 1000 AND NO FRAC IN RICH GAS-CONDENSATE 182

LIST OF TABLES

TABLE 3- 1: DESCRIPTION OF THE MAIN CHARACTERISTICS OF THE RESERVOIR MODEL 35

TABLE 7- 1: SHOWS PERFORATION, WORK STRING AND CASING DATA FOR THE STIMULATED WELL 117
TABLE 7- 2: MINI FRAC PUMPING SCHEDULE FOR THE FRACTURED WELL 117
TABLE 7- 3: DESCRIPTION OF THE MAIN CHARACTERISTICS OF THE GAS RESERVOIR MODEL 119
TABLE 7- 4: COMPARISON OF WELL TEST INTERPRETATION RESULTS OF ANALYTICAL & NUMERICAL 123
TABLE 7- 5: FRACTURE, FORMATION AND FLUID INPUT PARAMETERS USED IN THE NUMERICAL MODEL 124
TABLE 7- 6: SHOWS RESULTS COMPARISON BETWEEN NUMERICAL AGAINST ANALYTICAL SOLUTION 128
TABLE 7- 7: RESERVOIRS B, C & D DEPTHS, THICKNESS AND INITIAL PRESSURE PRESENT IN EACH LAYER. 129
TABLE 7- 8: FRACTURE LENGTH, HEIGHT AND CONDUCTIVITY OF THE INDUCED FRACTURE 130

NOMENCLATURE AND ABBREVIATIONS

A	area, ft^2
B	formation volume factor
BHP	bottom hole pressure, psi
C	wellbore storage coefficient, bbl/psi
C_D	dimensionless wellbore storage,
C_{Df}	dimensionless fracture storage
C_{rD}	dimensionless reservoir conductivity
c_t	total compressibility, psi^{-1}
FcD	dimensionless fracture conductivity
h	formation thickness, ft
hc_t	storativity, ft-psi^{-1}
h_f	fracture height, ft
k	permeability, mD
k_f	fracture permeability, mD
kh	permeability-thickness (conductivity), mD-ft
k_h	horizontal permeability, mD
k_r	reservoir permeability, mD
k_s	damaged zone permeability, mD
k_{fc}	choked fracture permeability, mD
k_z	vertical permeability, mD
m(p)	real gas pseudo pressure, $psia^2/cp$
m_{HKF}	slope of high conductivity fracture, psi/hr
m_{LKF}	slope of low conductivity fracture, psi/hr
m_{wbs}	slope of wellbore storage dominated regime, psi/hr
MW	molecular weight
Nre	reynolds number
P	pressure, psi
P_{av}	average reservoir pressure, psi
P_i	initial reservoir pressure, psi
p_d	dew point pressure, psi
p_D	dimensionless pressure

p_{wf}	flowing bottom hole pressure, psi
p_{1hr}	pressure at 1 hour on the Horner straight line (psi)
q	flow rate of oil or gas, STB/D or Mscf/D
r_D	dimensionless radius
r_e	drainage radius, ft
r_s	damaged zone radius, ft
r_w	well radius, ft
r_{wa}	equivalent wellbore radius, ft
$r_{w'}$	equivalent wellbore radius due to fracture, ft
S	skin factor, dimensionless
Sc	condensate saturation, percentage
S_d	effective skin factor caused by damage
S_f	pseudo skin factor due to fracture
S_{fc}	choked fracture skin, dimensionless
S_{ff}	fracture face skin, dimensionless
S_t	total skin
t	Time, hrs
t_D	dimensionless time
t_{De}	effective dimensionless time
t_{Dxf}	dimensionless time (with respect to fracture half-length)
t_e	equivalent pseudo time, hr-psia/cp
t_p	production time, hr
v	velocity
V_u	pipe capacity, bbl/ft
w	fracture width, ft
w_s	width (extent) of damaged fracture, ft
x_{cD}	dimensionless fracture choked damage,
x_{fD}	dimensionless fracture face damage
x_{ck}	fracture choke damage length, ft
x_{ff}	fracture Face damage length, ft
x_e	reservoir extent in x-direction, ft

x_y reservoir extent in y-direction, ft

x_f fracture half-length, ft

Z gas compressibility factor

Greek

β inertial effect coefficient/turbulence or non-Darcy effect

Δt elapsed time, hrs

μ viscosity, cp

v velocity

ø porosity

ρ density

σ interfacial tension

Subscripts

D dimensionless

f fracture

g gas

o oil

w water

t total

ABBREVIATION

BU build-up. This flow period corresponds to zero production rate. The preceding number is the flow period during well test

DD drawdown. This flow period correspond to production period. The preceding number represents the flow period during well test

FP flow period

MHF massive hydraulic fracturing

MLR multi-layered reservoir

N_c capillary number. This is as defined as $\frac{k\|\nabla\Phi\|}{\phi.\sigma}$ for this project

PVT pressure Volume Temperature

RCP resin coated proppant

TSO tip screen out

WBS wellbore storage

CHAPTER I

BACKGROUND AND MOTIVATION

1.1 Introduction

Hydraulic fracture stimulation makes development of tight formations and other unconventional reservoirs possible. Enhancing oil and gas wells with low and moderate productivity through hydraulic fracturing has been common practice in the industry for decades. The approach is to create a flow path that extends beyond the damaged zone surrounding the wellbore resulting from drilling and completion operations. The induced fracture is packed with proppant material that has permeability significantly higher than the formation permeability (*Figure 1-1*).

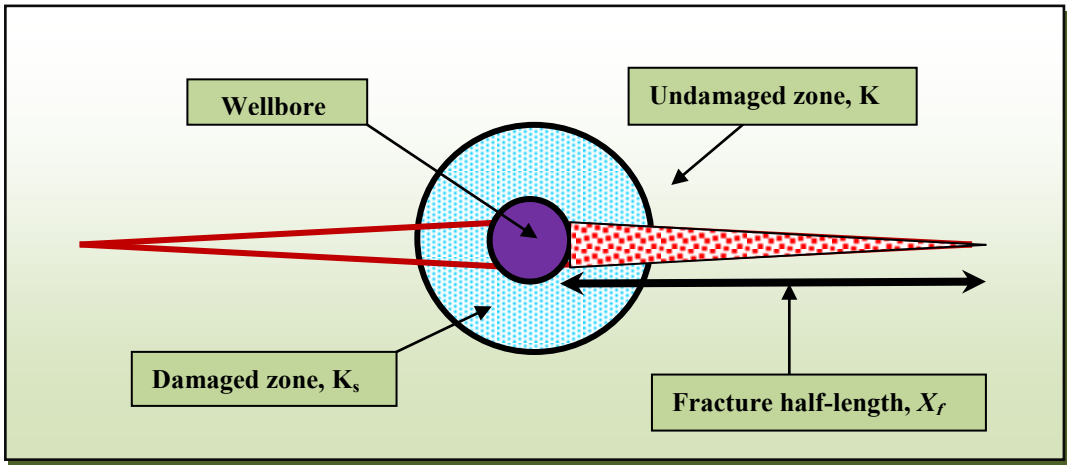


Figure 1- 1: Schematic of fractured well with damaged zone

A practical approach to evaluate the effectiveness of a stimulation job performed on a well is through post-frac well test analysis. On a log-log plot of pressure change and derivative versus elapsed time, the pressure transient response of a fractured well is expected to be different to a non-fractured well. In early time, a non-fractured damaged well will usually exhibit a unit slope corresponding to wellbore storage. The derivative will then decrease to a stabilisation level corresponding to infinite acting radial flow. Conversely, a fractured well is expected to exhibit early time slopes less than one (usually a half or quarter) and the derivative will approach the stabilisation level corresponding to infinite acting radial flow from below rather than above. This is the behaviour expected when skin is negative. However, it is observed that in some post-frac well tests, a unit slope line is reported instead of typical fractured well flow patterns, indicating a non-stimulated well feature.

1.2 Problem Recognition

After stimulating, some wells penetrating single or multi-layered oil and gas reservoirs, do not exhibit early time fracture flow patterns of half or quarter unit slope features in the post-frac well test. Instead, a unit slope line representing wellbore storage effect with reduced skin followed by radial flow behaviour is present on the log-log pressure change versus elapsed time plot (*Figure 1-2*). With this behaviour reduction in positive skin and improvement in well productivity are reported in post-frac tests. Mountford and Raghavan (1978) stated that if the wellbore storage effect dominates pressure data for a stimulated well, it is expected to observe unit slope line followed by half slope. However, the analytical solutions suggested that only the transition between the unit slope and half slope period will be seen and if the storage effect is large then the half slope line may be obscured by the transition period. In this study, hydraulically fractured wells exhibiting unusual flow behaviour at early time are investigated in detail.

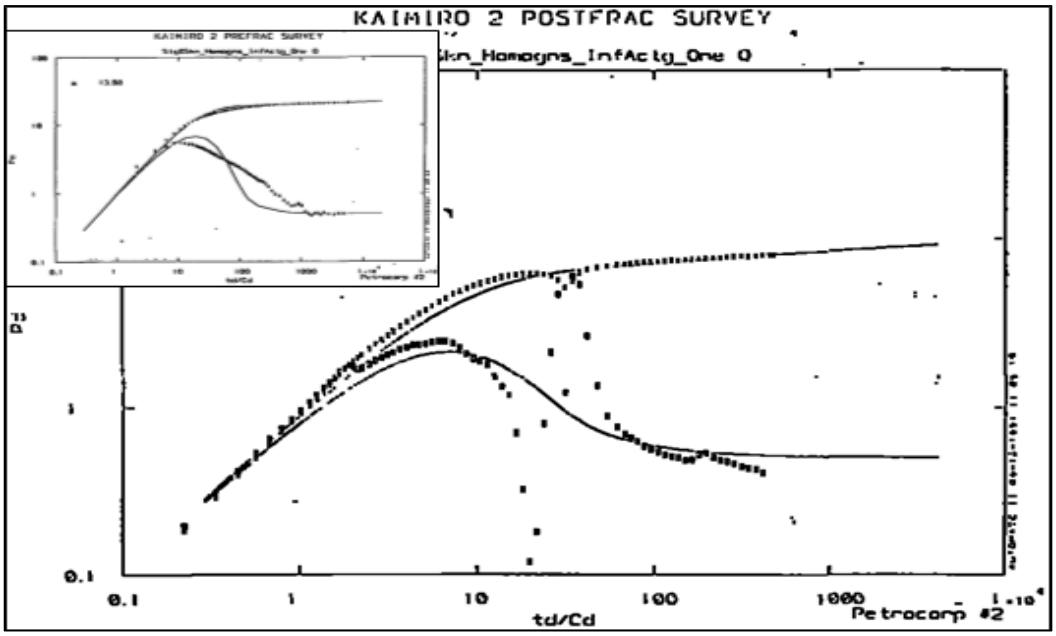


Figure 1- 2: Pre & Post-frac infrequent fracture behaviour indicating non-stimulated well

Figure above presents transient pressure behaviours of pre and post frac a fractured well with reduced damage (skin) followed by radial flow. As it can be noticed the early time behaviour is identical to that of a non-fractured well. This is an example of the infrequent behaviour of a fractured well that was published by Goodin (1991). The problem of observing uncommon fracture flow behaviour had been referred to briefly in the literature. The main objective of this study is to examine reasons for developing unusual fractured well flow behaviour at early times.

1.3 Methodology

Transient pressure responses are generated using 3-D numerical simulation model by changing flow conditions at the wellbore. The pressure data are then analysed by matching with an appropriate analytical solution model. Typical rock and fluid properties found in actual reservoir conditions were used in the study to model behaviour of hydraulically fractured wells penetrating single or multi-layered oil and gas reservoirs, using black oil and compositional numerical models. Conclusions drawn from the synthetic numerical simulation models will be used to interpret actual field cases illustrating unusual behaviour at early times.

Constant wellbore storage is assumed in most analytical models; however, the numerical model is not capable of modelling wellbore storage effect. The concept of skin effect is used to quantify impediment to flow in oil and gas wells, as introduced by Van Everdingen and Hurst (1953). The most common source of skin effect is mechanical skin around the wellbore, which forms an important part of the total skin denoted by S throughout this document.

A number of parameters are investigated with respect to their impact on the introduced unusual fractured well flow behaviour including the impact of reservoir heterogeneity. Fracture configuration parameters including fracture length, width, conductivity and damage caused to the induced fracture are investigated. In proppant fractured wells, damage can be due to a fracture face skin, S_{ff}, which is a permeability reduction normal to the face of the fracture or to a choked fracture, S_{fc} effect with reduced proppant permeability within the fracture close to the wellbore, as presented by Cinco-Ley and Samaniego (1981).

Black oil and compositional reservoir simulators (Eclipse-100 and 300) were used to simulate pressure drawdown (DD) and build-up (BU) well test data. It is common practice to model a single vertical non-stimulated well as part of a radial grid model. However, Lee and Spivey (1998) stated that a more practical approach to incorporate the fracture plane of high permeability cells into a Cartesian grid model where cells are specified by their length and width. The local grid refinement (LGR) approach is applied to model induced fractures in Cartesian coordinates, where flow geometry is modelled rigorously.The produced synthetic pressure transient versus elapsed time data is then analysed using commercial well test interpretation software packages.

1.4 Objectives

Many authors have studied the behaviour of fractured wells both analytically and numerically including Prats *et al*. (1962), Scott (1963), Russell and Truitt (1964), Millheim and Cichowicz (1968), Wattenbarger and Ramey (1969), Evans (1971), Raghavan *et al*. (1972), Gringarten *et al*. (1974), Gringarten *et al*. (1975), Ramey and Gringarten (1975), Locke and Sawyer (1975), Ozkan and Raghavan (1977), Cinco-Ley *et al*. (1978), Narasimhan and Palen (1979) and Lee and Brockenbrough (1988). From all these publications and others, infinite, uniform flux and finite fracture conductivity behaviours are well understood.

However, very a few workers have examined the unusual flow behaviour associated with hydraulically fractured wells, where typical fractured well flow patterns are not observed during early time. Instead, a wellbore storage with unit slope followed by radial flow behaviour had been described in some field cases. To the author's knowledge, so far no published study had investigated this problem in the literature. Therefore, the main objectives of the current study are to:

- Examine the unusual flow features associated with some fractured well tests following a proppant frac job;
- Determine conditions where the uncommon behaviour develops; what type of reservoirs and what are the main controlling parameters;
- Investigate the behaviour in homogenous and heterogeneous reservoirs including multi-layered, naturally fractured and gas-condensate reservoirs containing lean and rich fluids;
- Explore the effectiveness of hydraulically fractured vertical wells to improve well productivity in lean and rich gas-condensate reservoirs.

Study results present the main causes for observing infrequent flow behaviour in post-frac well tests, which is significantly important to most operator and service companies. As understanding causes for developing such unusual flow behaviour helps in evaluating the effectiveness of stimulation treatment performed on the well. This study is the first systematic and comprehensive work carried out on this problem associated with fractured wells.

1.5 Project outline

This report comprises the following chapters:

Chapter (I) introduce a brief description of the problem, methodology implemented in the project and the main objectives of the study.

Chapter (II) provides a review of the early time flow regimes associated with fractured wells including wellbore storage, skin and fractured well flow patterns; definition of dimensionless terms used in this study followed by research problem identification and literature review of the problem.

Chapter (III) highlights a description of the reservoir simulation model construction approach and methodology used for fracture modelling.

Chapter (IV) presents work done on numerical modelling of propped fractured wells in single and multi-layered reservoirs. Sensitivity runs on various cases including fracture configuration and reservoir settings are discussed in detail.

Chapter (V) shows results of modelling hydraulically fractured wells in naturally fractured oil and gas reservoirs and pressure transient analysis of the presented cases.

Chapter (VI) addresses results obtained from comparison of fractured well in lean and rich gas-condensate with emphasis on causes of the problem development in such reservoirs. Well productivities of fractured wells in such reservoirs are also investigated.

Chapter (VII) demonstrates application of the results obtained from the generic reservoir simulation models into real field examples to verify conclusions drawn from the study.

Chapter (VIII) summarises main conclusions and recommendations for future work. This chapter is followed by detailed biography and list of appendices.

1.6 Publication

The following paper was published as a result of this thesis:

Aram Amin: "Well Test Analysis of Infrequent Flow Behaviour of Fractured Wells in Oil and Gas Reservoirs," SPE 149887, paper presented at the SPE Annual Unconventional Gas Conference held in Abu Dhabi, 23-25 January 2012.

CHAPTER II

FRACTURED WELL: CONCEPT and FLOW PATTERENS

2.1 Introduction

The first hydraulic fracturing treatment was pumped in 1947 on a gas well operated by Pan American Petroleum Corporation in the Hugoton field in Kansas, USA (Howard and Fast, 1970). Since then hydraulic fracturing has been used quite successfully and has become a standard practice in the industry to improve productivity from oil and gas reservoirs. The fracturing processes include design, execution and post-frac analysis.

The fracture design process including selection of proppant/fluid type, pumping schedule, injected proppant concentrations, total job size, pump rate, and other parameters requires an understanding of the stimulation goals. For instance, what fracture length is required; what pack concentration can be placed? How much fracture can be cleaned-up? When all necessary inputs are specified to characterize the reservoir and the fracture design, the outcome can be accurately modelled with a simulator. The treatment goals listed above can be realized and an optimum design can be reached.

Following creation of the fracture, a practical way to assess the effectiveness of the stimulation work is through transient pressure analysis. For this purpose actual measured drawdown and build-up pressure and rates versus time data is required. The interpreted pressure transient allows engineers to identify important reservoir characteristics that are not possible to obtain through other sources of information of limited resolution such as cores and logs. By examining the shape of the generated pressure and pressure derivative on a log-log plot of pressure versus time, the interpreter should be able to describe certain characters of the reservoir and assess induced fracture properties.

Fractured wells often exhibit double lines of half or quarter unit slopes on a log-log plot of pressure change versus elapsed time. It is usual to observe such behaviour when analysing well test data from stimulated wells. In a fractured well multiple flow regimes are present including short wellbore storage (may or may not exist) followed by negative skin, bilinear flow, fracture linear flow, pseudo-linear flow. The following section discusses in detail all these flow regimes associated with fractured wells.

2.2 Wellbore storage

The surface flow from sand-face continues into the wellbore for some time after a well is shut-in. This time period causes flow regime behaviour called wellbore storage (WBS). This may last from a few seconds to minutes or even longer and it is also known as after flow, after production, after injection and wellbore unloading or loading in the literature (Olivier *et al.*, 2008). Wellbore storage affects well pressure responses during the first instants of each test period either drawdown (DD) or build-up (BU). Wellbore storage effect can be caused by either fluid compressibility or by changing fluid level inside the wellbore.

For instance, when the well is opened to flow the production at surface is initially due to the expansion of the fluid stored in the wellbore, and the sand-face contribution is insignificant. The reservoir begins to contribute flow until it becomes the same as the observed surface rate. Once this condition is reached the production is purely from the formation, then wellbore storage effects are over.

During shut-in period, the well will be shut-in either at the surface or at the sand-face. In the case of shutting the well at the sand-face there will be slight or no wellbore storage effect to develop. However, in the former case and after shut-in, the wellbore storage unit slope will end when the sand-face rate (after flow) starts to reduce significantly. Once the sand face flow becomes zero, wellbore storage effects are over.

The effect of wellbore storage was first introduced by Van Everdingen and Hurst (1949). They pointed out that the storage of fluid contained within the wellbore could cause a significant difference between the surface production rate and the sand-face flow rate. Wattenbarger and Ramey (1969) studied wellbore storage for gas flow case and found that under extreme conditions there could exist an initial period of storage control followed by a period of linear flow. As a result on a typical log-log type curve an initial line of unit slope followed by a second straight line of slope equal to half unit can be observed. They also stated that the half slope would occur whether the fracture orientation was horizontal, vertical or any other inclination.

In another study by Ramey and Gringarten (1975), wellbore storage effect in fractured wells of infinite conductivity fracture was considered. Ramey (1970) investigated wellbore storage effect on the early times pressure behaviour and as it can be seen from the graph below (*Figure 2-1*), plot of type curve and pressure build-up data shows data taken during the first 0.1 hour of build-up clearly form a line of unit slope indicating that wellbore storage is the controlling parameter. At about 0.25 hour, the build-up data form a line of half unit slope, representing a long period of linear flow.

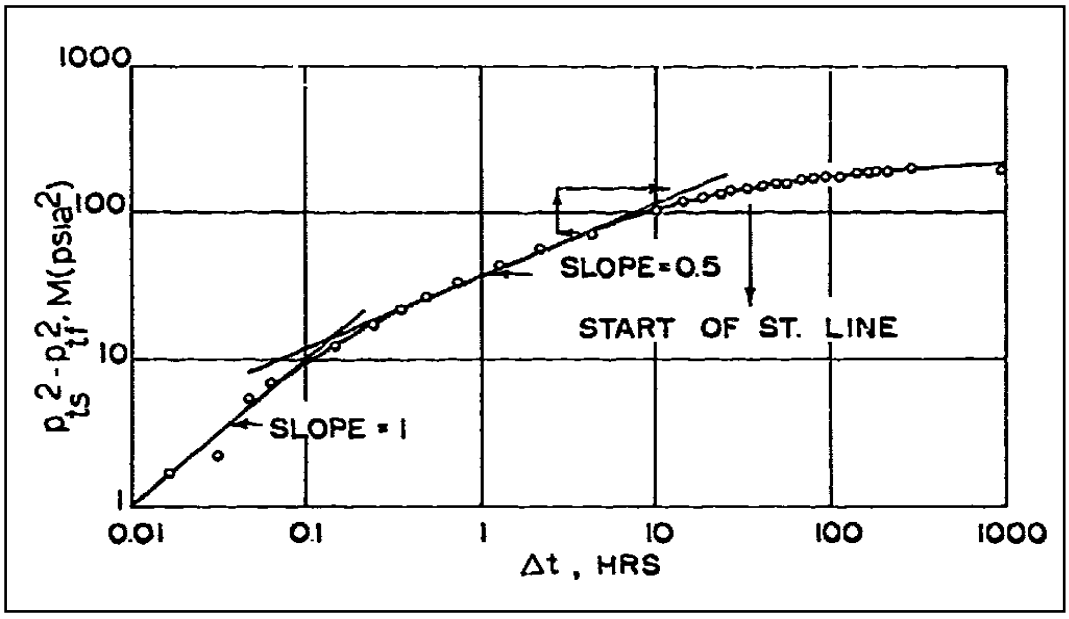


Figure 2- 1: Wellbore storage effect on fractured well flow behaviour (Ramey, 1970)

In a similar study, Raghavan (1976) investigated new solutions for the effects of wellbore storage and skin on pressure behaviour of vertically fractured wells. He noted that occasionally, data could be interpreted incorrectly if these two factors are not taken into account and that analyses of pressure transient data in vertically fractured systems are subject to distortion by wellbore storage and skin effects. He also stated that initially a short unit slope line representing wellbore storage effect is observed followed by a half unit slope indicating linear flow behaviour.

The wellbore storage coefficient, C defines the rate of pressure change during the wellbore storage flow regime. It is defined as the volume of fluid that the wellbore itself can produce due to unit drop of pressure. For a well full of a single phase fluid, wellbore storage is represented by a compressibility term. During the wellbore storage regime, the pressure change ΔP and the pressure derivative $\Delta P'$ are identical and follow a single

straight line of slope equal to unity on log-log scale as mentioned above. The relationship below describes the storage coefficient in the case of completely oil-filled well as introduced by Everdingen and Hurst (1949):

$$C = -\frac{\Delta V}{\Delta p} = c_w V_w \tag{1.1}$$

where:

C wellbore storage coefficient, bbl/psi

ΔV change in volume of fluid in the wellbore at wellbore condition, bbl

ΔP change in bottom-hole pressure, psi

V_w wellbore volume, bbl

c_w the liquid compressibility, psi^{-1}

When the relationship between $\Delta P = \rho g \Delta h$ and $\Delta V = Vu \Delta h$ does not change during the test, the wellbore storage coefficient is constant and can be estimated from the well completion design. Equation below describes the storage coefficient for well with changing fluid level as presented by Earlougher (1977):

$$C = 144 \frac{V_u}{\rho (g / g_c)} \tag{1.2}$$

where:

ρ liquid density, lb/ft3

g/gc gravitational acceleration, lbf/lbm

Vu wellbore volume per unit length, bbl/ft

The dimensionless wellbore storage coefficient is defined by Agarwal *et al.* (1970) as:

$$C_D = \frac{0.8936C}{\phi h c_t r_w^2} \tag{1.3a}$$

Ramey and Gringarten (1975) defined dimensionless wellbore storage coefficient for fractured well as:

$$C_{Df} = \frac{0.8936C}{\phi h c_t x_f^2} \tag{1.3b}$$

Where, C is the wellbore storage constant. During the wellbore storage flow period, the well is acting as a closed volume system, with a constant surface rate condition and the pressure changes linearly with time. The wellbore storage coefficient can be estimated on

a Cartesian scale plot of the pressure change (Δp) versus the elapsed time (Δt). At early time, the response follows a straight line of slope $m_{(WBS)}$, intercepting the origin and pressure changes versus elapsed time as defined below by Everdingen and Hurst (1949):

$$\Delta p = \frac{\Delta qB}{24C}\Delta t \tag{1.4}$$

The wellbore storage coefficient, C is estimated from the straight-line slope, m:

$$C = \frac{\Delta qB}{24m_{(WBS)}} \qquad (Oil\ and\ water) \tag{1.5}$$

$$C = 2348\frac{\Delta qT}{\mu m_{(WBS)}} \qquad (Gas) \tag{1.6}$$

In practice, wellbore storage is short-lived in fractured wells, and frequently is not observed on the recorded data. The response starts to follows the half unit slope infinite conductivity fracture or quarter slope finite conductivity fracture at early time according to Cinco-Ley and Samaniego, (1977). Wellbore storage effect may be present with infinite conductivity fracture response and it is indicated by a deviation below the half unit slope line, before linear flow becomes evident at early time. The next feature on the pressure transient response would be the skin, which can be either positive or negative and the following section will discusses this effect in more detail. Figure (2-2) below shows wellbore storage and skin effects for damaged homogenous reservoir.

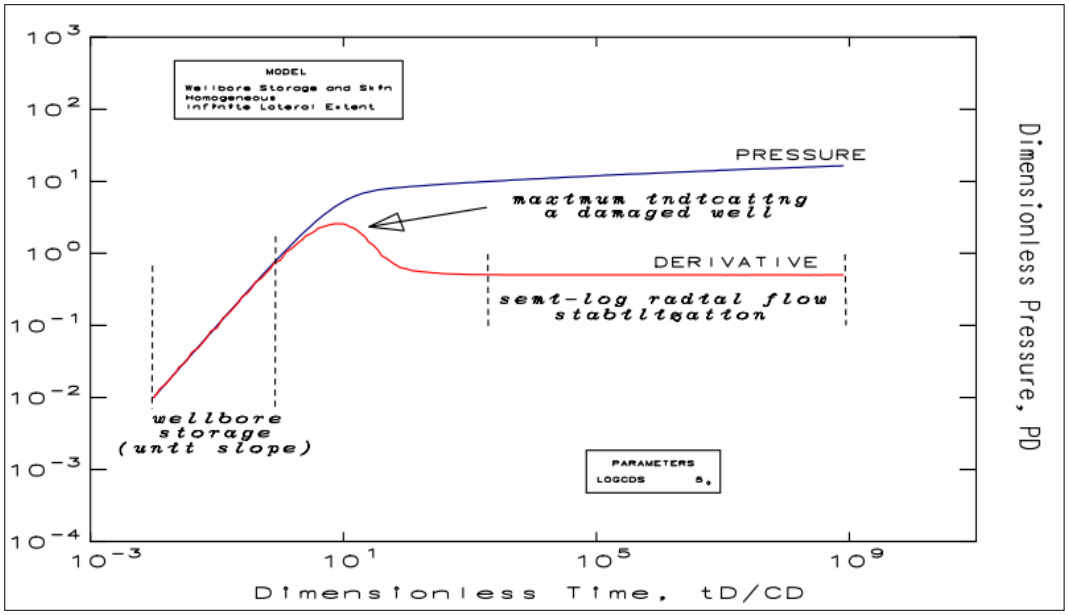


Figure 2- 2: Wellbore storage and skin features on log-log plot (Gringarten, 2002)

2.3 Skin

The skin effect represents the degree of damage caused to the immediate vicinity of the wellbore as a result of mud filtrate, drilling, cementing and work over processes. This effect can also be the result of flow convergence near the wellbore, viscous-inertial flow velocity and the blocking of fractures and pores damages that occur during the drilling and completion operations. The damaged zone has a reduced permeability, k_s from that of the formation permeability, k. The altered permeability around the well will cause significant pressure drop in the case of damage well or pressure enhanced in the case of stimulated well.

The skin factor is a dimensionless term used to quantify the increase (damaged) or decrease (stimulated) in pressure drop required for a given flow rate into the wellbore according to Hurst (1953) and Van Everdingen (1953):

$$S = \frac{kh}{141.2\Delta qB\mu}\Delta P_{skin} \tag{1.7}$$

In the case of a damaged well, a flow restriction is present at the interface between the reservoir and the wellbore, producing an additional pressure drop ΔP_{skin} when the fluid enters the wellbore. For a stimulated well, the flowing condition is improved near the wellbore and the pressure decline is reduced in a cylindrical shape near a wellbore reservoir region. In either case, the resulting positive or negative skin can be expressed by the difference between the pressure profile corresponding to the original reservoir permeability, k and the actual pressure profile due to the modified reservoir permeability, k_s as expressed in the following relationship, according to Hawkins (1956):

$$P_{w,S} - P_{w,S=0} = \frac{141.2\Delta qB\mu}{k_s h}\ln\frac{r_s}{r_w} - \frac{141.2\Delta qB\mu}{kh}\ln\frac{r_s}{r_w} \tag{1.8}$$

The skin value can be calculated from the Horner (1951) solution for pressure build-up (BU):

$$S = 1.151\left[\frac{P_{1hr} - P_{wf}}{m} - \log\left(\frac{kt_p}{(t_p+1)\phi\mu c_t r_w^2}\right) + 3.23\right] \tag{1.9}$$

where:

s skin factor, dimensionless

$1hr$ shut-in time, hr

P_{1hr} pressure intercept of semi-log straight line at a shut-in time of 1 hour, psi

P_{wf} measured wellbore flowing pressure prior to shut-in, psi

μ viscosity at reservoir conditions, cp

m slope of the semi-log straight line, psi/cycle

k permeability, mD

φ porosity, fraction

c_t total compressibility, psi^{-1}

r_w wellbore radius, fee

It is worth noting that the source of the damage caused to the wellbore can be related to:

- Sand control treatment
- Wettability changes as a result of fluid injection and drilling mud.
- Plugging by solid particles due to fluid injection
- Bacteria
- Cementing and Perforating damage
- Improper selection of drilling fluid
- Fines migration into the well bore
- Emulsion
- Swelling clays causing near-wellbore permeability reduction in the reservoir
- Scales due to presence of water

Skin due to formation damage, S_d is part of total skin, which can be removed by stimulations measures. Well stimulation is a procedure to increase well productivity by increasing effective wellbore radius; increasing permeability-thickness, kh value and reducing skin in the vicinity of the wellbore. The total skin factor, S is dimensionless parameter used to describe non-ideal near wellbore conditions due to formation damage and the main components according to Kabir (2009) are:

$$S_{total} = S_{perf.} + S_{dam} + S_{dev.} + S_{turb.} + S_{stim} + S_{gravel} + S_{fiss+} S_{temp.}$$

where:

$S_{perf.}$: skin as a result of perforation

$S_{dam::}$ skin caused by damage

$S_{dev.}$: skin due to well deviation

$S_{turb.:}$ skin resulting from turbulence flow (rate dependant skin)

$S_{stim.:}$ skin caused by well stimulation

$S_{gravel:}$ skin as a result of gravel packs installation

$S_{fiss:}$ skin due to fissures

Assuming the skin region has a finite radius of r_s with a skin zone permeability of k_s then the skin can be calculated from the Hawkins (1956) equation as described below:

$$S = \left(\frac{k}{ks} - 1 \right) \ln \frac{r_s}{r_w} \qquad (1.10)$$

Based on the relationship above and depending on the permeability ratio k/k_s and assume $\ln (r_s/r_w)$ value is positive; three possible cases in evaluating the skin factor (*Figure 2-3*):

I) Positive skin factor, when the damaged zone near the wellbore exists, k_s is less than k and S is a positive number. The magnitude of the skin factor increases as k_s decreases and as the depth of the damage r_s increases. Positive skin values may range between +5 for mechanical skin and up to +300 in the case of partial penetration completion (Gringarten, 2002).

II) Negative skin factor occurs when the permeability around the well k_s is higher than that of the formation k. This negative factor indicates an improvement of wellbore ability to flow. A negative value of -4 to -5.5 usually indicates a hydraulically fractured completion, whereas a negative value of -1 to -4 is typically expected from an acid stimulation job.

III) Zero skin factor occurs when no change in the permeability around the wellbore is observed when. k_s is equal to k.

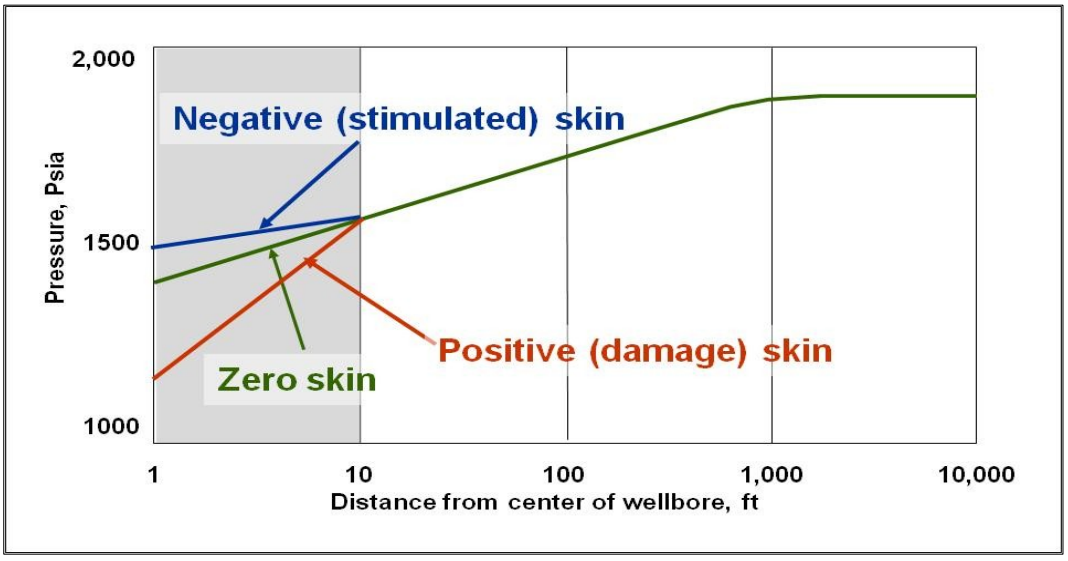


Figure 2- 3: Pressure profiles for damaged and stimulated well

Prats (1960) considered the skin factor as effective wellbore radius, which is the smallest radius the well appears to have due to the reduction in flow caused by the skin effect. The effective wellbore radius can be calculated from the following relationship:

$$r_{we} = r_w e^{-s} = x_f / 2 \tag{1.11}$$

In an artificially fractured well, two types of skin are recognised (*Figure 2-4*): fracture face skin (S_{ff}) and choked fracture (S_{fc}) as stated by Cinco-Ley and Samaniego (1977). Both types of damage can be calculated through:

$$S_{ff} = \frac{\pi w_s}{2x_f}\left(\frac{k}{k_s} - 1\right) \tag{1.12-a}$$

$$S_{fc} = \frac{\pi x_{ck}}{x_f}\left(\frac{k}{k_{fc}} - \frac{k}{k_f}\right) \tag{1.12-b}$$

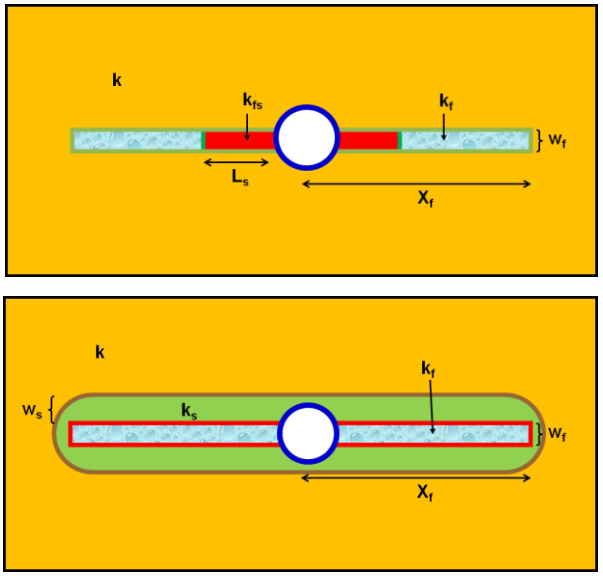


Figure 2- 4: Fracture choke damage (top) and face skin (below)

where:

S_{ff} fracture face skin

S_{fc} choked fracture skin

k formation permeability, mD

k_f fracture permeability, mD

k_s damage zone permeability, mD

k_{fc} choked fracture permeability, mD

x_f fracture half-length, ft

x_{ck} choked fracture length, ft

w_s damage extent, ft

Fracture face skin is due to reservoir permeability alteration along the fracture face surface and fracture choke referring to as reduction of fracture proppant pack conductivity within the fracture close to the wellbore. The former skin can be caused as a result of: fluid leak-off when damage extend deep into the formation particularly in high permeability reservoirs; saturation changes; clay swelling or fines migration; capillary pressure changes and pore throat blocking in the case of high permeability formations as presented by Holditch (1979), Iqbal *et al.* (1993), and Xinghui and Civan (1994).

The latter skin is caused as a result of proppant crushing, polymer damage; proppant over-displacement; formation fines migration into the fracture, fracture fluid residue or unbroken fracture fluid within the fracture and reduced fracture conductivity due to non-Darcy effect in gas reservoirs as stated by Holditch and Morse (1976), Bennett et al. (1983) and Azari *et al.* (1991).

Several workers investigated fracture damage to better understand well productivity impairment at the fracture face and within the fracture, Raghavan *et al.* (1972), Cinco-Ley and Samaniego (1977), Holditch (1979), Cinco-Ley and Samaniego (1981), Brannon and Pulsinelli (1990), Adegbola and Boney (2002), Romero *et al.* (2002). Fracture fluid leak-off effect and the clean-up process were examined in number of publications, Tannich (1975), Holditch *et al*. (1981), Johansen (1988), Robinson *et al*. (1988), Berthelot *et al*. (1990), Yizhu and Lee (1993), Voneiff *et al*. (1996) and Gdanski *et al.* (2006).

In addition, post-frac flow behaviour problems and calculated fracture properties were studied by Lee and Holditch and Gist (1981), Wong *et al*. (1986) , Elbel and Ayoub (1992), Davidson *et al*. (1994) and Rahim *et al*. (1995), Cipolla and Mayerhofer (1998), Alvarez *et al*. (2002), Barre *et al*. (2003), Lolon *et al.* (2003), Siddiqui *et al*. (2004), Davidson *et al*. (1994), Mathur *et al.* (1995) and Rahim *et al*. (1995).

Based on the literature review, in order to understand unusual fractured well flow behaviour, there are a number of considerations. For instance, has the fracture targeted the formation interval of interest? Is the induced fracture conductive enough? How damaged is the created fracture? How long is the actual induced fracture? What was the purpose of the frac job? Has the designed frac job achieved its goals? It is important to answer all the above questions when analysing post-frac well test data.

2.4 Fractured Well Flow Patterns

The interpretation of well test data from a stimulated well require clear understanding of different flow periods that are observed on the diagnostic log-log plot. Pressure transient analysis of fractured wells include identification of three flow periods, which are linear flow representing infinite facture conductivity for fractures with negligible pressure drawdown within the fracture and bilinear flow with finite conductivity fracture (linear flow from the formation into the fracture and linear flow within the fracture). The third main flow period that can be noticed in a fractured well is pseudo-radial flow.

It is reported that analysing pressure transient for a fractured well with finite conductivity fracture will reveal four distinctive flow periods as stated by Cinco-Ley *et al.* (1978). Initially, flow period of linear characteristic representing fracture flow followed by bilinear flow when linear from the formation into the fracture and linear flow within the fracture occur at the same time.

This will be followed by linear flow from the formation feeding the fracture before approaching pseudo radial flow. However, the second bilinear flow period will not be present for fractures with high conductivities. The schematics below (*Figure 2-5*) demonstrate various flow regimes associated with a fractured well depending on the conductivity of the induced fracture.

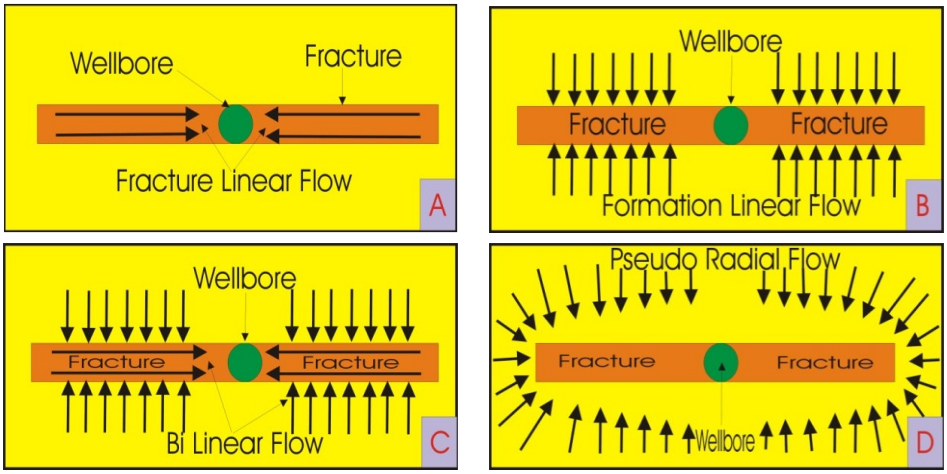


Figure 2- 5: Fracture flow patterns:
A) Linear flow within the fracture
B) Linear flow from the formation into the fracture
C) Bilinear flow within the fracture and formation fluid flow into the fracture
D) Pseudo radial flow

2.4.1 Linear Flow - Infinite Conductivity Fracture

The induced infinite conductive fracture is characterised by a very high conductivity, $k_f w_f$ path. It is assumed that the flow into the wellbore is only through the fracture and exhibits three flow periods namely: fracture linear flow period, formation linear flow period and infinite acting pseudo radial flow period. In this type of fracture, it is assumed that the fracture is symmetrical on both sides of the well and it intercepts the complete formation thickness and that the fluid flows along the fracture without any pressure drop.

It is the first flow regime which occurs in a fractured well system. Most of the fluid enters the wellbore during this period by fluid expansion within the fracture. It is assumed there is negligible fluid coming from the formation. Flow within the fracture and from the fracture to the wellbore during this time period can be described by the diffusivity equation as expressed in a linear form and is applied to both the fracture linear flow and formation linear flow periods similarly.

At early time, the flow lines are perpendicular to the fracture plane. Then, the formation surrounding the two ends of the fracture starts to contribute significantly to the flow. At this time the linear flow regime ends, and the flow will change into pseudo-radial regime. The well response demonstrates the characteristic of radial flow regime behaviour towards the late time period.

Clark (1968) stated that during linear flow, the pressure change is proportional to the square root of the elapsed time and pressure change and the derivative are both proportional to $\sqrt{\Delta t}$ on log-log scale. According to Alagoa *et al*. (1985), both pressure and derivative follow straight lines of half slope and the level of the derivative half-unit slope line is half that of the pressure, the following equations illustrates such relationship:

$$\Delta p = 4.06 \frac{\Delta q B}{k x_f} \sqrt{\frac{\mu}{\phi c_t k}} \sqrt{\Delta t} \tag{1.13}$$

The fracture half-length, x_f is calculated from:

$$x_f = 4.06 \frac{\Delta q B}{h m_{HKF}} \sqrt{\frac{\mu}{\phi c_t k}} \tag{1.14}$$

2.4.2 Bilinear Flow - Finite Conductivity Fracture

This was first developed by Cinco-Ley *et al.* (1978) and was considered as one of the crucial concepts in analysing fractured well test analysis. During this flow period the pressure drop within the fracture cannot be neglected. This happens when the linear flow from the formation into the fracture and linear flow through the fracture occur at the same time before the fluid starts to flow through the tip of the fracture when the effect of pseudo radial flow occurs. This flow pattern can be observed as quarter slope on the log-log plot of the pressure change versus elapsed time.

The bilinear flow pattern may occur for instance when the permeability of the fracture is not very high relative to the formation permeability. The duration of this flow pattern period depends on the dimensionless fracture conductivity (*FcD*), the dimensionless wellbore storage coefficient (C_D), the dimensionless fracture storage capacity (C_{Df}) and presence of non-Darcy effect in fractured gas and gas-condensate wells.

In the bilinear flow case, the fracture permeability, k_f is reduced as compared to that of the infinite conductivity fractures case. The finite conductivity vertical fracture exhibits a unique pressure response that can be distinguished from infinite conductivity fracture behaviour. The transient pressure behaviour for this system may include the following different flow regimes: initially linear flow within the fracture followed by bilinear flow then linear flow in the formation and finally infinite acting pseudo radial flow. It is worth noting that the duration of each of these flow periods may vary and might not comprise a complete test.

In bilinear flow regime system, the pressure change is proportional to the fourth root of the elapsed time ($\sqrt[4]{\Delta t}$). During bilinear flow geometry, both pressure and derivative responses are proportional to $(\Delta t)^{1/4}$. A log-log straight line of quarter slope can be established on the pressure and derivative curves and the derivative line is four times lower. The following relationship below explains such flow behaviour:

$$\Delta p = 44.11 \frac{\Delta q B \mu}{h\sqrt{k_f w_f}\sqrt[4]{\phi \mu c_t k}} \sqrt[4]{\Delta t} \tag{1.15}$$

Fracture conductivity, $k_f w_f$ can be calculated from:

$$k_f w_f = 1944.8 \left(\frac{\Delta q B \mu}{h m_{LKF}} \right)^2 \frac{1}{\sqrt{\phi \mu c_t k}} \tag{1.16}$$

2.4.3 Pseudo Radial Flow

After linear or bilinear flow depending on the induced fracture conductivity, the pressure response exhibits a pseudo-radial flow feature that displays the usual semi-log straight line behaviour. In addition, during this flow period the flow lines to the fracture are not radial, and this regime is affected by the near fracture tip condition. It is worth noting that the formation permeability thickness, kh product can be calculated from this flow period.

In addition, it is common practice in well test analysis to use general solutions in dimensionless terms that can be used for any studied well test problem. The following dimensionless pressure and time terms are used in this study and are defined as:

$$p_D = \frac{kh}{141.2\Delta qB\mu}\Delta p \tag{1.17}$$

$$t_D = \frac{0.000264k}{\phi\mu c_t r_w^2}\Delta t \tag{1.18}$$

Gringarten *et al.* (1975) proposed using a dimensionless time group defined as:

$$\frac{t_D}{C_D} = 0.000295\frac{kh}{\mu}\frac{\Delta t}{C} \tag{1.19}$$

Earlougher and Kersch (1974) proposed a new term called $C_D e^{2S}$ to describe the well condition and it ranges from 0.5 for a stimulated well and up to 1060 for a very damaged well. A series of type curves were generated that are still implemented in most well test software packages.

$$C_D e^{2S} = \frac{0.8936C}{\phi c_t h r_w^2} e^{2S} \tag{1.20}$$

In hydraulically fractured wells the following dimensionless variables are implemented:

$$t_{D_f} = \frac{0.000264k}{\phi\mu c_t x_f^2}\Delta t \tag{1.21}$$

$$p_D = \left(\pi t_{Df}\right)^{1/2} \quad Infinite\ Conductivity\ Fracture \tag{1.22}$$

$$p_D = \frac{2.451}{\sqrt{k_{fD}w_{fD}}} t_{Dx_f}{}^{1/4} Finite\ Conductivity\ Fracture \tag{1.23}$$

$$k_{fD} = \frac{k_f}{k} \tag{1.24}$$

$$w_{fD} = \frac{w_f}{x_f} \tag{1.25}$$

By combining two terms above 1.24 and 1.25, the dimensionless fracture conductivity, *FcD* term as introduced by Cinco-Ley *et al.* (1978) which will be referred to in this study:

$$FcD = \frac{k_f w_f}{k x_f} \tag{1.26a}$$

Bennett *et al.* (1983) introduced above term as:

$$k_{fD} w_{fD} = \frac{k_f w_f}{k x_f} \tag{1.26b}$$

where:

k_f fracture permeability, mD

w_f fracture width, inch

k formation permeability, mD

x_f fracture half-length, ft

Based on the above relationship, the dimensionless fracture conductivity is directly proportional to the fracture conductivity and inversely proportional to the reservoir permeability and fracture half-length. Also, small *FcD* will be obtained with high formation permeability or longer fracture length and vice versa.

As it can be noticed from the above formula, the *FcD* value is controlled by fracture permeability and half-length parameters. It is known that *FcD* value will determine the type of the conductive fracture obtained as result of stimulation process performed on the well. For instance, high dimensionless fracture conductivity indicates presence of linear flow with no pressure drop within the fracture. On the other hand, low values of *FcD* represent bilinear flow indicating of some pressure drop within the fracture that cannot be neglected.

Agarwal *et al.* (1979) used analytical approach and stated that the dimensionless fracture conductivity, *FcD* value for finite conductivity fracture is equal to 500 and any value higher than that indicates infinite conductivity fracture. However, Cinco-Ley *et al.* (1978) in similar approach showed that *FcD* value of 300 is the limit for bilinear flow to occur before it changes to linear flow behaviour. In this study both statements were verified numerically and found that not much difference between them. However, from a practical point of view, it is stated in the literature that *FcD* value of 1.6 can be considered as the limit representing finite conductive fracture according to Valko *et al.* (1998).

2.5 Research Problem Review

The investigated problem in this study had been referred to briefly in a few publications with no clear understanding of causes of the infrequently observed fracture flow behaviour in some post-frac tests. Some studies related the behaviour to fractures of short lengths and low conductivities, Goodin (1991) and Azari *et al.* (1992). Others have suggested that the problem occurs when resin-coated proppant, *RCP* is used in stimulating gas wells, e.g. Al-Ghurairi *et al*. (2006) and Duverney *et al.* (2007). A few workers suggested that fracture damage was the cause for the unusual behaviour such as Elbel and Ayoub (1992) and Garzon *et al.* (2008). In this study, causes of fractured wells exhibiting unusual flow behaviour is investigated in detail, below is a brief review of all publications on the problem.

Robinson *et al.* (1991) presented the first field case showing distinctive feature of fractured wells in post-frac well test. The fractures were designed with short half-lengths to overcome skin effect and improve well productivity. The objective of well stimulation work was to achieve relatively short fracture length (x_f < 20ft) to improve near wellbore damage (skin frac). As it can be noticed from the rate normalised plot below (*Figure 2-6*), early time pressure responses for pre/post-frac cases are identical with dominant WBS effect and some reduction of skin as a result of well stimulation. The study conclusion indicates that the problem is likely to be associated with short induced fractures.

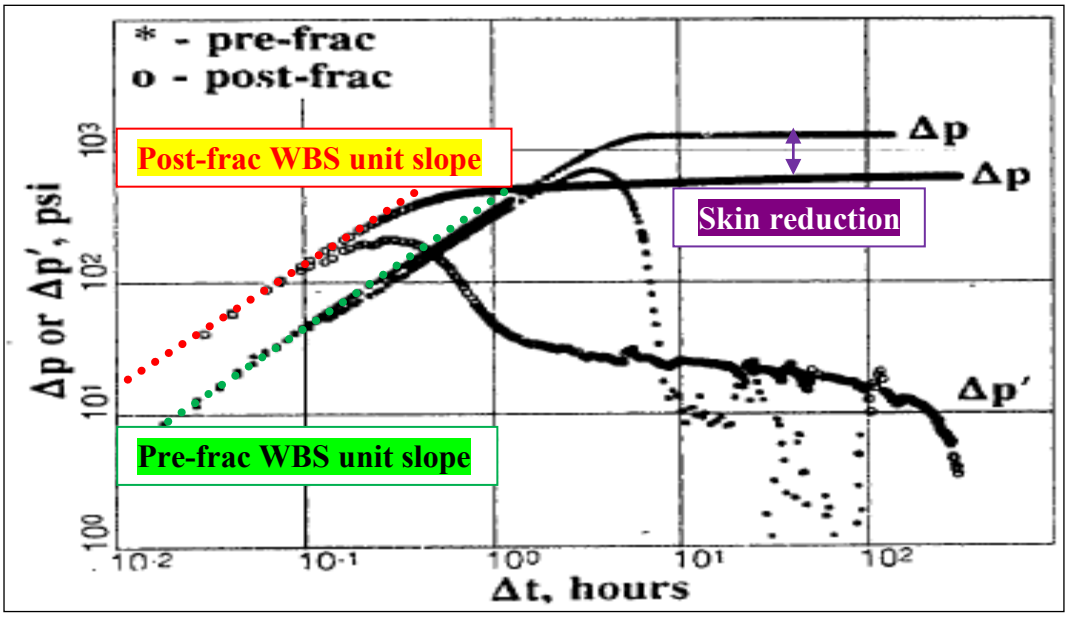


Figure 2- 6: Field case with similar pre and post-frac behaviours (Robinson *et al*. 1991)

Goodin (1991) presented the problem when analysed pressure transient of stimulated well onshore oil field in New Zealand. The well was hydraulically fractured to improve its productivity through reduction of skin effect. A short fracture treatment was designed to overcome near wellbore damage and improve well performance. The post-frac well test interpreted with wellbore storage followed by a radial flow model instead of a typical fractured well flow at early time. The paper showed clearly that the behaviour is associated with fractures of short lengths.

Azari *et al.* (1992) introduced type curves to compute wellbore storage, fracture conductivity, fracture half-length and formation permeability using analytical model. Some field and generic examples were included in their paper and stated that using type curve analysis based on radial flow assumption results in relatively accurate estimation of formation permeability but fracture half-length and conductivity parameters calculation will be associated with errors. They also stated that the problem is related to fractures of low conductivities ($FcD < 0.1$).

Elbel and Ayoub (1992) presented pressure transient analysis of post-frac tests of some cases with short, ineffective fracture treatment. Their study results suggested that inconsistency in induced fracture length compared to the designed length is due to damaged proppant permeability, incomplete proppant height and settling. The study introduced a number of single layer and multi-layer field examples with pressure behaviour features similar to the investigated problem in the current study.

Other workers, Chu and Shank (1993), investigated the effect of short length induced fractures within the radial composite region around the fracture and wellbore. Induced fractures that extend beyond the damaged radial zone surrounding the wellbore were examined by Chen and Raghavan (1995). It is worth noting that in all these studies relatively short fracture lengths were considered (typically tens of feet). Hence, there is clearly indication the relationship between short length fractures and occurrence of the behaviour.

Hunt *et al.* (1994) and Al-Haddad *et al.* (1994) investigated pressure behaviour of proppant fractured wells in high permeability reservoirs and presented some results indicating similar pressure behaviour to the investigated problem. They considered effects of parameters such as permeability, skin, fracture length, conductivity and damage

in their study. They concluded that fracture damage is due to fracture fluid leak-off into the formation. To model this type of damage they assumed a composite radial region of altered permeability around the fracture.

Yadavalli *et al.* (1996) studied fractured gas-condensate wells, which exhibit unusual behaviour using compositional simulation model. They demonstrated that production impairment from hydraulically fractured wells is due to condensate banking in the vicinity of the wellbore. They presented a classification of two types of reservoirs: one with small condensate bank and another with large bank effect. Both these exhibit two distinctive early time pressure features for a fractured well. However, their study did not consider critical factors such as the non-Darcy effect within the reservoir. More importantly, wellbore storage and capillary number dependant relative permeability in the fracture were not considered, which indicates the limitations of the study.

Chu (1996) investigated fractured wells in high permeability oil reservoirs and demonstrated that with short fracture lengths only the skin value will be reduced as a result of stimulation and that well pressure profile for a fractured will be identical to that of non-fractured well behaviour. The paper showed the effect of low fracture conductivity on benefits achieved from stimulation high permeability formations (*Figure 2-7*).

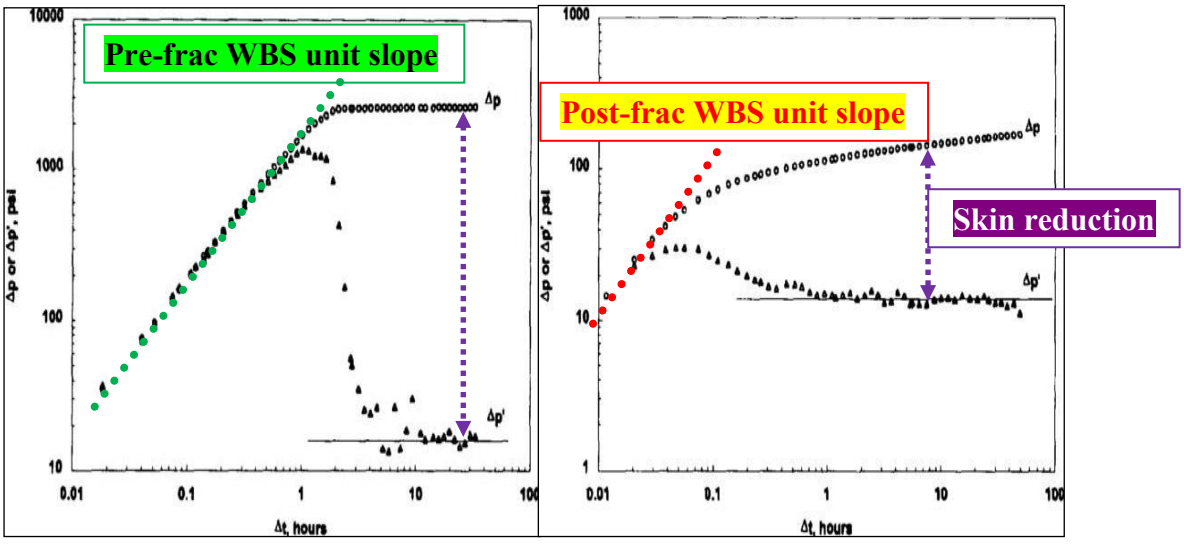


Figure 2- 7: Pre and post-frac identical flow behaviours (Chu, 1996)

Ning *et al.* (1996) investigated re-fracturing oil wells in high permeability reservoirs in the Valhalla Field, Alberta. The objective of the well stimulation was to bypass the near wellbore damage and enhance well productivity. The initial induced fracture length was

relatively short but following re-fracturing process, an estimated longer fracture length was obtained based on the simulated model results. Bertram *et al.* (1997) studied a similar problem using compositional modelling. Their study results were associated with discrepancy and proposed additional future work to achieve a better understanding of physical phenomenon associated with stimulating gas-condensate wells.

Settari *et al.* (2000) examined hydraulic fracturing application in high permeability gas reservoirs to investigate the non-Darcy effect in both fracture and formation on well performance. They introduced various correlations between fracture half-lengths and the calculated non-Darcy values. The objective of the study was to predict well productivity in high permeability formations considering turbulence flow effect. Results indicated that the investigated problem is more likely to occur in fractured wells of short lengths.

Skaar *et al.* (2000) investigated well performance in two gas-condensate fields using single well simulation model to match actual data. Results showed good agreement between numerical and analytical interpreted data. The range of fracture half-length used in the study was varied from 15ft to 100ft and *FcD* from 0.5 to 3. By examining the presented plots, it can be concluded that the investigated behaviour is similar to the current study problem, which is due to short fracture length.

In a another approach, Al-Ghurairi *et al*. (2006) and Duverney *et al.* (2007) related the causes of the investigated problem to occur to resin-coated proppant, *RCP* used in fracturing gas wells. The material is used as inhibiter of formation fines flow back during post-frac and clean-up process. They presented some field examples to demonstrate their findings. However, it is not possible to verify their results in this study due to limited resources.

Economides *et al.* (2007) presented pressure transient analyses of hydraulically fractured wells in the Gulf of Mexico. Similar pressure behaviour to this study was presented in their work. The deep-water oil well was stimulated and the well test analysis of the post-frac test indicated no fracture flow pattern presence at early time. Their interpretation for the unusual behaviour was due to short length fractures.

Shaoul *et al.* (2007) presented field example of a tight, gas-condensate reservoir following a frac job in India. The illustrated fracture flow behaviour in the paper is similar to the

non-stimulated well flow behaviour that is investigated in the current study. However, the authors did not explain what caused the behaviour and why they were unable to match typical linear or bilinear fracture flow behaviour on log- log pressure versus elapsed time diagnostic plot.

Garzon *et al.* (2008) investigated fracture flow behaviour and stated that the cause of the problem is related to improperly performed frac jobs. Their interpretation of the behaviour was attributed to damage within the fracture near the wellbore that prevents fracture flow into the wellbore. The transient pressure behaviour from pre-frac and post-frac tests showed two distinctive features not only at early times but also at late times (*Figure 2-8*).

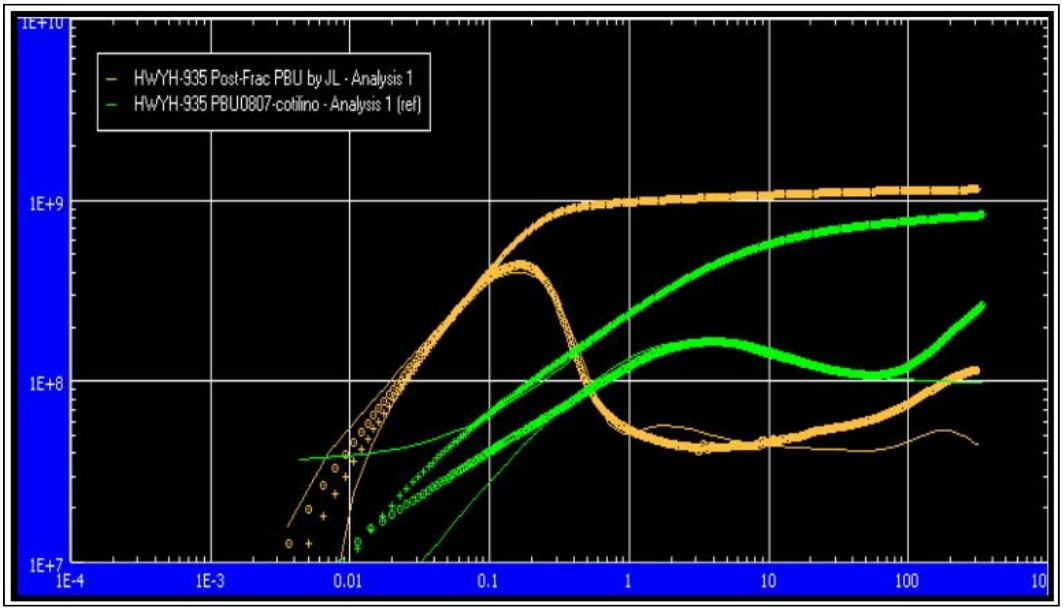


Figure 2- 8: Log –log plot of pre-frac (yellow) and post-frac (green) infrequent behaviour

It is notable that fracture damage is considered one of the prime causes for the investigated problem. Many workers investigated various problems associated with fractures including fracture face skin and choke damage including Creamer (2005), Mayerhofer *et al.* (2005), Akram, A.H, and Samad, A. (2006), Zillur, R. and Ismail B., (2006), Liu *et al.* (2006), Sanchez *et al.,* (2007). Yatindra, B. (2008), Al-Naimi *et al.* (2009) and Heydarabadi *et al.* (2010).

Figure (*2-9*) below presents multi-frac well test result for a stimulated oil well onshore Kazakhstan. The post-frac test results indicate no fractured well flow feature, with a clear reduction in the skin value in the second post-frac test and significant improvement of formation permeability-thickness value.

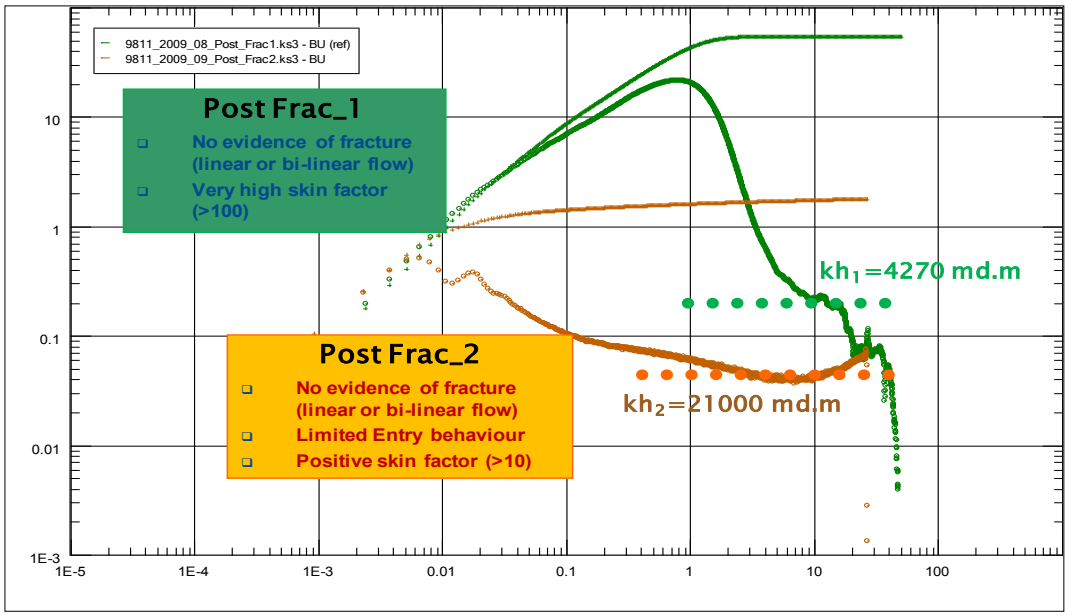


Figure 2- 9: Unusual flow behaviour of a stimulated well with improved skin and kh

2.6 Conclusions

The reviewed publications in the above section represent the most up to date, published work relevant to this research problem. The control parameters are fracture length, fracture conductivity, fracture damage and non-Darcy effect of the pressure response in the case of fractured gas wells.

Based on the literature review, the investigated unusual fractured well flow behaviour is more likely to be associated with short length fractures and low conductivity fractures relative to the formation conductivity. Damaged fractures including choked fracture and less importantly face skin may also impacts the pressure data in post-frac tests. As part of the current study, many subsurface and fracture uncertainty parameters will be investigated.

Furthermore, many other factors will be considered with respect to their impact on developing unusual fracture flow behaviour. Sensitivity cases of different reservoir parameters and fracture configuration will be studied in addition to investigating fracture leak-off, unequal fracture half-length and many other effects, such as flow behaviour of fractured wells in naturally fractured reservoirs and effect of fluid richness in gas-condensate reservoirs.

CHAPTER III

FRACTURED WELL NUMERICAL MODELLING

3.1 Introduction

The simplest approach for modelling a fractured well is to mimic fracture with a modified negative skin or productivity index enhancement but none of these methods represent actual physics of fluid flow into and through the fracture. It is common practice to use a radial model in the reservoir simulation for numerically modelling of vertical non-fractured wells. The well is placed at the centre of the grid, and the radial grid mesh size typically increases logarithmically to give the optimal representation of the actual pressure distribution of the field in reality. However, the practical approach for modelling a fractured well is to represent the fracture explicitly as a plane of thin, high permeability grid cells in the simulation grid (*Figure 3-1*).

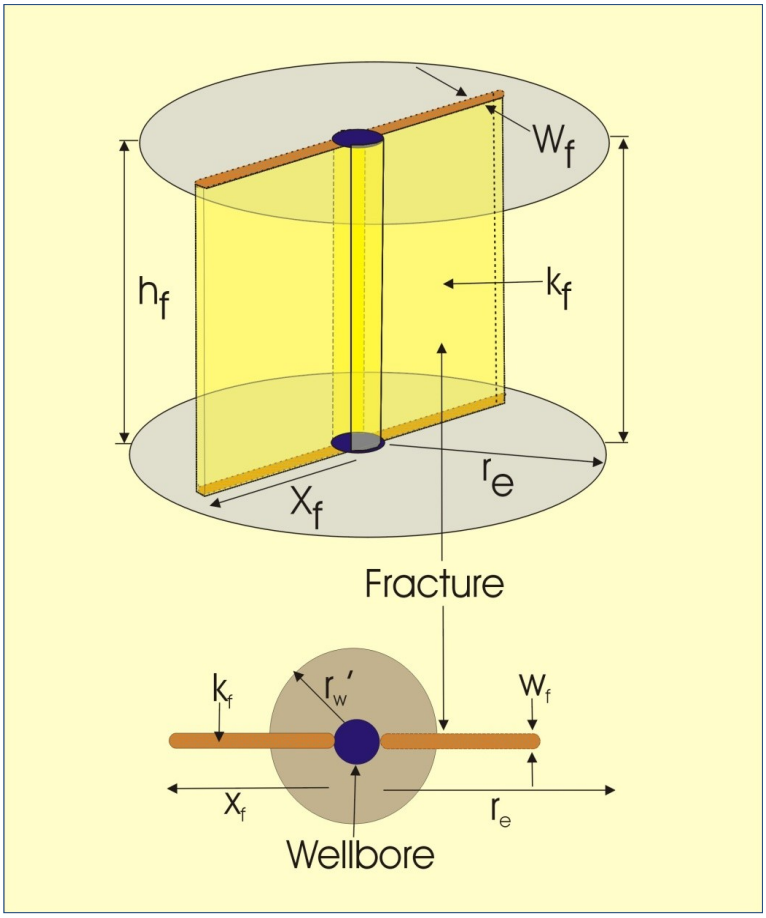


Figure 3- 1: Schematic of typical fractured well design and parameters

The synthetic fracture illustrated above consists of vertical fracture, which intersects the wellbore with equal fracture half-lengths, X_f. The fracture height (h_f) is assumed to be equal to the formation thickness and fracture width (w_f) is assumed to be constant and independent of the vertical ordinate. It is worth noting that fractures are characterized in terms of the dimensionless fracture conductivity, *FcD* value that measures the relative importance of pressure drops in the formation and the fracture. It is stated in the literature that large *FcD* values of 300 and 500 corresponds to an infinite conductivity fracture, where the pressure drop within the fracture can be neglected as proposed by Cinco-Ley and Samaniego (1978) and Agarwal *et al.* (1979) respectively.

3.2 Fracture Modelling

Modelling a fracture using Cartesian grid is more practical approach and provides closer representation of flow geometry than radial grid mesh. The problem associated with modelling a fracture as part of a radial grid is that cell widths increase with distance from the wellbore, which is not representative of actual fracture (*Figure 3-2*). Thus, it is more convenient from modelling point of view to implement the fracture plane into a Cartesian geometry grid where cells are specified by their lengths and widths.

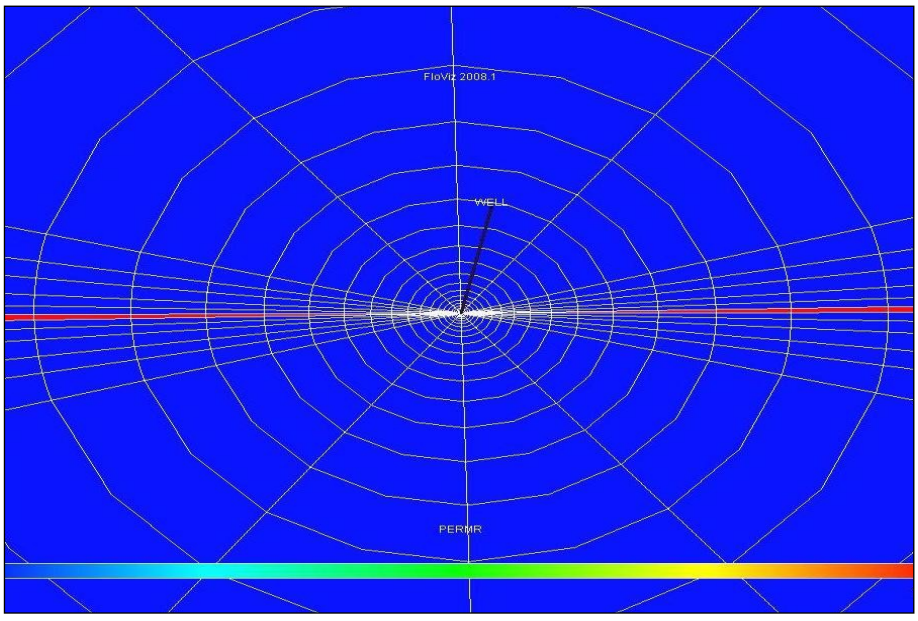


Figure 3- 2: Radial grid model for fracture modelling

In devising the Cartesian grid, a symmetric modelling approach is used to model quarter of the reservoir only. Local grid refinement "LGR" is implemented in the region of the fracture and its tip to capture the radial flow pattern at the tip of the fracture.

Also, fracture width is fixed in the simulation model, with a corresponding increase of the fracture permeability so that the conductivity (product of permeability and thickness) is preserved. Increasing the fracture width reduces the severity of the numerical problems and has minor effect on the results. Sensitivity cases run by Hegre (1996) and Kroemer *et al.* (1997) indicated that fracture width changes led to nearly identical results. However, it was possible to use actual fracture dimensions in the simulation model constructed in the current study.

Another important consideration is the grid around the fracture. If a vertical fracture is in the x-z plane, a fine grid is needed in the Y direction close to the fracture and this is how the fracture is modelled here. Near to the tip of the fracture, the flow will be cylindrical and a fine grid is also needed in the x direction. The fracture plane is parallel to the drainage boundary and the fracture is symmetric with respect to the wellbore. Consequently, one quarter of the system was modeled in this study (*Figure 3-3*).

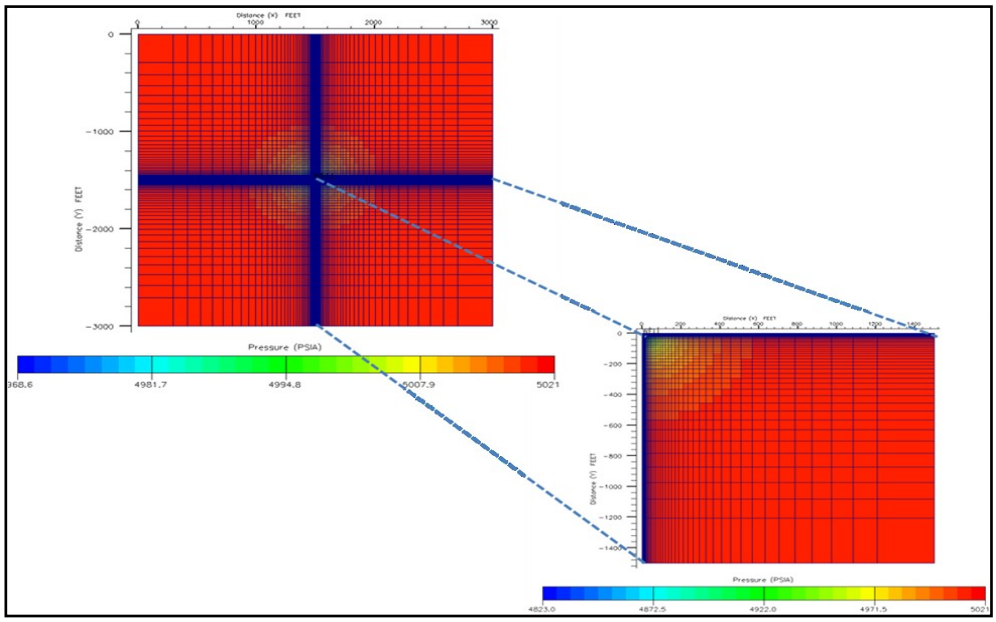
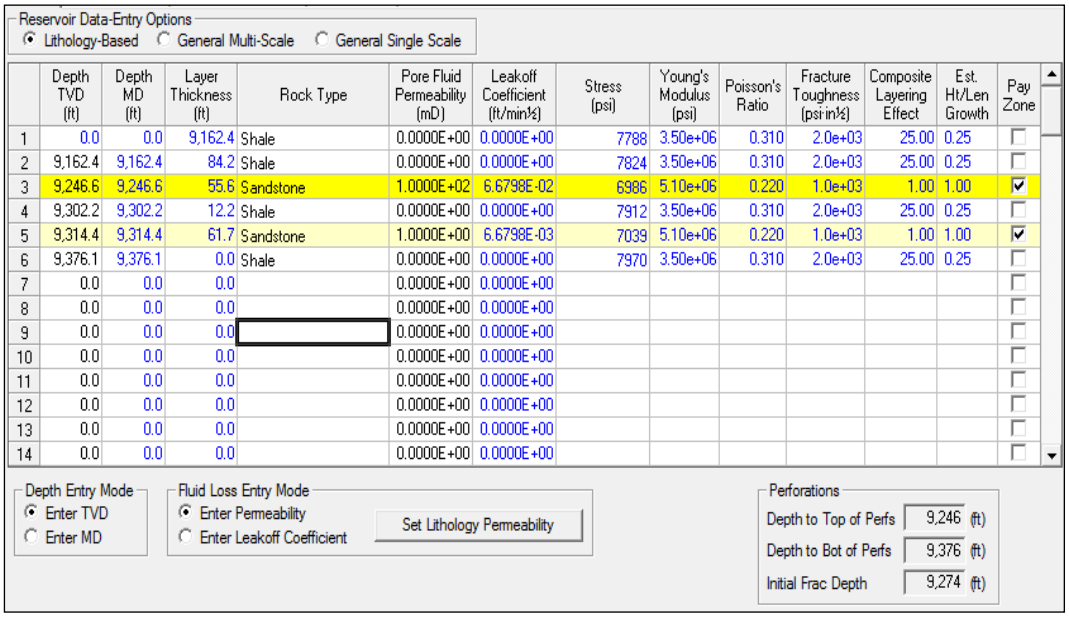


Figure 3- 3: Cartesian grid used for fracture modelling in the study

In addition, the grid blocks increase in size with increased distance from the fracture in both x and y directions and the minimum grid size are dependent on the induced fracture half-length, x_f. The grids in the z direction are based on reservoir layering, where in layers with higher thickness are subdivided into smaller grid sizes to achieve uniform grid blocks in the z direction. The fine grids of the fracture extends about 1.5 times along the fracture half-length in the x direction and 2 times in the direction normal to the fracture, y.

In order to compare fracture model used with the computer designed model, the leading industry fracturing analysis software FRAC PRO PT tool is used to generate realistic fractures that consider complex physical processes related to rock mechanics (*Figure 3-4*). The software is well known for hydraulic fracturing design and analysis. It is a product that utilises real data that enable user to build fracture models that include real reservoir properties pre and post-frac treatment. Figure (*3-5*) below shows two layers commingled case with designed fracture half-length of almost 300ft using the software. Results from fracture model in the study and computer built synthetic model were similar.



	Depth TVD (ft)	Depth MD (ft)	Layer Thickness (ft)	Rock Type	Pore Fluid Permeability (mD)	Leakoff Coefficient (ft/min½)	Stress (psi)	Young's Modulus (psi)	Poisson's Ratio	Fracture Toughness (psi·in½)	Composite Layering Effect	Est. Ht/Len Growth	Pay Zone
1	0.0	0.0	9,162.4	Shale	0.0000E+00	0.0000E+00	7788	3.50e+06	0.310	2.0e+03	25.00	0.25	☐
2	9,162.4	9,162.4	84.2	Shale	0.0000E+00	0.0000E+00	7824	3.50e+06	0.310	2.0e+03	25.00	0.25	☐
3	9,246.6	9,246.6	55.6	Sandstone	1.0000E+02	6.6798E-02	6986	5.10e+06	0.220	1.0e+03	1.00	1.00	☑
4	9,302.2	9,302.2	12.2	Shale	0.0000E+00	0.0000E+00	7912	3.50e+06	0.310	2.0e+03	25.00	0.25	☐
5	9,314.4	9,314.4	61.7	Sandstone	1.0000E+00	6.6798E-03	7039	5.10e+06	0.220	1.0e+03	1.00	1.00	☑
6	9,376.1	9,376.1	0.0	Shale	0.0000E+00	0.0000E+00	7970	3.50e+06	0.310	2.0e+03	25.00	0.25	☐
7	0.0	0.0	0.0		0.0000E+00	0.0000E+00							☐
8	0.0	0.0	0.0		0.0000E+00	0.0000E+00							☐
9	0.0	0.0	0.0		0.0000E+00	0.0000E+00							☐
10	0.0	0.0	0.0		0.0000E+00	0.0000E+00							☐
11	0.0	0.0	0.0		0.0000E+00	0.0000E+00							☐
12	0.0	0.0	0.0		0.0000E+00	0.0000E+00							☐
13	0.0	0.0	0.0		0.0000E+00	0.0000E+00							☐
14	0.0	0.0	0.0		0.0000E+00	0.0000E+00							☐

Figure 3- 4: Reservoir properties input into FracProPT fracture design

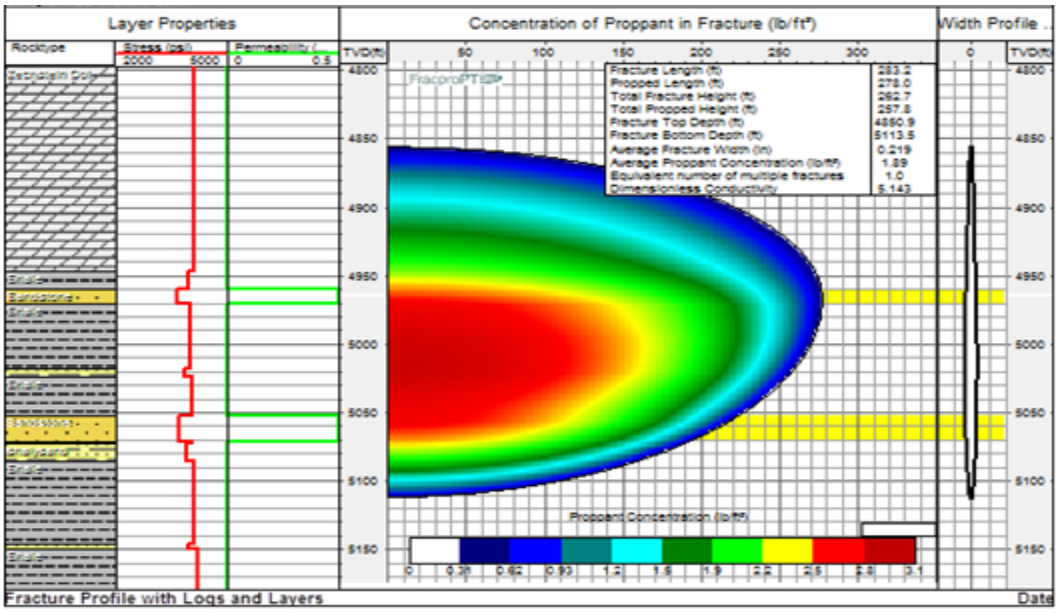


Figure 3- 5: Induced fracture design in two layers commingled model

In modelling the fracture various rock properties were considered including rock related stress, fractured /perforated thicknesses , rock type, Young's modulus, Poisson's ratio, fracture toughness formation permeabilities and pay zone intervals. In the presented example a two layered reservoirs separated by an impermeable layer penetrated by a single designed fracture targeting both layers using the software.

3.3 Model Description

A conceptual reservoir system that is being drained by a finite conductivity vertical fractured well, which fully penetrates a single layer reservoir, is modelled as the base case (*Figure 3-6*). The reservoir with finite dimensions in x and y directions (10,000ft in both axes) consists of homogenous reservoir with uniform thickness and closed outer boundaries. This single layer closed model is assumed to be porous medium that is filled with a fluid of constant compressibility. The vertical permeability, k_v is different from the horizontal permeability, k_h. The reservoir has a uniform pressure distribution before well starts production and the pressure gradients are very small throughout the formation.

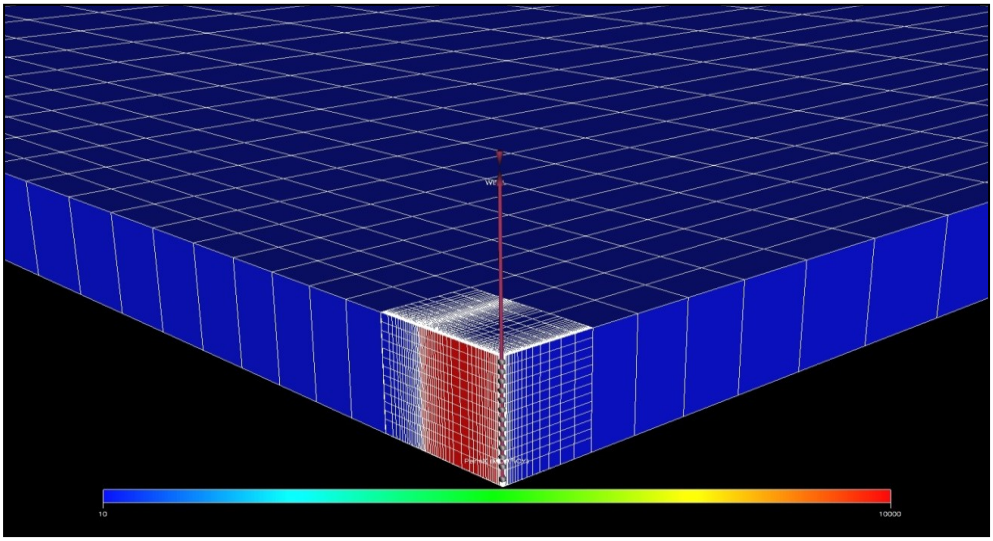


Figure 3- 6: Single layer induced fracture model

In the multi-layered case, a commingled (*Figure 3-7*) and cross-flow (*Figure 3-8*) reservoir system that is penetrated by a fracture were modelled that consists of two or more fractured layers isolated by an impermeable layers (*Figure 3-9*). Vertical communication can be established at the wellbore through the fracture. Fracture half-lengths are assumed to be equal in each layer; however, cases with different fracture half-lengths were also investigated.

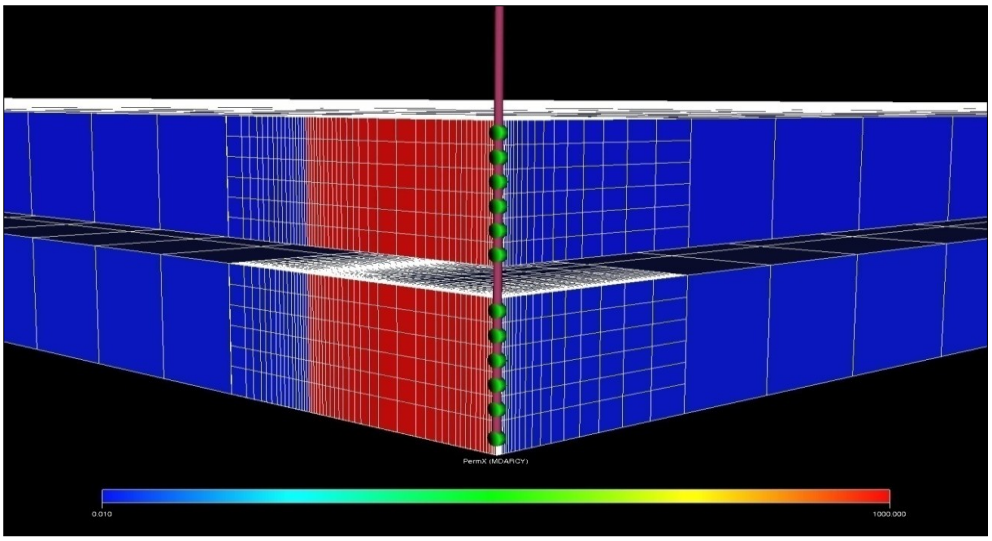


Figure 3- 7: Fractured well design in two layers commingled model

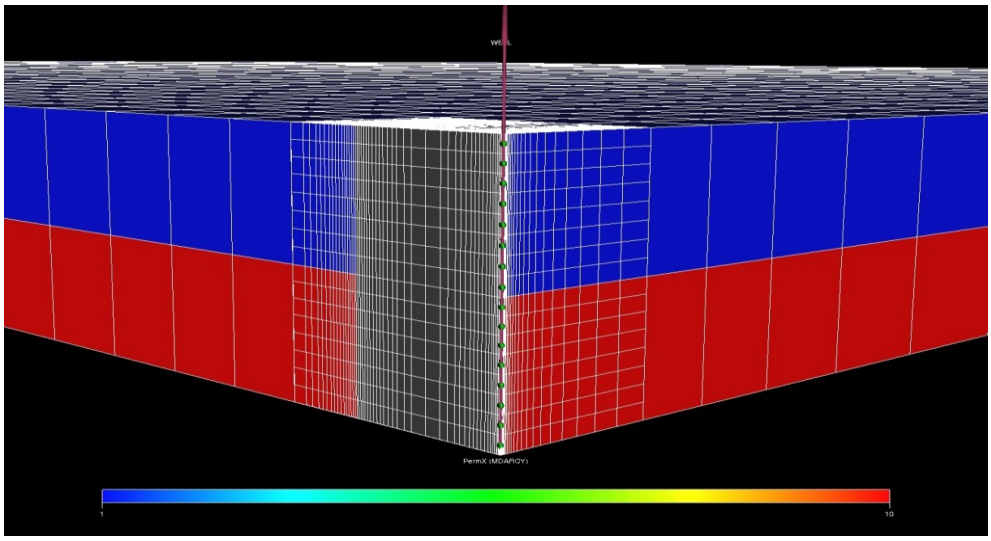


Figure 3- 8: Fractured well profile in two layers cross flow model

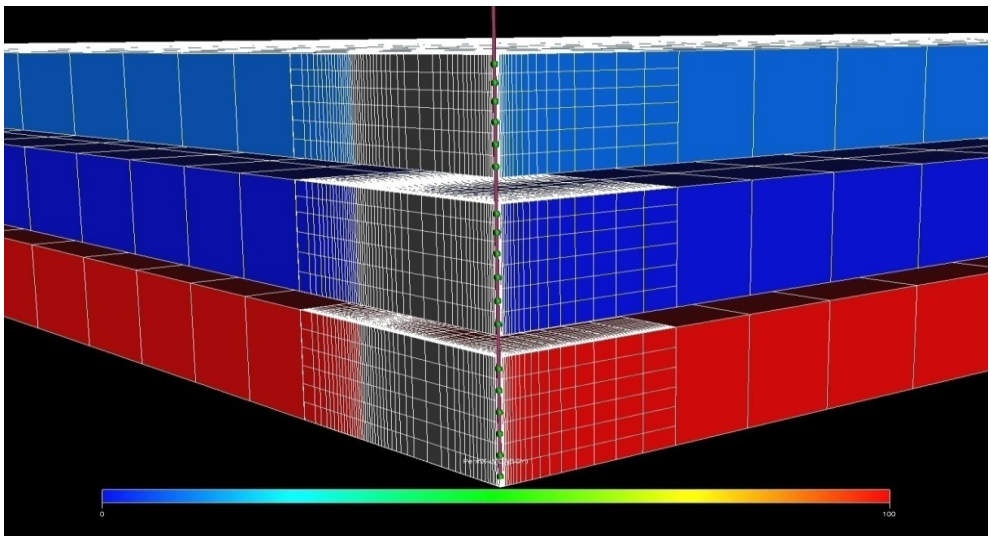


Figure 3- 9: Fractured well in multi-layered commingled model

In another phase of the study, cases of gas and gas-condensate (lean and rich) fluids with non-Darcy and capillary number effects are considered utilising a compositional simulation model. It is concluded from the literature review that the impact of not considering non-Darcy effect will result in error in terms of fracture and well performance parameter calculations.

3.4 Relative Permeability Modelling

The Corey relationship was used in the study to model relative permeability of the fluids present in the model. For instance, for the case of oil-water system the following Corey equations below were used for both oil and water relative permeabilities. To investigate reservoir heterogeneity effect, three sets of relative perms were generated representing clean, shaley and silty sand cases to use in the study (*Figure 3-10*). The objective was to investigate the impact of heterogeneity that might have on the generated early time flow behaviour of fractured wells.

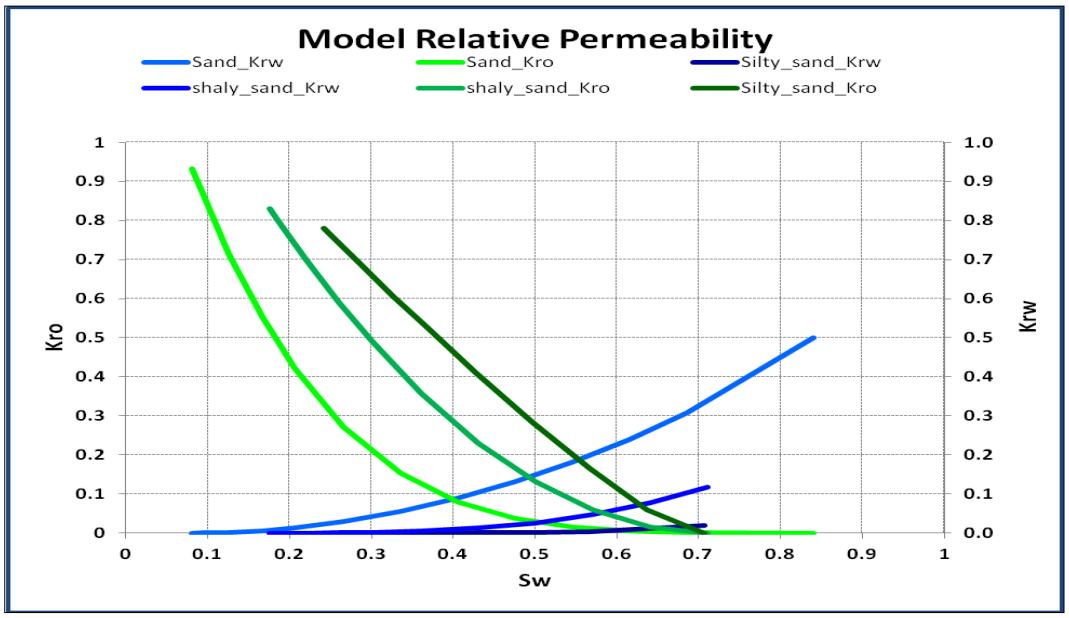


Figure 3- 10: Heterogeneity effect on oil and water relative permeability curves

$$k_{rw} = k_{rw}' \left(\frac{S_w - S_{wc}}{1 - S_{wc} - S_{or}} \right)^{n_w}$$

$$k_{ro} = k_{ro}' \left(\frac{1 - S_w - S_{or}}{1 - S_{wc} - S_{or}} \right)^{n_o}$$

where:

Kr_w: water relative permeability

Kr_w': end point relative permeability

Sw: water saturation

Sw_c: connate water saturation

n_w: Corey water exponent

Kr_o: oil relative permeability

Kr_o': end point oil relative permeability

Sor: residual oil saturation

n_o: Corey oil exponent

The relative permeability in the fracture was calculated using straight line approach with end point saturations of zero values. In the reservoir, relative permeability tables were used from field examples to obtain reasonable results that can be expected from actual cases. In compositional runs the variation of the relative permeability as compared to capillary number effects was modelled using velocity dependant relative permeability keywords, as defined by Henderson *et al.* (1995). At high rates flow periods the relative permeability curves tends to be straight lines to represent total miscibility case. This effect is most significant for the high flow rates occurring in the near well region of non-fractured gas and gas-condensate wells.

The influence of boundaries is not considered in this work and the total flow rate from the well is assumed to be constant. Production rate from quarter model is multiplied by four to account for the whole model. The input files for reservoir models used using Eclipse100 and 300 packages can be found in the Appendix-A in this document.

3.5 Model Verification

Initially a propped fractured well completed in a single layer homogenous model filled with a single phase constant compressibility fluid used to investigate the pressure behaviour of finite conductivity fracture case. In this model, many parameters were investigated in detail that believed to have impact on the development of unusual fractured well flow behaviour such as formation permeability, layer thickness, fracture damage; fracture half-length, conductivity, height and width effects.

The reservoir is assumed at constant pressure and the fluid flows from the formation into the fracture and then into the wellbore. Pressure gradients are small throughout the model and gravity effect is considered negligible, which is not a critical problem, as only single phase flow is modelled initially. However, cases of saturated oil with pressure drops below bubble point and dry, wet gas with reservoir pressure above and below dew point pressure were modelled.

In addition, the impact of the fracture properties was investigated by varying the fracture half-length, x_f, conductivity, $k_f w_f$ and width. The fracture conductivity is dependent on fracture permeability and width, which can be assumed constant, and the fracture half-lengths were varied from 10 to 1500 feet. However, models having fractures with variable conductivities were also examined.

To obtain constant dimensionless fracture conductivity, *FcD,* it is usually the fracture conductivity parameter that can be modified accordingly. The fracture conductivity is found to be influencing well performance and the fracture half-length is predicted to become important in developing the investigated problem in the case of short induced fractures.

All reservoir fluid characterizations used in the study were modeled using PVTi package, which can be found in the Appendix-B in this document. Table (*3-1*) below shows the main reservoir and fluid properties used in the base case fracture model with *FcD=1.6*. It is worth noting that exhibiting infrequent fracture flow behaviour may occur in any reservoir type containing any type fluids. Figure (*3-10*) shows well test result of fractured well with *FcD* of 1.6 that is considered as minimum dimensionless fracture conductivity that is expected to achieve from typical frac job according to Valko *et al.* (1998).

Reservoir Properties	
Initial pressure	5021
Formation permeability	10
Formation porosity, fraction	0.15
Rock compressibility, psi-1	3.35E-6
Well bore radius, ft	0.345
S_w	0
S_t	-5.5
Wellbore storage, bbl/psi	0.00035
Reservoir thickness, ft	117.5
drainage area, acres	80
Fluid Properties	
Oil Compressibility, psi-1	1.36E-5
Viscosity, cp	0.3745
FVF, rb/stb	1.496
Temperature, ^oF	135
Bubble point pressure (p_b), psi	4228
Fracture Properties	
Fracture half-length, ft	100
Fracture width, ft	0.01
Fracture permeability, D	74

Table 3- 1: Description of the main characteristics of the reservoir model

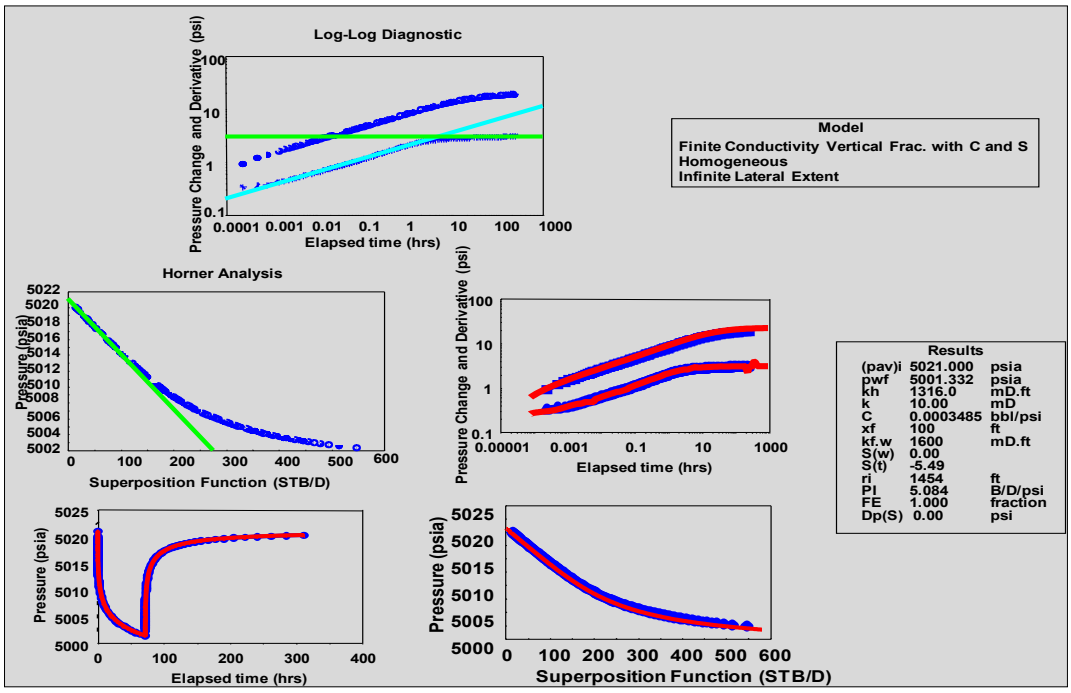


Figure 3- 11: Verification of the numerical model with the analytical solution for *FcD* of 1.6

To validate robustness of the constructed numerical model, a vertical fracture model penetrating single layer is designed with *FcD* values ranging from one up to 500. The plots below (*Figures 3-11 and 3-12*) show a comparison of the numerical model with analytical solutions for different dimensionless fracture conductivities, which indicate robustness of the numerically designed fracture in the study in generating any fracture configuration.

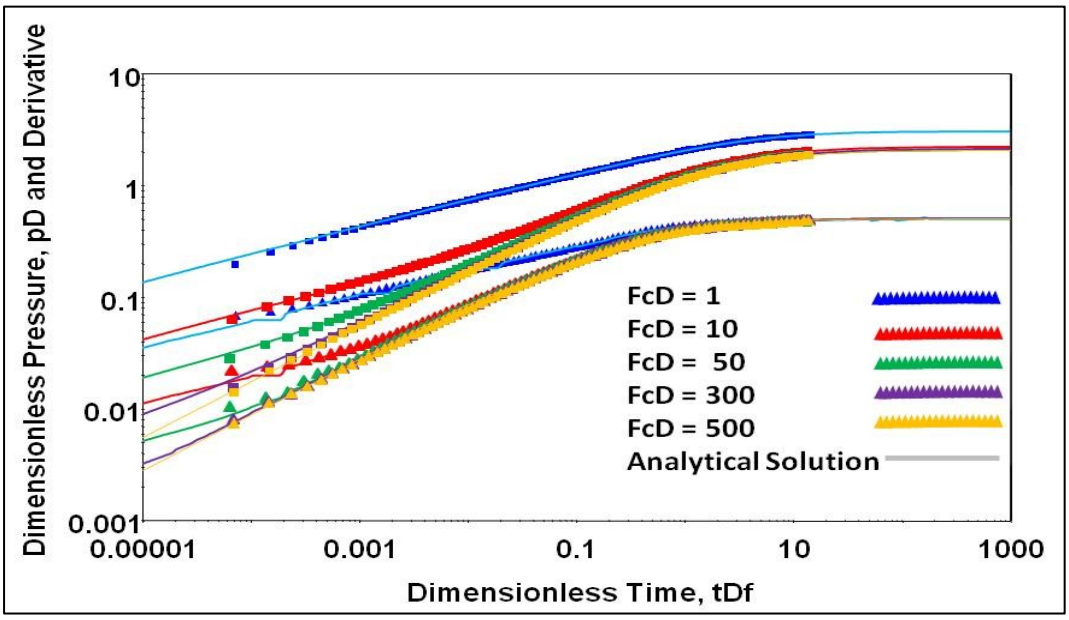


Figure 3- 12: Verification of the numerical model versus analytical solution for various *FcD*

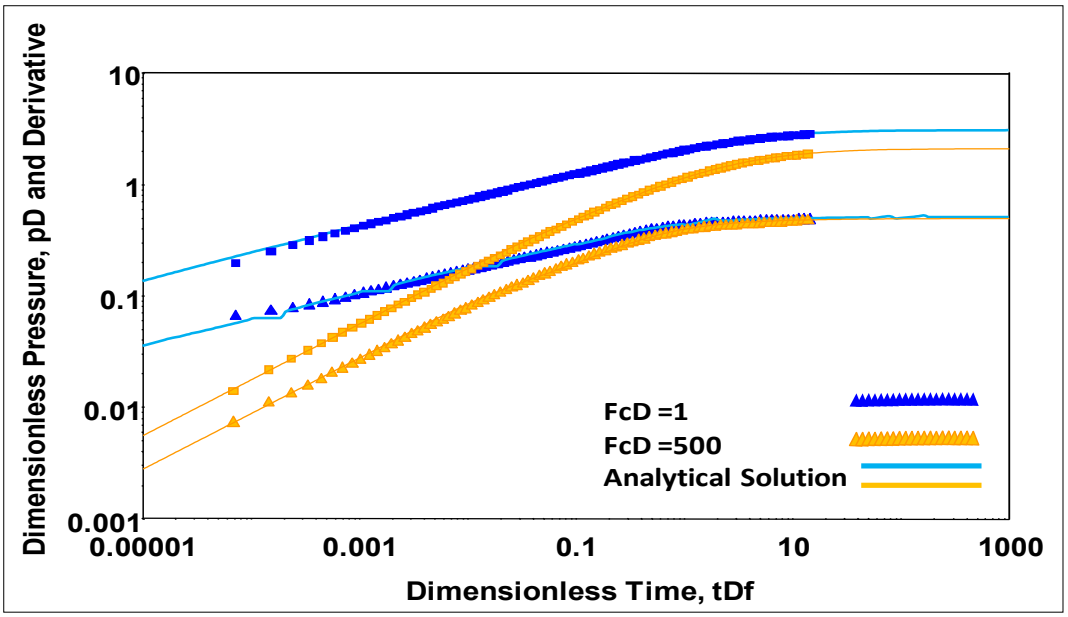


Figure 3- 13: Analytically verified Infinite versus finite conductivity fracture models

Fracture damage is believed to be one of the main causes for developing infrequent behaviour in fractured wells. Formation fines migration towards the wellbore considered being one of the critical problems that is responsible for permeability reduction at fracture face and within the fracture. Field operation activities such as drilling, completion, and production processes may also cause some permeability reduction in the vicinity of wellbore. The resulting depth of damage may extend from a few inches to several feet into the formation as it is reported in the literature. One of the main sensitivity parameters that need to be well understood in fractured wells is the effect of the fracture damage on fracture conductivity.

Fracture choke damage has significant impact in developing the investigated problem in this study. The second lower impact damage is the fracture face skin due to reduced permeability caused by leak-off of fracturing fluid. To investigate the importance of fracture damage, both fracture choke and face skin damage were modelled. In order to mimic fracture damage, a permeability reduction along the fracture face and close to the wellbore in choked fracture case was modelled and the graph below shows post-frac pressure behaviour of fractured well with no indication of fractured well flow feature at early time due to fracture choke effect.

3.6 Conclusions

It is common practice to use a Cartesian grid in modeling an induced fracture in the reservoir simulator. Therefore, the Cartesian grid using local grid refinement "LGR" too in the numerical simulation has been used to model fracture. To test the approach used in the study in modeling a fracture accurately, an industry leading fracture software "Frac pro PT" was tested to verify various fracture designed models. The software is powerful tool in modeling proppant fracture as it takes into account fracture, rock, fluid and other physical properties when a frac job is designed. For fracture modeling purpose:

- A single vertical well Cartesian model was constructed with rock and fluid properties obtained from simulated PVT data and the numerical model results were verified against analytical solutions. Modeling the induced fracture using the Cartesian grid approach represents best practice as indicated in the literature. In order to investigate formations and fracture sensitivity parameters, various sensitivities have been run.

- Actual field samples of oil, gas, lean and rich gas-condensate fluids were obtained from different sources and simulated with appropriate equations of state using fluid characterization PVTi package. Good matches were achieved between the actual measured data and the simulated data for most fluids.

- The saturation tables needed for the reservoir simulation model were generated using Corey functions as well as from real field data. In the gas-condensate case the designed capillary model by Herriot-Watt (through use of velocity dependent relative permeability) will be included in the compositional numerical simulation section in this document.

- Finite conductivity fractures have been used throughout this study, because the vast majority of fractures created in real field examples tend to have finite conductivity rather than infinite conductivity. Both black oil and compositional simulators were utilized to investigate the problem in simple and complex fluid cases.

CHAPTER IV

FRACTURED WELL FLOW BEHAVIOUR ANALYSIS

4.1 *Introduction*

The first study investigating the flow behaviour of fractured wells using a steady state analytical model was presented by Muskat (1949) followed by Poollen *et al.* (1958) study. Since then many papers have been published that have investigated the pressure transient analysis of stimulated wells. Some workers examined the steady-state flow behaviour towards the fractured well; a few studied the unsteady-state flow case; others considered infinite, finite and uniform flux conductivity fractured wells. The first study on the unsteady-state (transient) flow behaviour for fractured wells was presented by Dyes *et al.* (1958). In their case they studied the influence of a vertical fracture on the semi-log straight line.

Prat *et al.* (1962) were the first to investigate the performance of a vertically fractured well in a reservoir with compressible fluid produced at constant flowing pressure. They considered semi steady-state constant production rate behaviour for vertically fractured wells. They demonstrated that the effective wellbore radius of a fracture is a function of dimensionless fracture conductivity, *FcD* and fracture length (*Figure 4-1*). They also indicated that for the case of an infinite conductivity fracture system and relatively large drainage area, the effective wellbore radius is equal to one half the fracture half-lengths.

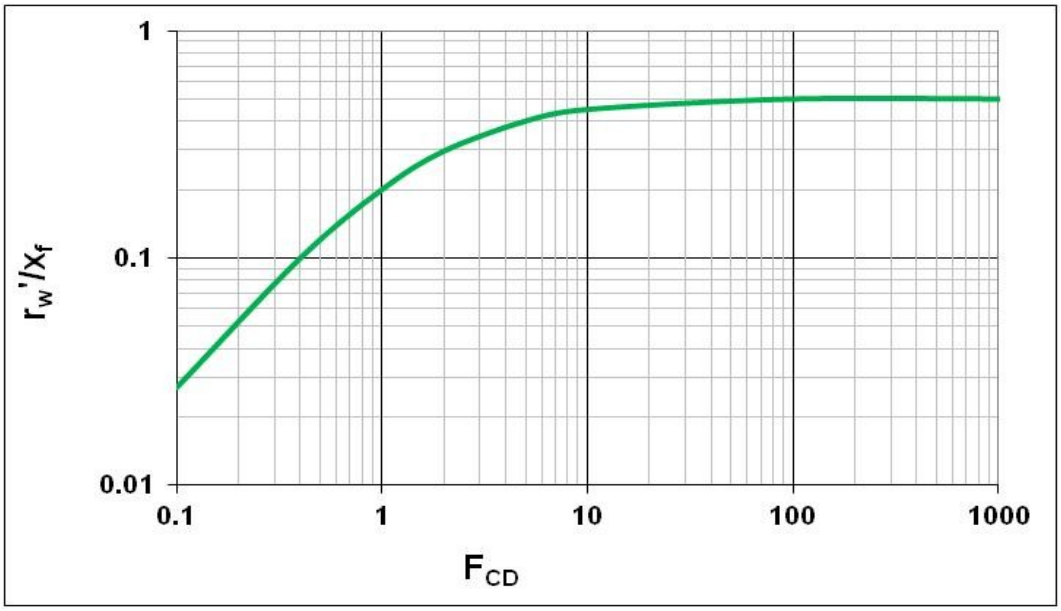


Figure 4- 1: Effective wellbore radius versus *FcD* (Prats *et al.* 1962)

Russell and Truitt (1964) were first to show that fractured well flow behaviour develops into pseudo radial flow and introduced a correction factor for the kh values computed from semi-log graph for cases where the fracture penetration is high. They examined the transient pressure behaviour for an infinite conductivity vertical fracture in a closed square reservoir system. They also analysed the wellbore pressure as a function of time for several fracture penetration ratios.

Lee (1967) used a numerical simulator to examine the effect of both vertical and horizontal finite conductivity fractures and proposed correlations to estimate reservoirs and fracture properties. It is worth noting that unsteady-state linear flow theory was first applied to fractured wells by Millheim and Cjchowicz (1968); Clark (1968) presented a graph he called a linear flow, in which plotting wellbore bottom hole pressure versus the square root of time yields a straight line whose slope is inversely proportional to the fracture area and the slope depends on fracture half-length and formation permeability.

One of the most significant contributions to the transient pressure analysis theory for fractured wells was made by Gringarten and Ramey (1973). In another study Gringarten *et al.* (1974) used an analytical approach by implementing Newman's product method, combined with Green's and source functions, to generate a large number of reservoir solutions. Also, they introduced three solutions: infinite conductivity for vertical fracture and uniform flux solutions for vertical and horizontal fractures.

Sawyer and Locke (1973) examined the transient pressure behaviour of finite conductivity vertical fractures in gas wells. They introduced a numerical simulation of production wells intercepted by a finite conductivity fracture. Their solutions were of limited use in analysing transient pressure data as they were applicable to few cases presented.

Gringarten and Ramey (1975) were the first to introduce the mathematical solution for an infinite conductivity fracture in an infinite acting reservoir, and it has been used since in well test applications for wells intersecting large natural fractures. In another study, Gringarten *et al.* (1975) investigated three models of infinite conductivity vertical fracture, uniform flux vertical fracture and uniform flux horizontal fracture to find solutions for transient flow behaviour for fractured wells.

Locke and Sawyer (1975) in a study examined reservoirs with low permeability producing at constant bottom hole pressure using an infinite conductivity fracture and finite fracture conductivity concepts. They used a finite difference model to generate type curves for infinite conductivity vertical fractures in bounded reservoirs producing at constant pressure. They presented various type curves to estimate both formation and fracture characteristics by analysing flow rate data.

Cinco-Ley and Samaniego (1977) introduced a set of dimensionless variables to specify the performance of fractured wells. The concept of dimensionless fracture conductivity has been used in the well test analysis as the dominant indicator of relative improvement in fluid flow due to an induced fracture compared to the non-fractured well. Cinco-Ley *et al.* (1978) presented a paper that is considered being one of the milestones in the analysis of fractured wells in which they pointed out that the infinite fracture conductivity assumption is not valid when pressure along the fracture is considerable, that is, when the dimensionless fracture conductivity is less than 300.

Barker and Ramey (1978) in another study investigated the influence of a closed external boundary on the behaviour of finite conductivity fractured well. They indicated that with a large production time the systems reach pseudo-steady state flow conditions and demonstrated that the use of type curves may result in a unique problem.

Agarwal *et al.* (1979) presented that transient pressure data from a vertically fractured well could exhibit flow behaviour that is different from uniform flux or infinite conductivity fracture models. The new flow regime, called bilinear flow, represents linear flow from formation to the fracture and linear flow within the fracture. In fact they extended Cinco-Ley *et al.* (1978) constant rate type curves to early times and produced constant pressure type curves for finite conductivity fracture generated by massive hydraulic fracturing.

In a study Scott (1979) introduced a new graph called the time power function graph to analyse pressure data for small and intermediate values of elapsed time. He demonstrated that the pressure behaviour of a well intercepted by a finite conductivity vertical fracture can be approximated as a function of a time power being the exponent dependent on the fracture conductivity.

Cinco-Ley and Samaniego (1981) in another study concluded that a fracture with intermediate or low conductivity exhibits bilinear flow period in addition to the linear and the pseudo radial flow period and new type curves were introduced. They pointed out that plotting pressure data versus the fourth root of time results in a straight line whose slope is inversely proportional to the square root of fracture conductivity.

Cinco-Ley (1982) published a work in which he presented an evaluation of pressure transients generated by hydraulically fractured well for diagnostic purposes. He demonstrated the importance of the application of type cures as a diagnosis tools in interpreting pressure data and also showed applicability of infinite conductivity fracture for fractures with high permeability and finite conductivity.

Cinco-Ley *et al.* (1984) investigated the pressure transient analysis from moderate to high conductivity fractures using linear flow and pseudo-linear flow models. They found that pseudo-linear flow pattern could be used to analyse transition period between bilinear and linear flow periods rather than using a type curve technique.

Bennett *et al.* (1986) studied infinite acting multi-layered commingled reservoirs with finite conductivity fractures using the concept of dimensionless reservoir conductivity, *CrD*. They proposed that commingled reservoir solutions are identical to single layer solutions throughout the infinite acting period. Camacho *et al.* (1987) addressed the pressure transient response of wells producing from commingled reservoirs with unequal fracture lengths. They showed that the solution for a fractured well producing from such a system is identical to the corresponding single layer solution when equivalent fracture half-length and fracture conductivity are used.

Osman (1992) investigated pressure and flow behaviour of fractured wells in multi-layered bounded square reservoir and found that fracture extension play a significant role in controlling pressure and derivative features. In a similar study, Osman (1993) presented a mathematical model to study pressure behaviour of a vertically fractured well of finite conductivity.

Based on the above literature review, it can be concluded that none of these of studies examined the unusual flow behaviour of fractured wells. The following section investigates the main causes and controlling parameters for developing such behaviour.

4.2 *Fracture and Formation Parameters Sensitivities*

A wide range of fracture and formation parameter sensitivity cases are run to investigate the impact of each parameter on fractured well flow behaviour in single and multi-layered reservoirs. The investigated parameters include: single versus multi-layered reservoirs; commingled versus interlayer cross-flow scenarios; fracture conductivity and length effects; fracture and formation permeability contrasts; fracture damage including fracture face and choke damage; fractured interval lengths effect; mechanical skin effect; proppant damage effect, fluid leak-off effect and many other scenarios of fractured wells.

To model typical fractured well flow behaviour in the reservoir simulator, a commercial fracturing package of "FRAC PRO PT" was used to investigate how fracture is induced in different formations and to design fractures of various configurations in different reservoir settings. The software is a powerful tool for modelling fractures that consider various physical aspects (stresses and strains) related to hydraulic fracturing process. Sensitivities run examined effects of fracture configuration including length, conductivity, width and reservoir settings containing different fluid types. In the next section a detailed review of all these sensitivities are presented.

The cases run were for different fluid types (oil, gas, and lean, rich gas-condensate fluid in reservoirs with permeability ranges from low (1mD) to moderate (10mD) and high (100mD). Based on the literature review it is concluded that the investigated problem may occur in any reservoir type including single layer or multi-layered of low and high permeability formations containing oil, gas, lean and rich gas-condensate fluids. For this reason, the study is considered a challenge to examine the problem in such wide range of reservoir settings.

The study results suggest that fracture conductivity and half-length are the key causes in developing the investigated problem in the study. Other reservoir parameters such as permeability appear also contributing in causing the investigated behaviour. The main results are presented in the following sections and different plots are illustrated accordingly. Below is a list of fracture and formation sensitivity parameters that were investigated in detail.

4.2.1 Effect of Fracture Half-Length, X_f

One of the critical fracture parameters to consider when designing a frac job is the fracture half-length, x_f. Often the resultant fracture half-length following stimulation work is different from the designed length. The type and stimulation target needed will determine the required length to achieve. For instance, the required half-length for skin-frac job is 1-10 feet; whereas, stimulating tight formation would require 100s of feet half-length. Thus, achieving appropriate fracture length is important in any stimulated job. For this reason fracture length sensitivity is investigated in the study.

In addition, accurate calculation of dimensionless fracture conductivity, the *FcD* value, for any fracture is dependent on accurate calculation of the induced fracture half-length and conductivity. The *FcD* is product of the formation and fracture permeability, width and half-length. Therefore, it is very important to calculate fracture half-length as accurately as possible. To investigate the effect of induced fracture half-length on the fractured well behaviour, a single layer model penetrated by vertical fracture was built with fracture half-lengths of 10ft and 100ft and *FcD* of one and ten. Results indicate that the investigated behaviour is likely to occur in fractures of short lengths (*Figures 4-2 and 4-3*). Obviously, fractured well flow behaviour is more evident in the case of a longer fracture half-length of 100ft and a higher *FcD* value of 10.

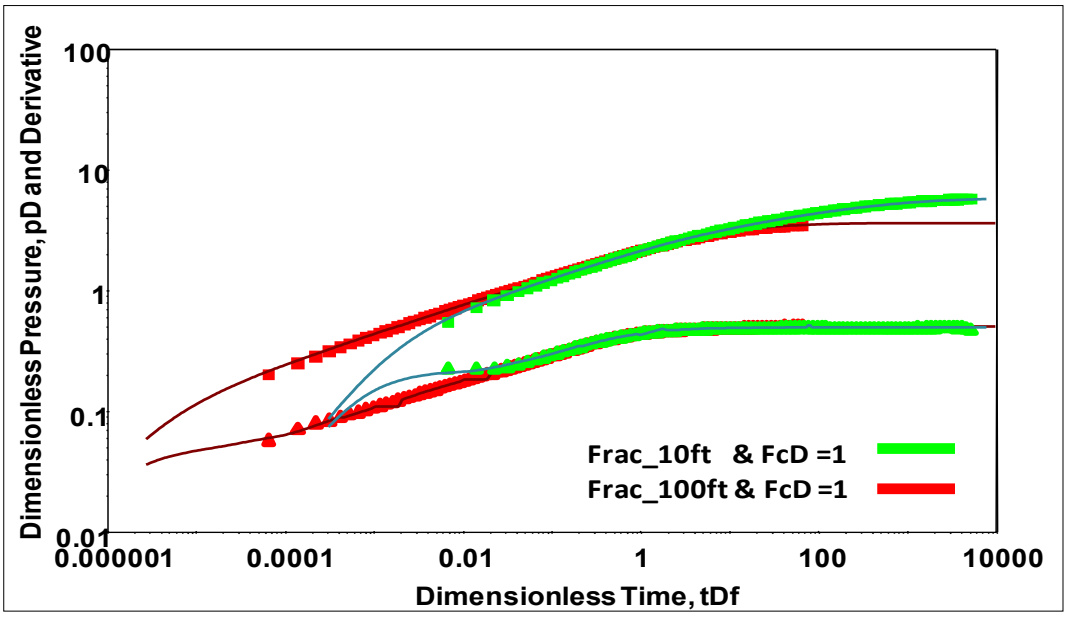


Figure 4- 2: Comparison of fracture half-lengths of 10 and 100ft with FcD of one

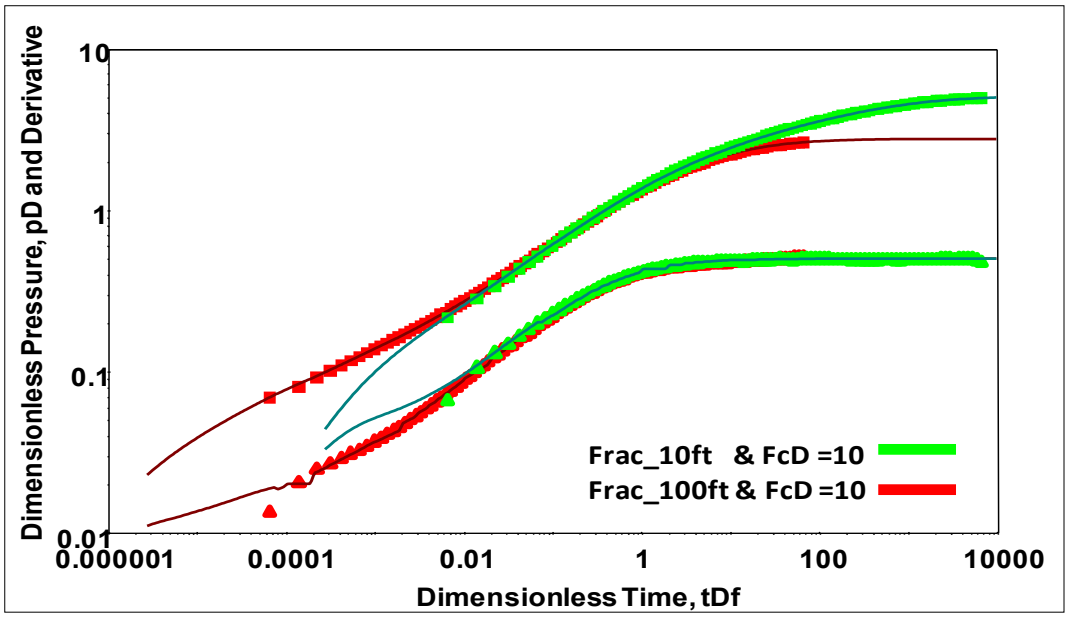


Figure 4- 3: Comparison of fracture half-lengths of 10 and 100ft with FcD of 10

To further investigate fracture length effects on the generated pressure behaviour of fractured wells, a single layer model penetrated by vertical fracture was constructed with *FcDs* of 1 and 10 and fracture half-lengths of 10, 100 and 1000ft.

The graphs below (*Figures 4-4, 4-5 and 4-6*) show clearly the effect of the induced fracture half-length on the introduced fractured well flow behaviour. As it can be seen that fracture flow feature is more evident in the case of 1000ft half-length and *FcD* of 10 compared to fracture half-length of 10ft and *FcD* of one.

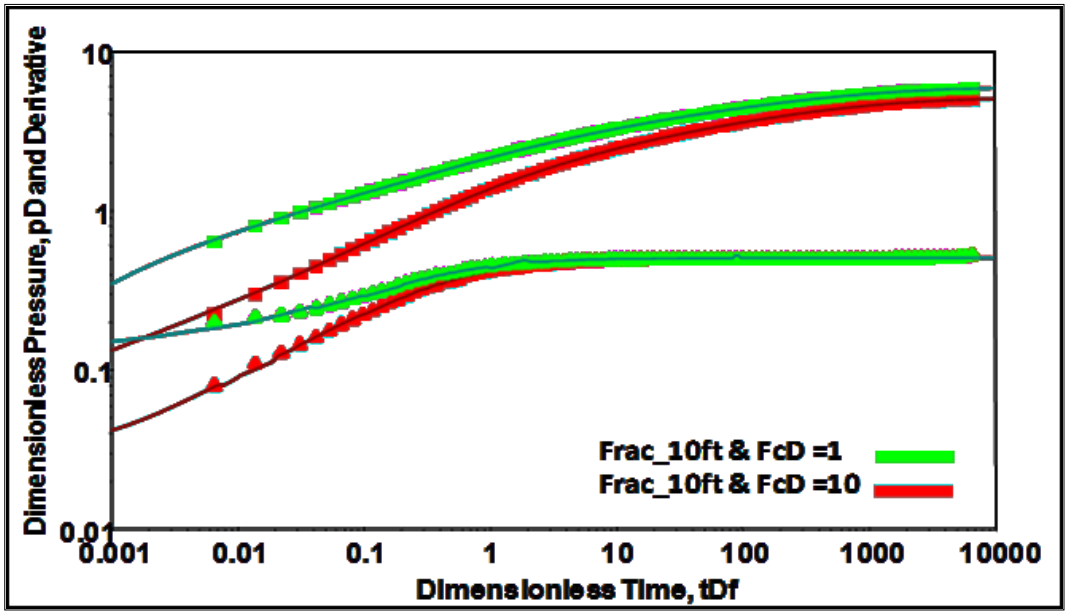


Figure 4- 4: Fractured well pressure behaviour with FcD of 1 and10 and X_f of 10ft

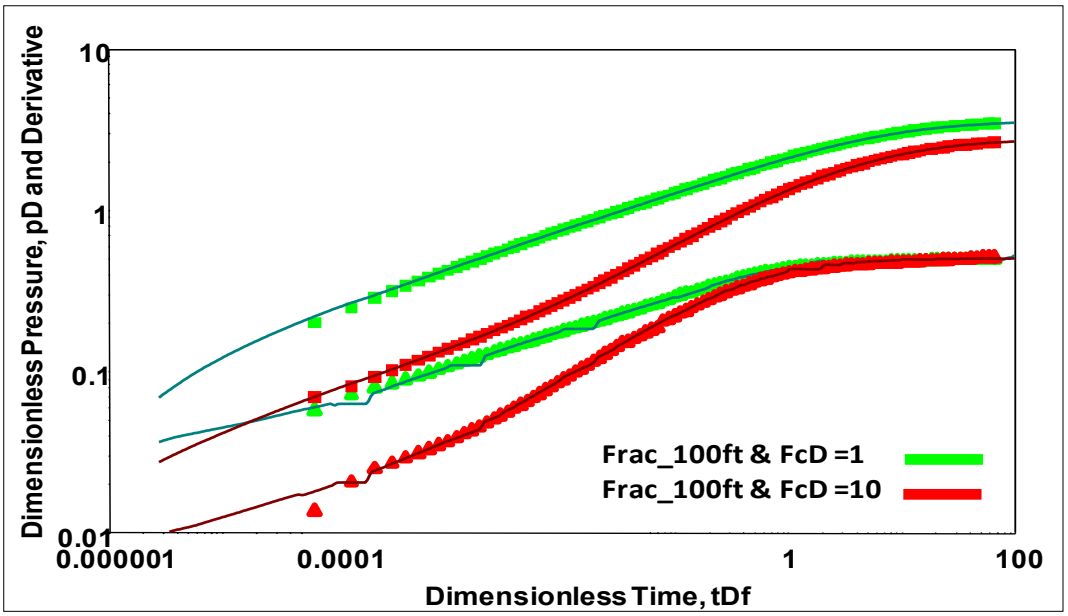


Figure 4- 5: Fractured well pressure feature with FcD of 1 and10 and half-length, X_f of 100ft

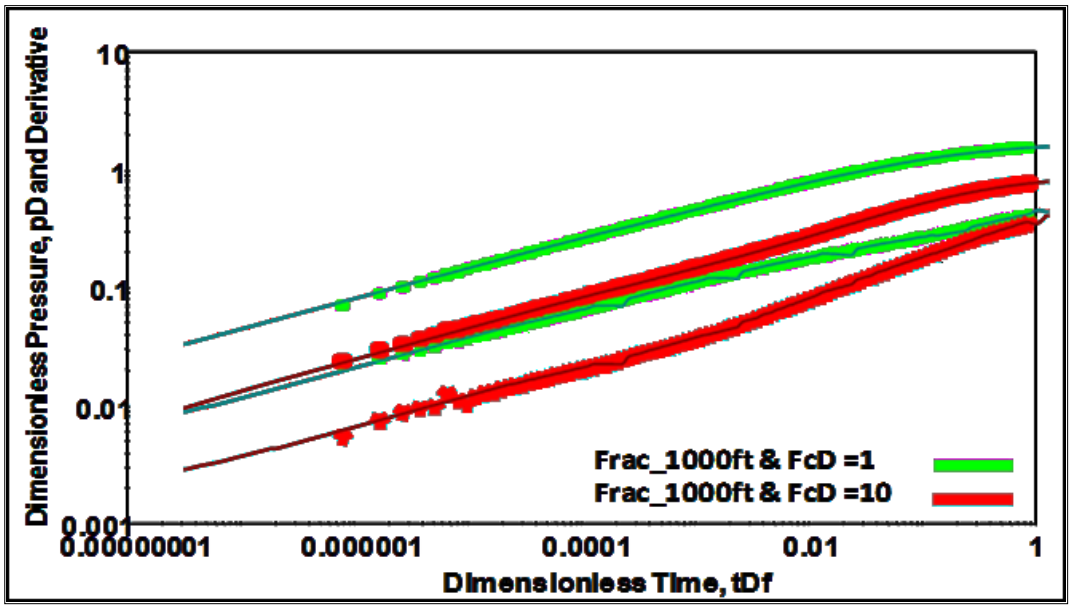


Figure 4- 6: Fractured well pressure behaviour with FcD of 1 and10 and X_f of 1000ft

To investigate the effects of different *FcD* values, the model was run with *FcDs* of 0.25, 1, 5 and 10 and various fracture half-lengths, x_f of 10, 100 and 1000ft. As can be seen in the presented graphs (*Figures 4-7, 4-8 and 4-9*), a fracture behaviour with low *FcD* of 0.25 is close to the non-fractured pressure behaviour. The study results suggest that developing unusual fracture flow behaviour is related to short induced fracture half-length and low fracture conductivity, which can be considered as critical control parameters in causing the investigated behaviour.

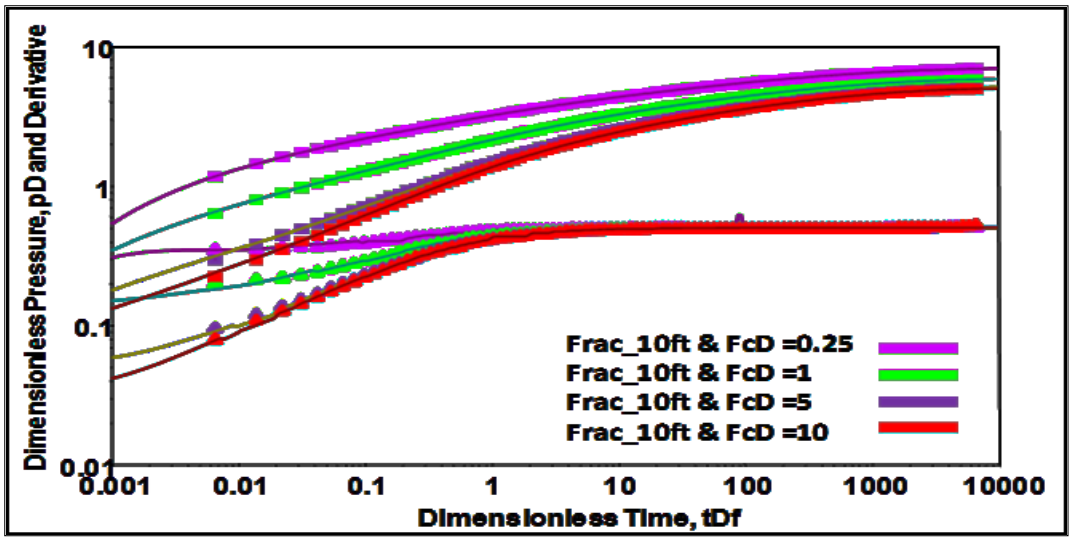


Figure 4- 7: Log-log plot of fractured well with FcD of 0.25, 1, 5 and10 and half-length of 10 ft

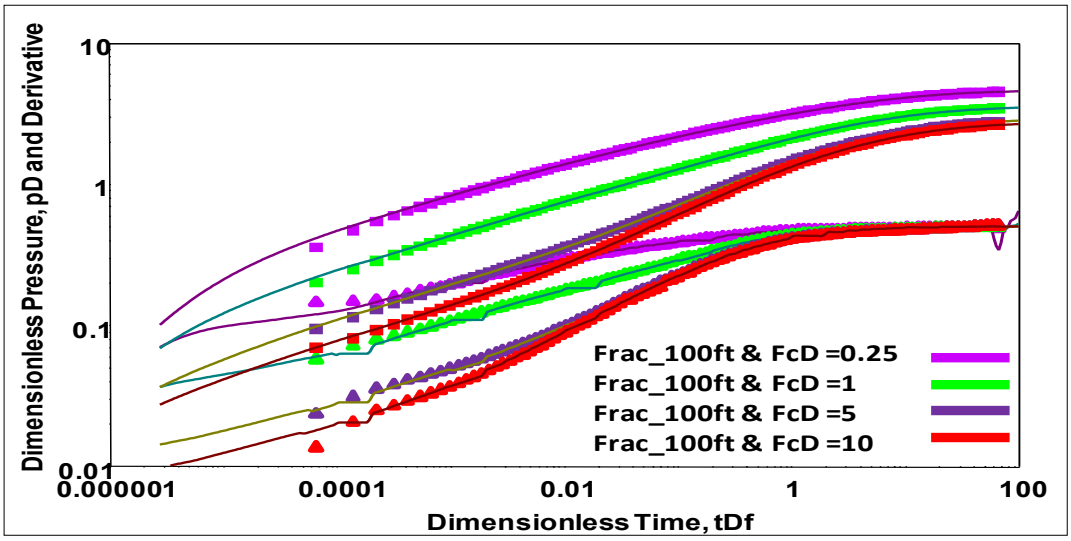


Figure 4- 8: Log-log plot of fractured well with FcD of 0.25, 1, 5 and10, half-length of 100 ft

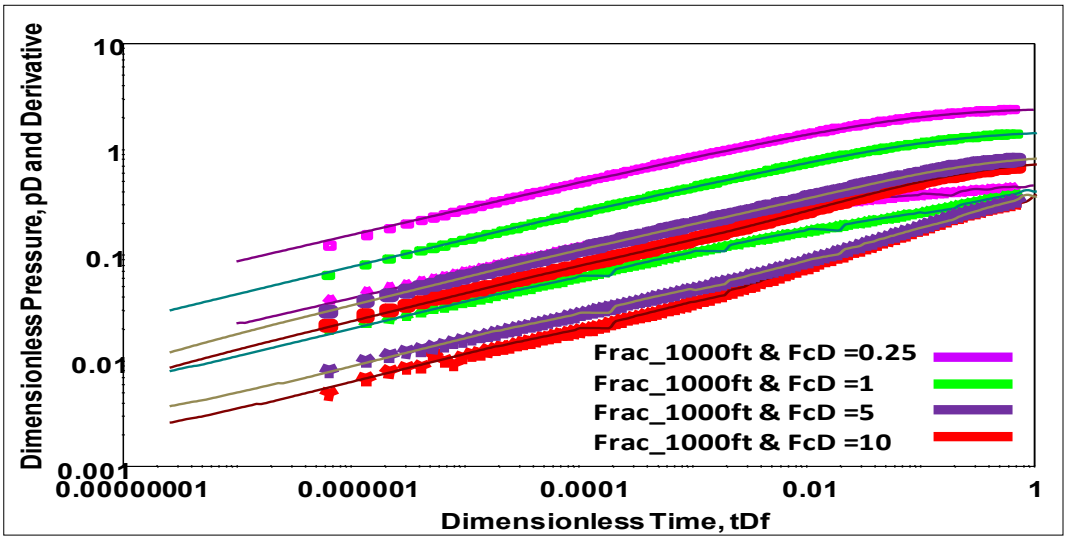


Figure 4- 9: Log-log plot of fractured well with FcD of 0.25, 1, 5 and10, half-length of 1000 ft

4.2.2 Effect of Fracture Permeability, K_f

After performing a stimulation work on a well, calculation of fracture parameters, including length and conductivity through well test analysis would be the next exercise for practice engineers. Well test engineers are often keen verify the calculated fracture parameters against the proposed values in the fracture design model prior to well stimulation. The study suggests that accurate calculation of the fracture conductivity, $K_f w_f$ value; hence, fracture permeability together with fracture half-length, x_f is the key parameter to assess in any frac job.

To investigate the fracture permeability effect, vertical fracture models with permeabilities of 10D, 40D and 400D and a fracture half-length of 100 ft penetrating 10 mD single layer formations were constructed. Clearly, pressure behaviour of lower fracture permeability and hence of low dimensionless fracture conductivity, *FcD* is closer to the non-fractured well flow behaviour compared to one of high fracture permeabilities *(Figure 4-10*).

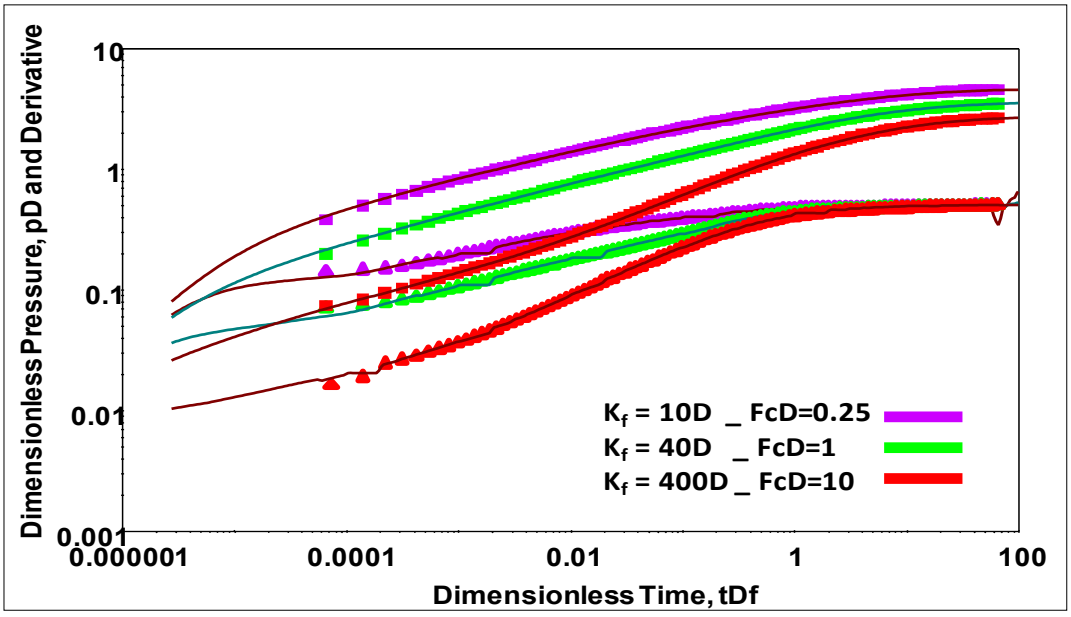


Figure 4- 10: Pressure behaviour of 100ft x_f and fracture permeability of 10, 40 and 400D

In order to investigate the impact of fracture permeability on the generated pressure responses in more detail, a single model of 1, 10 and 100mD permeabilities penetrated by 100ft vertical fracture was constructed. Figures *4-11, 4-12 and 4-13* demonstrate the generated pressure profiles for each individual case. For this purpose various fracture permeabilities were used in the model ranging from half a Darcy to tens of Darcies as such range of fracture permeabilities is believed to be result of a stimulation process.

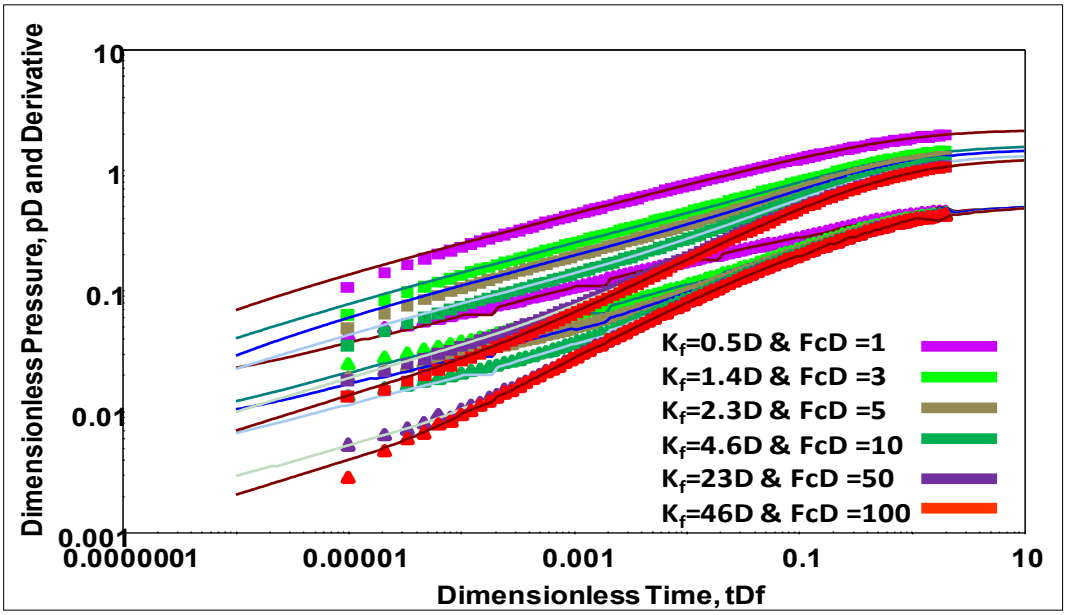


Figure 4- 11 : Fractured well of 1 mD model with FcD of 1, 3, 5, 10, 50 and 100 and X_f=100ft

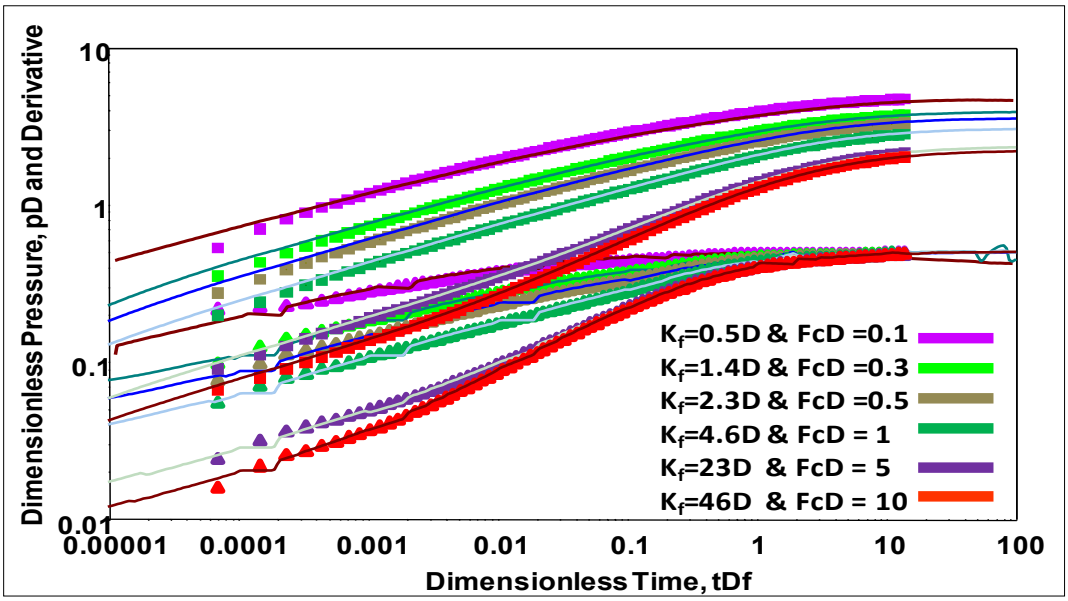


Figure 4- 12: Fractured well in 10 mD model with FcD 0.1, 0.3, 0.5, 1, 5 and 10 and, X_f=100ft

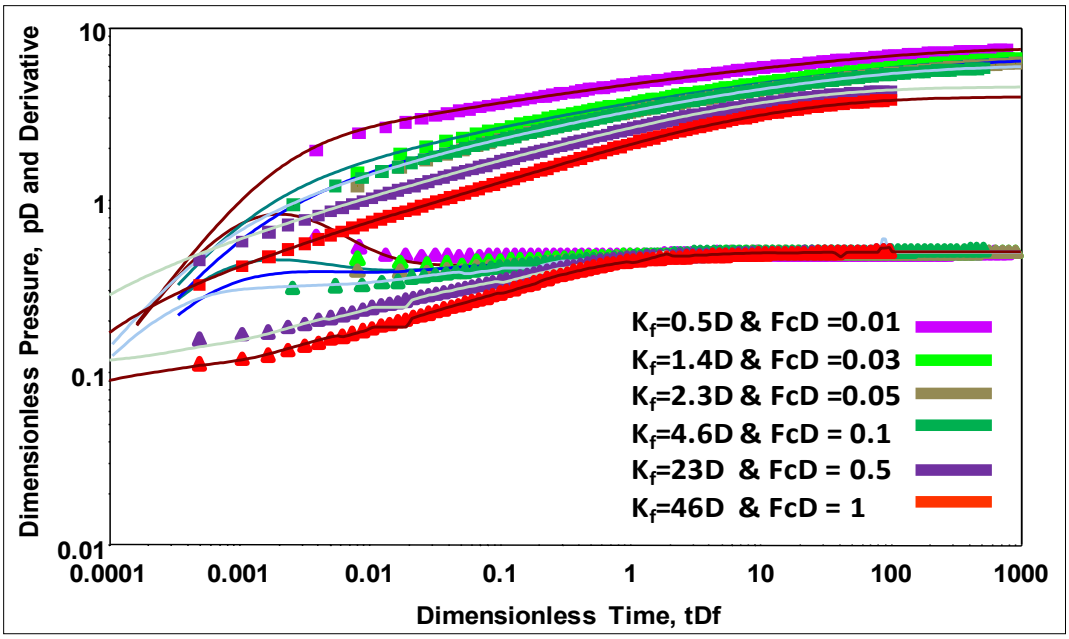


Figure 4- 13: Fractured well in 100 mD with FcD of 0.01, 0.03, 0.05, 0.1, 0.5 and 1, x_f=100ft

Based on the above presented graphs, it can be concluded that fracture permeability has a significant impact on the generated pressure profiles from stimulated wells. In practice achieving a good frac job is mainly dependent on the induced fracture conductivity and fracture permeability in particular. By examining the above plots, it can be observed that fractures of low permeabilities; hence, low fracture conductivities have similar pressure behaviour to the non-fractured wells.

Results indicate that the investigated problem in the current study is most likely to be associated with fractured wells of low induced fracture conductivities due to improperly performed frac job. Thus, the studied infrequent flow behaviour in fractured wells in this research project is expected to occur in fractures with dimensionless fracture conductivity, *FcD* of less than 0.1.

4.2.3 Effect of Formation Permeability, *K*

Formation permeability effect is yet another important factor in developing the investigated behaviour in this study. To examine the effects of this parameter, a single layer model of different formation permeabilities (1, 10, 50 and 100mD) penetrated by a vertical fracture was constructed. The reason for selecting such a range of permeabilities was to consider tight to high permeability formations. Fracture half-length and permeability was set to 100ft and 50D respectively in all cases. The simulation run results suggest that the higher the formation permeability relative to low fracture permeability, the more likely unusual flow behaviour occur.

As it can be seen in the graphs below (*Figures 4-14 and 4-15*), a range of *FcD* values of 0.1 to 10 were used to represent the results of typical frac jobs. Results suggest that the behaviour is likely to occur in fractures of low *FcD* value and low fracture permeability relative to high formation permeability. When stimulating high permeability formations through the "Frac Pack" process if the induced fracture is of low conductivity relative to the formation, the fracture flow behaviour will be identical to non-stimulated wells.

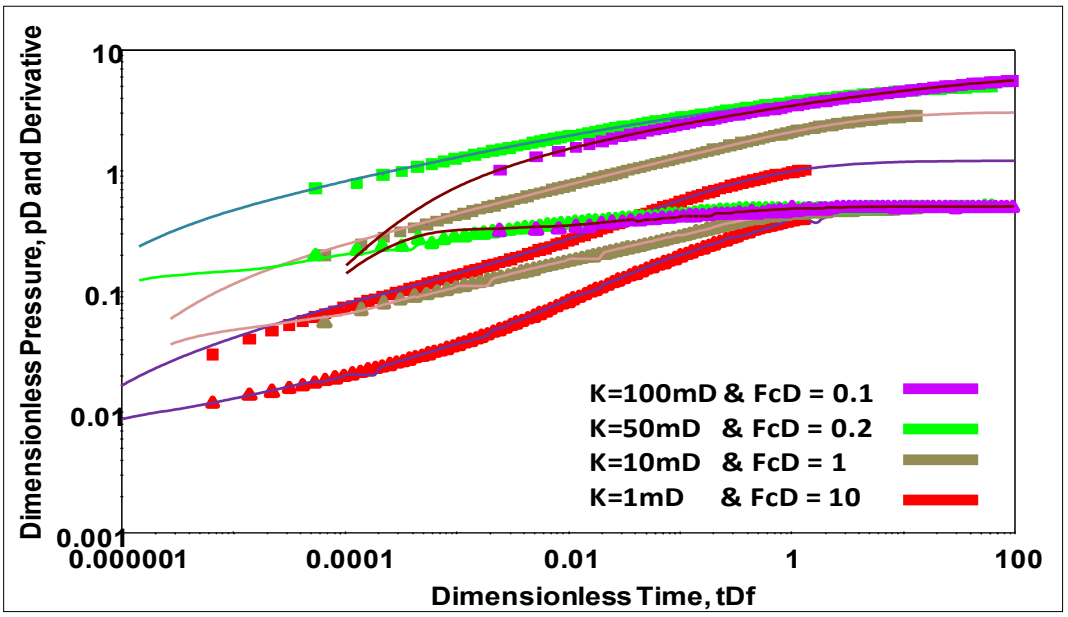


Figure 4- 14: Log-log plot of fracture permeability of 50D and fracture half-length, X_f=100ft

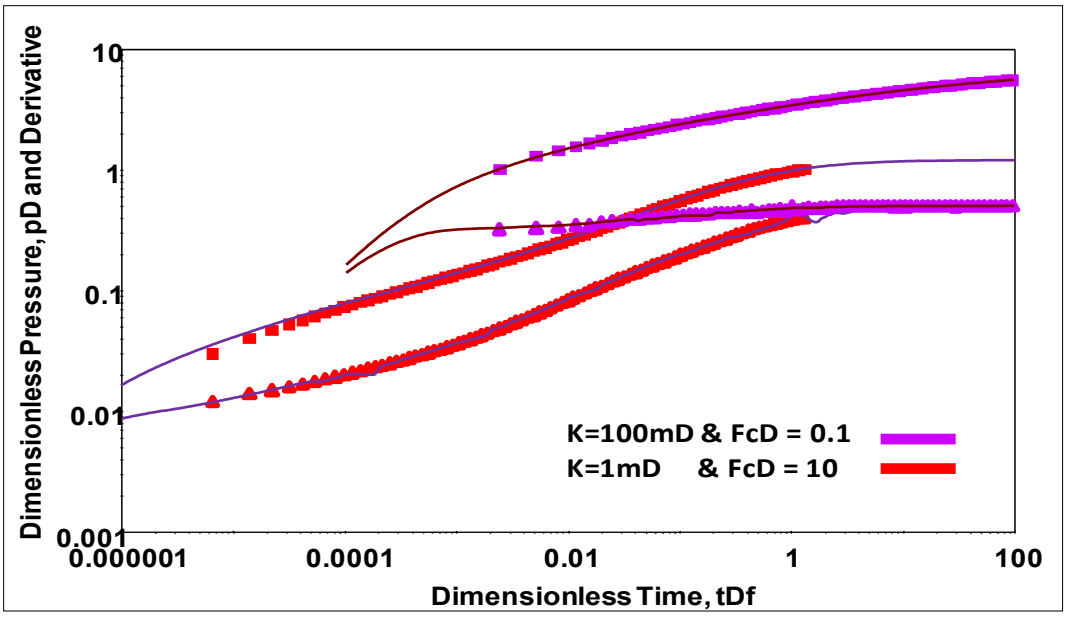


Figure 4- 15: Two models with formation permeabilities of 1 and 100mD and X_f of 100ft

4.2.4 Effect of Fracture Fluid Leak-off

The leak-off effect occurs as a consequence of proppant fracturing, and is considered one of the complicated processes in modelling propped fractures that affects effectiveness of any stimulation job. Modelling fracture fluid leak-off and clean-up processes is important following stimulation treatment to assess well productivity. The depth of filtrate leak-off varies depending on the penetrated formation permeability and the leak-off effect may extend from a centimetre to tens of centimetres and more in the case of high permeability reservoirs.

To model the leak-off effect it is assumed that the highest water saturation occurs close to the wellbore. Fracture fluid leak-off is normally simulated numerically by injecting fracture fluid at a constant pressure into cells representing the created fracture, which initially have same water saturation as other parts of the model. The injection pressure will be slightly higher than the formation pressure and the fracture leak-off fluid is usually a water-based fracturing fluid. The water is injected first into the cell representing the wellbore then the injection continues progressively outward until the tip of the induced fracture is reached. For this purpose, a simple model was constructed to mimic leak-off effect on the generated pressure profile following the well stimulation.

Figure (*4-16*) shows the water saturation profile with injected water distribution along the fracture face and the nearby wellbore area. Obviously, the highest water saturation will be within the fracture and in the vicinity of the wellbore along the fracture face. In the graph, the blue part represent fracture fluid invaded area within the fracture and at fracture face.

This injection technique represents the fracture growth and leak-off versus time during the hydraulic fracture treatment. The water is injected for a certain period and the amount of water injected for given formation permeability and propped fracture half-length is then calculated. It is known that a higher permeability formation has a greater volume of water leaked-off into the formation along the fracture face than a lower permeability reservoir case.

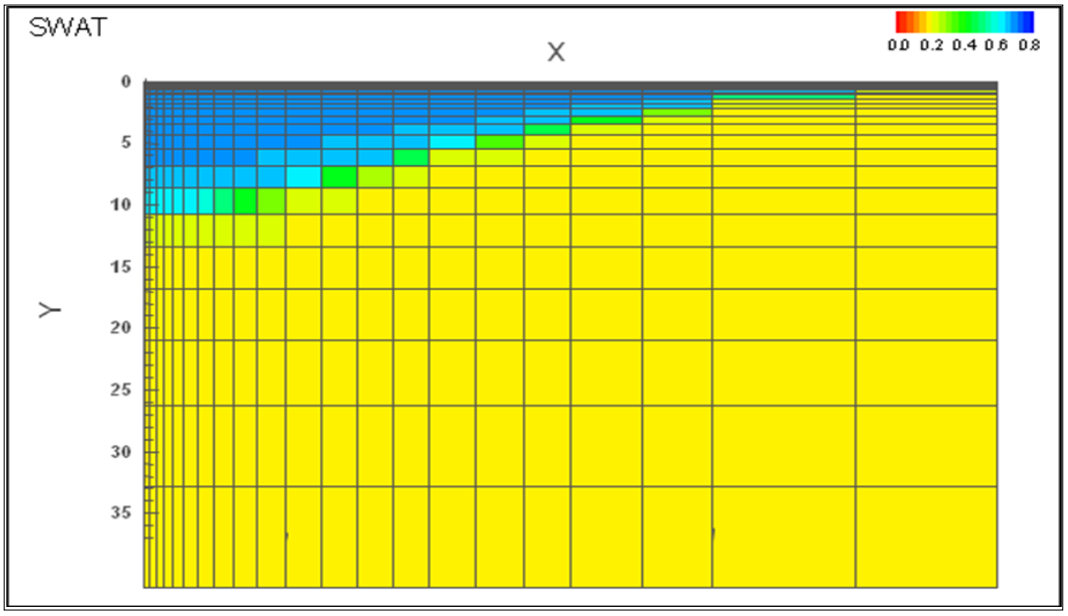


Figure 4- 16: Cross section showing effect of facture fluid leak-off effect

Similarly, the amount of water leaked-off into the formation for a long fracture is greater than that for a short fracture. The invaded water volume represents the amount of the fracturing fluid leaked-off during the fracture treatment. At the end of the injection, the saturation and pressure distributions will be used in the numerical simulation. The stimulated well will then be put on production and closed for pressure build-up and the generated pressure responses are exported into a well test package for interpretation.

During the clean-up period the initial produced fluid will be mainly water combined with oil. This gradually reduces to minimum rate as the fracture cleans-up and connection between wellbore and formation is established (*Figure 4-17*). The introduced pressure behaviour of the induced fracture is interpreted and the graph below (*Figure 4-18*) represents the expected behaviour of stimulated well affected by fluid leak-off effect.

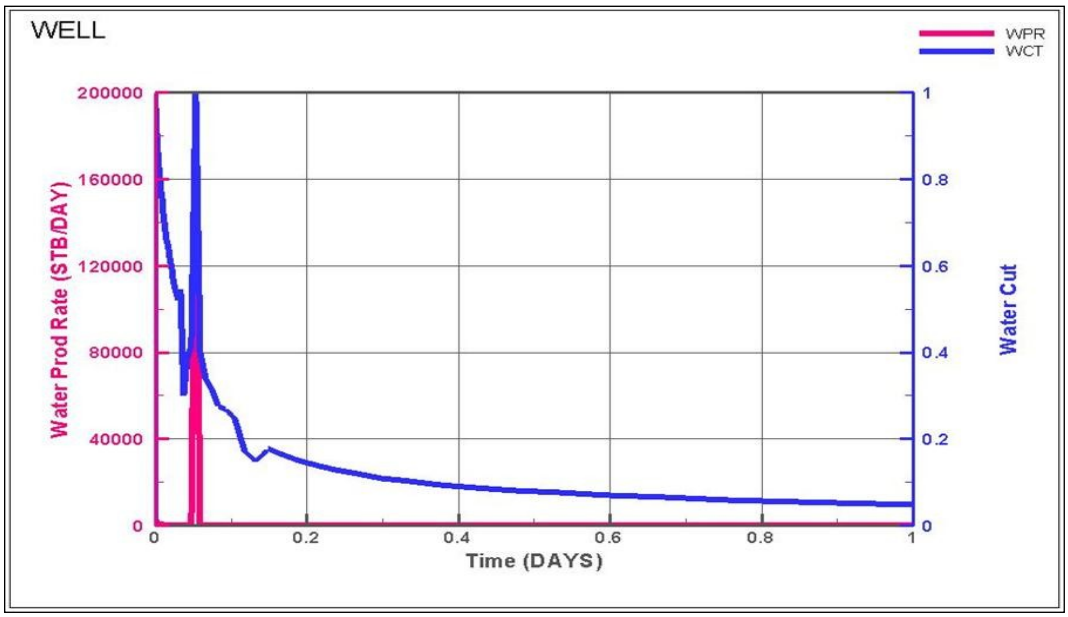


Figure 4- 17: Water production rate during clean-up period following well stimulation

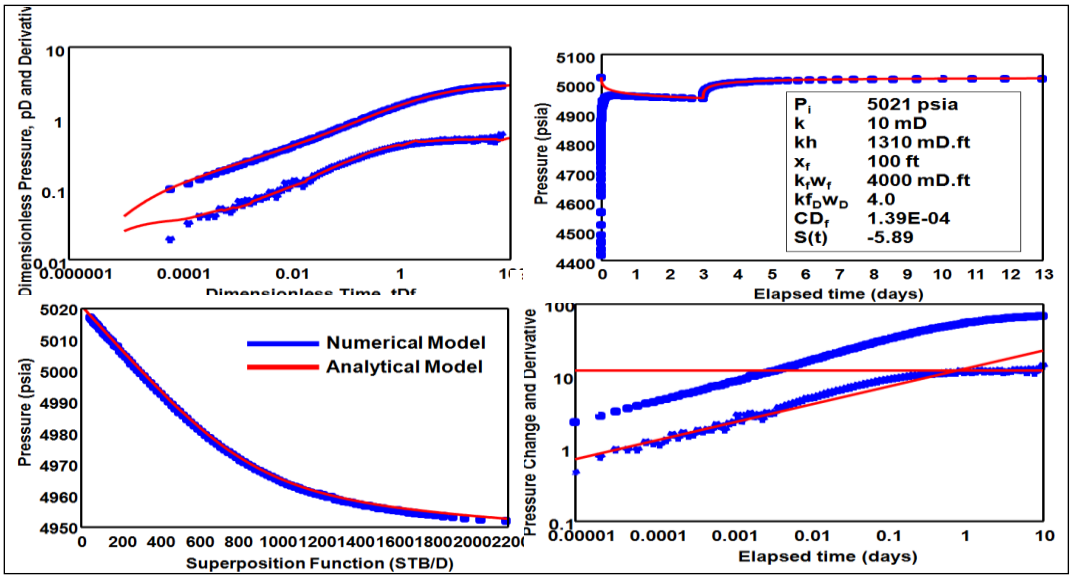


Figure 4- 18: Fracture leak-off effect in 10 mD formation with *FcD* of 4 and x_f of 100ft

4.2.5 Effect of Fracture Choke and Face skin

To investigate the effect of damage caused to the fracture as a result of stimulation process, a single layer model with formation permeability of 10 mD penetrated by a vertical fracture half-length of 100ft and fracture permeability of 10D was constructed. In order to mimic fracture choke effect, an altered (reduced) permeability zone was assigned within the fracture close to the wellbore of various dimensionless distances (x_{cD} is the damaged length, x_c to the fracture half-length, x_f ratio) from the wellbore. The results suggest that this type of fracture damage is considered the main cause of production impairment and introducing pressure profile similar to the investigated behaviour in this study (*Figure 4-19*).

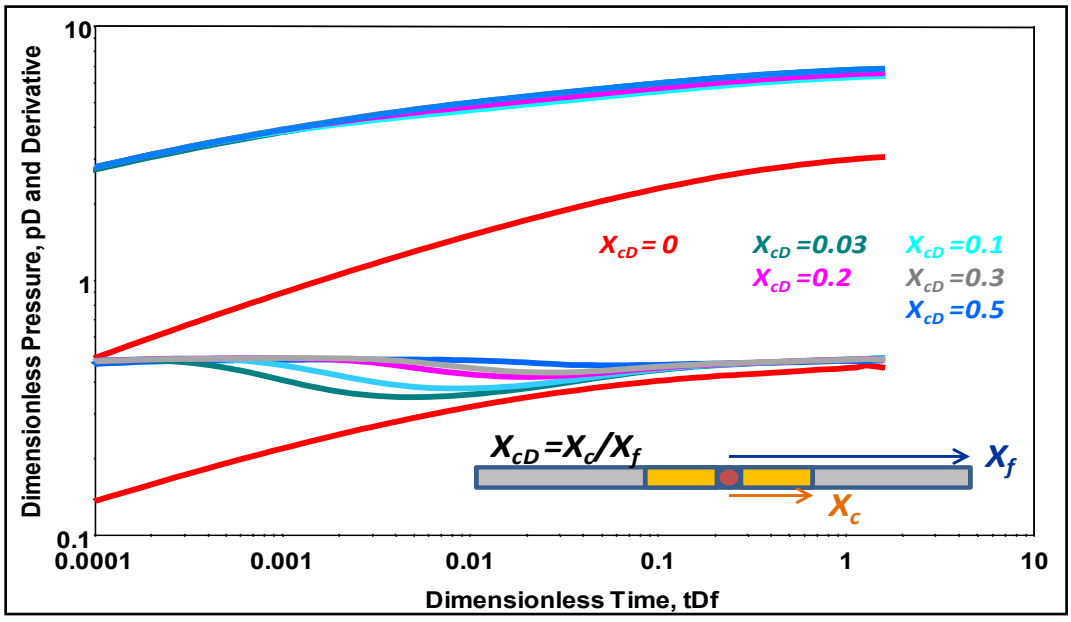


Figure 4- 19: Fracture choke effect on the pressure profile of fracture half-length of 100ft

In the above graph, it is assumed that the fracture choke will exist close to the wellbore and extends to various distances from the wellbore within a fracture length of 100ft. The plot shows that deeper choke extension; hence, more damage caused to the fracture will result in the possibility of not observing fracture flow pattern completely resulting in confusion with non-fractured well flow behaviour.

Another type of fracture damage examined in the study was fracture face skin (*Figure 4-20*). The face skin is assigned to the fracture face only (x_{fD} is the fracture length of reduced perm due to damage, x_s to the half-length, x_f ratio) up to various distances away from the fracture face. These distances with reduced permeability (up to tenth of the formation permeability) are believed to be representative of the fracture face damage in the model.

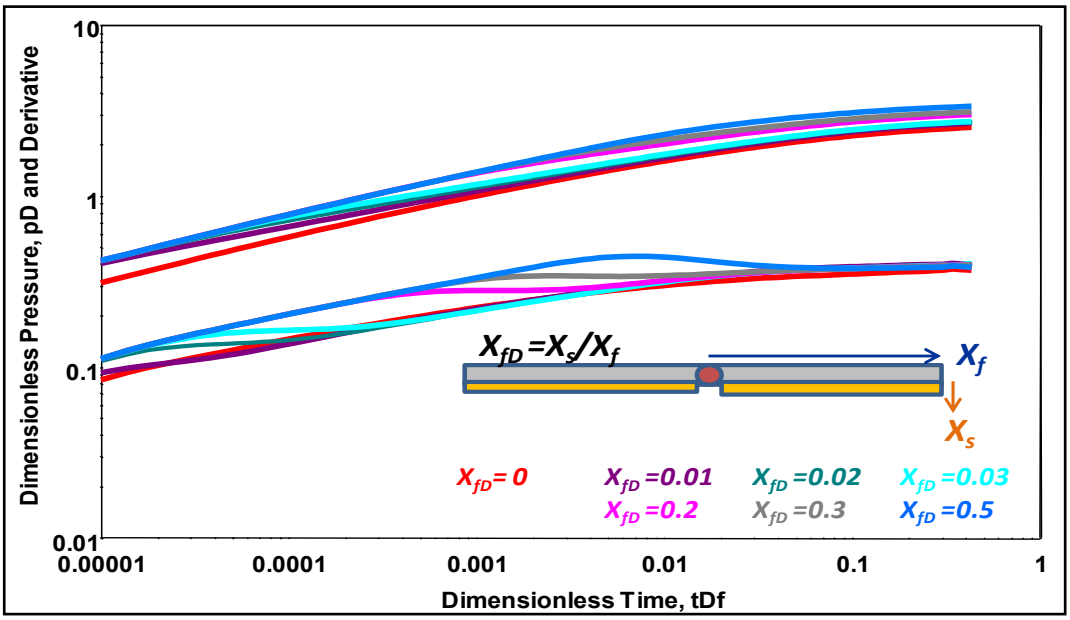


Figure 4- 20: Fracture face skin pressure profile of fracture half-length of 100ft

It is also possible that both types of damage (choke and face) may associate with the same induced fracture and this case would result in difficulty recognizing fractured well from non-stimulated well flow behaviour particularly in poorly performed frac jobs. In order to investigate the combined impact of choked and face skin damage on different reservoir settings, three cases were considered for low permeability of 1mD; moderate permeability of 10mD and high permeability formations of 100mD.

Figures (*4-21*) *and* (*4-22*) show the impacts of fracture choke and face skin on low permeability reservoir of 1 mD and 100md cases. The pressure behaviour of choke and face damaged fracture wells is similar to the behaviour of the investigated problem in this study of fractured well with some skin reduction.

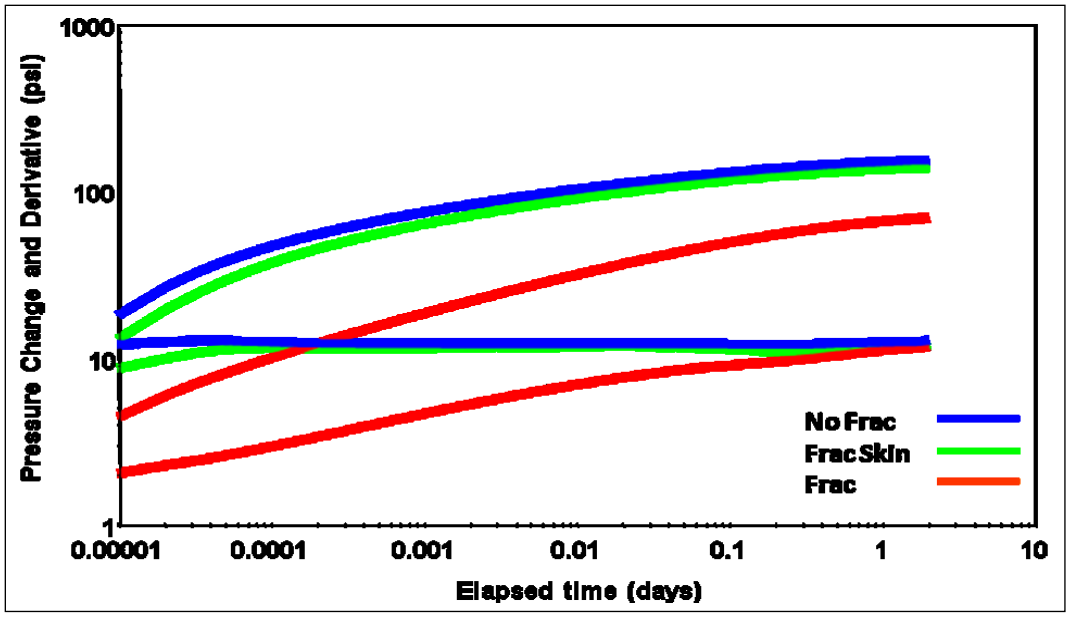


Figure 4- 21: Fracture face and choke effects in low permeability reservoir of 1mD

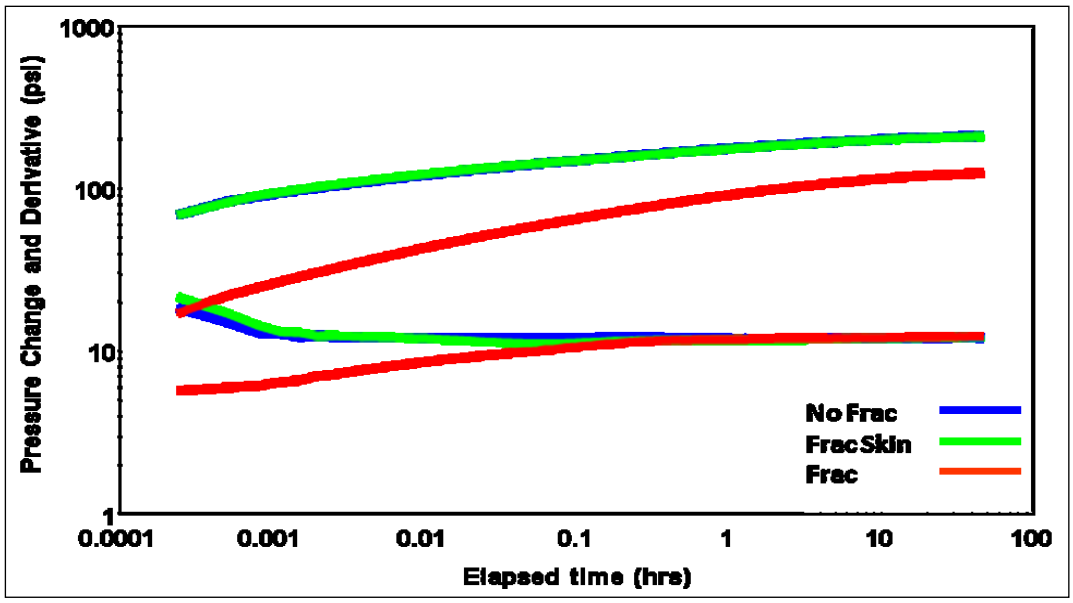


Figure 4- 22: Fracture face and choke effects in moderate permeability reservoir of 100mD

In addition, to investigate the flow behaviour of longer fractures, a fracture half-length of 500ft was considered. All cases run previously for 100ft damaged fracture (choked and face) cases were re-run and the results are illustrated below (*Figures 4-23 and 4-24*).

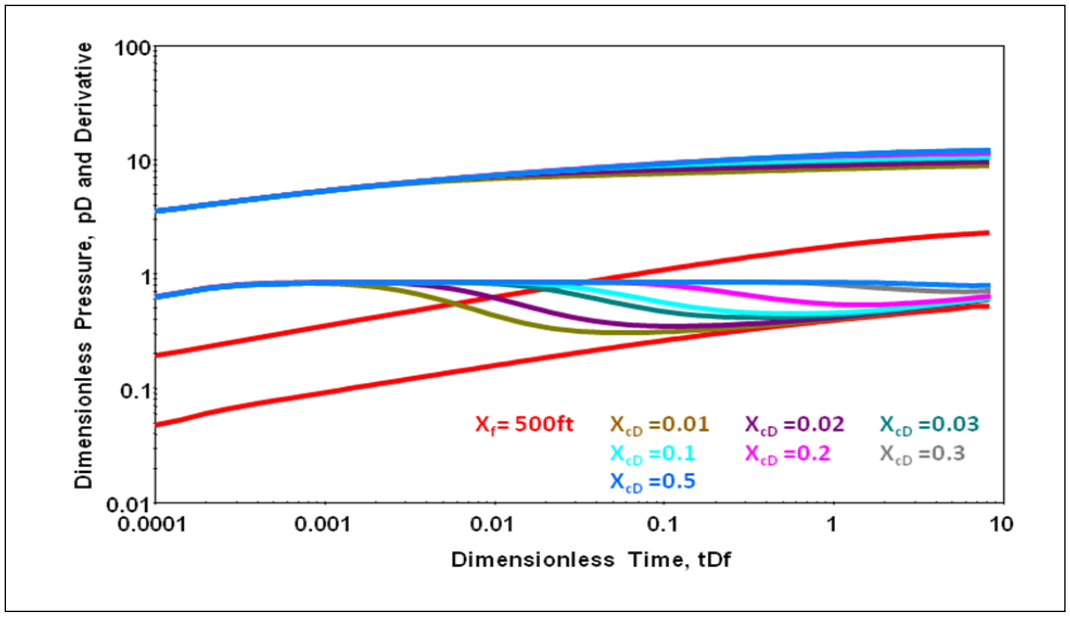


Figure 4- 23: Fracture choke effect on the pressure profile of fracture half-length of 500ft

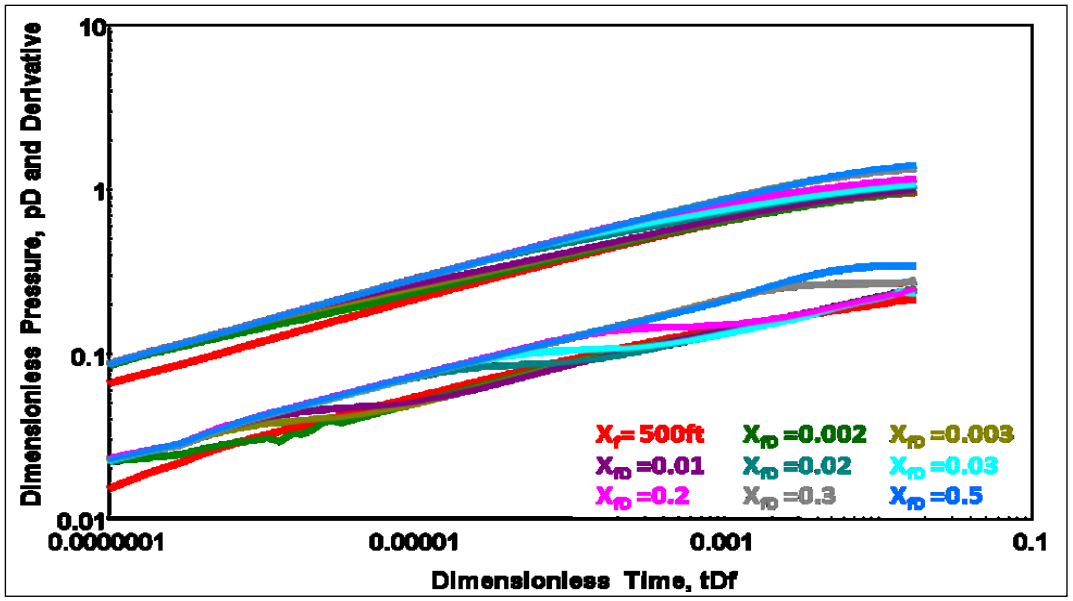


Figure 4- 24: Fracture face skin on the pressure profile of fracture half-length of 500ft

Figures (*4-25 and 4-26*) show fracture damage impact on the fractured well feature and the results suggest that the behaviour is more likely occurring in short damaged fractures.

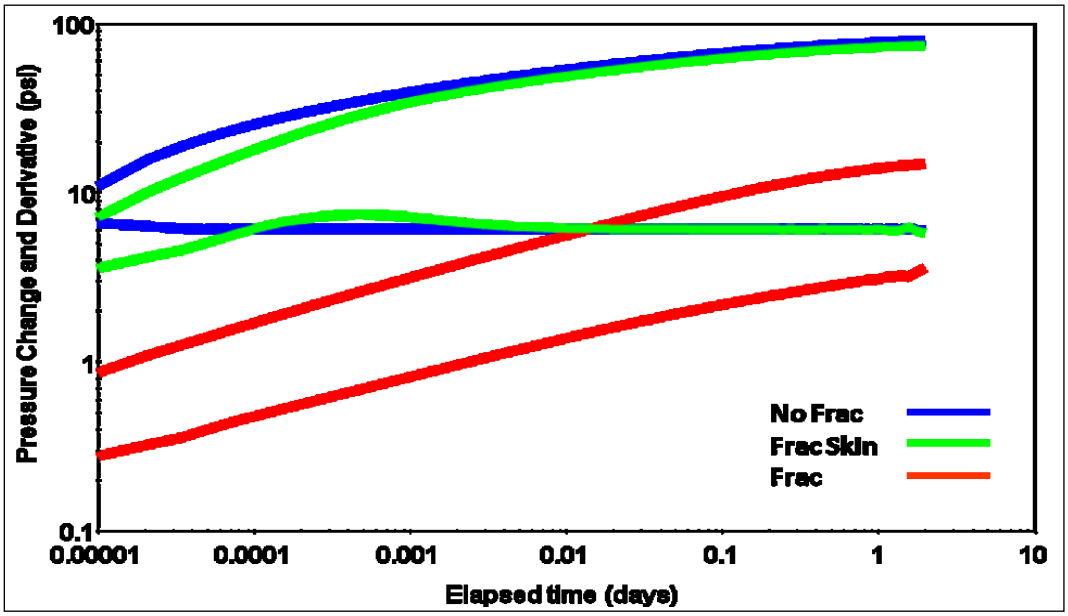


Figure 4- 25: Fracture choke and face skin effect in 1mD and fracture half-length of 500ft

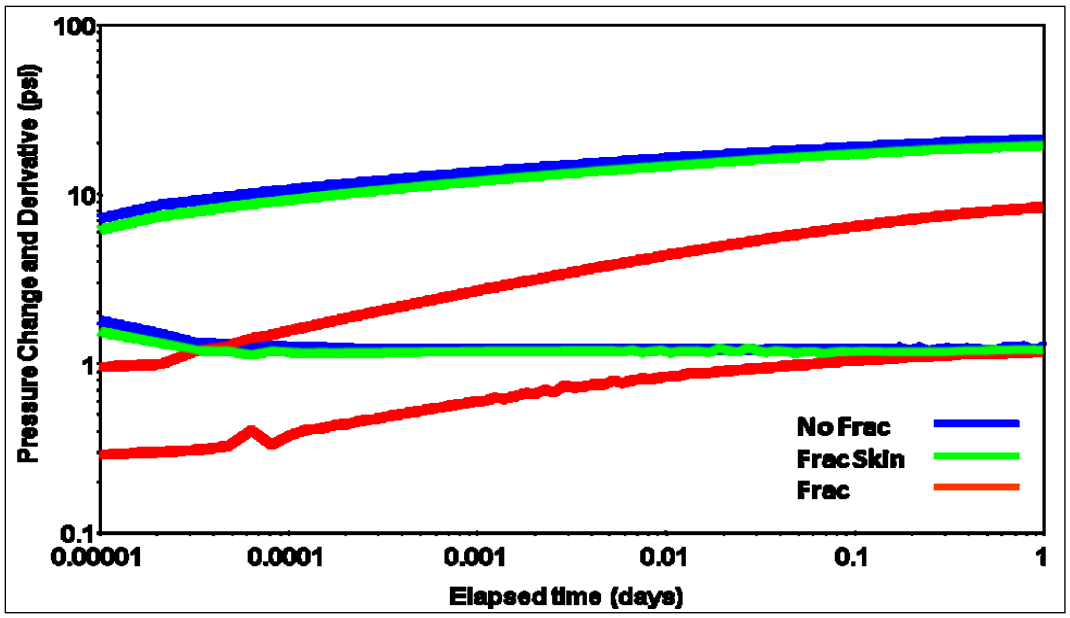


Figure 4- 26: Fracture choke and face skin effect in 100mD and fracture half-length of 500ft

Due to the significant impact of fracture choke and less effectively face skin damage on the flow behaviour of fractured wells, a single layer model with formation permeability of 10mD and fracture half-lengths of 10ft and 100ft was investigated individually. As stated previously in this document, the induced fracture half-length and conductivity; hence, fracture permeability play critical role on the developed shape of the generated

pressure profile of fractured wells. Detailed results of work performed to examine fracture choke and face skin impact on the generated pressure profiles can be found in Appendix – C in the document. As it can be seen in the graphs (*Figures 4.27 and 4.28*) for a fractured well with half-lengths of 10ft and 100ft associated with fracture choke damage (x_{cD} of 0.5), it is likely that the derivative shape will be similar to the non-fractured well derivative behaviour in the case of fractured well of short half-length of 10ft.

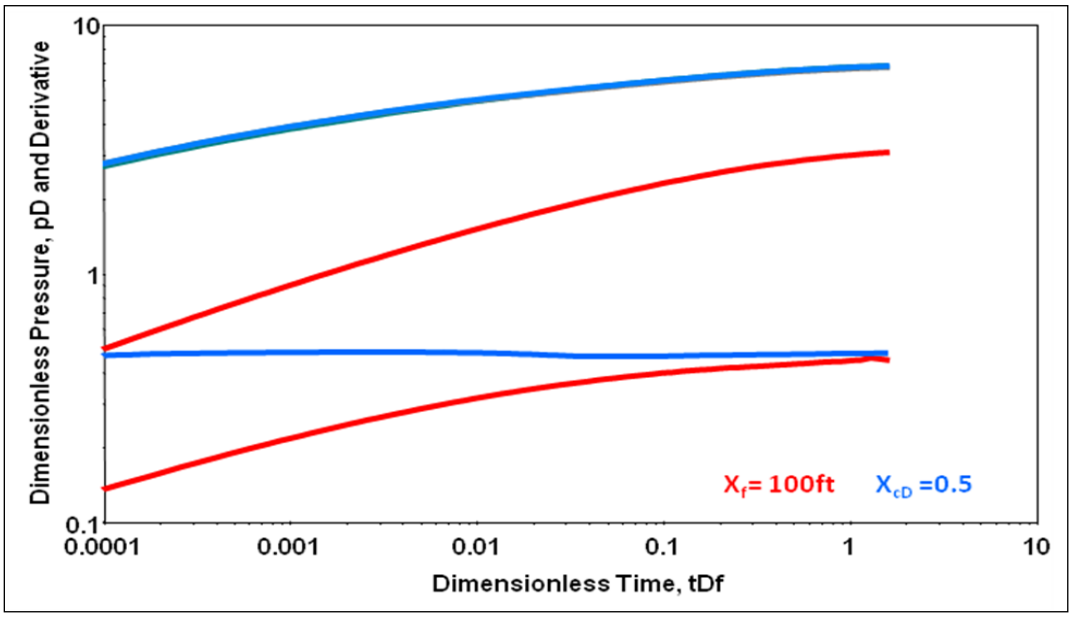


Figure 4- 27: Fracture choke effect on the pressure profile of fractures half-length of 10ft

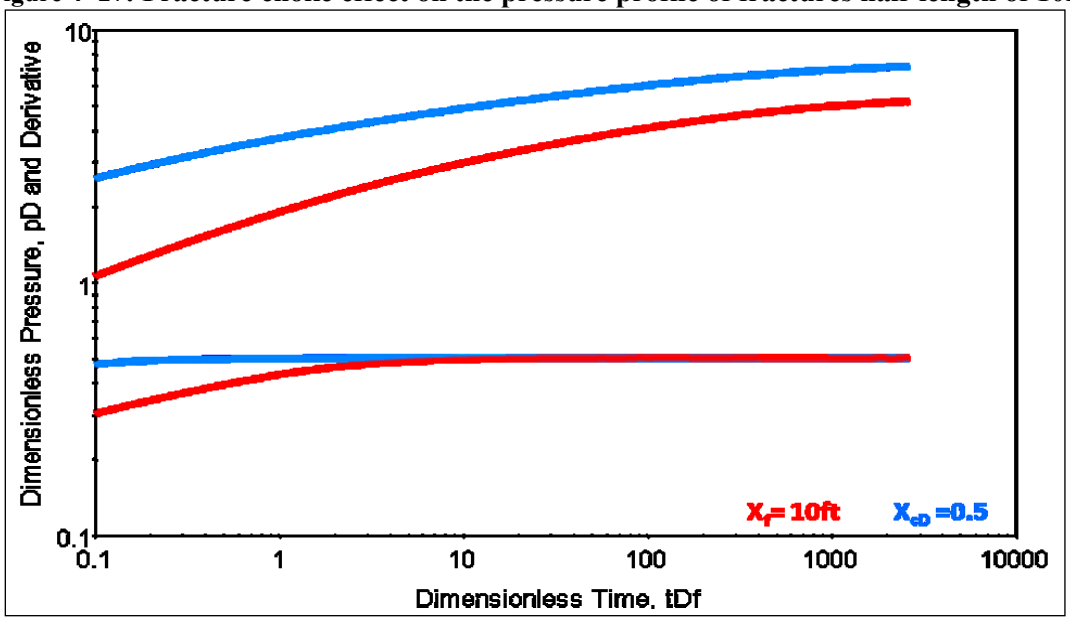


Figure 4- 28: Fracture choke effect on the pressure profile of fractures half-length of 100ft

Similarly the fracture face skin was investigated to understand fractured well behaviour in the presence of fracture face skin (x_{fD} of 0.5) and the results can be found in the graphs below (*Figures 4-29 and 4-30*).

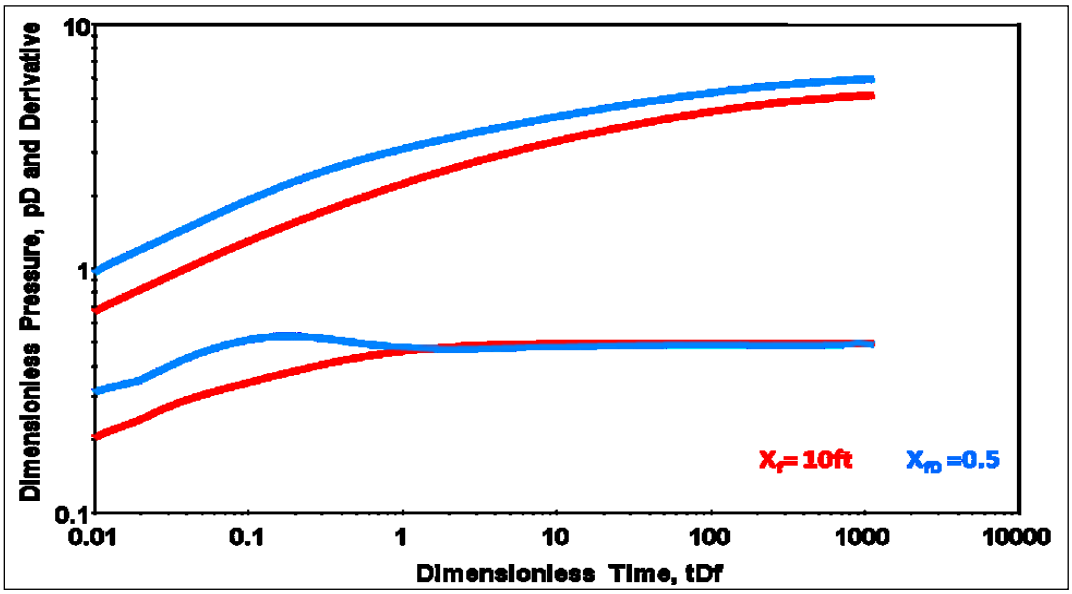


Figure 4- 29: Fracture face skin effect on the pressure profile of fracture half-length of 10

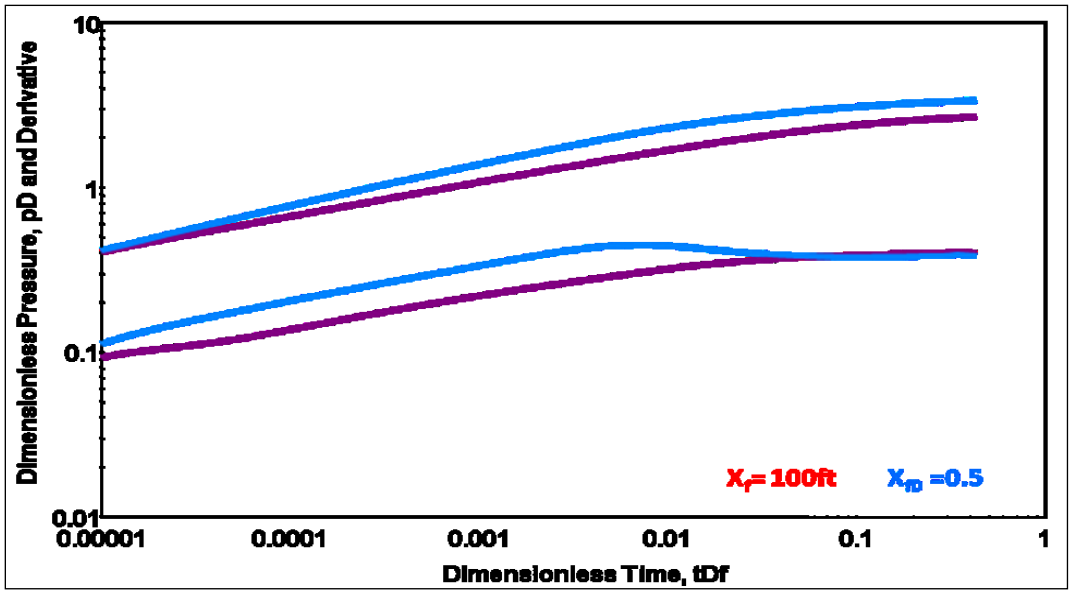


Figure 4- 30: Fracture face skin effect on the pressure profile of x_f of 100ft

By comparing behaviours resulted from implementing fractures with half-lengths of 10ft and 100ft and fracture choke and face skin effects, it appears that the reduced skin value for a fractured well as a result of the stimulation would be greater in long fracture half-length case. This indicates the fact that the shorter the induced fracture half-length, the less benefit is derived from the stimulated well particularly if the fracture job was not performed properly. The results can be seen in the plots below (*Figure 4-31*). More cases are modelled to demonstrate fracture damage effect can be found in the Appendix-C in this document.

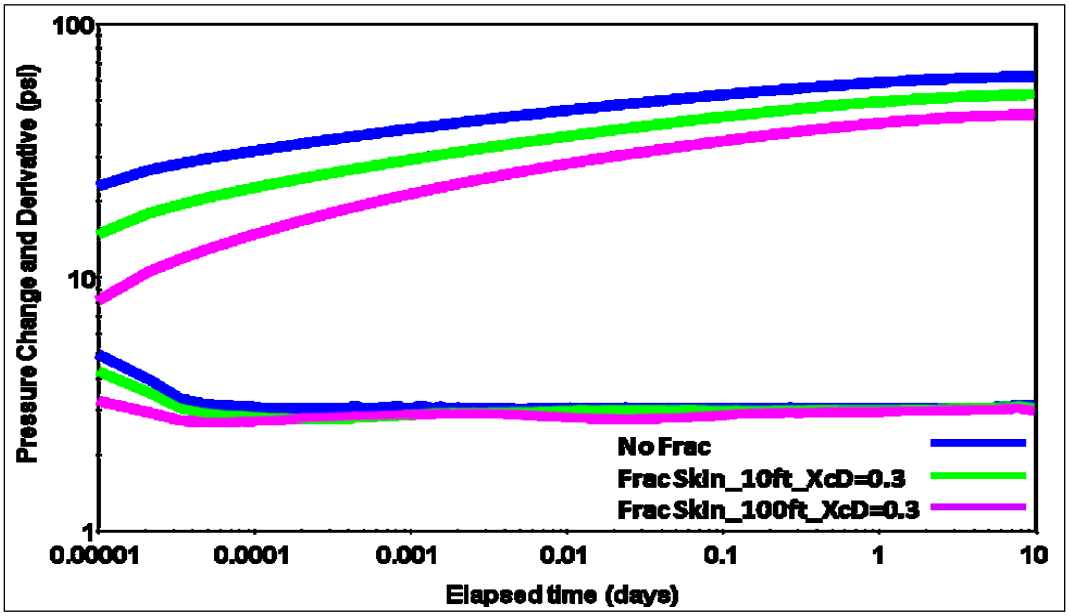


Figure 4- 31: Fracture choke effect comparison on the pressure profile of fractures half-lengths of 10ft and 100 ft

To conclude, fracture damage appears to be one of the control parameters in developing unusual fracture behaviour in not observing fractured well flow feature during the early times in post-frac well tests. Also, the current study results indicate that fracture choke effect is more effective in causing the fractured flow feature not to be seen compared to the fracture face skin. Therefore, it is critical to accurately design a frac job and execute the stimulation job as neatly as possible to avoid any difficulties in not observing fractured well flow behaviour and to obtain a good conductivity required to enhance productivity of the stimulated oil and gas wells.

4.2.6 Effect of Un-equal Fracture Half-length

It is a common assumption in the literature to propose that the induced fracture will have equal half-lengths on both sides of the wellbore. However, this assumption may not be valid as it is difficult to predict fracture directions when extending away from the well when one side of the fracture propagates longer or shorter than the other side into the formation. This problem has been investigated in both commingled and cross-flow system to examine the impact of communication between adjacent layers on the generated pressure responses.

For this purpose, a model of moderate permeability of 10 mD penetrated by a fracture of 200ft length initially of equal half-lengths of 100ft on each side of the wellbore . Three cases were then run in which fracture half-lengths were 10ft by 100ft, 25ft by 100ft and 50ft by 100ft. The generated pressure data was interpreted and the results can be found below (F*igures 4-32 and 4-33*). The results indicate that the interpreted fracture half-lengths are 55ft, 70ft and 80ft respectively and similar pressure behaviour were found in commingled and cross-flow cases.

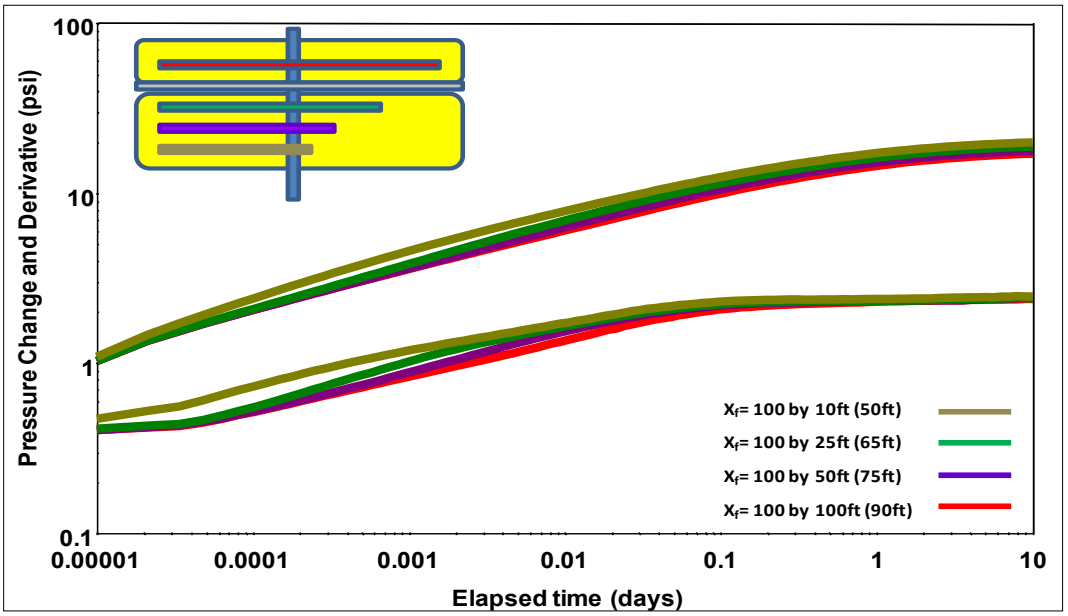


Figure 4- 32: Un-equal fracture half-length effect in commingled layers case

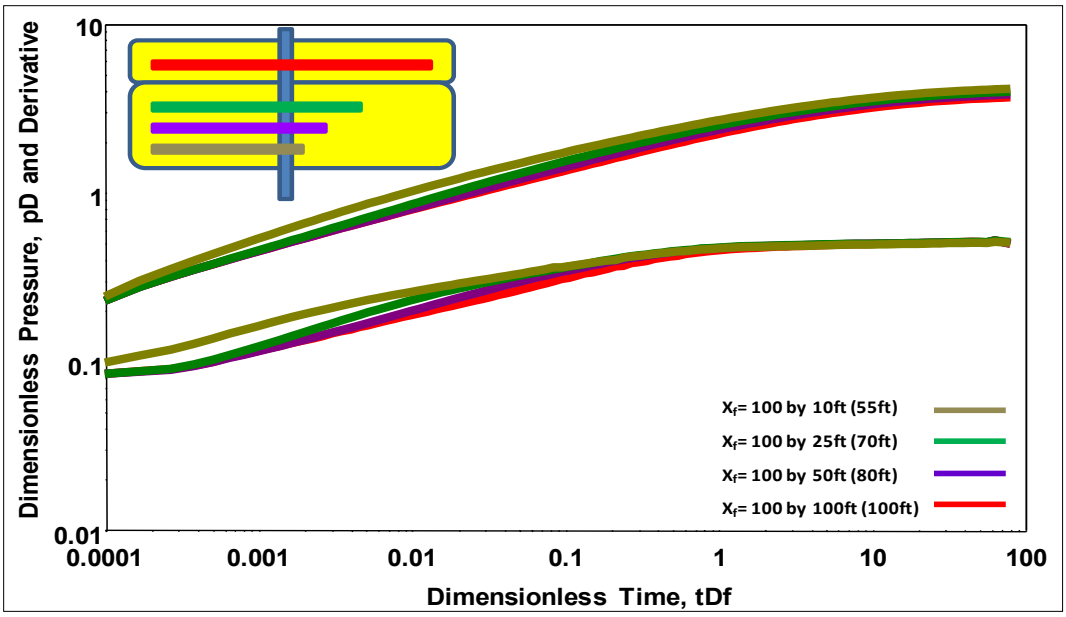


Figure 4- 33: Un-equal fracture half-length effect in cross-flow scenario

4.2.7 Effect of Fracture Width, w_f

The effect of fracture width on the generated pressure feature is investigated in a single model with different widths. As it can be noticed in the plot below (*Figure 4-34*) the smaller the width, the closer the pressure response to the non-fractured well behaviour.

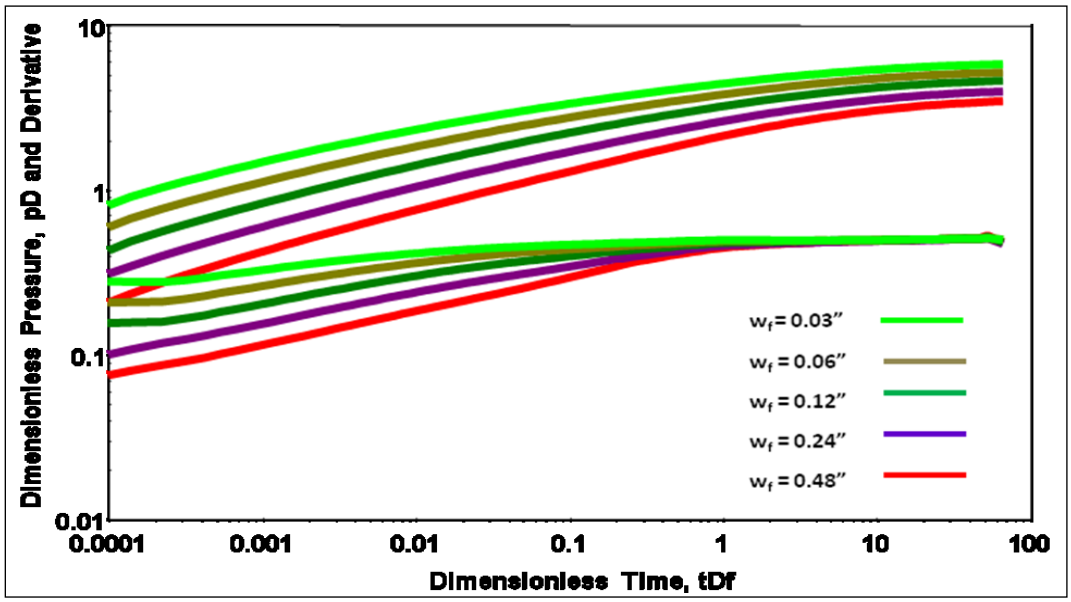


Figure 4- 34: Fracture width effect on the pressure response

4.2.8 Effect of Fracture Conductivity, $K_f w_f$

To investigate the fracture conductivity effect on the pressure response of proppant fractured wells, a model was constructed in which a 100ft fracture half-length penetrating 117.3ft of 10md formation. A range of fracture models with dimensionless fracture conductivity values of (1, 1.6, 10, 30 and 50) were built. The graph below (*Figure 4-35*) illustrates the results of all the runs, which show that the smaller the *FcD* value, the closer the flow behaviour of a fractured well is to a non-fractured well response. Also, as can be seen from the plot, there is very little difference between pressure derivative responses from fractures above *FcD* value of 10.

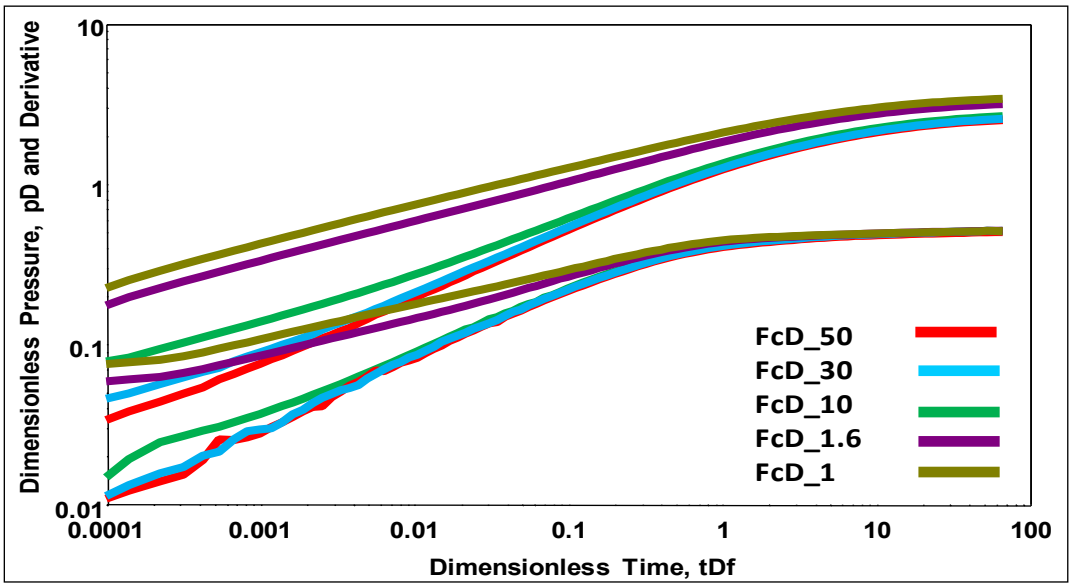


Figure 4- 35: Fracture conductivity value effect on the well flow behaviour

In this study, an *FcD* value of 10 is considered as the optimum dimensionless fracture conductivity that can be obtained from properly performed frac job. Based on the above plot, it appears that the investigated behaviour is likely to occur in fractured wells with *FcDs* of less than 0.1; any values higher than that will clearly illustrate fractured well flow behaviour.

4.2.9 Effect of Formation Fractured Interval

In order to investigate fractured interval height effect, a 10 mD single layer model with fracture height of 120ft and completed fractured thicknesses of 30, 60, 90 and 120ft was constructed. Such sensitivity is important when the formation is partially fractured and plot below (*Figure 4-36*) shows the results obtained from the runs. The results indicate that the behaviour may occur in fractured wells of low *FcD* in partially fractured formation. By examining the generated plots in this section, it can be concluded that a partially completed fracture may cause the problem of not observing fractured flow behaviour in post-frac well tests.

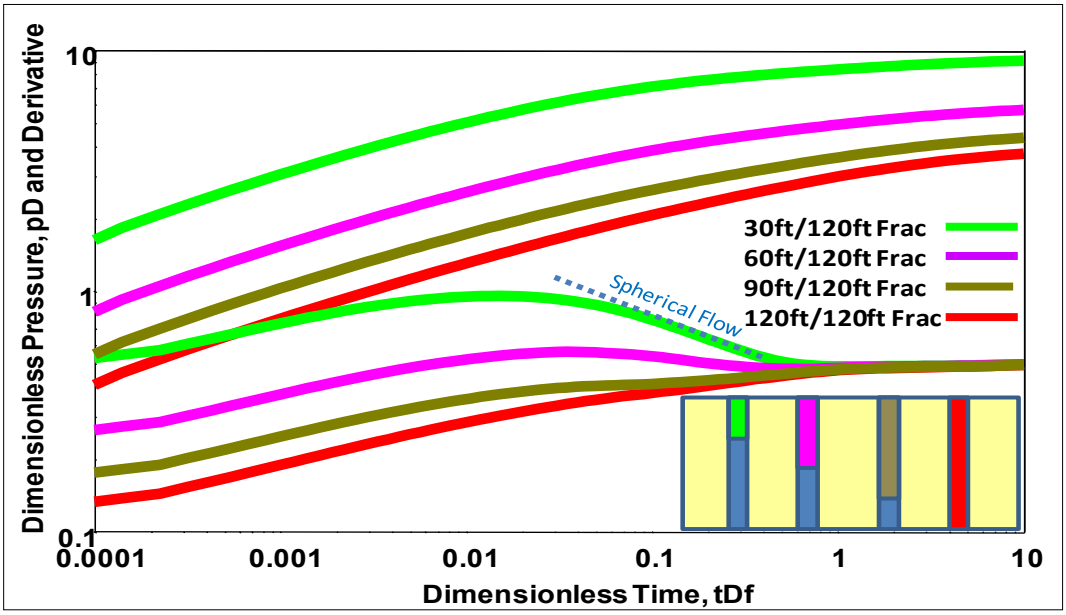


Figure 4- 36: Partially fractured formation effect with X_f=100ft and 10mD formation

Another two scenarios with *FcD* of 0.1 and 1 were considered in which the formation was partially fractured at a depth of 10, 20, 40, 60, 80 and 100ft thickness from the mid interval rather than at the top of formation. Such sensitivity is important when the formation interval is partially fractured and the following plots (*Figures 4-37 and 4-38*) show the results obtained from two cases.

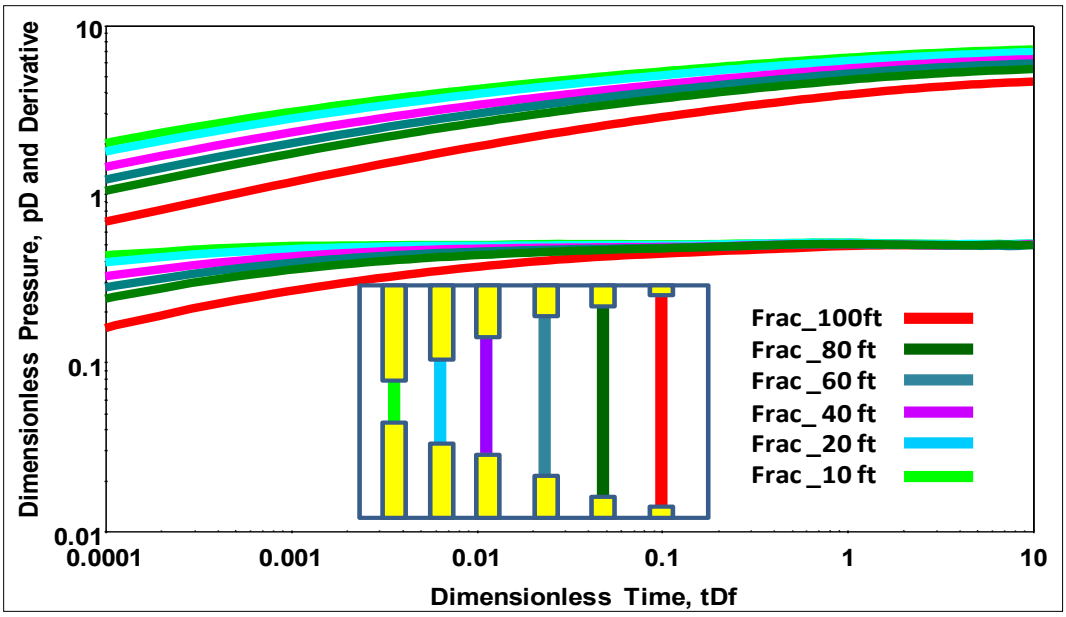


Figure 4- 37: Completed fractured interval effect on the fractured well flow behaviour (FcD=0.1)

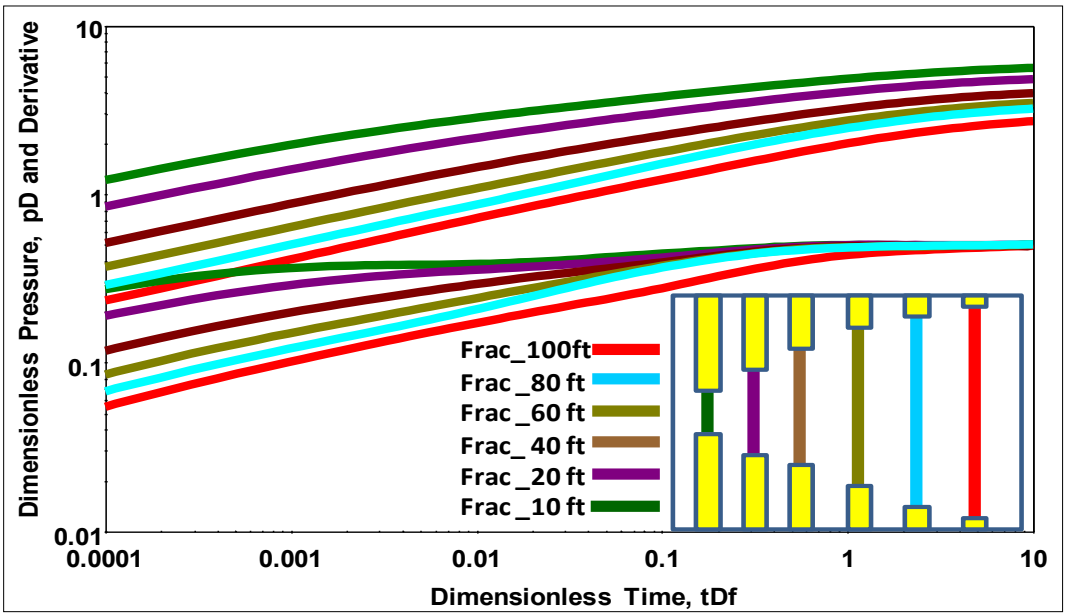


Figure 4- 38: Completed fractured interval effect on the fractured well flow behaviour (FcD=1)

4.2.10 Effect of Non-Darcy in Gas Reservoirs

The non-Darcy effect (*Figure 4-39*) in gas reservoirs was investigated to assess the importance of such a parameter that impacts significantly the productivity of the well through increasing pressure drawdown due to high velocity fluid flow particularly in the fracture close to the wellbore and in the vicinity of the well (*Figure 4-40*).

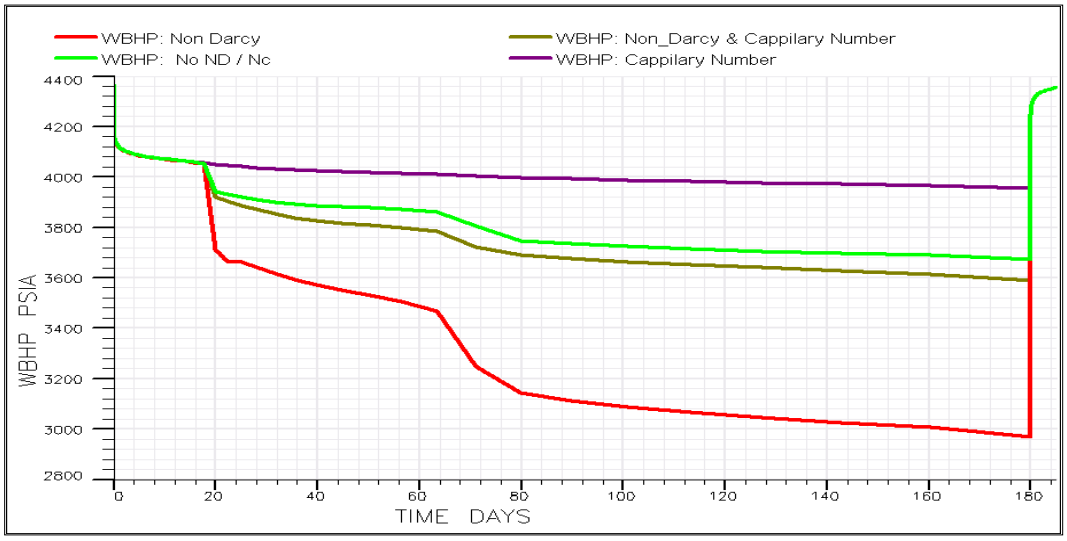


Figure 4- 39: Effects of non-Darcy (red) and capillary number (purple) on the pressure

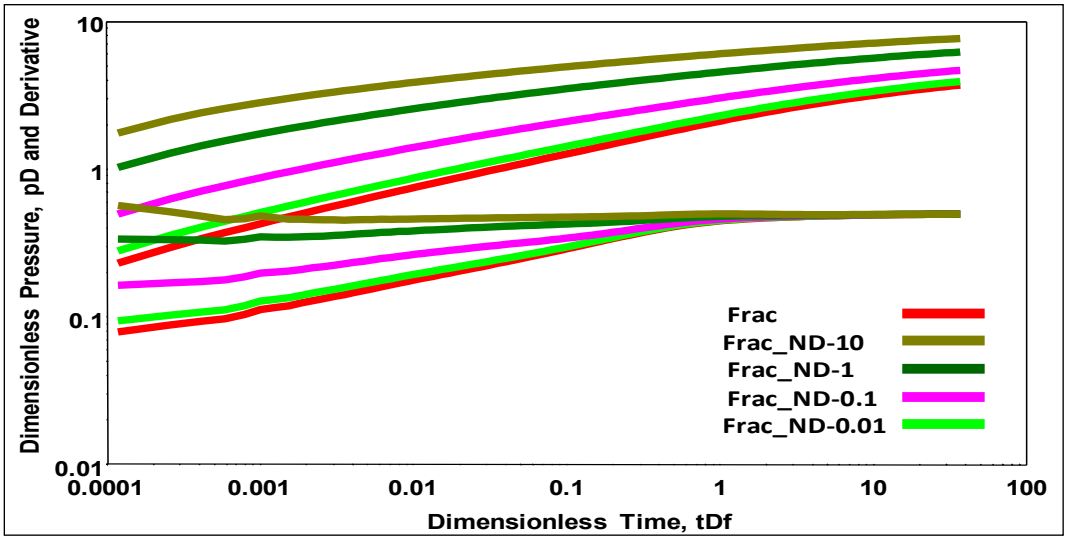


Figure 4- 40: Non-Darcy effect on the generated pressure behaviour of fractured wells

Keyword "VDFLOW" enables the treatment of non-Darcy effect in inter-block flow, and specifies the non-Darcy flow coefficient. This is commonly known as β, the non-Darcy flow coefficient, and is entered in units of atma.s^2.g^{-1} (the Forchheimer unit) and typical

value of $\beta = 10^7 cm^{-1}$, which is 9.86 Forchheimer units. Initially a value of 10 was used followed by runs with non-Darcy flow coefficient of 1, 0.1 and 0.01. The results indicate that non-Darcy is the most critical parameter that causes infrequent flow behaviour problem to develop

4.2.11 Effect of Proppant Agent Type

In the literature some workers like Al-Ghurairi *et al* (2006) and Duverney *et al* (2007) have related the investigated behaviour problem in the current study to the use of certain proppant agents called Resin Coated Proppant, in stimulating gas reservoirs in particular. To investigate this theory and its validity in causing the problem, a model with two layers of 10 mD each separated by a barrier was constructed; RCP was then used as the fracturing material with different damage degrees of 10% (up to 8.6D of proppant permeability) and 90% (up to 1.6D proppant permeability).

As can be seen in the plot below (*Figure 4-41*) in the case of 90% proppant damage, fracture half-length of 33ft only are calculated from well test analysis as compare to 10% damage, which shows that the designed 100 ft fracture half-length in the simulator was obtained from the well test analysis. This demonstrates the fact that proppant permeability within the fracture controls the value of calculated fracture length form well test analysis.

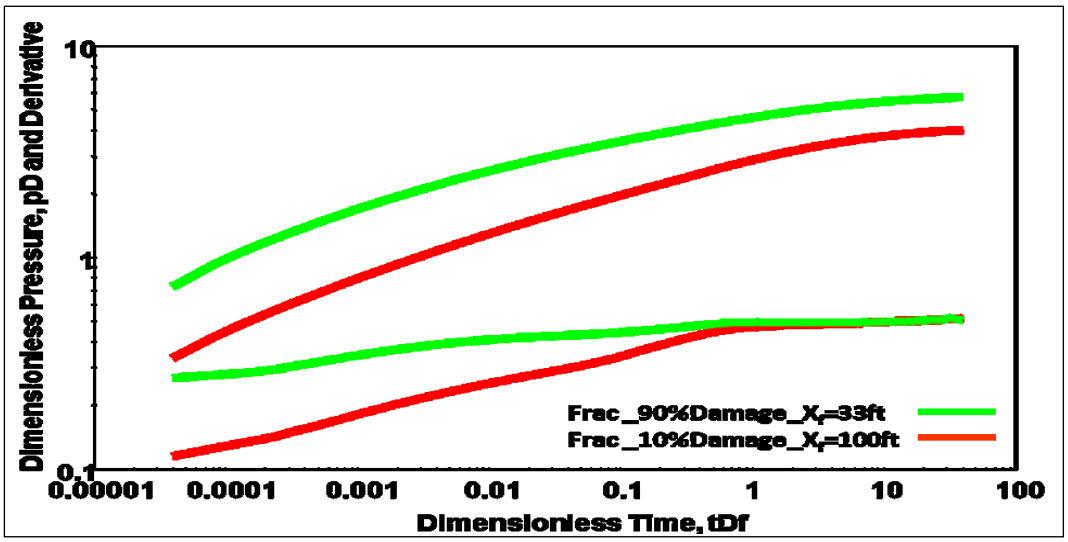


Figure 4- 41: RCP as fracturing proppant agent with different damage effects

4.2.12 Effect of Multi-layered (Two Layers)

In another approach to investigate unusual fractured wells behaviour in heterogeneous multi-layered reservoirs with a permeability contrast between layers, two cases of commingled two layers model with permeabilities of 0.1 by 10mD in the low to moderate permeability scenario and 10 by 100mD in the moderate to high permeability case were investigated. In a similar approach to the homogeneous single layer scenario, various sensitivities were investigated assuming various fracture half-lengths (10, 25, 50 and 100ft) and various fracture permeabilities of 0.1, 0.5, 1 and 1.5D in the case of low permeability reservoirs and 1, 1.5, 2 and 5D for high permeability formations (*Figures 4-42 and 4-43*).

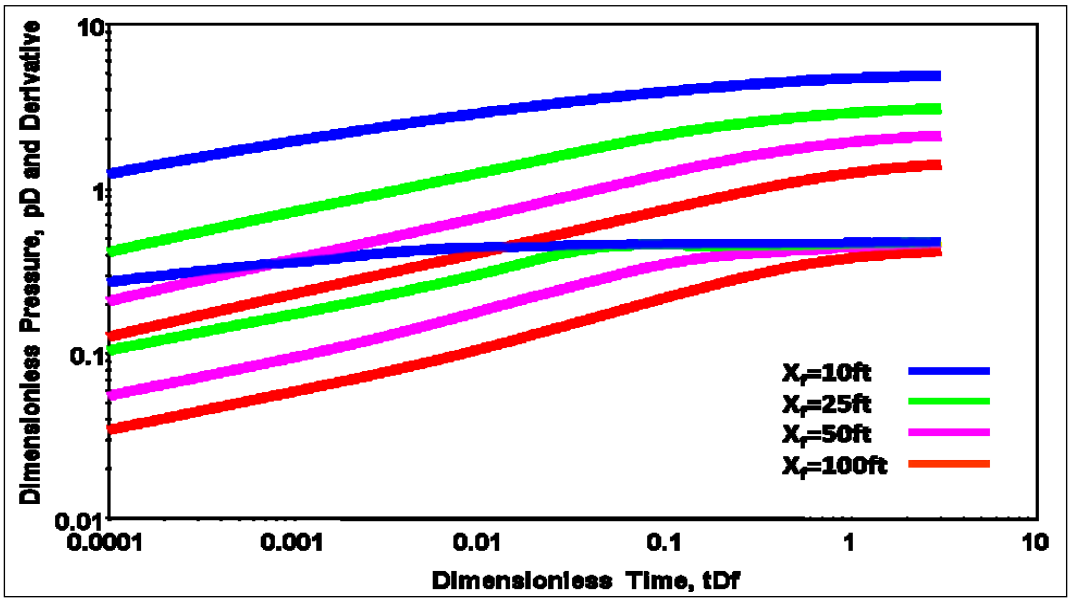


Figure 4- 42: Two layers of 0.1 by 10 mD with fracture permeability of 0.1, 0.5, 1 and 1.5D and fracture half-lengths of 10, 25, 50 and 100ft

Based on the simulation run results, it can be concluded that short fracture half-length is a critical parameter in causing the behaviour investigated in the study. As it can be seen from examining the following plot, the shorter the fracture created the closer the generated behaviour to the non-fractured well flow feature.

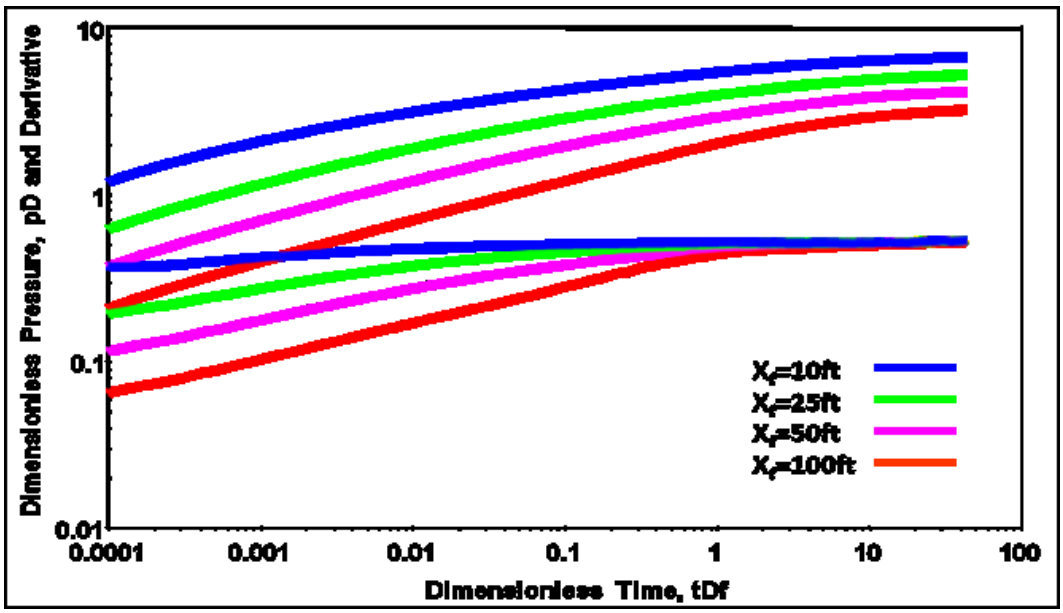


Figure 4- 43: Two layers of 10 by 100 mD with fracture half-lengths of 10, 25, 50 and 100ft

To investigate longer fracture half-lengths, a new model was constructed to include fracture half-length of 500ft and *FcD* of 1, plots below show the results (*Figures 4-44 and 4-45*).

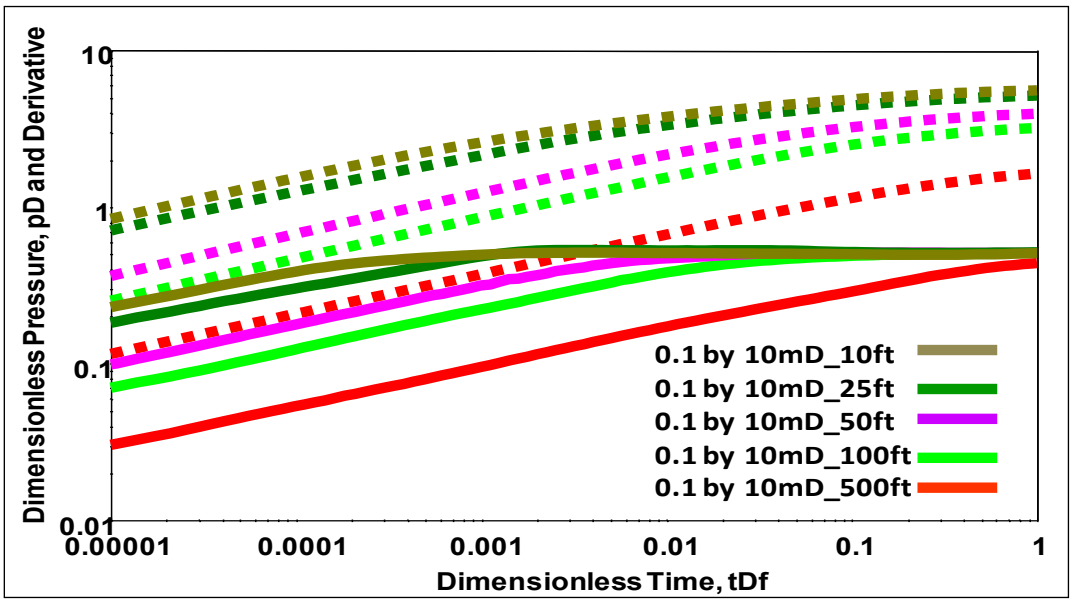


Figure 4- 44: Two layers of 0.1 by 10mD and fracture half-lengths of 10, 25, 50,100 and 500ft

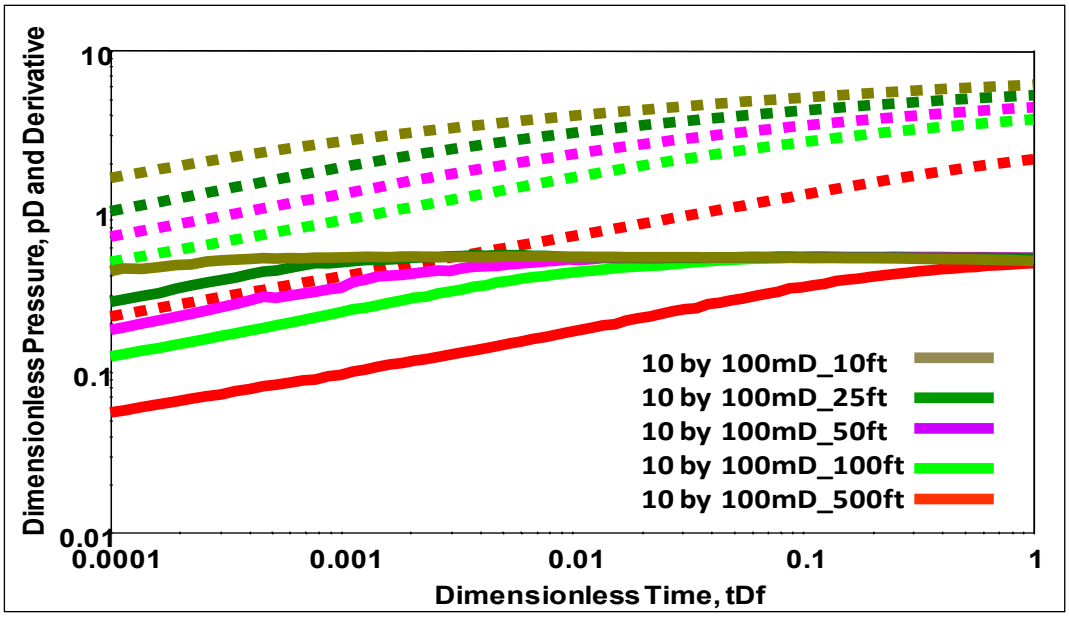


Figure 4- 45: Two layers of 0.1 by 10mD and fracture half-lengths of 10, 25, 50,100 and 500ft

In addition, a model consisting of two layers with permeabilities of 0.01 and 100 mD separated by a barrier was set up to investigate a high permeability contrast between layers and fracture configuration impact on the pressure responses of a fractured well. As can be seen from the plots (*Figures 4-46and 4-47*).; when fracturing the top layer of low permeability (0.01mD) only, multi-layer flow behaviour can be observed clearly with increasing fracture permeability, which results in combination behaviour of fractured flow behaviour together with multi-layer effect at early time.

However, when the bottom layer of high permeability (100mD) is stimulated only, the signature of fractured flow pattern can be noticed more clearly as fracture permeability increases, which indicates the importance of such a parameter in causing infrequent fractured well flow behaviour. In this case, fracture permeabilities used were 1, 2.5, 5, 10 and 20D, a range of permeabilities that can be expected from typical fractured wells. The results indicate that for the unusual behaviour to develop in a multi-layered case with significant permeability contrast between layers, the fracture must be propagating into lower permeability layer with lower conductivity fractures.

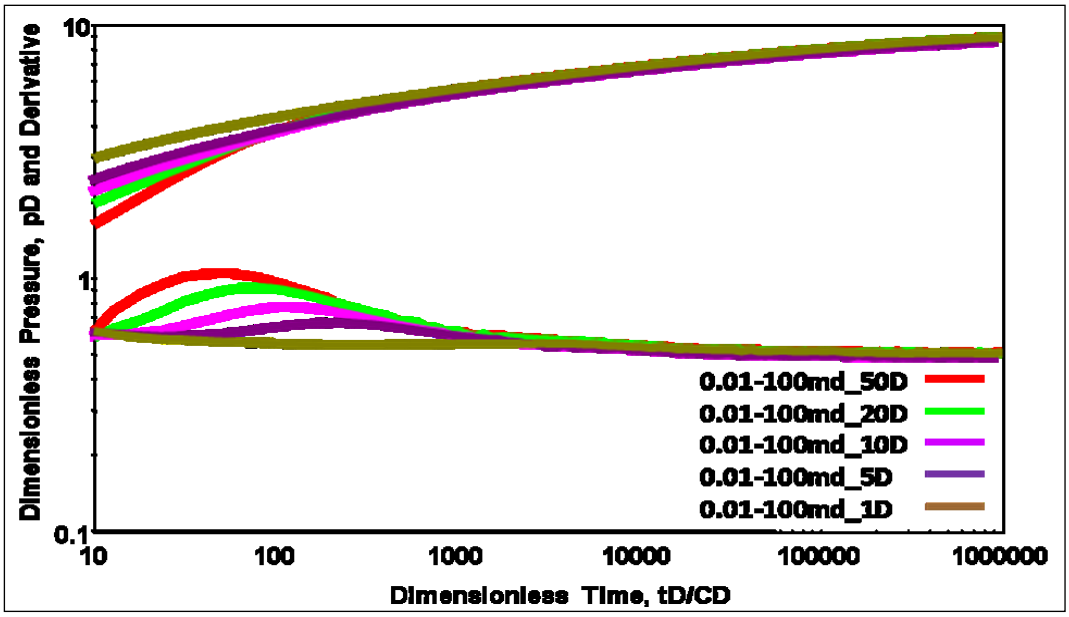


Figure 4- 46: Two layers with top layer (0.01mD) fractured only

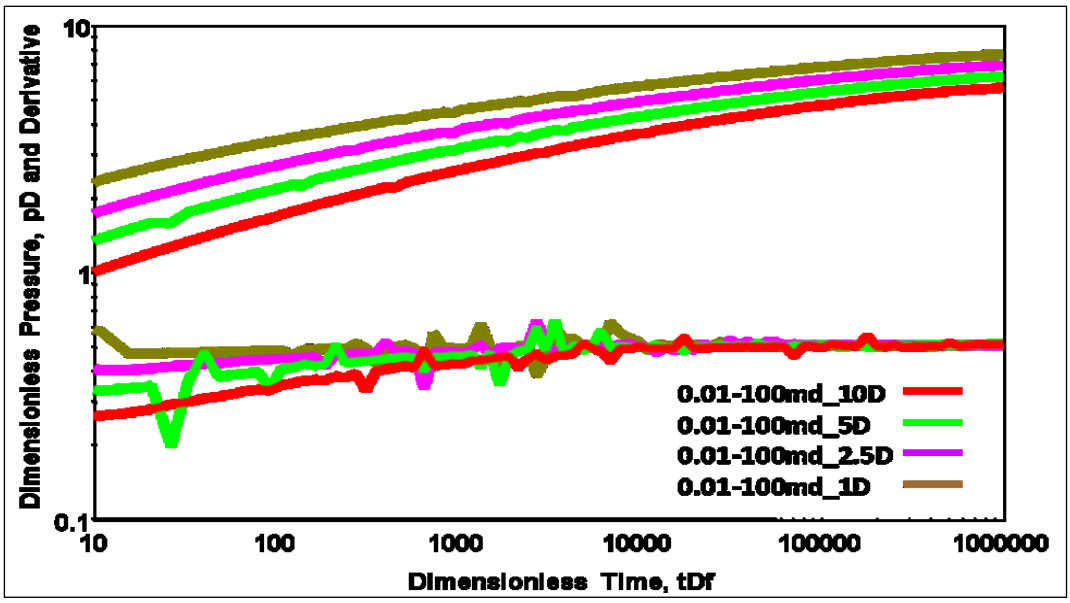


Figure 4- 47: Double layers with lower layer (100mD) fractured only

Furthermore, to examine formation permeability effect in multi-layered system, two layers with permeabilities of 0.1 by 10mD; 0.01 by 10mD; 0.1 by 100mD and 0.01 by 100mD were investigated. By examining the graph below (*Figure 4-48*) it can be observed that in layers with low permeability (0.1 by 10 and 0.01 by 10mD) the fracture flow pattern is clearly observed even with low fracture permeability of 1D.

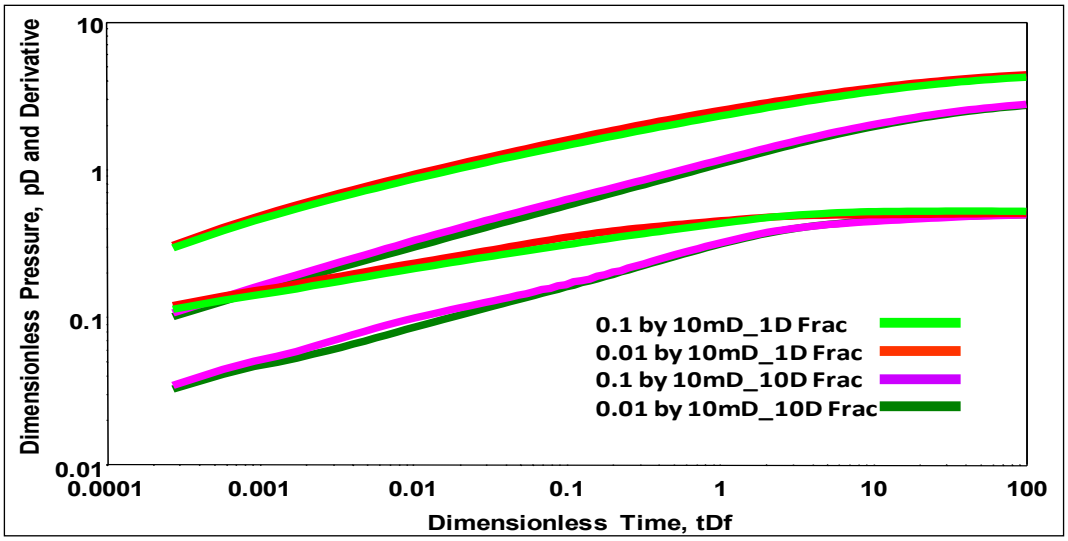


Figure 4- 48: Two layers of 0.1 by 10mD and 0.01 by 10mD, clear fracture flow behaviour

However, with higher formation permeability of 0.1 by 100 and 0.01 by 100mD as can be seen in the following plot (*Figure 4-49*) there is no indication of fracturing in the case of low fracture permeability of 1D. This indicates that for low fracture permeability cases and as formation permeability increases it is unlikely to observe induced fracture of low conductivity (low permeability) clearly in the post-frac well test. To conclude, in the case of multi-layered reservoirs with high permeability contrast between layers, the fracture has to propagate into the lower permeability layer rather than higher permeability layer in order to introduce behaviour similar to non-stimulated well behaviour.

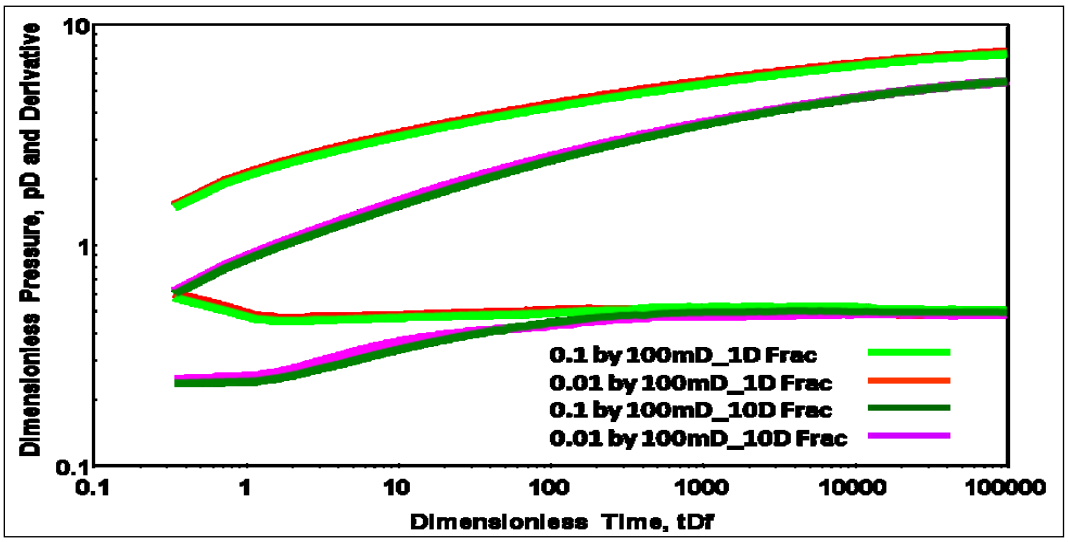


Figure 4- 49: Two layers of 0.1 by 100mD and 0.01 by 100mD, no fracture flow behaviour can be observed in low fracture permeability case of 1D

In addition, in another approach a two layers model was built (*Figure 4-50*) with top layer of 0.01mD and bottom layer of 100mD stimulated with fracture permeability of 1 and 10D. The results indicate low fracture permeability relative to the formation is critical factor in the development of unusual fractured well flow behaviour.

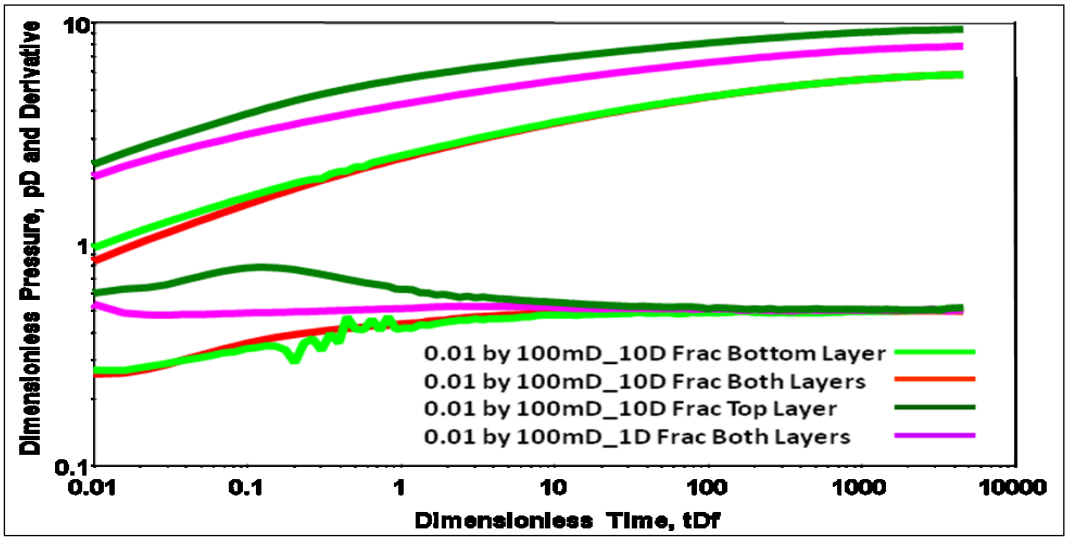


Figure 4- 50: Two layers of 0.01 by 100mD perm with fractured permeabilities of 1 and 10D

To examine the impact of the permeability contrast between layers on the generated flow behaviour features in multi-layered system, a two layers model was constructed with a bottom layer permeability of 100mD and top layer permeabilities of 0.001, 0.01, 0.1 and 1mD (*Figure 4-51*).

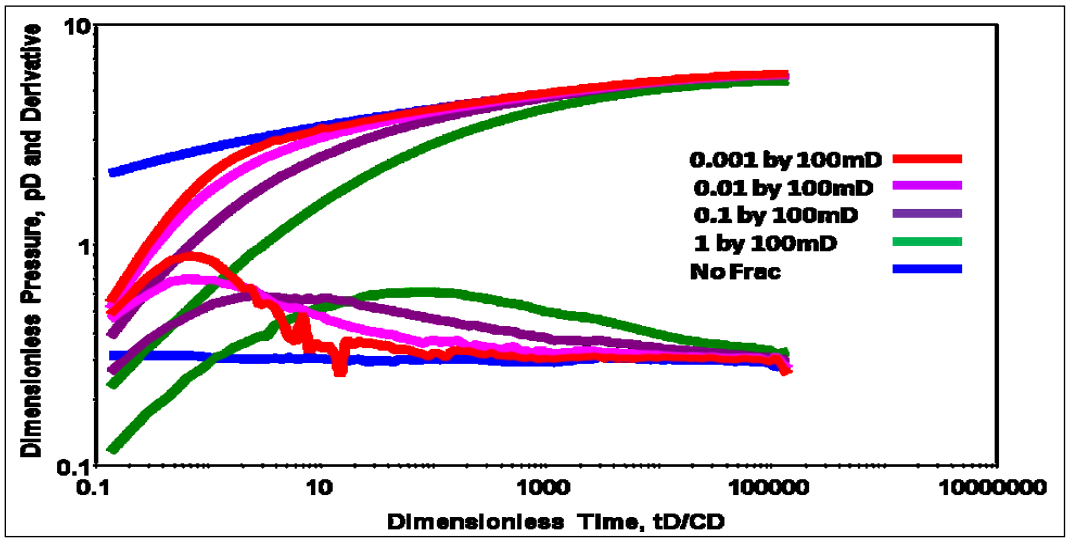


Figure 4- 51: Two layers of 0.001. 0.01. 0.1 and 1D by 100mD perm with fractured permeabilities of 1 and 10D

The results demonstrate that fracturing the top layer with a low permeability of 0.001mD only results in the investigated unusual behaviour to occur. By reducing the permeability contrast between the layers, the multi-layered flow behaviour feature is observed together with the fracturing effect.

To conclude, the investigated infrequent fracture flow behaviour in this study is likely to occur when the fracture propagates to the layer of lowest formation permeability. Also, results suggest that the lower the permeability contrast between layers, the less likely it is that the unusual behaviour will develop. Finally, low fracture length and conductivity (i.e. low fracture permeability) are two critical factors to cause the problem investigated in this study.

4.2.13 Effect of Multi-layered (Three layers)

To examine the behaviour in heterogeneous formations consisting of more than two layers, a model was constructed comprising three layers of 0.1, 10 and 100mD permeability separated by barriers with no communication between layers (commingled) and in contact at the wellbore only. For this purpose the top, middle and bottom layers were fractured individually; then, all three layers were stimulated simultaneously. The aim was to examine the effect of fracturing individual layer in multi-layered systems and analysing the pressure response from each scenario. Fracture half-length of 100 ft and permeabilities of 1, 5, 10 and 50D were assumed (numbers expected following typical frac job).

As can be seen from the plot below (*Figure 4-52*), when the top layer of 0.1mD is stimulated only, the resulting pressure behaviour varies depending on the fracture conductivity and permeability. For instance, for the low fracture permeability case of 1D, there is no indication of fracture flow behaviour; however, as the fracture permeability increases to 50D the multi-layered flow behaviour is seen with clear stimulation effect.

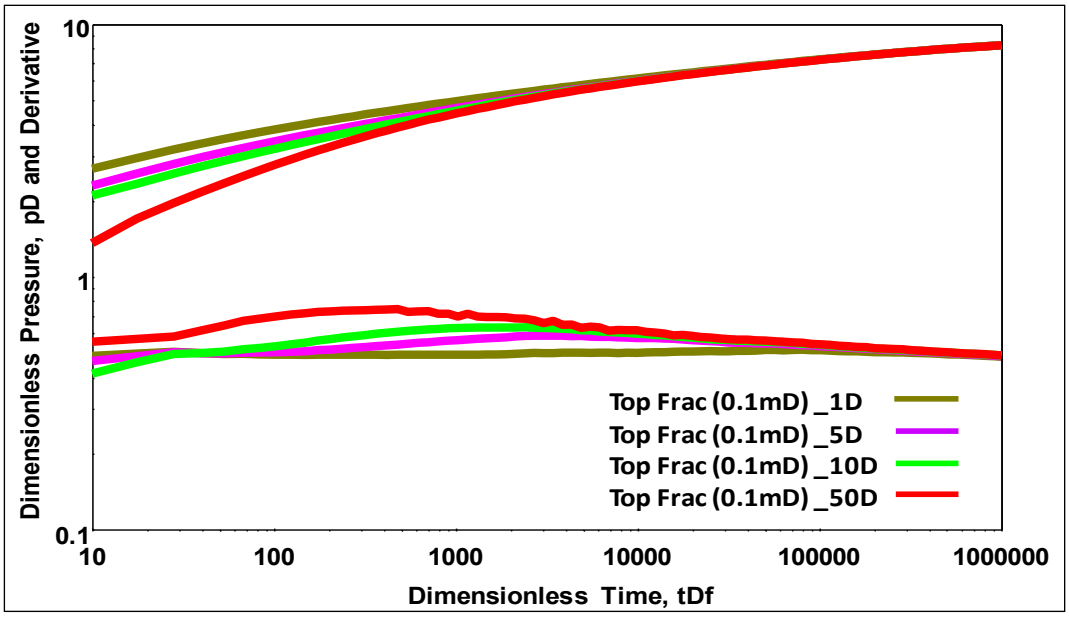


Figure 4- 52: Multi-layered system (three layers) with top layer (0.1mD) fractured only

Additionally, when fracturing the middle layer of 10mD, similar to the previous case the generated pressure responses will also depend on the fracture permeability. In this case, as the fracture conductivity increases a combination of fracture linear flow and multi-layered flow feature will soon be observed. The result is similar to that from two layers scenario where the fracture conductivity is considered as important parameter controlling the fractured well behaviour (*Figure 4-53*).

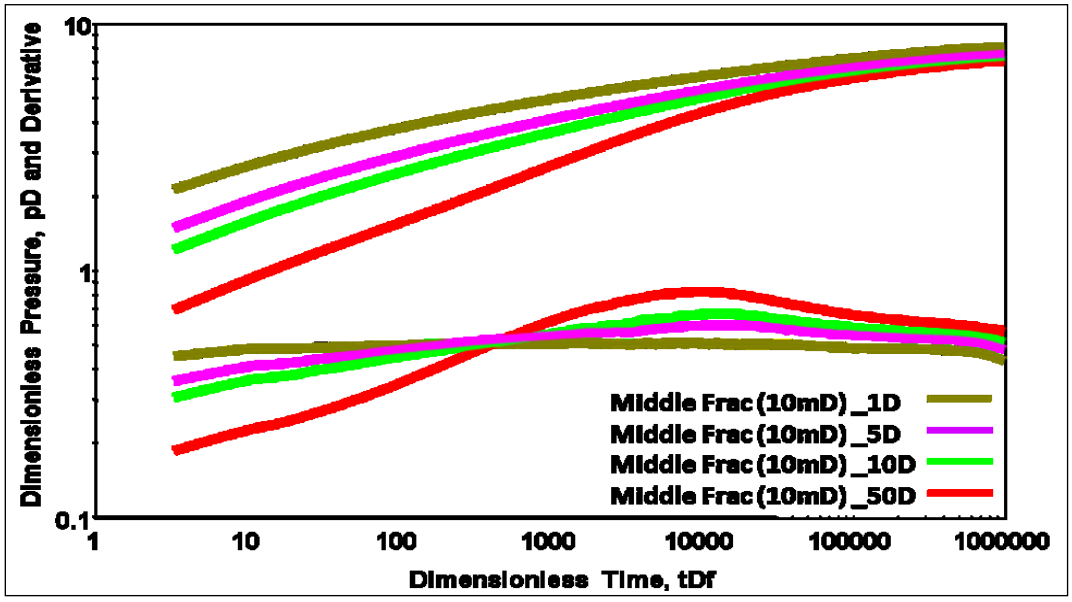


Figure 4- 53: Multi-layered system (three layers) with Middle layer (10mD) fractured only

When the bottom layer (100mD) is targeted for stimulation, the pressure response will exhibit fractured well flow behaviour (*Figure 4-54*) and obviously the higher fracture conductivity the more obvious linear flow indicating fractured well flow feature. However, when all three layers are stimulated simultaneously, the generated pressure behaviour (*Figure 4-55*) is similar to fracturing the bottom layer only case with more evident fractured well flow behaviour at an early time on the log-log plot of pressure change and derivative versus elapsed time. The results confirm the fact that induced fracture half-length and conductivity are critical parameters to consider when investigating early times unusual fracture flow behaviour seen in post-frac well tests.

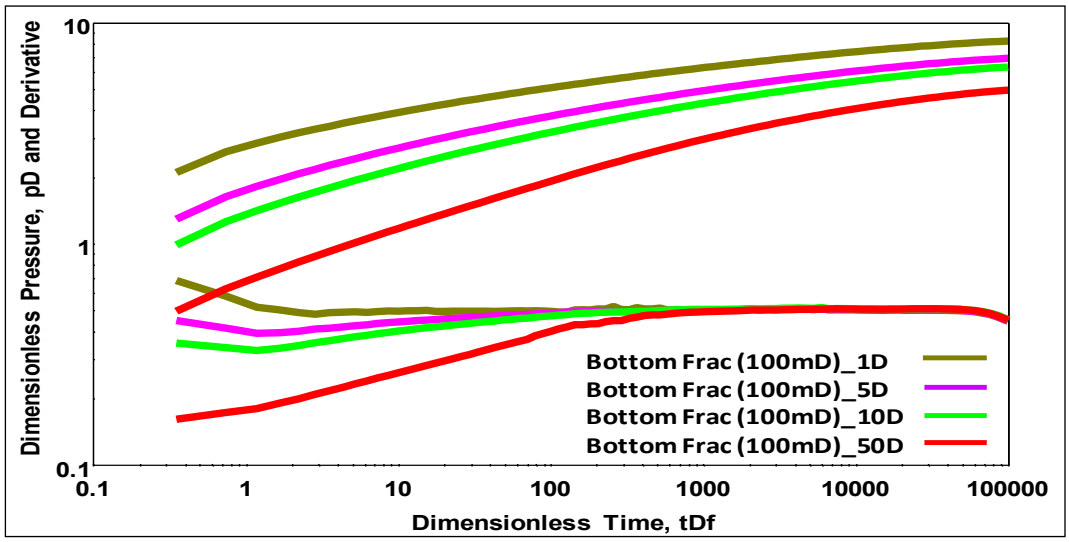


Figure 4- 54: Multi-layered system (three layers) with Bottom layer (100mD) fractured only

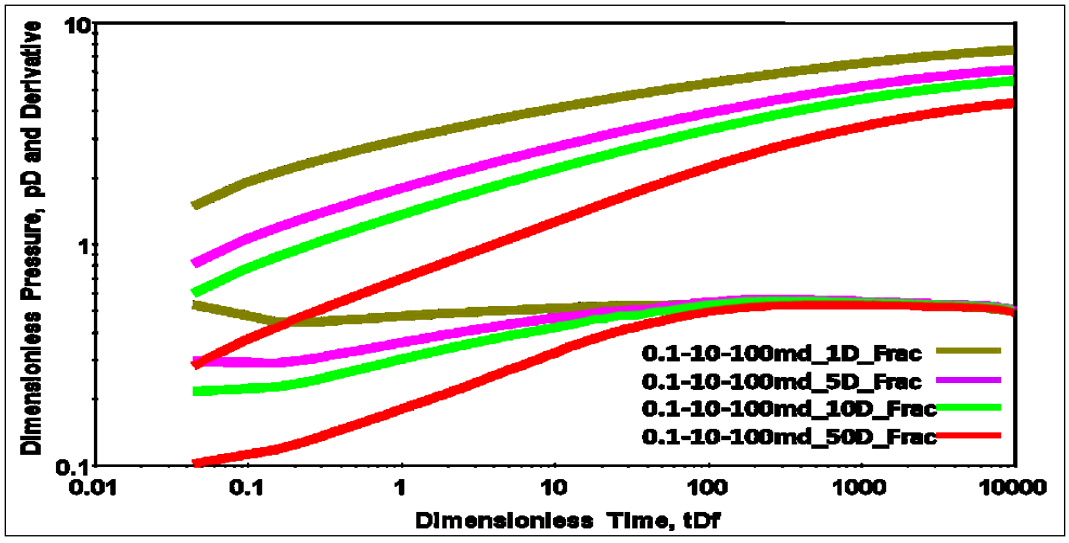


Figure 4- 55: Multi-layered with three layers (0.1-10-100mD) fractured stimulatingly

In another approach to investigate fracture half-length effect on the generated pressure behaviour from stimulating three layers model individually and simultaneously. The previous three layers model was re-run with an induced fracture half-length of 1000ft which is typical length expected from a massively hydraulically fractured well. The same scenarios that were investigated previously were re-run as part of the sensitivity analysis. The results (*Figures 4-56, 4-57, 4-58 and 4-59*) indicate similar results were obtained in the case of fracture half-length of 100ft. Again, fracturing the top low permeability layer of 0.1mD would result in a multi-layer feature present on the generated pressure behaviour.

When fracturing higher permeability layers of 10 and 100mD, the indication of fractured well flow behaviour is recognised clearly as fracture permeability increases significantly, especially in the case of 50D fracture permeability. However, pressure behaviour from fracturing middle layer seems more complicated than fracturing other layers as in this case the model demonstrate combination of fractured well flow behaviour and multi-layered flow behaviour, which make it more difficult to interpret as there is no analytical solution developed in any pressure transient analysis software packages available to use.

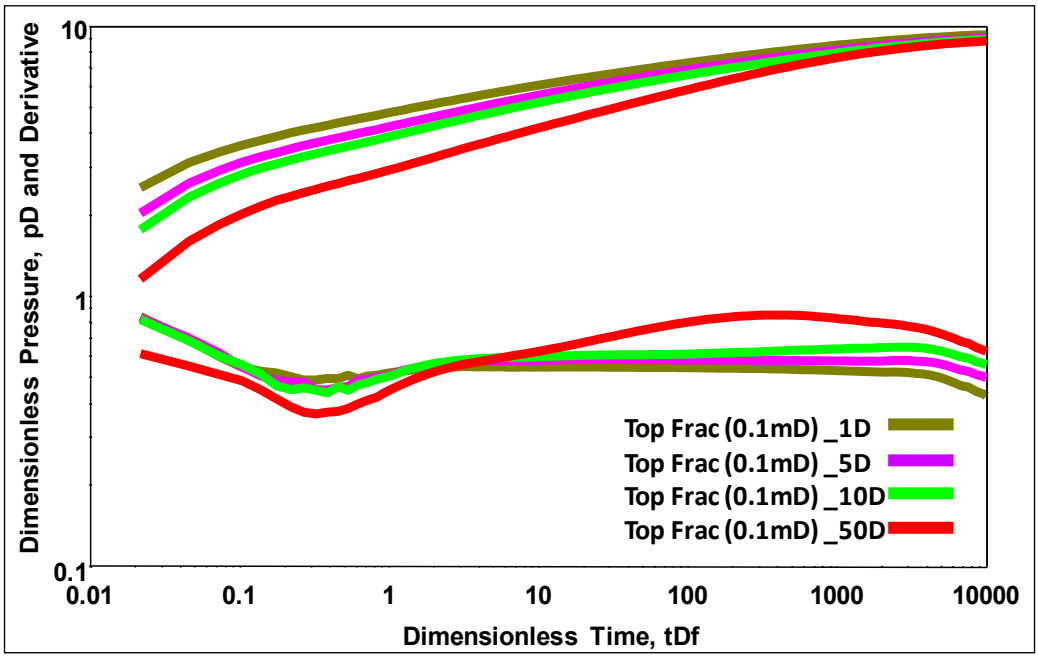


Figure 4- 56: Three layers with top layer (0.1mD) fractured only and X_f = 1000ft

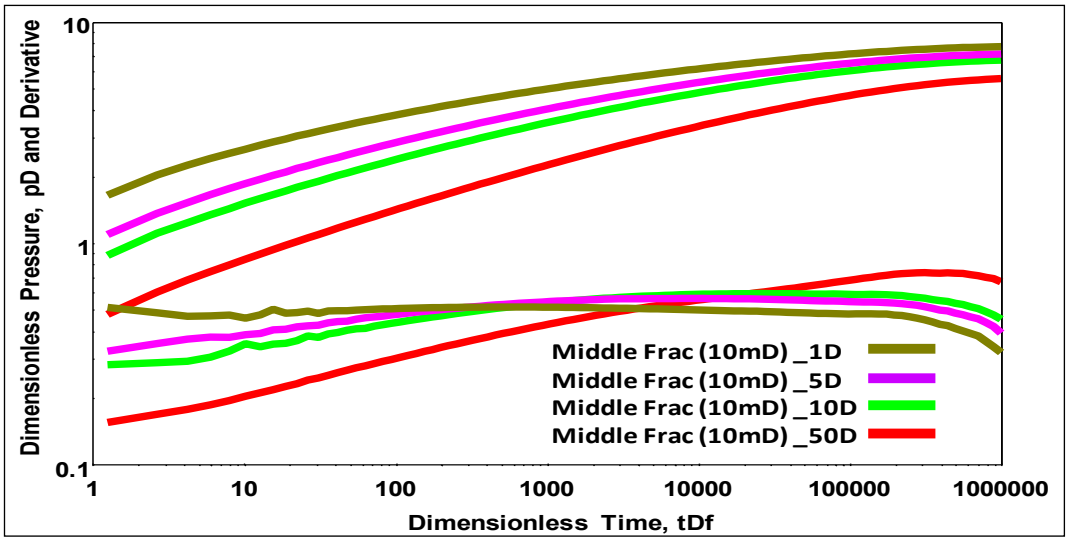


Figure 4- 57: Three layers with middle layer of10mD fractured only and x_f= 1000ft

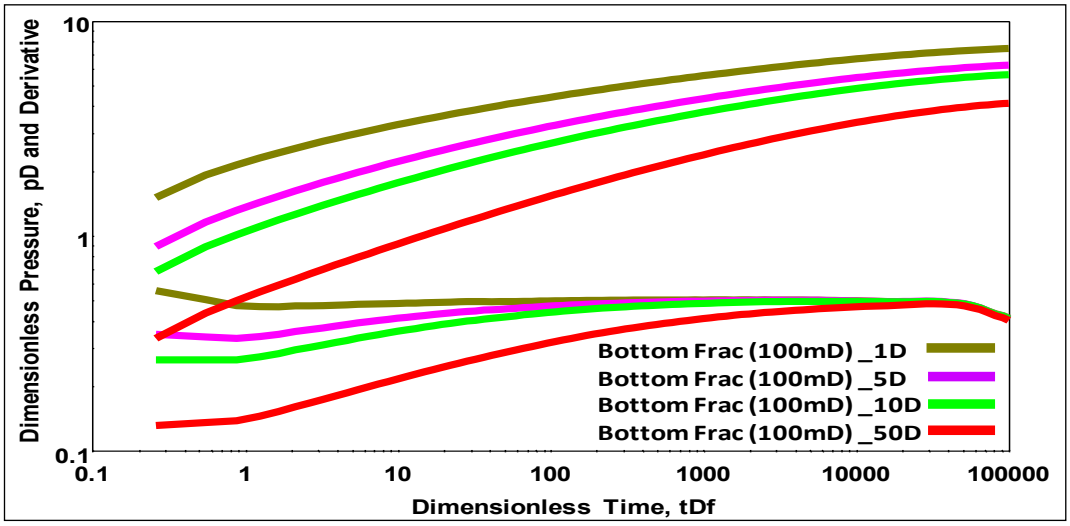


Figure 4- 58: Three layers with bottom layer of100mD fractured only and x_f= 1000ft

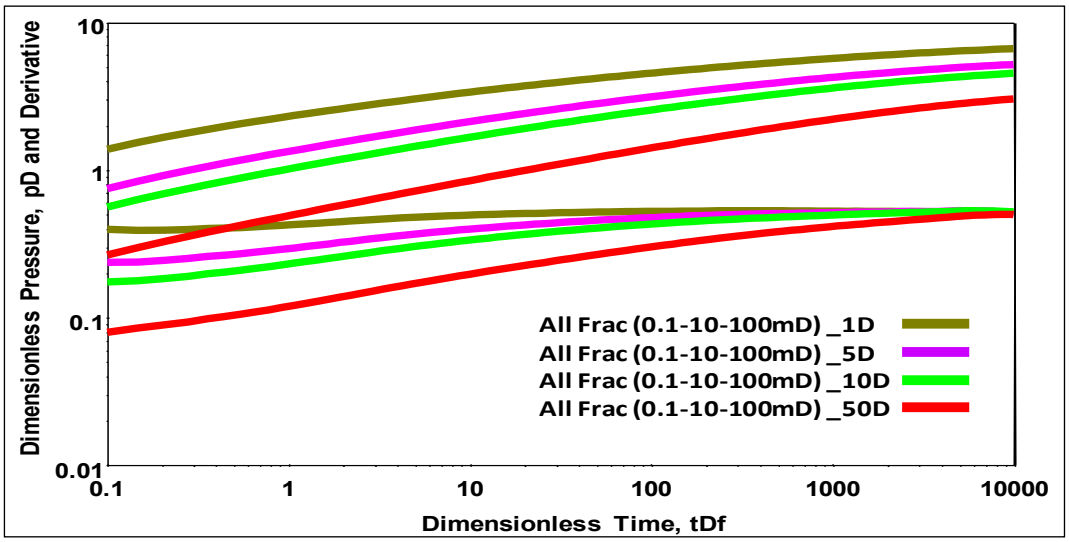


Figure 4- 59: Three layers of 0.1-10-100mD fractured stimulatingly with X_f= 1000ft

4.2.14 Effect of Fractured Layer Position in Multi-layered System

As part of the study sensitivities of the effect of fracturing, three layers with different layer positions and fracture permeabilities of 1 and 50D were investigated. The layer distribution in the model was set in the following layout: (0.1-10-100mD); (10-100-0.1mD); (10.0.1-100mD). The aim from such scenario was to study the effect of different layer setting with permeability contrasts and observe the pressure behaviour following a frac job. By examining the plot below (*Figures 4-60 and 4-61*), the impact on layers in different positions within the model and how they would affect the pressure behaviour can be seen; also clear is the impact of high permeability fracture on the pressure responses as compare to lower fracture permeability effect.

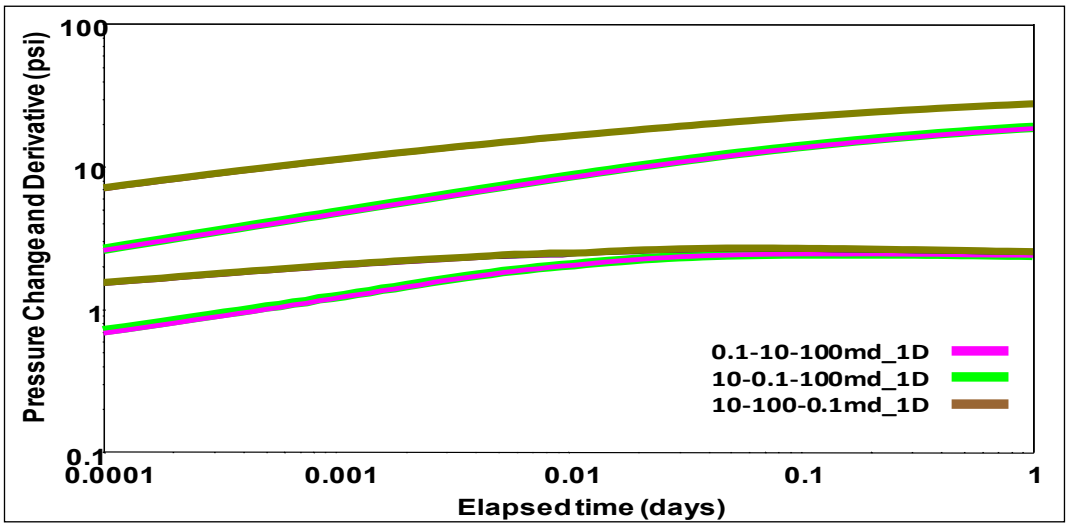


Figure 4- 60: Three layers fractured with different layer positions and K_f of 1D

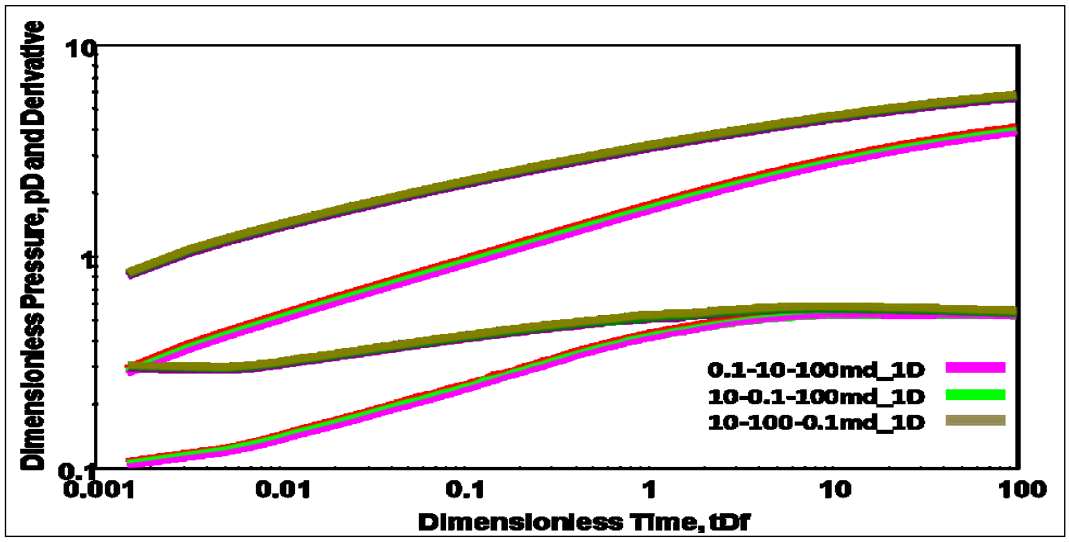


Figure 4- 61: Three layers with all layers fractured stimulatingly and different layer positions and fracture permeability of 1D

4.3 *Discussions*

Three types of fracture are known in the literature namely infinite conductivity, uniform flux and finite conductivity. The former two types are of high conductivity featured with two parallel lines of half slope. Whereas, finite conductivity fractures exhibit two parallel lines with a quarter slope and pressure drop occurring in the fracture during flow. Literature review indicates it is most likely that the researched behaviour is associated with improper frac jobs. Hence, the objective of this study is to examine the problem in hydraulically propped fractures of finite conductivity only.

Pressure transient interpretation of a post-frac test is done using analytical solutions, which can be divided into the semi analytic model for infinite conductivity fractures developed first by Gringarten *et al.* (1974) and the asymptotic model, which was introduced by Cinco-Ley *et al.* (1978). Analytical solutions for hydraulically fractured wells were developed based on a bilinear and tri-linear flow approach as introduced by Lee and Brockenbrough (1988). In this study, a numerical modelling approach is used to investigate flow behaviour of propped fractured wells exhibiting infrequent features similar to non-fractured well behaviour at early times. The result is then verified against the available analytical solutions to estimate fracture and formation parameters.

Various fracture and formation sensitivity parameters were examined that impact on flow behaviour of propped fractured wells. Results suggest that the problem is likely to be associated with fractures of low conductivity typically $FcD<0.1$ and short half-lengths. Analysing this unusual behaviour requires an understanding of fracture flow behaviour in low conductivity propped fractures. In the case of infinite conductivity fractures, it is assumed that the fluid flux is perpendicular to the fracture face at all times. However, as the conductivity decreases for the fracture exhibiting bilinear flow, another component of flow parallel to the fracture will flow. As the former flow become slower due to low fracture conductivity compared to the parallel flow in the formation, the overall fracture flow changes to an elliptical shape forming semi radial or pseudo radial flow with time.

According to Azari *et al.* (1990) as the fracture conductivity reduces, the elliptical shape of the flow towards the fracture changes to a circular shape, which results in short lived bilinear flow duration for low dimensionless fracture conductivity of 0.05. Since there will be no chance for formation linear flow development, the end of the bilinear flow is

followed by a transition and then the start of pseudo radial flow. Low *Fcd* reduces the bilinear flow duration that will be masked by *WBS* effect. Therefore, transient pressure features for fractures of *FcD* of <0.1 illustrates wellbore storage effects followed by pseudo radial flow behaviour. Based on the literature review, there are a number of causes for fracture permeability reduction resulting in the reduction of conductivity including:

- an increase in dimensionless wellbore storage, which indicates that it is unlikely to achieve high conductivity fractures;
- flow back of fracture fluid, which results in crushing and proppant embedment due to stresses applied prior to fracture closure;
- fracture choke damage can be a control parameter for the occurrence of the behaviour;
- knowledge of the true formation permeability is crucial in achieving accurate design and analysis.

In addition, in order to understand causes for this behavioural problem to occur, it is important to verify that the:

1- Designed fracture has targeted the formation interval of interest.
2- Designed fracture parameters in pre frac model are similar to the calculated values from post-frac tests.
3- The purpose of well stimulation and objectives are well understood.
4- Induced fracture with damage especially fracture choke damage has a critical impact on the fractured well behaviour with fracture face skin of less importance.
5- Fracture conductivity has not been reduced significantly due to non-Darcy effects in stimulated gas wells.
6- High permeability contrast between formation together with low conductive induced fracture may cause development of the behaviour problem
7- Fractures with low conductivity penetrating gas-condensate well experienced liquid bank accumulation nearby wellbore may result in developing the behaviour.
8- It is likely that skin frac may cause the behaviour to develop due to short induced fracture half-length.
9- Liquid flow back from the formation into the wellbore through the fracture path causing blockage and proppant embedment of the fracture.
10- Frac pack of high permeability formations with low induced fracture conductivity may result in developing the behaviour problem.

4.4 *Conclusions*

In this chapter, a number of cases of fracture and formation parameters were investigated to study their impacts on the generated pressure response that might result in fractured well flow behaviour similar to the non-stimulated well behaviour. Below are the main conclusions drawn based on the results obtained from the current study:

- Fracture conductivity is the most important factor in determining effectiveness of any frac job. The lower the fracture conductivity ($FcD < 0.1$) the more likely for infrequent fractured well flow behaviour to occur.
- Fracture length is considered to be the second critical factor controlling the development of unusual fractured well flow behaviour. It is found that the investigated behaviour is likely to develop in fractured wells of short half-lengths usually of less than tens of feet or metres.
- Fracture permeability is the crucial parameter in causing the problem. The results indicate that fractured wells with low fracture permeability are considered prime candidates for the unusual behaviour to exist.
- Fracture face skin and choked fracture damage effects were examined in details and the results suggests that fracture face skin has less impact on the pressure response compared to the choked fracture effect. The results indicate that damaged fracture (choked) plays a significant role in developing the investigated behaviour.
- Fluid leak-off as a result of the well stimulation process may slightly impact the generated pressure behaviour depending on the formation permeability and duration of the well clean-up period.
- Non-Darcy effect in stimulated gas reservoirs may cause unusual flow behaviour to develop.
- Fractured wells penetrating high permeability formations would result in fractures having conductivity less than the formation, which means of low dimensionless conductivities resulting in development of infrequent flow behaviour.
- Un-equal fracture half-length on either side of the wellbore are found to have minimal effects on development of unusual fractured wells behaviour.

CHAPTER V

FRACTURED WELL IN NATURALLY FRACTURED RESERVOIRS

5.1 Introduction

Some wells penetrating naturally fractured reservoirs that have experienced damage as a result of drilling or completion operations are hydraulically fractured in order to increase well productivity. These reservoirs had been studied intensively by many workers: Barenblatt and Zeltov (1960); Warren and Root (1963); Kazemi (1969); De Swaan (1976); Mavor and Cinco-Ley (1979); Najurieta (1980); Bourdet and Gringarten (1980); Cinco-Ley and Samaniego (1982); Streltsova (1983); Serra *et al.* (1983); Bourdet (1983, 1984); Aguilera (1987) and Olarewaju and Lee (1989). Stimulating wells penetrating such reservoirs is not common practice due to fracture fluid loss into natural fractures effect; resulting in not achieving stimulation targets.

Transient pressure analysis of fractured wells penetrating these reservoirs indicates typical fracture flow behaviour followed by a dual porosity feature at early times. However, it is stated in the literature that the problem investigated in this study may occur in naturally fractured formations according to Gringarten *et al.* (1975). They stated that observing unit slope at early time instead of half or quarter unit slope is common in naturally fractured reservoirs. It is also believed that the problem is associated with multi-layered formations with high permeability contrast between different layers (verbal communication with Prof. Gringarten). In order to investigate the problem in these particular reservoirs, some sensitivity cases were run in the current study.

Gringarten (1984) in a study presented the most remarkable work on the analysis of pressure data for multi-layered and naturally fractured reservoir systems under practical conditions with high permeability contrasts between layers. The study presented a new type curve for identification of the flow periods and estimation of the system parameters.

Aguilera (1987) analysed data from multi-layered naturally fractured reservoir with ten layers, with a range of fracture permabilities and constant fracture spacing using numerical simulation. It was found that on the pressure derivative a partial penetration effect could be noticed as the effect of a multi-layered reservoir as if all layers are perforated. The next section discusses behaviour of fractured wells in these reservoirs.

5.2 Fractured Well in Naturally Fractured Reservoirs

A number of studies investigated fractured wells flow behaviour in fractured reservoirs. For instance, Lancaster and Gatens (1986) proposed some practical measures to analyse hydraulically fractured wells in naturally fractured reservoir system. The study's conclusion was that from the pre fracture test one could obtain natural fracture permeability, lambda and omega, which are critical parameters for the post-fracture well test interpretation.

Aguilera (Sept, 1987) investigated the effect of wellbore storage; skin, and constant pressure reservoir boundaries on the transient behaviour of naturally fractured reservoirs intercepted by a hydraulic vertical fracture of infinite conductivity. Study results showed that there are different flow regimes in the transient behaviour of a hydraulically fractured in such reservoir. The first regime might be masked by wellbore storage and is recognized by a unit slope on a log-log plot. The second regime is linear flow from the natural fracture into the hydraulic fracture with a half unit slope.

The third flow regime is a transition period whose behaviour depends on the transient (unrestricted) or pseudo steady state (restricted) interporosity flow assumption. The transient approaches a quarter slope for small values of omega suggesting bilinear flow between (a) the natural and the hydraulic fractures and (b) the matrix blocks and the natural fractures. The forth flow regime is pseudo steady state and is characterised by a 1.151 slope on a conventional semi-log plot. The fifth regime is dominated by outer boundaries.

Cinco-Ley and Meng (1988) studied transient behaviour of a well intersected by a finite conductivity vertical fracture in a naturally fractured reservoir system. They investigated two procedures of fluid transfer between matrix blocks and fractures that are pseudo steady-state and transient matrix flow models. They presented a general semi analytical model and simplified fully analytical models. The study stated that these systems exhibit the basic behaviour of a well with a finite conductivity fracture feature that is bilinear flow, pseudo linear flow and pseudo radial flow in addition to the transition flow periods between some of the periods. It showed that each of these flow periods is under the influence of the different states of the fluid transfer between matrix and fractures, fracture dominated period, transition period and total system.

Houze *et al.* (1988) examined flow behaviour of a fractured well in infinite acting dual porosity reservoir and found that a log-log plot of Δp vs. time should result in an early straight line with a half unit slope, followed by a transition period, and reaching pseudo radial flow when pressure in matrix and fractures become equal. In another study, Olarewaju and Lee (1989) presented an analytical solution for pressure transient tests from a well intercepting multi-layered reservoir with or without interlayer cross flow. They modelled multi-layered reservoir systems with unsteady-state or pseudo steady interlayer cross flow, commingled flow, and dual porosity systems with pseudo steady matrix-to-fracture transfer in the presence of skin, wellbore storage, and phase segregation.

Okoye *et al.* (1989, 1990) examined transient behaviour of a well intersected by a finite conductivity vertical fracture in a closed square multilayer naturally fractured reservoir system using analytical, semi analytical and numerical models in their approach. They used the analytical solutions for early, intermediate and late times that can be used to analyse transient pressure data if the flow period is recognised. The semi-analytical solution was for all times for the purpose of type curves generation. The numerical solution was used to verify and validate the semi analytical solution and vice versa. They also studied both pseudo-steady-state and transient matrix flow models for fluid transfer between matrix blocks and fractures in their analyses.

Aguilera (1989) presented an analytical solution for the analysis of naturally fractured reservoir systems penetrated by hydraulic vertical fractures of finite conductivity with the effect of wellbore storage, skin and unsteady or pseudo steady state interporosity flow. The study indicated that four flow regimes periods can be recognised, first period of bilinear flow effect, which is sign of finite conductivity fractures with quarter slope on a log-log plot. This was followed by second period, which is the transition period characterised by straight line on the semi log plot. The third period is of a straight line slope on the conventional semi-log plot indicating pseudo radial flow. A fourth period is the boundary effect. In another study Aguilera and Aguilera (2001) a numerical model of a previous study was used to investigate the effect of variation of fracture permeability, layer thickness, fracture spacing and fracture porosity. It can be concluded from the above presented literature review that the investigated problem in this study is unlikely to occur in naturally fractured reservoirs.

5.3 Numerical Simulation of Fractured Well in Naturally Fractured Reservoirs

The investigated fractured well flow behaviour problem in this study has not been reported to be associated with any type of naturally fractured reservoir in the literature. However, as part of the sub-surface parameter sensitivity in the study a dual porosity model intercepted with a hydraulically fractured well was constructed to examine the possibility that the investigated problem might occur in oil and gas wells penetrating such reservoirs. For this purpose, a single layer fractured reservoir intercepted by vertical fracture model is constructed. In the example presented below a clear fractured well feature can be observed at early time compared to non-fractured well behaviour (*Figure 5-1*).

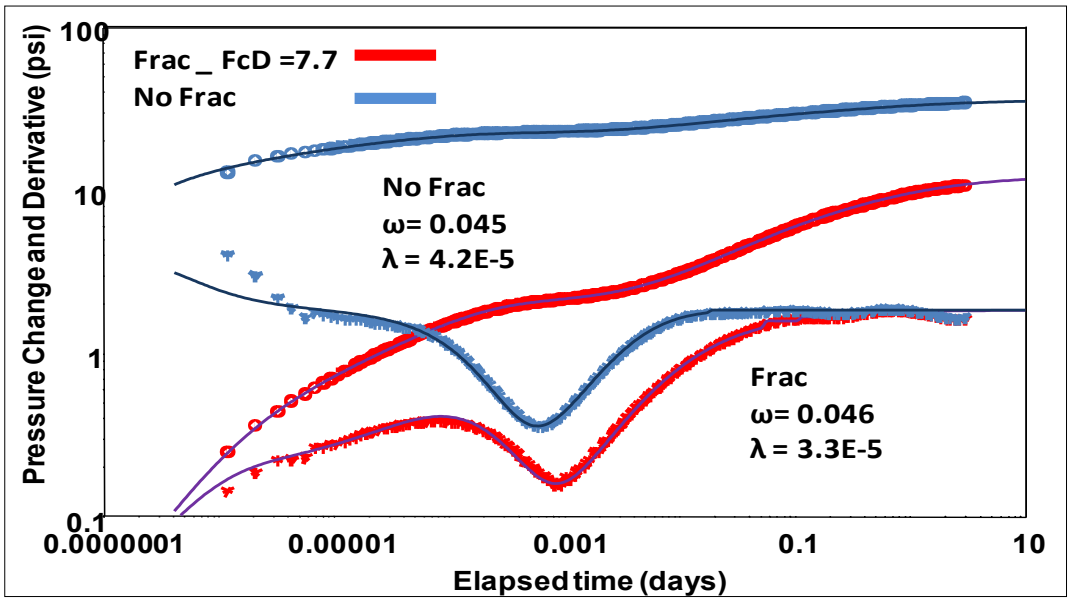


Figure 5- 1: Verification of numerical and analytical models for a fractured well

In addition, a number of cases were run to explore fracture configuration changes effect on the generated pressure behaviour. Figures (*5-2 and 5-3*) show single layer naturally fractured formation model of 1mD penetrated by a fractured well of various fracture permeability values ranging from 5D up to 500D. As it can be noticed due to high conductivity of the natural fracture there is no indication of fractured well response for low fracture permeability which indicates that any induced fracture of permeability of up to 100D will not be observed at early times.

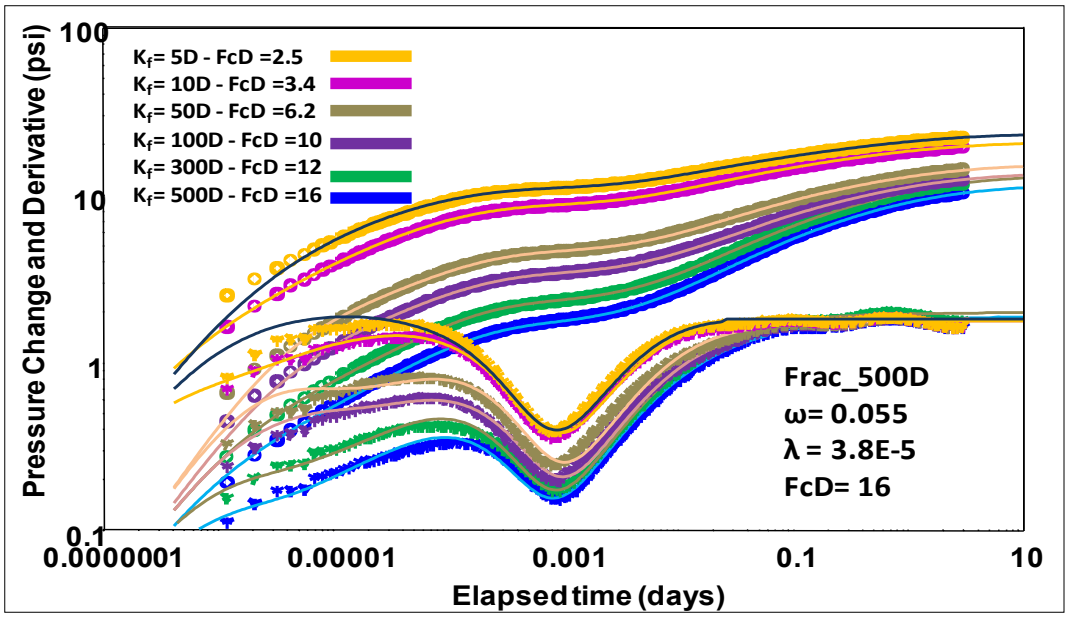


Figure 5- 2: Verification of numerical vs. Analytical solution of various fracture permeability in single layer fractured formation

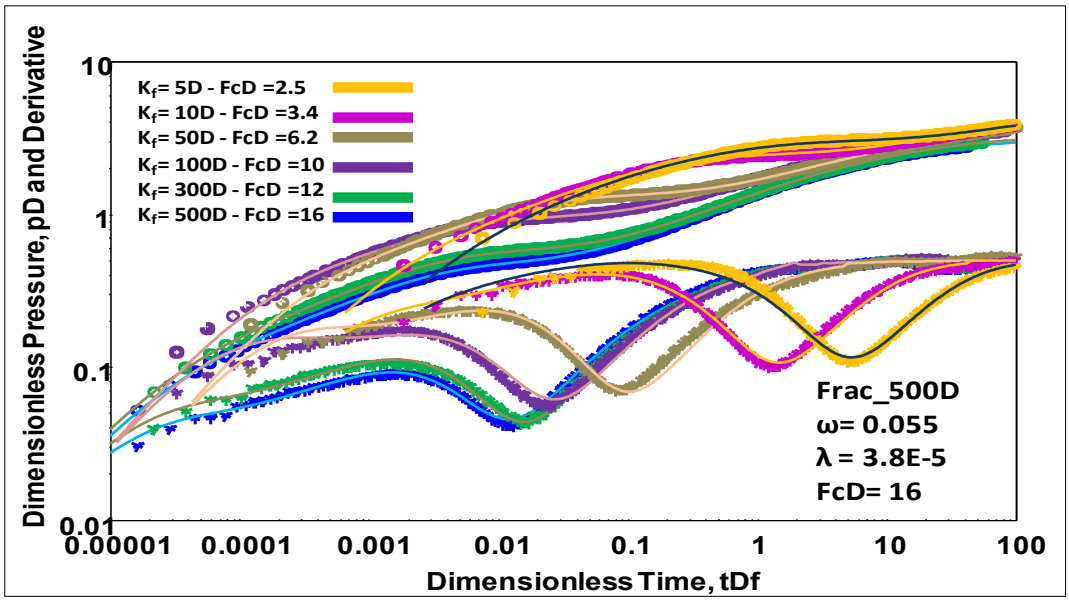


Figure 5- 3: Dimensionless pressure behaviour of various fracture permeability in single layer fractured formation

As it is concluded from the literature review in this document, the investigated problem might occur in any type reservoir setting containing any fluid type. Since liquid drop out effect in the case of gas-condensate reservoirs might influence pressure response. Thus, one of the sensitivity parameters examined in the study was production rate effect, which impacts a condensate bank feature in hydraulically fractured wells penetrating natural fractured reservoirs.

In order to examine the effect of fluid richness on the pressure response of fractured well in naturally fractured gas-condensate formations, a single layer model containing lean and rich gas-condensate was constructed. A number of cases were run with and without fracture and plots (*Figures 5-4, 5-5 and 5-6*) below demonstrate the results indicating less liquid drop out effect in the lean case compared to rich fluid case.

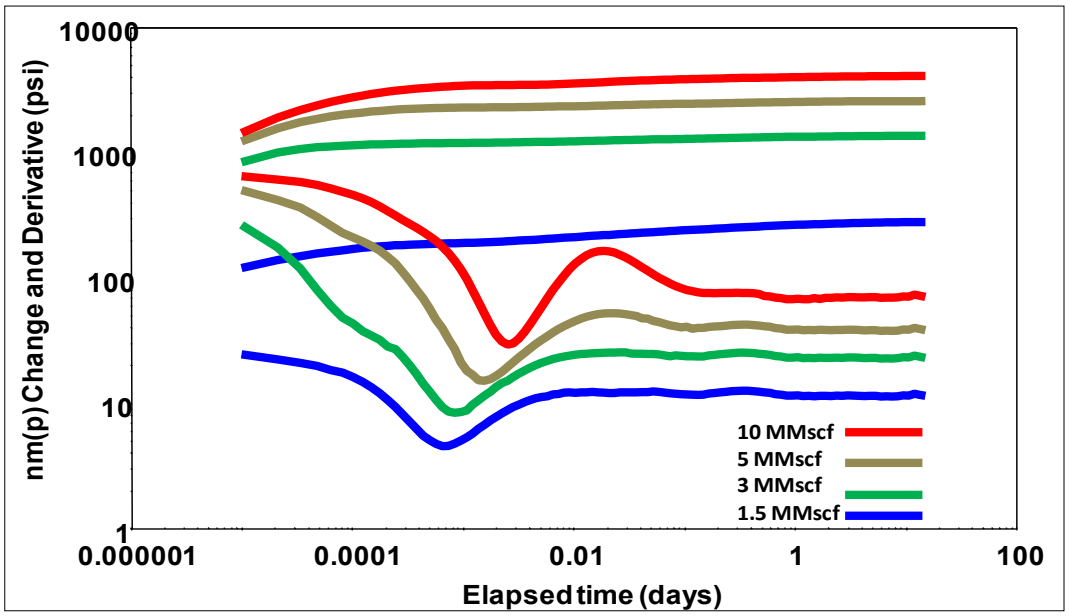


Figure 5- 4: Pre frac pressure behaviour of lean gas-condensate of various production rates

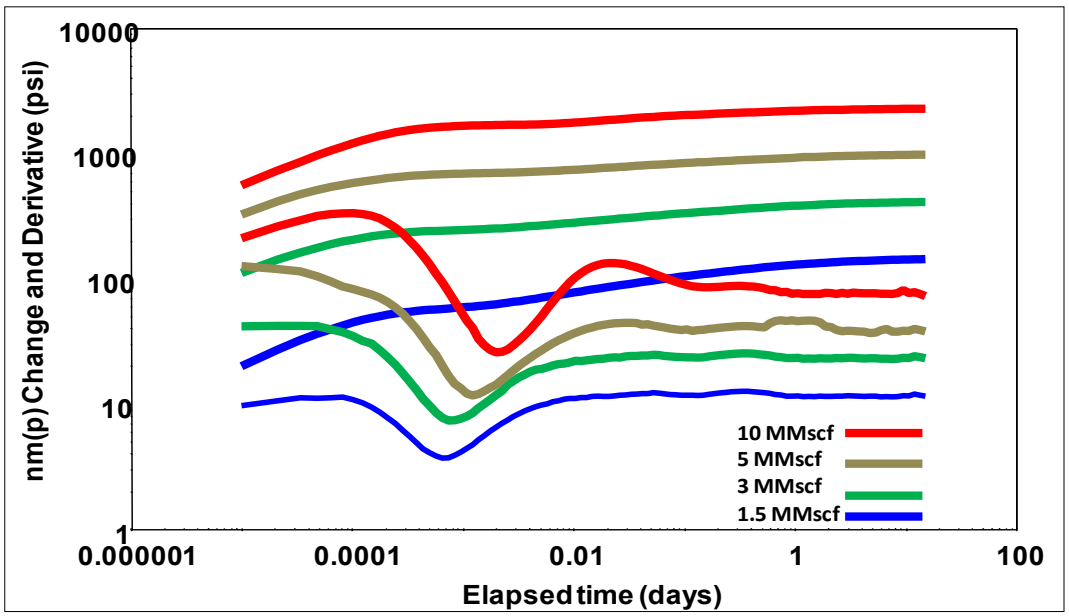


Figure 5- 5: Post-frac pressure behaviour of lean gas-condensate of various production rates

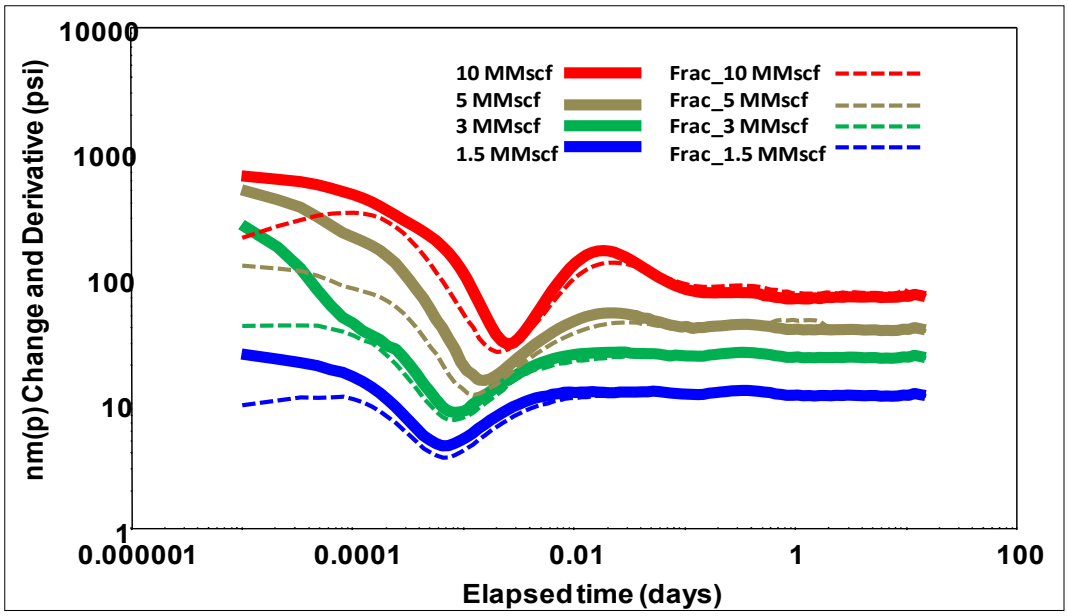


Figure 5- 6: Pre and post-frac pressure behaviour of lean gas-condensate fractured well

Similar cases were re-run with and without fracture for a rich gas-condensate fluid and plots (*Figures 5-6, 5-7 and 5-8*) below illustrate liquid drop out effect in rich case. As it can be noticed due to condensate bank in the case of high production rate the induced fracture has not much impact on the pressure behaviour apart from skin reduction and slight improvement of kh value. It also suggests that it is recommended to produce the stimulated well at lower rates to avoid condensate bank accumulation effect.

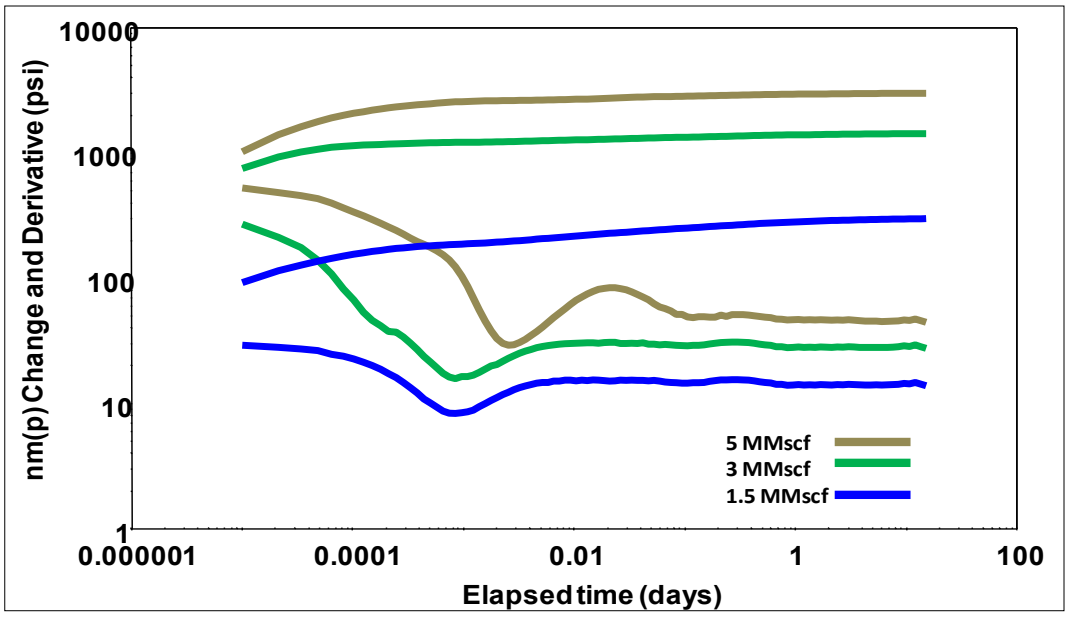


Figure 5- 6: Pre frac pressure behaviour of rich gas-condensate of various production rates

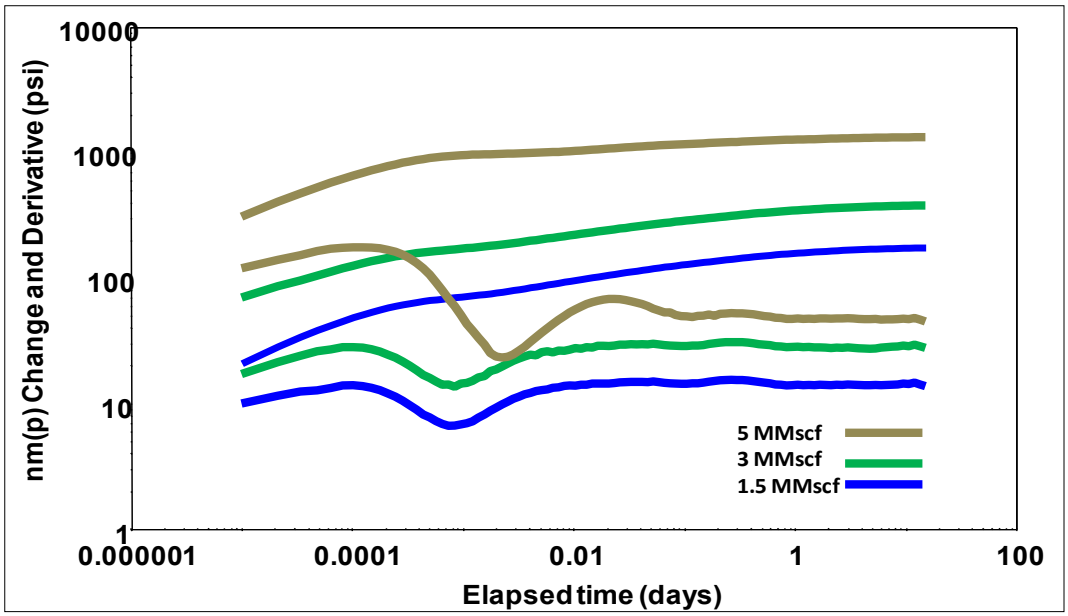


Figure 5- 7: Post-frac pressure behaviour of rich gas-condensate of various production rates

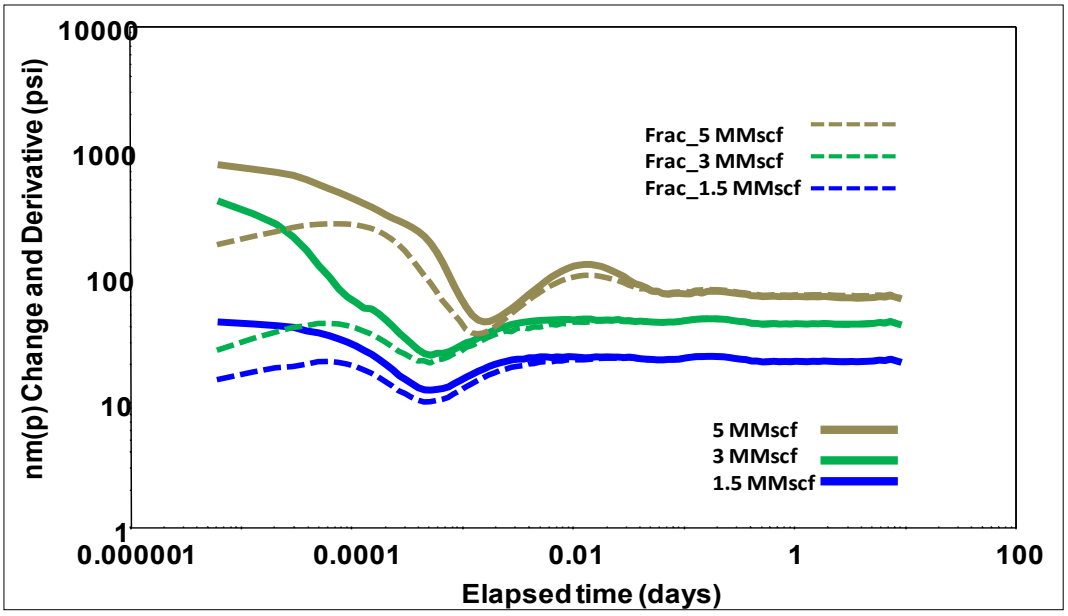


Figure 5- 8: Pre and post-frac pressure behaviour of rich gas-condensate fractured well

In another approach to investigate the effect of fracture damage including fracture face and choked fracture on the generated pressure response. For this purpose a simple dual porosity model that is penetrated by a fractured well. Results indicate sever liquid drop out effect in the case of fracture face skin case compared to choked fracture (*Figure 5-9*).

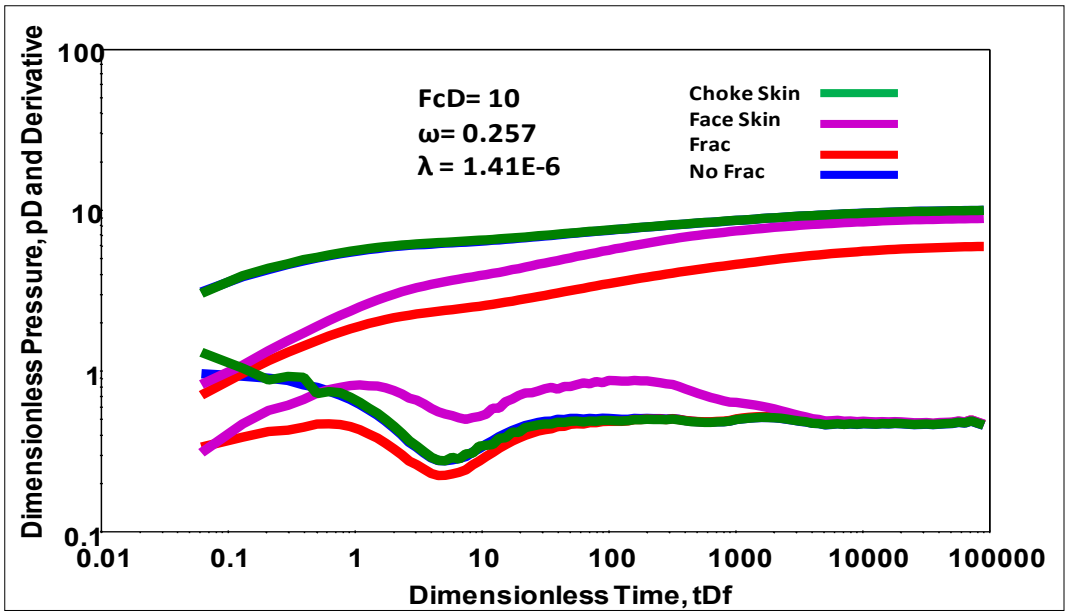


Figure 5- 9: Post-frac pressure response of fractured well affected by fracture damages

5.4 Conclusions

It was mentioned in the literature that observing a unit slope feature instead of half unit slope at early time of a stimulated well is common in naturally fractured reservoirs according to Gringarten *et al.* (1975). In order to investigate this, a dual porosity models was constructed to investigate fractured well flow behaviour in such reservoirs. Also, since it is a common practice to stimulate gas-condensate wells penetrating naturally fractured reservoirs. Therefore, investigating the unusual flow behaviour of fractured wells in these reservoirs is important to fully understand effects of natural fractures on the introduced pressure responses. Results from the cases run indicate that:

- Observing the unusual flow behaviour investigated in this study in naturally fractured reservoirs is dependent on the induced fracture permeability, typically fractures with low permeability may be masked by high conductivity naturally fractured behaviour.
- Early time flow behaviour of damaged fractured wells associated with choked fracture effect may cause the infrequent feature investigated in this study.
- Induced fractures face damage effect may cause extra liquid drop out problem.

CHAPTER VI

FRACTURED WELL IN LEAN AND RICH GAS-CONDENSATE RESERVOIRS

6.1 Introduction

Gas-condensate wells experience rapid decline in productivity when the near wellbore pressure goes below the dew point pressure causing liquid drop to accumulate in the near wellbore region. Many workers have studied such decline in the well productivity and investigated control parameters for the liquid drop out effect. Condensate bank forms due to an increase in condensate saturation around the wellbore that reduces the effective permeability to gas and results in a quick decline in well productivity once the near wellbore pressure drops below the dew point pressure.

However, productivity above the dew point pressure is controlled by the reservoir permeability thickness and viscosity of the gas. Whereas, below the dew point pressure the productivity will be controlled by critical condensate saturation (Sc) and the shape of the gas and condensate relative permeability curves. It is also stated in the literature that in the retrograde condensate region, the degree of interfacial tension (IFT) between the gas and the condensed phase is rather low. Thus, it is predicted that the capillary forces will play a lesser role compared to gravity and viscous forces.

A number of studies examined gas-condensate wells productivity in detail including O'Dell and Miller (1965), Hinchman and Barree (1985), Barnum *et al*. (1995); some other workers investigated fluid characterisation of gas-condensate wells such as Saeidi and Handy (1974), Metcalfe *et al*. (1988), Fevang *et al*. (2000) . Others studied liquid bank development in the vicinity of the wellbore and relative permeability variation effects in such reservoirs including Danesh *et al*. (1988), Asar and Handy (1988) , Jone and Raghavan (1989), Whitson *et al*. (1999) and Gringarten *et al*. (2000) . However, a few workers investigated the unusual fractured well flow behaviour in gas reservoirs, Cramer (2005), Mayerhofer (2005) and gas-condensate reservoirs, Yadavalli *et al.* (1996), Shaoul *et al.* (2007) and Yatindra (2008). Thus, it is one of the objectives of this study to examine the behaviour problem of hydraulically fractured wells in gas-condensate reservoirs.

6.2 Fractured Well in Gas-condensate Reservoirs

Often hydraulic fracturing is proposed to overcome formation damage in the near wellbore region to improve the flow path of fluids, which can be either gas or oil to the wellbore. It has been found to be effective not only in low permeability reservoirs but also in improving the productivity of gas-condensate reservoirs due to condensate bank accumulation around the wellbore region. The investigated unusual behaviour in this study has been reported to be associated with gas-condensate wells. Therefore, it is one of the objectives of this study to examine early time flow behaviour of fractured wells producing gas-condensate fluids. Also, it is important to investigate the impact of fluid richness on the pressure behaviour. Due to the economic importance of gas-condensate wells, large numbers of workers have studied in detail fractured well performances in gas-condensate reservoirs.

Sognesand (1991) investigated the effect of a retrograde condensate bank on long term well performance of vertically fractured gas-condensate wells. The study introduced the concept of time dependent skin factor to correct for the effect of condensate blockage. The study also investigated differences in productivity loss due to condensate blockage for non-fractured and fractured wells, which showed the importance and effectiveness of well fracturing. The study also indicates that the condensate bank depends on the relative permeability characteristics and production rates.

Carlson *et al.* (1995) examined the effects of retrograde liquid condensation on single well performance in a low permeability reservoir using radial compositional modelling of a hydraulically fractured well. They found that assuming the presence of a radial flow into a wellbore, there would be significant productivity impairment by a condensate bank accumulated in the vicinity of the wellbore. A hydraulic fracture treatment reduces the amount of pressure drawdown in the well and nearby area due to reduced condensate precipitation.

Settari *et al.* (1996) performed a study on the effect of condensate bank on the productivity index of hydraulically fractured wells in a complex, highly heterogeneous gas-condensate reservoir. In the study a two components black oil simulation model was used for simulating productivity of the Smorbukk field, Norway. They found that

proppant fracturing was effective in mitigating the effect of developed condensate blockage on productivity index. The effectiveness depended primarily on the fracture conductivity, fracture length and reservoir heterogeneity.

Hashim and Hashmi (2000) stated that hydraulic fracturing is effective in enhancing well productivity for gas-condensate wells with bottomhole pressure above and below the dew point pressure by circa three times compared to the non-fractured wells. The study also suggested that well fracturing can prolong cumulative production above the dew point pressure case and that the higher the *FcD* values, the more well performance improvement can be achieved.

El-Banbi *et al*. (2000) investigated the well productivity of vertical wells in a moderately rich gas-condensate reservoir where initially they decreased rapidly and then increased as the reservoir was depleted. Their explanation for this phenomenon was that when the well goes below the dew point, the productivity decreases because of the high condensate saturation in the vicinity of the wellbore, which severely reduces the effective permeability to gas; hence, reducing gas productivity.

Wang *et al*. (2000) examined the effects of gas permeability reduction through introducing a model that predicts a fractured well performance in gas-condensate reservoirs. However, it is worth noting their approach for the calculation of the appropriate pressure drawdown during production to optimize well performance was not clear in the study.

Indriati *et al*. (2002) presented a model that predicts the performance of fractured gas-condensate reservoirs. Issues investigated in their study include the effects of gas permeability reduction, optimum fracture design through calculating the optimum fracture configuration and the introduction of guidelines for the calculation of the optimum pressure drawdown during production to maximize well performance. They found that in rich gas-condensate reservoirs there is an optimum flowing bottomhole pressure in which the lowest bottomhole pressure no longer provides the highest production. However, for the lean gas-condensate reservoir case, the optimum flowing bottomhole pressure is the lowest bottomhole pressure values.

One of the important parameters to consider when analysing fractured gas and condensate wells is the effect of non-Darcy. Several workers studied the influence of non-Darcy flow on the pressure transient response of hydraulically fractured wells in gas reservoirs when high gas velocity is reached, especially within the fracture and near wellbore. Based on a literature review it is concluded that the non-Darcy effect within the fracture is more important to understand compared to its effect in the formation. This effect is mainly rate dependant and can affect the results obtained from gas well stimulation in terms of estimated fracture configuration parameters.

Forchheimer (1901) was first to propose a generalized equation that takes into account the additional pressure drop resulting from high flow velocities and is illustrated in the following equation:

$$-\frac{dp}{dx} = \frac{\mu v}{k} + \beta \rho v^2 \tag{6-1}$$

$$\beta \approx \frac{0.005}{k^{0.5}\phi^{5.5}S^{5.5}} \quad (\text{cm}^{-1}\text{ unit}) \tag{6-2}$$

$$\beta = \frac{1.570766957E-3}{\phi^{5.5}K^{0.5}} \quad (\text{Forchheimer unit}) \tag{6-3}$$

Since then different techniques were proposed to understand the effect of non-Darcy flow behaviour in porous media including McGuire and Sikora (1960); Millheim and Cichowicz (1968); Wattenbarger and Ramey (1969); Holditch and Morse (1976); Lee and Holditch (1979); Guppy *et al.* (1981); Guppy *et al.* (1982); Guppy *et al.* (1982); Gidley (1991); Settari *et al.* (2000); Umnuayponwiwat *et al.* (2000), Gil and Ozkan (2001), Cesar *et al*.(2002) and Smith *et al.* (2004).

By reviewing the studies published on the non-Darcy effect so far, it can be concluded that when non-Darcy flow effect occurs in a fracture, the estimated fracture conductivity and half-length represent only a small fraction of the actual values. It is worth noting that understanding gas-condensate well performance requires proper fluid characterisation and the next section will discuss PVT analysis in details.

6.3 PVT Analysis

The most important issue for understanding gas-condensate reservoir performance is fluid characterisation providing representative samples are collected from intervals of interest and at the surface. Understanding compositional gradients present in the field and setting up an appropriate Equation of State, *EOS* model, which is representative of the actual reservoir fluids are key points in understanding and developing any gas-condensate reservoir. When analysing gas-condensate samples, an EoS package is required to perform a series of calculations on the basis of a set of input data to predict the PVT behaviour of the fluid for a variety of PVT experiments, mainly constant composition expansion (CCE) and constant volume depletion (CVD).

The first step in fluid analysis task is to simulate a CCE to determine change in Z factor from initial reservoir conditions to dew point. Then, a CVD experiment is modelled and both the incremental well stream produced at each depletion step and the produced well stream compositions determined. Note that any liquid condensed in the reservoir is considered immobile. Each of the produced well streams was then flashed through the surface separation process and the relative amounts of surface gas and liquid obtained.

For the purpose of fluid characterisation in this study, the PVTi package was used to perform PVT analysis on various fluids used in the study. For this purpose, data on gas phase composition versus pressure can be found in a constant volume depletion test, *CVD* experiment and this makes the, *CVD* a much more useful experiment than constant composition expansion, or *CCE* experiment. Both experiments were analysed on fluid samples examined in this study. In addition, when modelling a gas-condensate the liquid drop out curve is usually thought to be the most important characteristic of the fluid. In fact, the liquid drop out curve has little direct impact on reservoir recovery mechanisms.

It is worth noting that the most critical fluid data to examine in detail are the gas Z-factor and the change in gas phase composition as pressure declines below the dew point pressure. Detailed results of fluid analysis used in this study can be found in Appendix-B in this document. The next most important issue related to gas-condensate reservoir is modelling relative permeability.

6.4 Relative Permeability Modelling

Relative permeability curves allow the calculation of fluid movement within a porous medium under the combined action of gravity and viscous forces. Saturation changes can be produced in a variety of ways and different relative permeability curves might be applicable in each case. Thus, relative permeabilities should be measured using techniques that mimic the actual reservoir characterisation as closely as possible. One of the important aspects of understanding gas-condensate behaviour is through producing gas oil relative permeabilities at conditions that are representative of the near wellbore region.

The variation in relative permeability found at the higher IFT values may be erroneous, due to neglect of capillary pressure in the analysis of the measurements; however, the strong variation observed at low IFT is well established in the literature. The exact dependence on the IFT has not been studied in details in the literature so far, and it might well be that it is the capillary number rather than the IFT alone, which is the controlling factor that needs to be understood well.

It is worth noting that lab studies to address gas-condensate productivity issues are often of a hybrid nature, with an initial liquid saturation being formed by condensation and then altered by injection of equilibrium oil and gas phases. These demonstrate increasing relative permeability with increasing rate and decreasing IFT, suggesting a dependence on the capillary number**.** It is recommended measuring relative permeabilities at a range of flow rates to understand the effect of high capillary number flow.

As the well productivity is proportional to the effective gas permeability in the near wellbore area, the most important parameter for understanding condensate well productivity is the gas relative permeability as a function of the ratio k_{rg}/k_{ro}. The ratio k_{rg}/k_{ro} is reported to be about 0.1 to 1 for a very rich condensate case, 1 to 10 for a medium to rich gas-condensate and 10 to 100 for a lean gas-condensate fluid. The degree of condensate banking depends on the relationship between k_{rg} and k_{rg}/k_{ro}, which is strongly dependent on the value of k_{rg} where the k_{ro} and k_{rg} curves cross over. Hence, relative permeability plays an important role in determining the productivity loss due to condensate blockage.

6.5 Near Wellbore Effects

Near wellbore effects can significantly influence the flow of oil and gas in gas-condensate system. In order to understand performance of typical gas-condensate well, there are three effects that impact well productivity to consider:

1. Condensate banking, in which liquid drops out as a result of well bottom hole pressure, BHP dropping below dew point pressure.
2. Velocity stripping, critical at high velocities, the oil and gas perm abilities are increased and the gas flow near the wellbore is improved. Velocity stripping only affects multi-phase systems and the effect is mainly dependent on capillary number, N_c value.
3. Non-Darcy flow, which is also function of velocity that causes negative impact on well productivity as reported in the literature.

Two special phenomena affect high velocity flow in gas-condensate reservoirs, which are non-Darcy or inertial flow, and changes in relative permeability due to velocity stripping' or positive coupling. Non-Darcy flow reduces productivity whereas the relative permeability effects increase productivity. In most cases, the relative permeability change is more important, so that the high rate phenomena have a beneficial effect on well productivity. Effects of capillary number and non-Darcy effects are acting simultaneously, one improves productivity as a result of high capillary number and other reduces it due to non-Darcy effect and hence called coupling effect.

To understand the flow to a gas-condensate production well, it is recommended as a good practice to divide the area around the wellbore into three regions as proposed by Fevang and Whitson (1996). Most of the pressure drop occurs in Region 1 in the vicinity of the wellbore, a region which typically extends up to about 100 feet away from the wellbore, where both gas and condensate phases are mobile. In this region, semi-steady state conditions can be applied and the flowing composition does not vary with distance from the well. The third region is located away from the wellbore where single phase gas is present only.

6.5.1 Effect of Condensate Banking

The main difference between a gas-condensate and dry gas reservoir is the formation of a liquid dropout in the reservoir as pressure declines below dew point, by a process known as retrograde condensation. This extra liquid phase has low or zero mobility, trapping liquid components in the reservoir and reducing recovery. The condensate may build-up for 10s or 100s of feet around production wells (*Figure 6-1*) depending on gas richness as well as production time and rate, impeding the flow of gas and reducing well productivity.

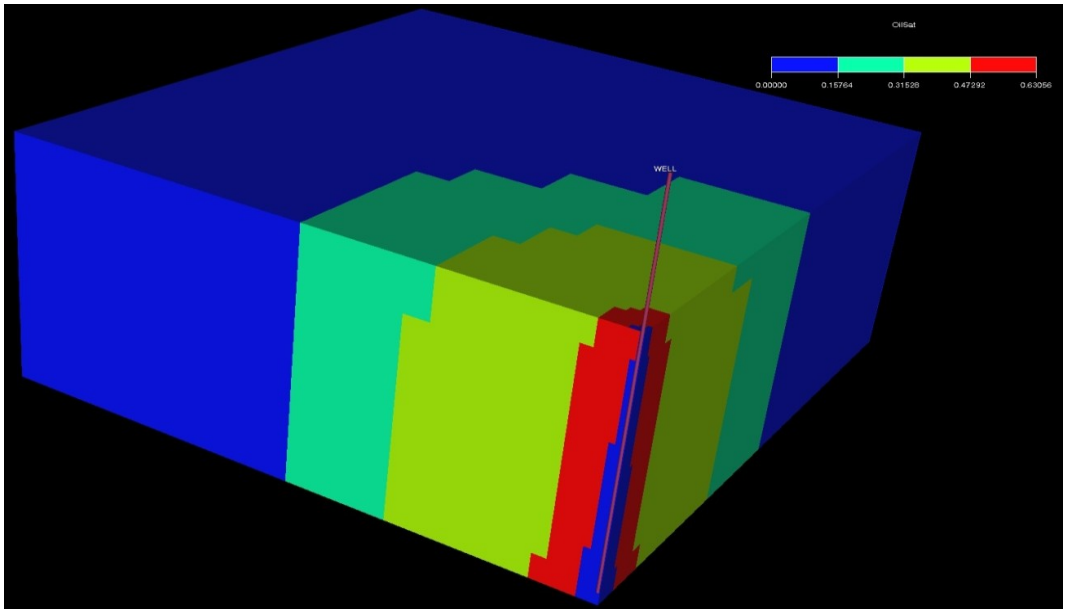


Figure 6- 1: shows near wellbore liquid drop out end of 5days BU following 180 days DD

The plot illustrates liquid saturation distribution in a single layer gas-condensate reservoir model with liquid drop out accumulated around the wellbore. As it can be seen the liquid saturation reduces away from the wellbore. However, in the vicinity of the wellbore there is no indication of any liquid drop out and this behaviour is due gas re-vaporisation during the build-up period. According to Mott (1999) pressure and liquid saturation around a producing well varies as a function of the distance from the wellbore. It is reported that away from the well, only the gas phase will be mobile. As gas flows towards the well and its pressure falls, the capacity of the gas to vaporise oil will reduce, so that liquid will condense from the flowing gas phase. This liquid condensate will initially be immobile and will accumulate in the near wellbore region. As the flow rate of the gas phase is greater near the well, liquid will continue accumulate faster in the region near to the wellbore until its saturation exceeds its critical value and then liquid will start to flow.

6.5.2 Effect of Velocity stripping

It is known that relative permeability is increased at high capillary number, which is a dimensionless quantity that measures the ratio of viscous to capillary forces, and is defined by the following equation:

$$N_c = \frac{(flow\ rate).\ (viscosity)}{IFT}$$

According to the above relationship, capillary number is proportional to flow rate. Thus, high capillary number values can occur in the vicinity of a gas-condensate well. Experiments showed that significant improvements in mobility will occur above a threshold capillary number, which has been found to be around 10^{-5} for gas and this value was obtained from experiment results.

Using rock relative permeability curves in the near wellbore region will certainly under predict well productivity because it ignores the increase of mobility at high velocity in the vicinity of the wellbore region known as velocity stripping phenomena, which can be observed from analysing pressure transient data and saturation profiles. An increase in mobility at high velocities near wellbore is reported based on lab experiments and gathered field results. Since the benefits of velocity stripping decline as production rate falls, it is not possible to define a single set of near well relative permeabilities that can model real well performance. It is worth noting that the improvement in productivity due to velocity stripping (due to high capillary number) is usually less significant than non-Darcy flow effect.

6.5.3 Effect of Non-Darcy Skin

In addition to capillary number, another critical parameter that impacts well productivity is the non-Darcy or inertial flow effects, which has a negative effect by reducing well productivity. The magnitude of this effect will depend on the value of the non-Darcy flow coefficient used in the model. Estimating non-Darcy values is a challenging task, as there is a wide variation between results of the different published correlations particularly as a function of permeability and porosity.

According to Mott (1999), non-Darcy flow effect reduces effective permeability near to the wellbore, causing a reduction in well productivity. The non-Darcy skin is included in

well inflow equations as a flow dependent addition to the skin factor as it can be seen in the relationship below:

$$S' = S + D.Q \tag{6-4}$$

where:
S' = total skin
S = mechanical skin factor
D = non-Darcy skin factor
Q = Flow rate.
For a *dry gas* system:

$$D = 2.912x10^{-14}\ \frac{k.\beta.\rho_g^{surf}}{\mu_g h.r_w} \tag{6-5}$$

where:
D = non-Darcy skin factor, (1/Mscf/day)
k = permeability, mD
β = non-Darcy constant, depending on type of rock and its permeability to the fluid, (1/ft)
ρ_g^{surf} = surface gas density, lb/ft^3
μ_g = in-situ gas viscosity, cp
h = thickness, ft
r_w = wellbore radius, ft

6.5.4 Effect of Miscibility

Gas-condensate well productivity presents some special problems for reservoir engineers. There is a need to understand the complex phenomena that occur in the near wellbore region, including condensate blockage, changes in relative permeability at high velocity and non-Darcy flow. Acquiring the necessary relative permeability data can be time consuming and expensive. Special techniques are needed for representing near wellbore effects in field scale simulation models.

In addition, conventional deep reservoir gas-condensate relative permeability measurements are usually conducted at very low rate to obtain relative permeability data at low capillary number, typically Nc =10^{-6}. In the current project a series of new relative permeabilities curves were generated that consider change in curves curvature, which will impact oil and gas flow in the reservoir. (*Figure 6-2*) shows changes in fluid miscibility effect on the oil and gas saturation curves. As it can be noticed a straight line represents the total miscibility case.

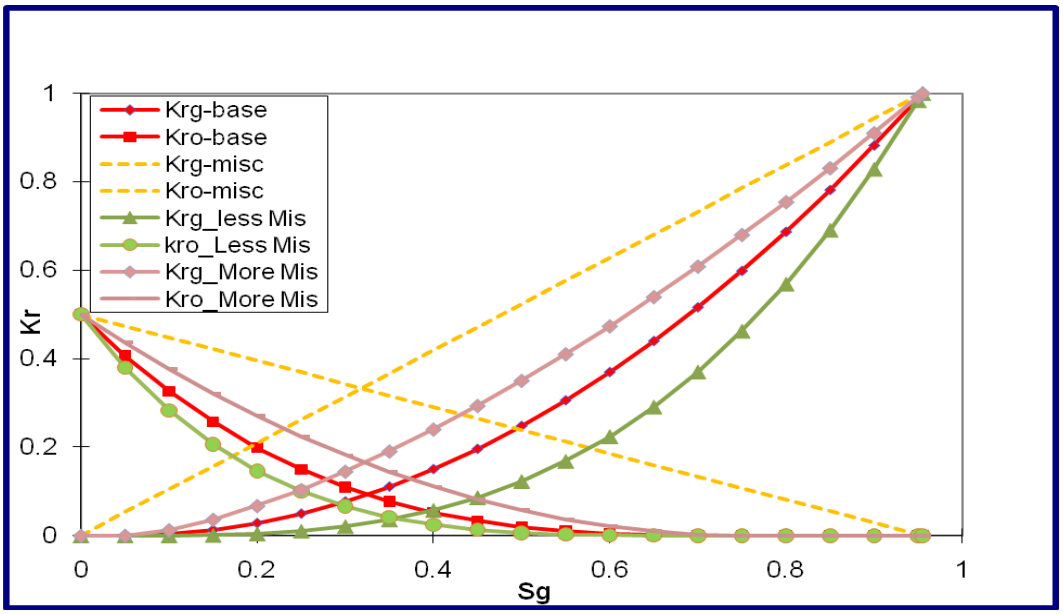


Figure 6- 2: Relative permeability curves for miscible, less, base and high miscible

Henderson *et al.* (1995) introduced a correlation for the change in relative permeability at high capillary number that is used in the Eclipse 300 simulator. This correlation is based on a conventional treatment of relative permeability in terms of saturation. It also uses an interpolation between 'base' and 'miscible' relative permeability curves; however, the interpolation is between values at the same value of gas saturation. The 'miscible' relative permeabilities are assumed to be straight lines with zero end point saturations and maximum values of 1. This correlation has the advantage of simplicity, with only 2 empirical parameters.

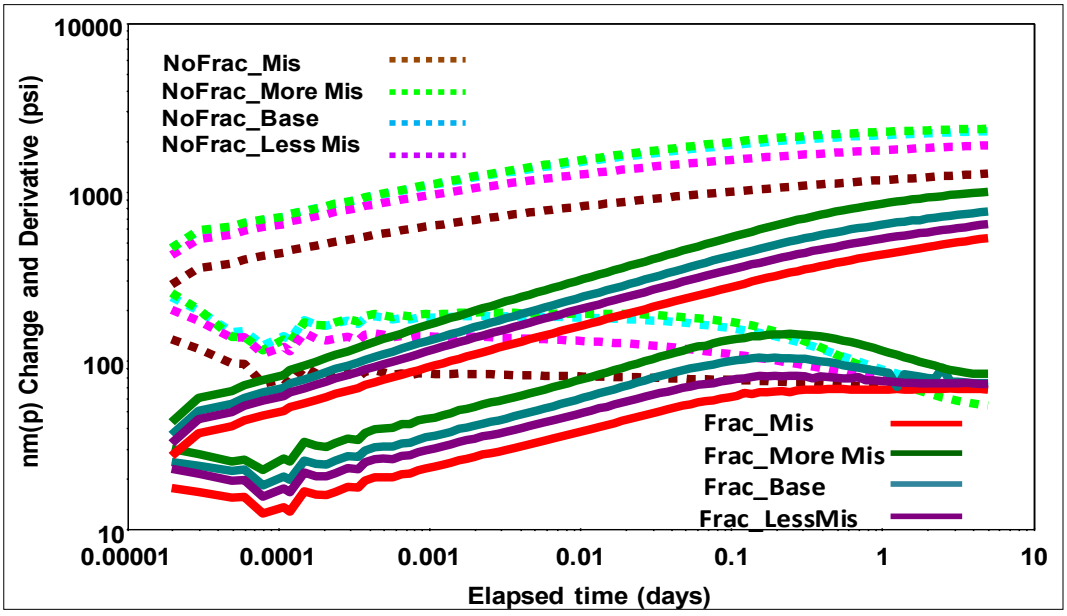


Figure 6- 3: Cases with/out fracture of miscible, and base, high and low miscibility fluids

By examining Figures (*6-3, 6-4 and 6-5*) of fractured and non-fractured wells behaviour with various miscibility runs it clearly can be noticed that the miscibility parameter is affecting the pressure response. For instance, in the case of total miscible run, the pressure behaviour is for typical fractured well feature (red). On the other hand, when the relative permeability curve of less miscibility effect, the generated pressure behaviour is different of normal fractured well response and some indication of skin can be seen (green). The plots indicate that the uncertainty associated with relative perm curves will impact the pressure behaviour of fractured wells significantly.

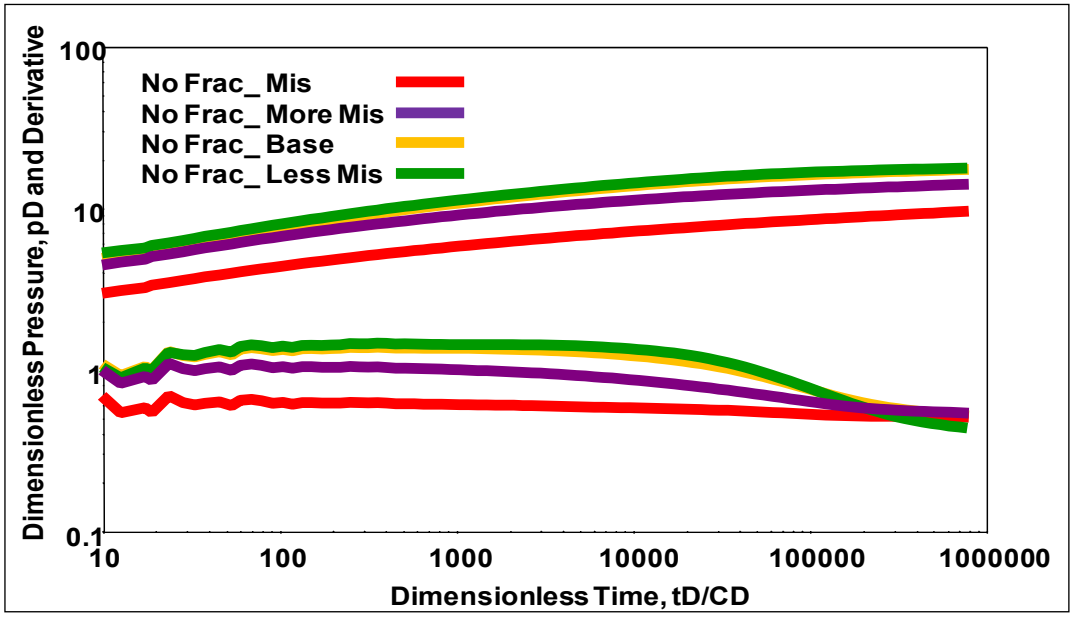


Figure 6- 4: Log-log plot of non-fractured well of mis, less miscible base and more miscible.

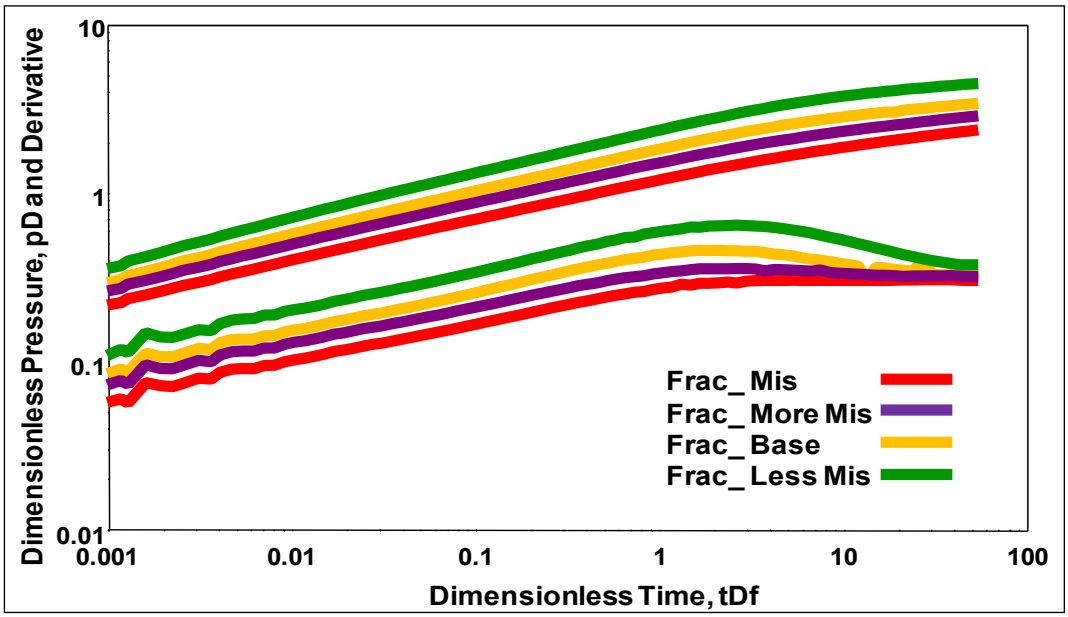


Figure 6- 5: Log-log plot of fractured well of mis. , less miscible, base and more miscible

6.6 Well Productivity

Well productivity is a critical issue in the development of many gas-condensate reservoirs. Accurate prediction of well productivity is needed to select the best development plan and to set gas sales contracts. It is found from experience that gas-condensate reservoirs require special practices for modelling well productivity due to liquid condensation phenomena in the vicinity of the wellbore. According to Mott (1999), much of the pressure drop from condensate blockage occurs within a few feet of the wellbore, where velocities are very high; therefore, it is important to understand the flow characteristics in this region to be able to forecast well productivity appropriately.

A very important phenomenon in the near wellbore region is the increase in relative permeability at high capillary numbers, while other significant effects include inertial or non-Darcy flow and the potential for water vaporisation. Thus, it is vital to understand and accurately predicting well productivity as much as possible. As part of the current study sensitivity cases were run exploring the impact of implanted production rate constraints in the base case model. For this purpose low and high production rates were assumed for individual well to investigate production rate effect as uncertainty parameter in the model. In addition, to investigate the impact of fluid richness on the generated pressure behaviour, both lean and rich gas-condensate fluids (*Figure 6-7*) were examined and various fracture half-lengths impact on well productivity were investigated.

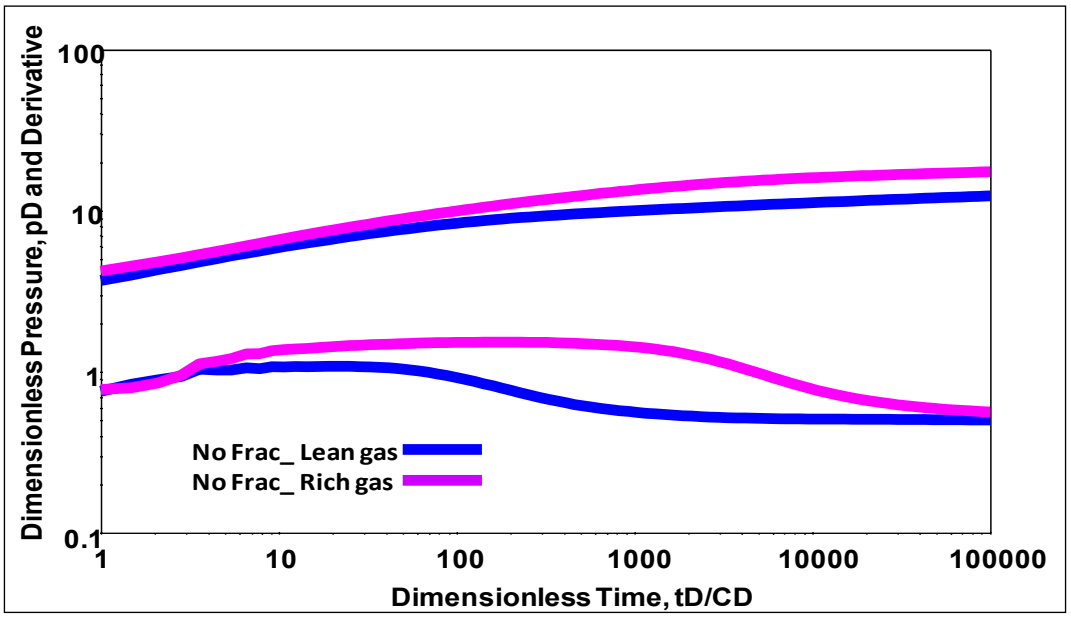


Figure 6- 6: Comparison of flow behaviour of lean and rich gas-condensate fluid

The numerical simulation results indicate the significance impact of fluid richness on the well productivity not only in the case of non-stimulated wells but also fractured wells. In the graphs below (*Figures 6-7, 6-8 and 6-9*), the well is fractured with different fracture half-lengths using lean and rich gas-condensate in the model. Results indicate that for short fractures there will be no indication of stimulation; however, fractured well flow behaviour can be seen clearly at early times for long fractures. Also, it seems condensate bank masks early time behaviour for short fractures with no significant effect on longer fractures.

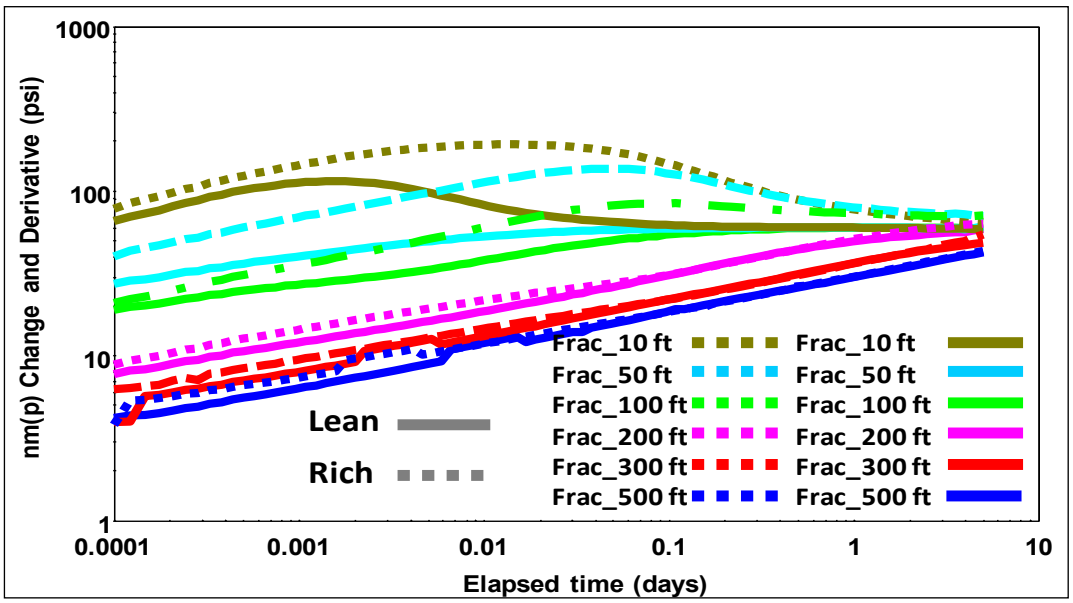


Figure 6- 7: Flow behaviour of fractured well in lean and rich models

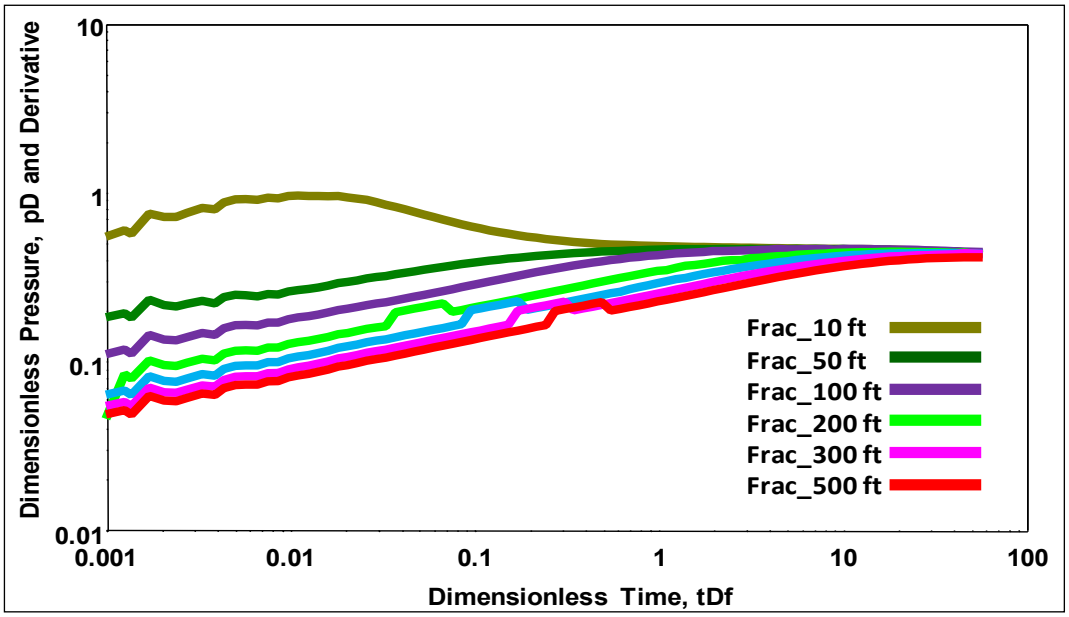


Figure 6- 8: Impact of short fracture half-length in lean case model

Based on the introduced pressure behaviour, fractured wells of short lengths demonstrate behaviour similar to the non-fractured well in both lean and rich fluid cases. The same model was run with damaged choked fractures (*Figure 6-10*) and the pressure behaviour shows no fractured well flow feature indication even for a massively fractured well (> 500ft). The graph shows the impact of performing an improper frac job or well stimulation resulting in a damaged fracture. These results demonstrate that a condensate bank will develop and mask early times fracture flow behaviour of induced damaged fractures.

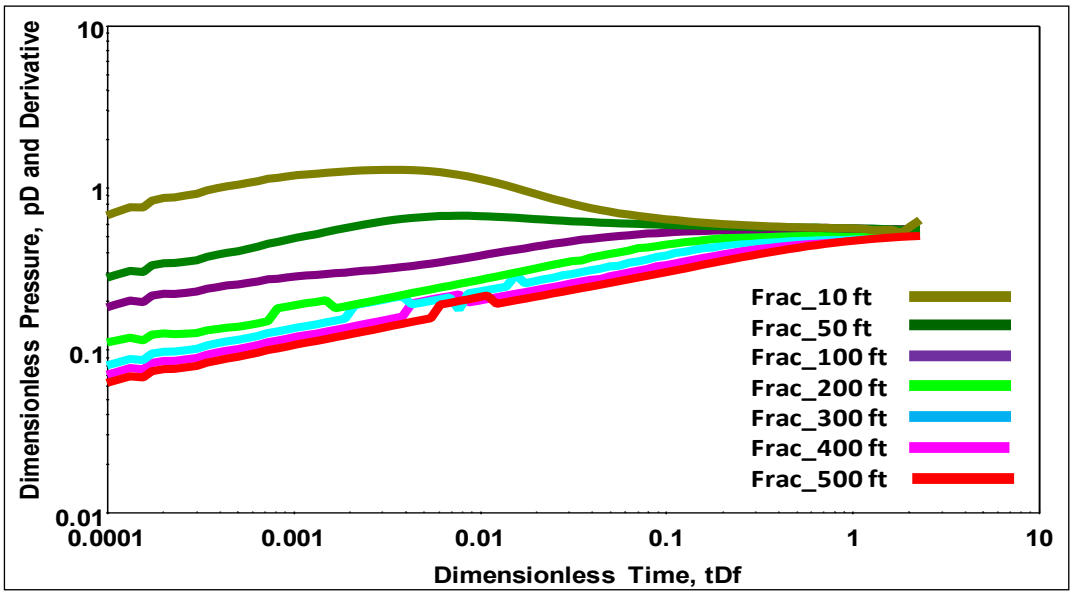


Figure 6- 9: Effect of short fracture half-length in the rich case

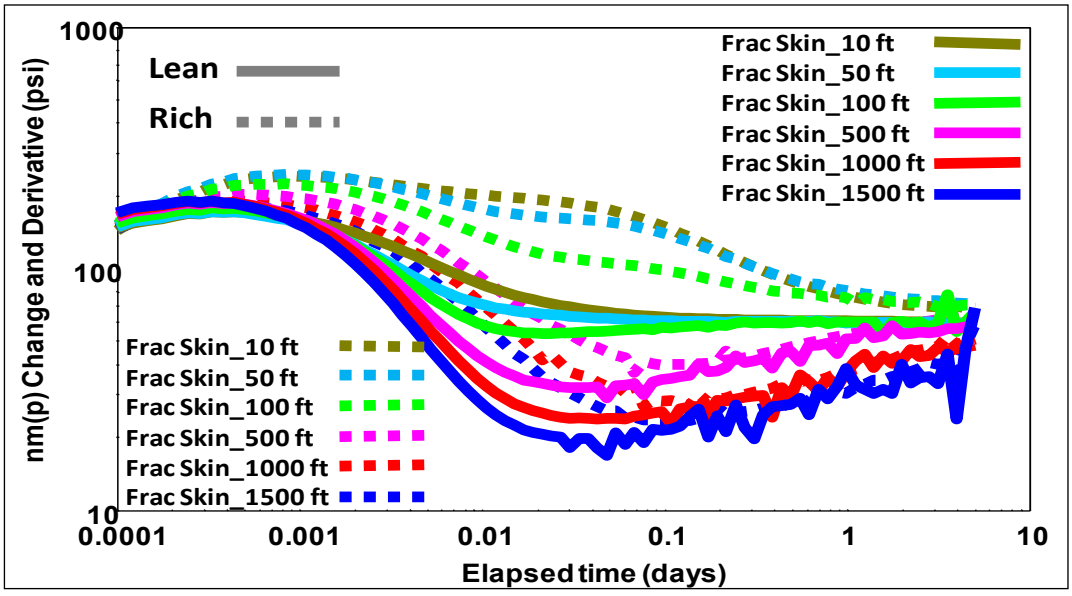


Figure 6- 10: Fracture choke damage effect on well behaviour in lean and rich condensate

In Appendix C in this document a range of fracture half-lengths were examined to investigate the impact of fracture damage on the generated well pressure behaviour.

To investigate production time effect on condensate bank accumulation, a single layer non-fractured model was run for different periods of 1, 2, 3, 6, 12, 24 and 36 months. Results are illustrated in Figure (*6-11*) below, where case A represents the model after 30 days drawdown followed by 5 days build up presented in case B. Cases C, D, E, F, and G are models run for 2, 3, 6, 12, 24 months drawdown followed by a 5 days shut-in period with case I representing the model at the end of 5 days build-up following a drawdown of 36 months period. As can be seen, the saturation near the wellbore changes significantly with increased saturation away from the wellbore and reduced saturation in the vicinity of the wellbore due to gas re-vaporisation effect during build-up period.

As production time increase with 36 months in case H, the reduced saturation in the vicinity of the well disappears. The results clearly demonstrate that the saturation profile is modified due to liquid condensation during draw downs and the gas re-vaporisation effect during subsequent build-up period. The purpose of running these models was to examine production time effect on the introduced saturation profiles pre frac and run the same models with different fracture half-lengths in post-frac tests to investigate the effect of stimulation on the generated saturation profiles.

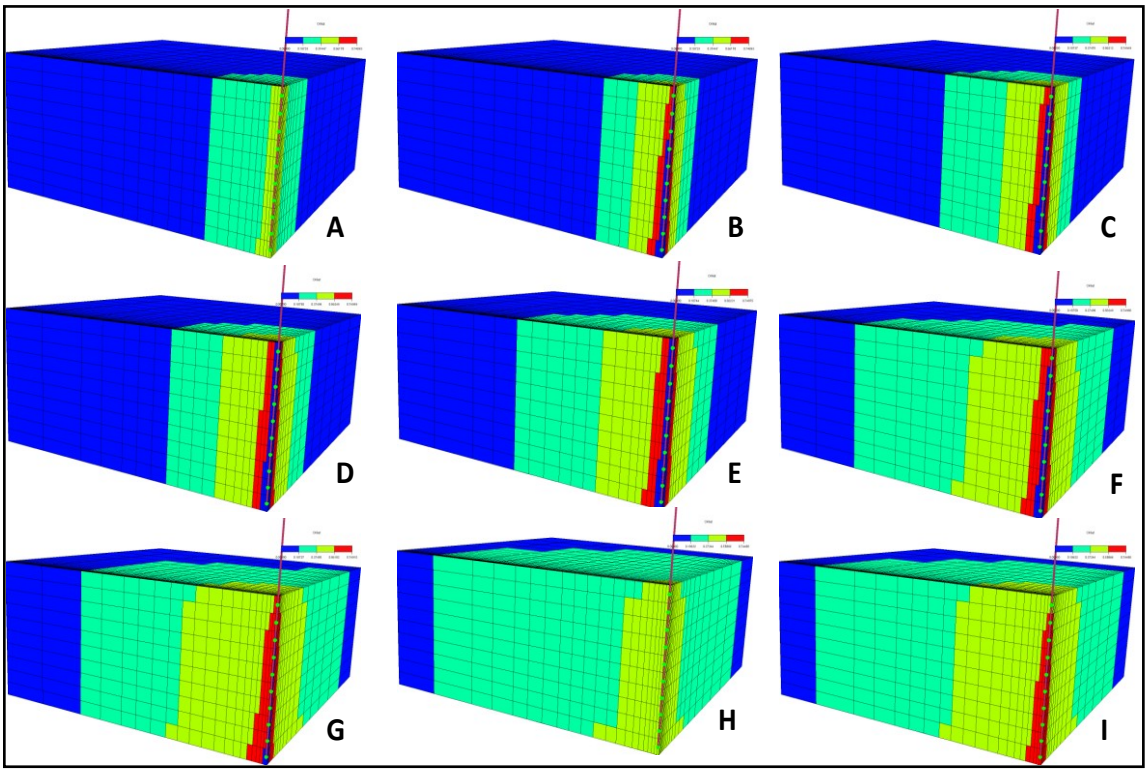


Figure 6- 11: Production time effect on condensate bank development after 1, 2, 3, 6, 12, 24 and 36 months with Case A and H showing end of DD and rest shows saturation at end of BU period following DD period

To further investigate the effect of production time cases of lean and rich fluids were examined for a drawdown of 30 days. By examining the plots below (*Figures 6-12 and 6-13*), the effect of fracture half-length on the liquid saturation distribution can be observed clearly. Results indicate that the liquid saturation is reduced along the fracture length and continued beyond the fracture tip in the case of short fractures. In addition, as fracture half-length increases more benefits can be observed through enhancing well productivity. However, results suggest that a fracture half-length of 400ft represents optimum length that can be designed in rich gas-condensate wells. It is worth noting that these saturation values were taken along the fracture length and liquid remains at the fracture face. Also, some spikes can be seen at the tip of short length fractures, which is more obvious in the rich gas condensate cases. As the fracture half-length increases with less liquid saturation (< 0.1), the spikes disappear. This suggests that liquid saturation is reduced along fracture lengths and remained beyond fracture tip with no effects for long fracture half lengths.

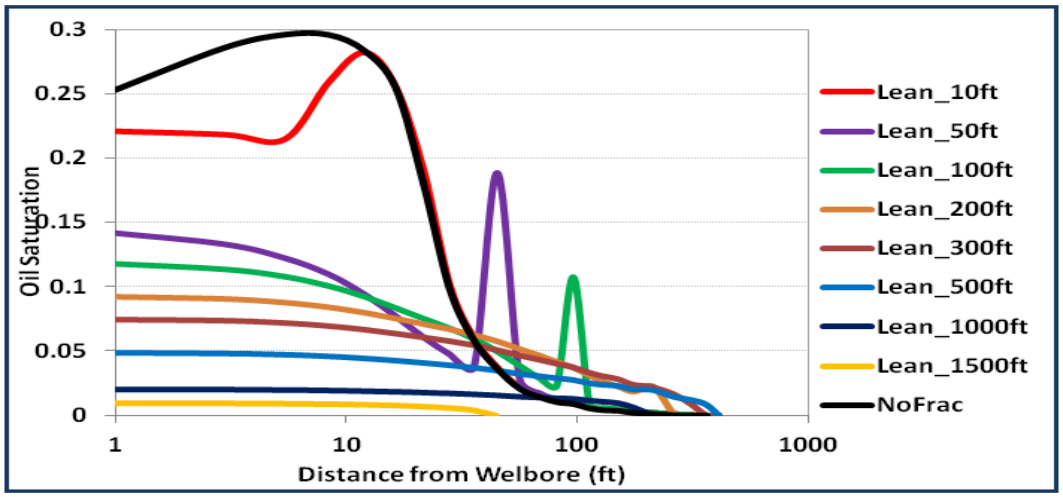


Figure 6- 12: Fractured well behaviour of various lengths at end of 30days DD

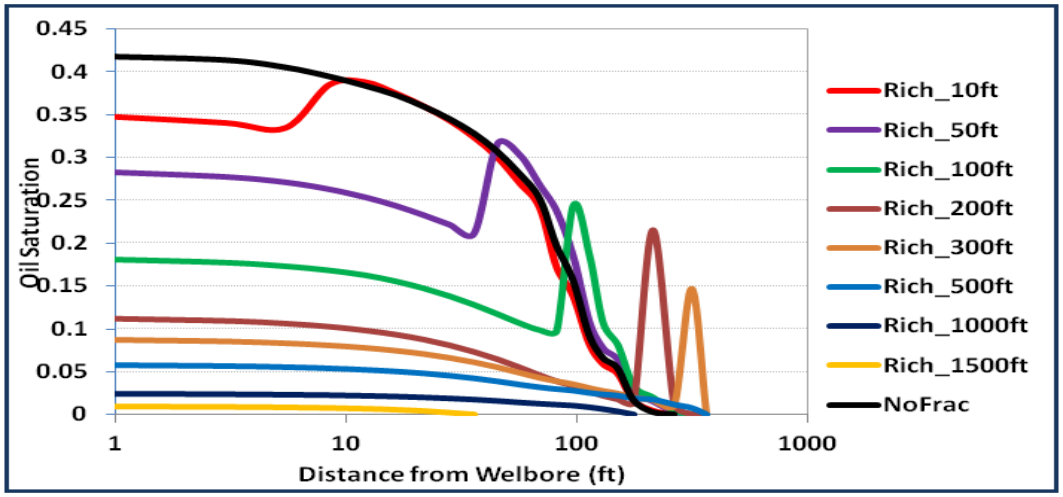


Figure 6- 13: Fractured well behaviour of various lengths at end of 30days DD

In addition, to examine longer production period effect, models were run for a drawdown of 180 days (*Figures 6-14 and 6-15*). The generated pressure profiles are obviously indicating that liquid saturation is widely distributed for longer production duration period. However, it appears that the lean case indicate less liquid saturation than rich fluid for longer drawdown periods due to low CGR effect. By examining the saturation profiles for the short fracture lean case in both 30 days and 180days periods, it can be observed that the liquid saturation for 10ft fracture half-length has dropped significantly in the 180days DD case and this is perhaps due to time allowed for gas re-vaporisation effect. It also shows condensate bank radius, which is different in lean and rich gas-condensate.

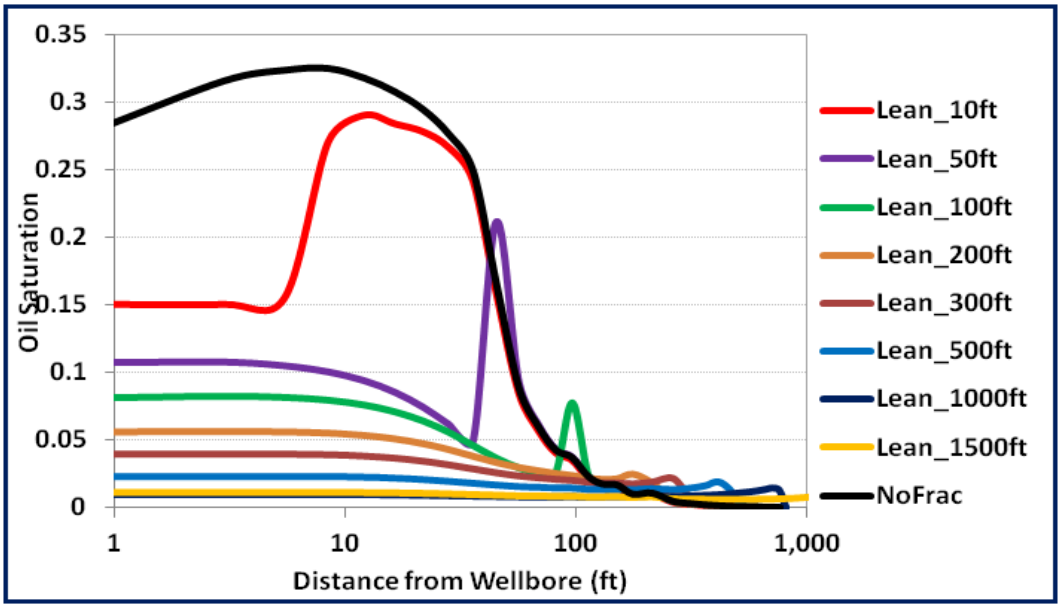


Figure 6- 14: Fractured well behaviour of various lengths at end of 180days DD

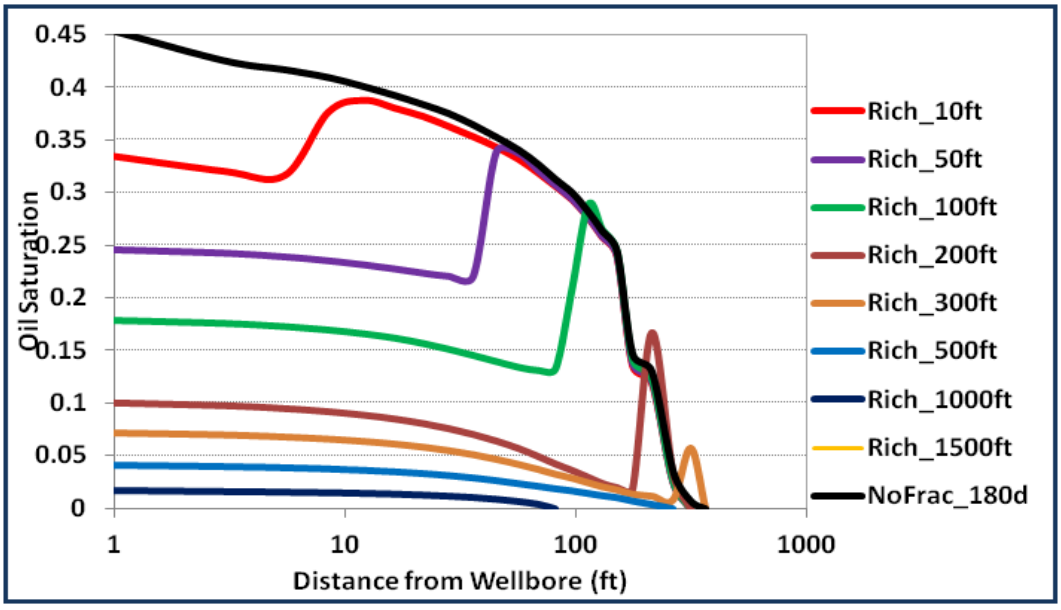


Figure 6- 15: Fractured well behaviour of various lengths at end of 180days DD

The graphs below (*Figures 6-16 and 6-17*) show a comparison between the two cases run with drawdowns of 30 days and 180 days for lean and rich fluid. Results indicate clearly the production time duration effect on the generated saturation distribution in both cases. Also, show that there will be not much benefit achieved from stimulation a well with fracture half-length longer than 400ft in the case of rich condensate and about 100ft in the lean fluid. By comparing the liquid saturation curves for both 30days and 180days production time, it demonstrates that more condensate is accumulated during the short production time compared to the longer production time due to gas re-vaporisation effect.

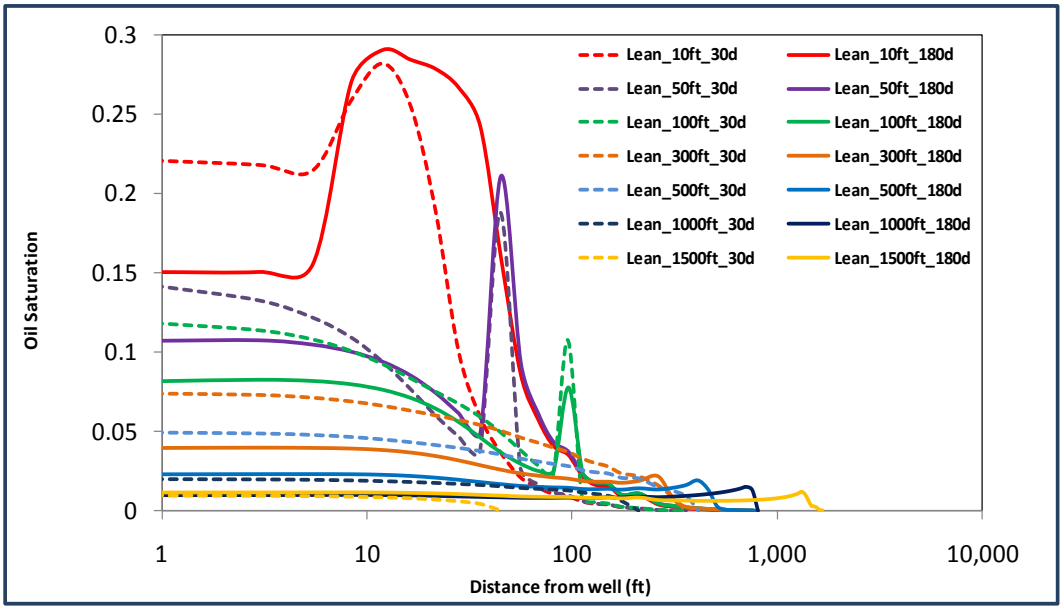


Figure 6- 16: Flow behaviour comparison in lean fluid of 30dand180d production periods

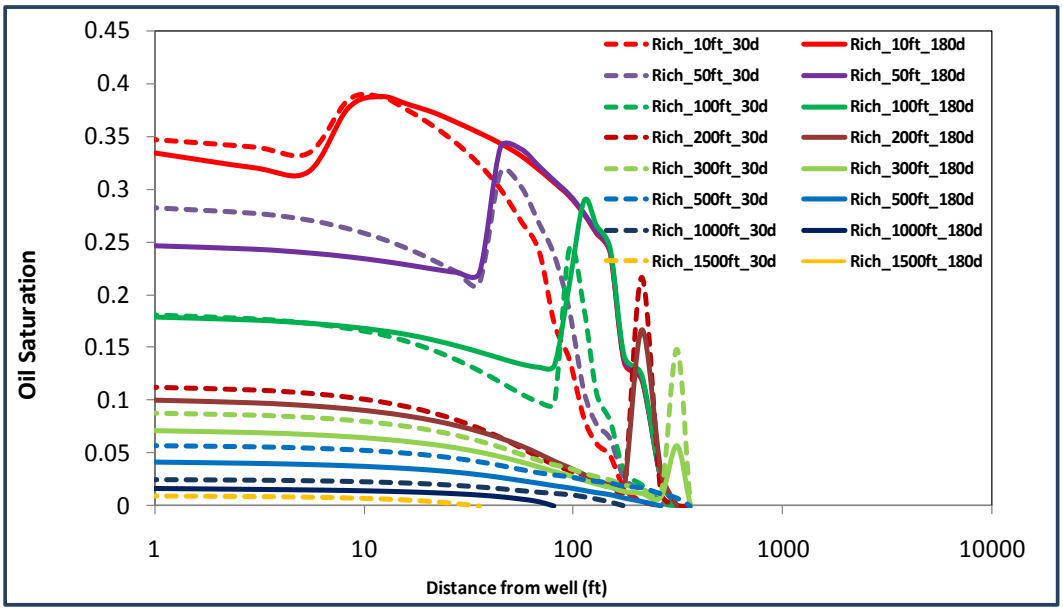


Figure 6- 17: Flow behaviour comparison in rich fluid of 30d and 180d production periods

In order to investigate the best time to stimulate a gas-condensate well, either at the beginning before putting the well on stream or after sometimes of liquid accumulation to enhance well productivity. Results indicate clearly that introducing a fracture at start of well production will improve well performance significantly than following condensate bank accumulation. For this purpose models of lean (*Figure 6-18*) and rich (*Figure 6-19*) gas-condensate consisting of fracture half-lengths of 50, 100, 500 and 1000ft were run for a month DD followed by a 5 days BU then fracture introduced and run for another month of DD and a 5 days of BU in parallel models with similar fracture half-lengths introduced before well commence production and for the same flow periods.

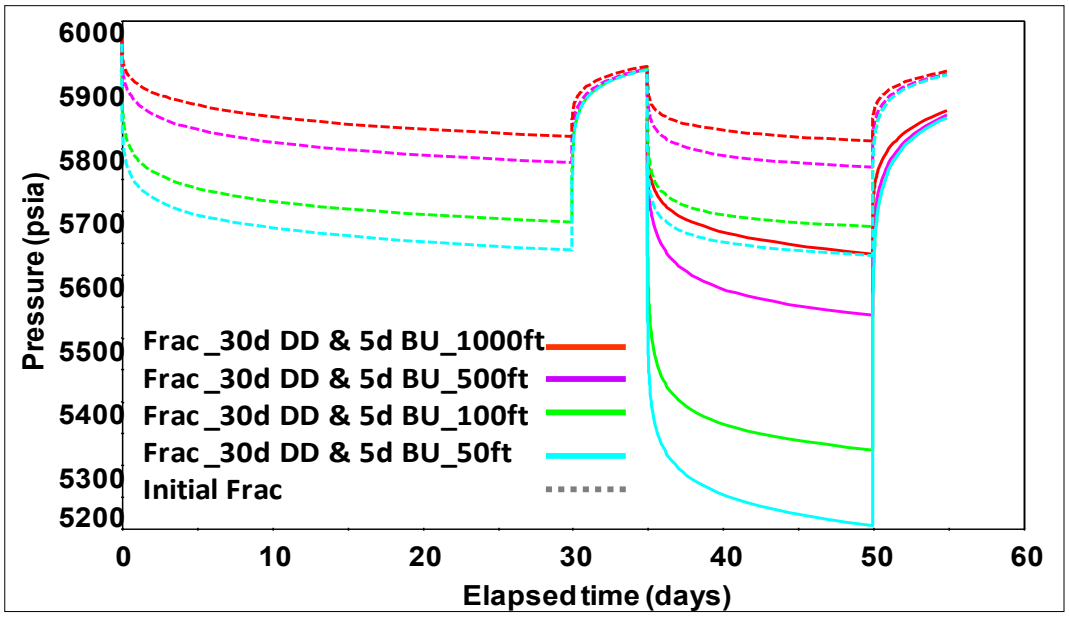


Figure 6- 18: Flow behaviour of lean fluid for fractured well during four low periods

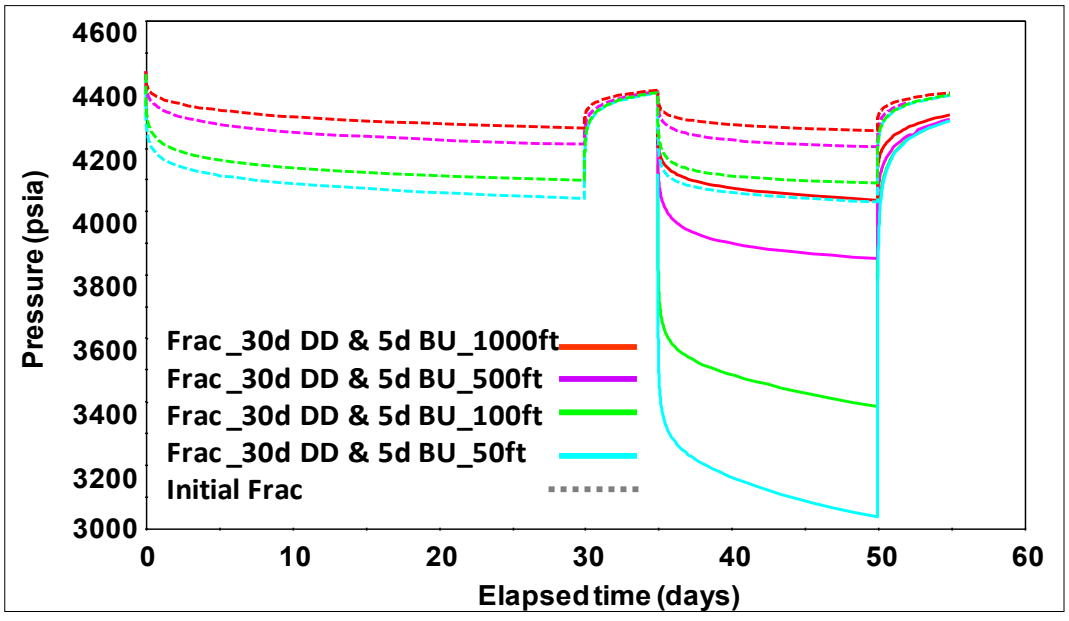


Figure 6- 19: Flow behaviour comparison in rich fluid of four flow periods

In another approach to investigate fractured well flow behaviour penetrating multi-layered lean and rich gas-condensate reservoirs. Initially, a non-fractured well examined consists of three layers allowing for cross flowing between adjacent layers. For this purpose both lean and rich fluid were examined with middle and bottom layers perforated only. Results indicate that the condensate bank accumulation feature is superimposing multilayer effects for both fluid types as it can be seen in Figure (*6-20*) below. In this graph a model with single layer of equivalent permeability of 35 mD is compared to the ones present in the multi-layered case of 1, 10 and 100mD. This is to show multi-layering feature and also to show behaviour of lean condensate compared to rich fluid case. As it can be seen the multi-layering feature is superimposing the condensate bank behaviour in both the lean and rich gas-condensate cases.

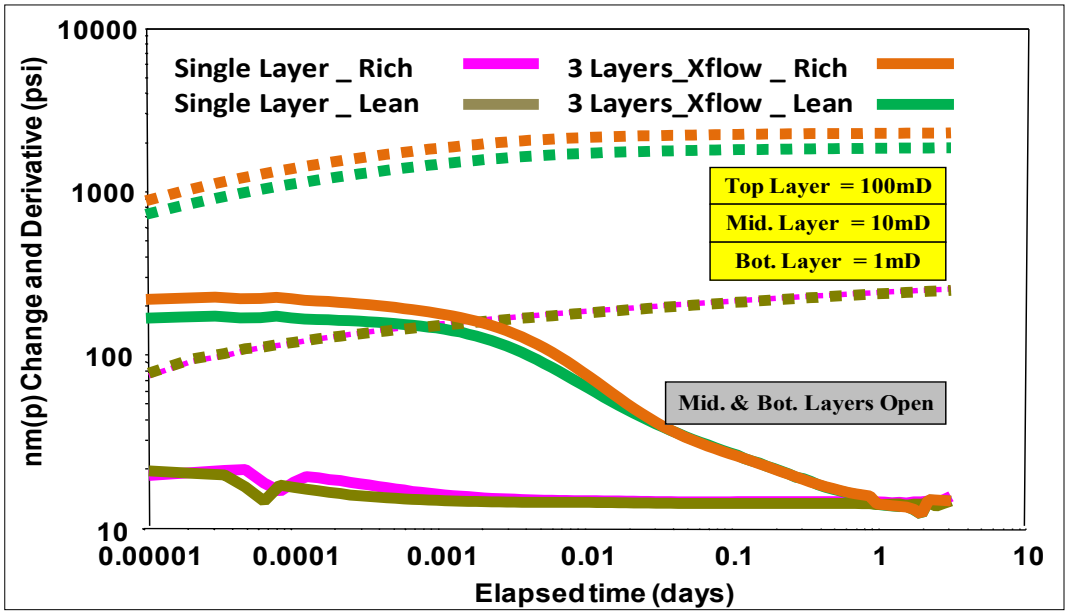


Figure 6- 20 : Flow behaviour comparison of multi-layered model of lean and rich fluid

To demonstrate a more detail graphical illustration of fracture half-length effect on the liquid saturation distribution and well productivity, some snap shots were taken for different scenarios, which can be found in the Appendix-D in this document. Liquid saturation distribution is presented in the first part and well productivity in the second part of the appendix. All graphs demonstrate the importance of fracture half-length effect in enhancing production and reducing liquid distribution nearby the wellbore. Results suggests that introducing fractures before condensate bank creation would improve well productivity by preventing liquid deposition within the fracture ;however, the liquid bank at the fracture face will remain even in the case of massive fracture half-length cases.

6.7 Conclusions

A number of single and multi-layered numerical models containing lean and rich gas-condensate fluid were constructed to investigate the liquid drop out effect on the performance of fractured wells; to examine condensate bank impact on generating flow behaviour that is similar to the investigated unusual fractured well flow feature in the study. Results from all case runs of fractured wells in lean and rich gas-condensate reservoirs suggest that induced fracture lengths would impact the benefits derived from any frac job. They also show that optimum fracture half-length in the rich case is 400ft with only 100ft in the lean case. In addition, radius of the created condensate bank will depend on the fluid richness, well production rate and the duration and radius of condensate bank that can be approximated from the induced fracture length. A number of conclusions were drawn as a result of hundreds of simulation runs of both lean and gas-condensate models:

- Different saturation zones develop around the wellbore indicating improved gas mobility due to capillary number effects, condensate drop out stabilization and dry gas behaviour at late time in gas-condensate reservoirs.
- Proppant fracturing of gas-condensate wells is certainly an effective approach for enhancing well productivity. The induced fracture reduces the rate at which condensate drop out by reducing pressure drop occur close to the wellbore.
- Induced fracture damage would impact the introduced fractured well flow behaviour and result in features similar to non-stimulated well. Interpretation of actual field well test data in North Sea verifies the results obtained from numerical simulation.
- Results indicate that liquid saturation near the wellbore for short production time is more than case of longer production time period due to gas re-vaporisation from the liquid during long drawdown periods.
- Results indicate that introducing hydraulic fractures before putting the production well on stream is more beneficial than some time after commencing production and a condensate bank has built. The simulation results show that that delaying fractures until the condensate bank is formed, then performing a frac job beyond the bank reduces saturation to minimum depending on the induced fracture half-lengths.
- Composite behaviour due to condensate bank and a multi-layered behaviour are superimposed, with the layering effects appearing first at early time on top of the condensate bank.

CHAPTER VII

FIELD APPLICATIONS OF FRACTURED WELL

7.1 Introduction

In this chapter, a number of fractured well field examples are presented that show flow behaviour similar to the behaviour of non-fractured well. It is worth noting the fact that finding actual field examples data demonstrating similar behaviour to the investigated problem in this study is not a simple task. As the study results suggest that the behaviour problem is likely to be associated with improper performed frac jobs. Unfortunately, usually service companies conducting the well stimulation work are not reporting bad performed frac jobs. For this reason finding field examples to include in this study was a challenge approach; however, three examples are investigated in the study.

The first case is a gas well test from Canada that was stimulated by proppant frac. The post-frac test showed an improvement of skin with no indication of fractured well flow behaviour at early time. Analysis results indicate that the behaviour is due to presence of fracture skin (choke damage) that prevents the fracture flow behaviour to occur.

The second example is from an SPE 23630 paper published by Azari *et al.* (1992), in which they related the problem of not observing the fracture flow feature to fractures having short lengths and low conductivities (*FcD* lower than 0.1). The cause of the problem in this particular example is due to short fracture half-length and low fracture conductivity.

The third field case is from a commingled gas-condensate and volatile oil well in the Central North Sea. This field is very complex from geology and fluid characterisation point of view. It is a multi-layered reservoir consisting of 43 interbeded layers of sand and shale producing gas-condensate and volatile in commingled system. The induced fracture lengths in this case were designed to be (60 to 80 m) to bypass the damage in the vicinity of the wellbore. Post-frac well test analysis indicated improvement of well production and skin. However, post-frac well test data exhibited wellbore storage and skin followed by radial flow pressure response on the log-log plot, which is typical behaviour of non-fractured well. Below is an illustration of the three field examples mentioned above in more detail.

7.2 Case (I): Fractured Gas Well_ (Fracture damage)

The first example is from a dry gas field in Canada where the well is stimulated by propped fracture with no indication of fractured well flow behaviour on the post-frac pressure response. Table (*7-1*) below illustrates perforation data for the fractured well with work string and casing data with Table (*7-2*) presenting results of mini frac test as provided by the service company. The table also demonstrates fracture properties comparison between designed mini frac and analyses. Often the frac job is designed in terms of fracture configuration prior to execution of actual stimulation work.

Perforation Data						
Top MD (ft)	**Top TVD** (ft)	**Bottom MD** (ft)	**Bottom TVD** (ft)	**Shot Density** (shot/ft)	**Number**	**Diameter** (in)
14137.0	14137.0	14167.0	14167.0	6.00	180	0.40

Work string Data			
OD (in)	**Weight** (lb/ft)	**ID** (in)	**Depth** (ft)
5.500	20.0	4.778	11771.0

Casing Data			
OD (in)	**Weight** (lb/ft)	**ID** (in)	**Depth** (ft)
9.625	53.5	8.535	11728.0
7.000	32.0	6.094	12380.0
5.500	20.0	4.778	14600.0

Table 7- 1: Shows perforation, work string and casing data for the stimulated well

Mini Frac Test Pumping Schedule				
Injected Fluid	**Pump Rate** (bbl/min)	**Pump Time** (min)		**Volume Injected** (gal)
Cross Link Pad	43.2	23.7		43060
	Closure Pressure	**Closure Time**		**ISIP**
	11551 psi	14.2 min		12364 psi
	Analysis Results	**Job Simulation Results**	**Calibration on Young's Modulus**	**Calibration on Height**
Modulus	3.182E+6 psi	3.182E+6 psi	15159631 psi	3.182E+6 psi
Toughness	1270 psi.in0.5	1270 psi.in0.5	1270 psi.in0.5	1270 psi.in0.5
Height	213.5 ft	213.5 ft	213.5 ft	75.4 ft
Net Pressure	813 psi	185 psi	813 psi	813 psi
Half-length	66.3 ft	85.0 ft	316.1 ft	531.9 ft
Leak-off Coeff.	1.0E-2 ft/min0.5	1.0E-2 ft/min0.5	2.1E-3 ft/min0.5	3.4E-3 ft/min0.5
Spurt	0.0 gal/100ft2	0.0 gal/100ft2	0.0 gal/100ft2	0.0 gal/100ft2
Fluid Eff.	0.30	0.08	0.30	0.30

Table 7- 2: Mini frac pumping schedule for the fractured well

Figure (*7-1*) below presents the results from the propped frac treatment performed on the well with Figure (*7-2*) showing fracture half-length as designed prior to the well stimulation. It is worth noting that the induced fracture might have different properties in terms of half-length and conductivity compared to the designed model. Figure (*7-3*) illustrates designed fracture width versus fracture half-length. It is worth noting that actual propped fracture half-length is more important to consider when analysing a post-frac well test data. Well test interpretation results of the actual measured data indicate that the frac process has resulted in damage fracture close to the wellbore. This particular case is an example of a fractured well with no clear indication of fracture pressure behaviour at early time.

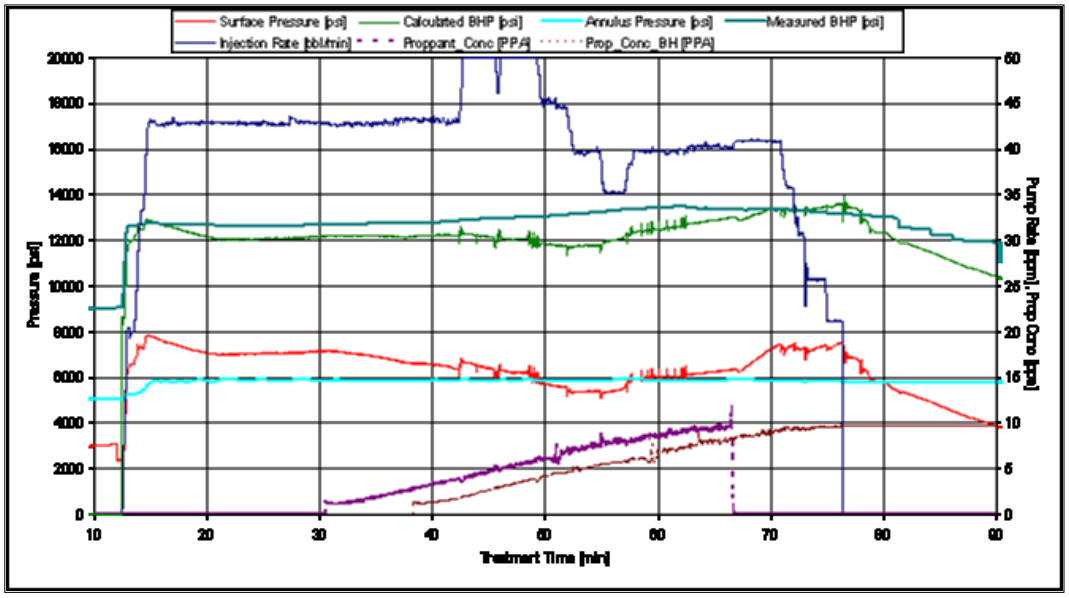


Figure 7- 1: Main frac job treatment results of the stimulated well

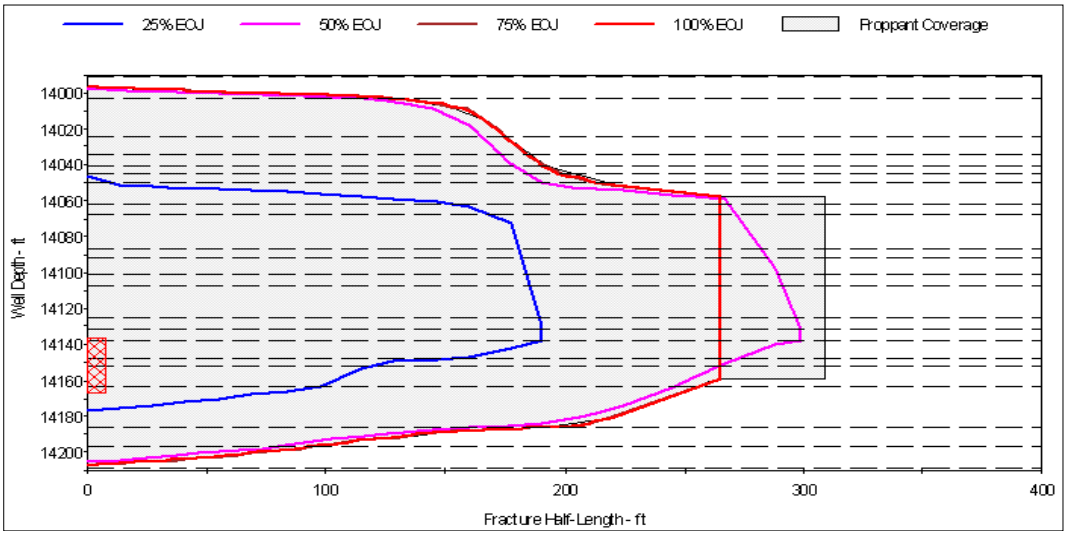


Figure 7- 2: Designed fracture half-length with perforated interval location

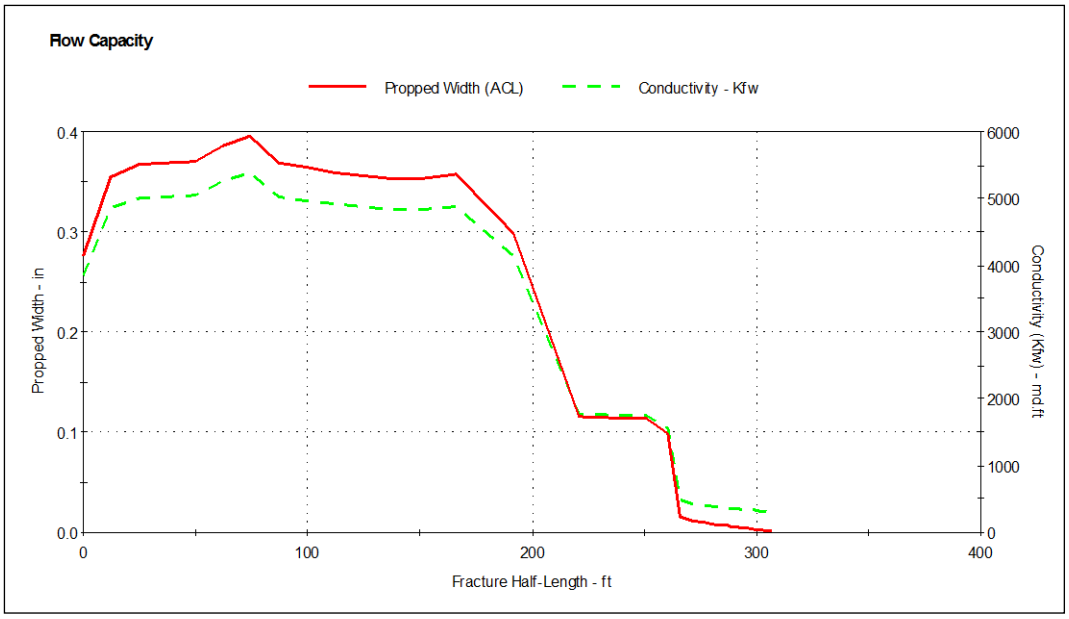


Figure 7- 3: Designed fracture width, length and conductivity profiles.

The main formation, fluid and fracture input parameters used to construct the numerical fracture model are illustrated in Table (*7-3*). Following the well stimulation work, a drill stem test, *DST* was run over the stimulated interval and the well test interpretation result is presented in Figure (*7-4*). The DST consists of well clean-up period followed by drawdown and short build-up with a second drawdown and long build-up period (FP # 4).

Reservoir Properties	
Initial pressure, psia	8840
Formation permeability	3
Formation porosity, fraction	0.3
Rock compressibility, psi-1	3.356E-6
Well bore radius, ft	0.3
Sw	2
St	-1.3
Wellbore storage, bbl/psi	0.00446
Reservoir thickness, ft	214
drainage area, acres	80
Fluid Properties	
Gas Compressibility, psi-1	3.82E-5
Viscosity, cp	0.04333
FVF, cf/scf	0.002652
Temperature, ^{o}F	150
Fracture Properties	
Fracture half-length, ft	65
Fracture width, ft	0.02
Fracture permeability, D	10

Table 7- 3: Description of the main characteristics of the gas reservoir model

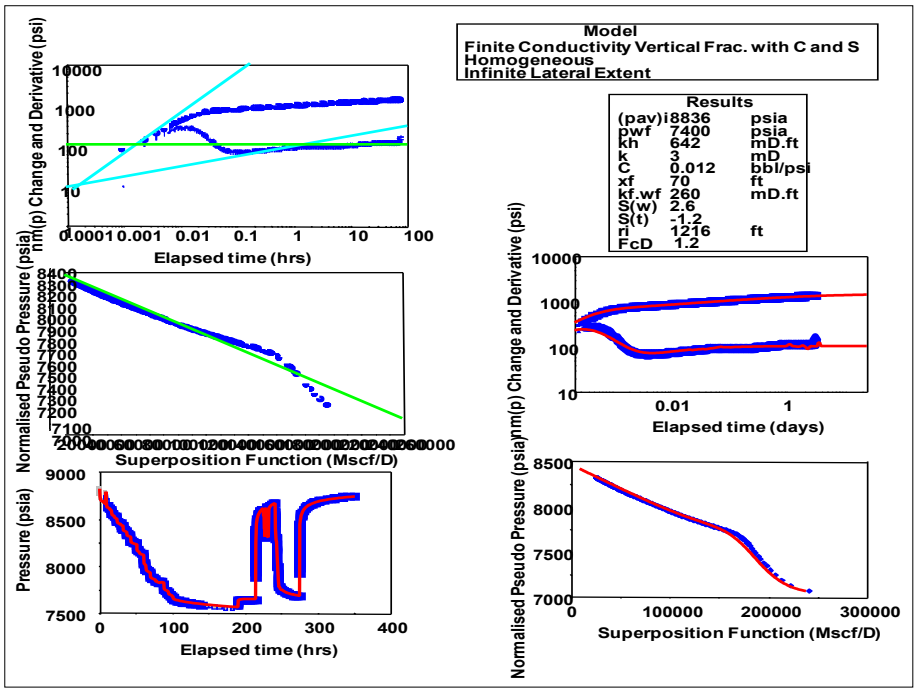


Figure 7- 4: Analytical well test interpretation result of the actual measured data (FP#4)

The interpreted forth build-up flow period data indicates *FcD* of 1.2, a fracture half-length of 70 ft and kh of 642 mD-ft. Figures (*7-5 and 7-6*) verify results of well test interpretation for the flow period #4 of the DST. The results also indicate a damaged fractured well response and in order to model the effect of fracture damage, a single layer numerical model was constructed and similar time step found in the history was used in the model.

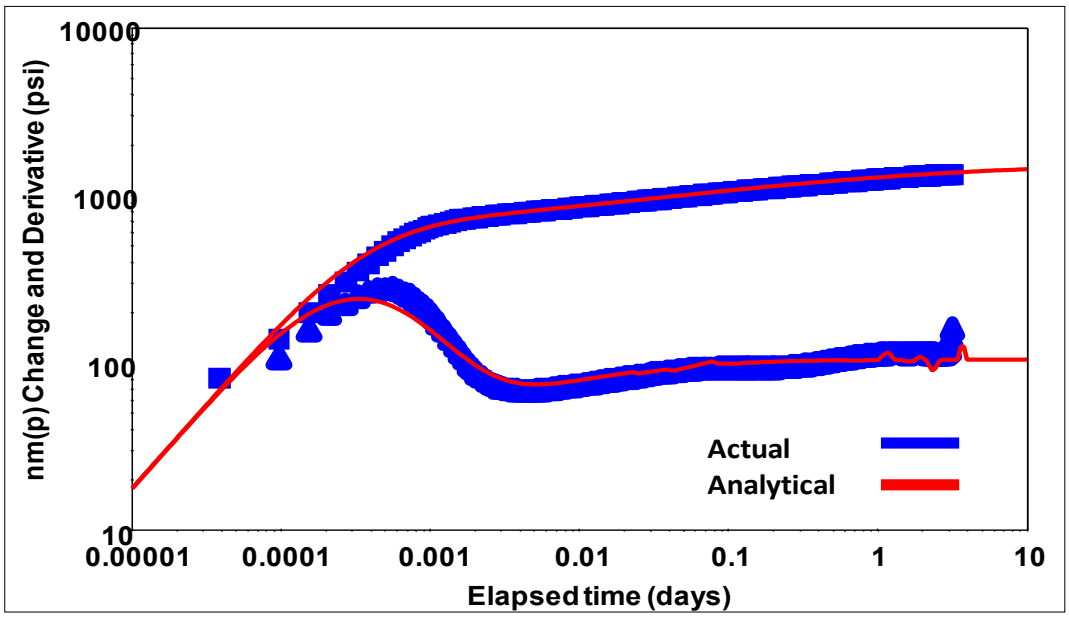


Figure 7- 5: Log-log diagnostic analytical solution match against actual data for FP#4

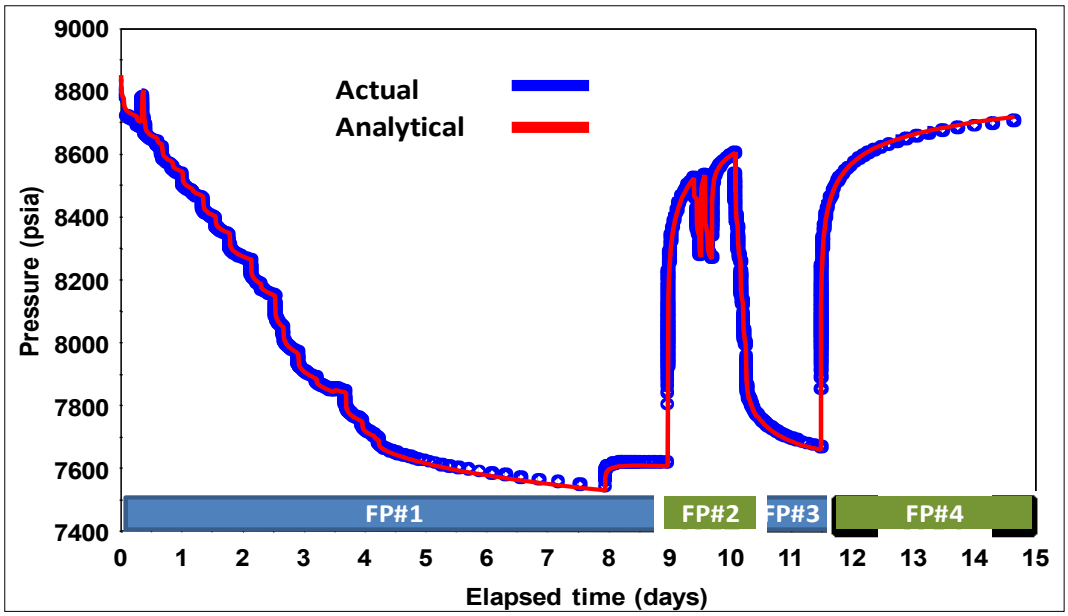


Figure 7- 6: Showing total production history of the DST run over the fractured interval

Fracture choke damage effect was implemented in the numerical model through altering the permeability within the fracture close to the wellbore, which can be resulted from performing improper frac job by inducing short fracture half-length of low conductivity relative to the formation conductivity. Well test interpretation result of the numerical model is presented in Figure (*7-7*) and as it can be noticed the results in good agreement with the measured data wish slight difference in calculated, x_f of 65ft due to the damage.

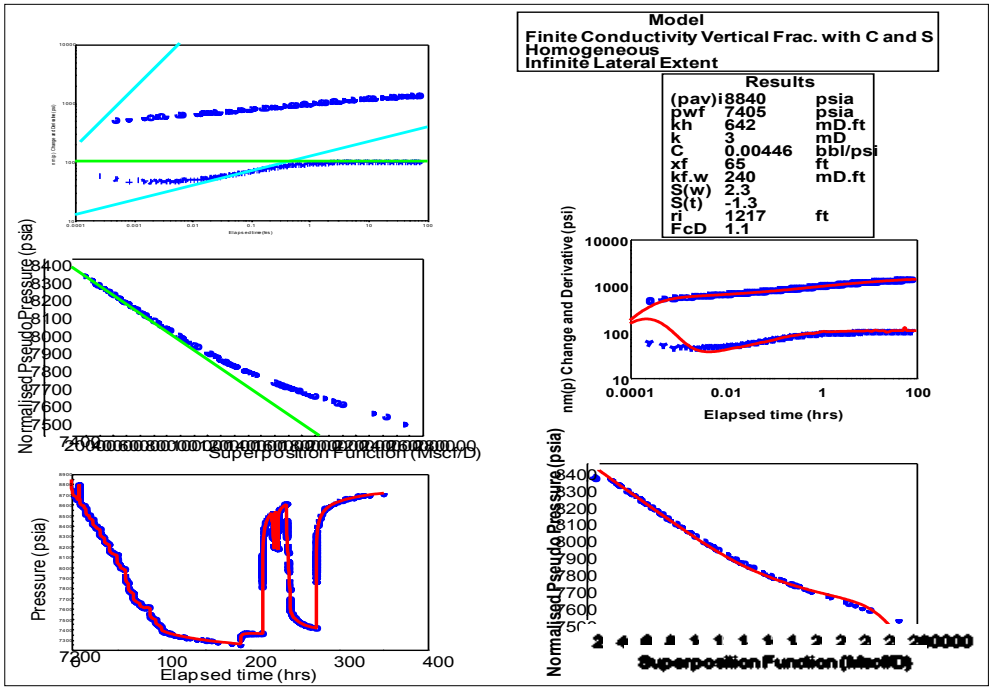


Figure 7- 7: Analytical well test interpretation of the numerical model results (FP # 4)

Figures (*7-8 and 7-9*) illustrate log-log diagnostic plot of the numerical fracture model with fracture chock effect versus analytical solution and total history match for the main flow period. Results also suggest that the investigated behaviour is most likely associated with fracture choke damage and relatively short induced fracture half-length. The example demonstrates the fact the behaviour resulted from a fracture damage effect, relatively short half-length and dominant wellbore storage impact at early time. The results also indicate that the numerical model is capable of introducing appropriate fracture properties and mimicking well behaviour following stimulation.

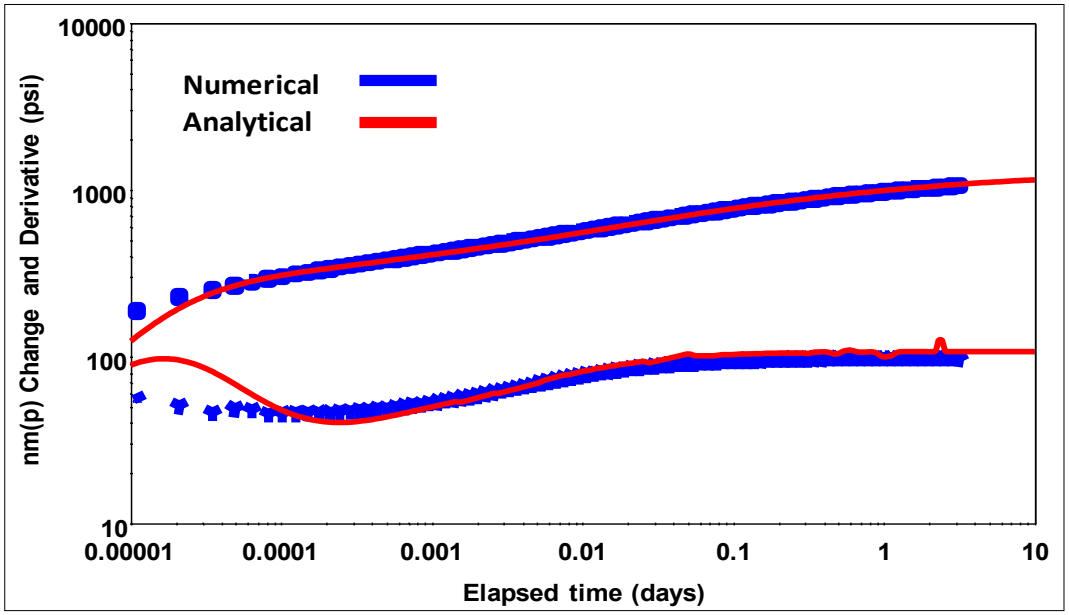


Figure 7- 8: Log-log pressure match for the main build-up flow period

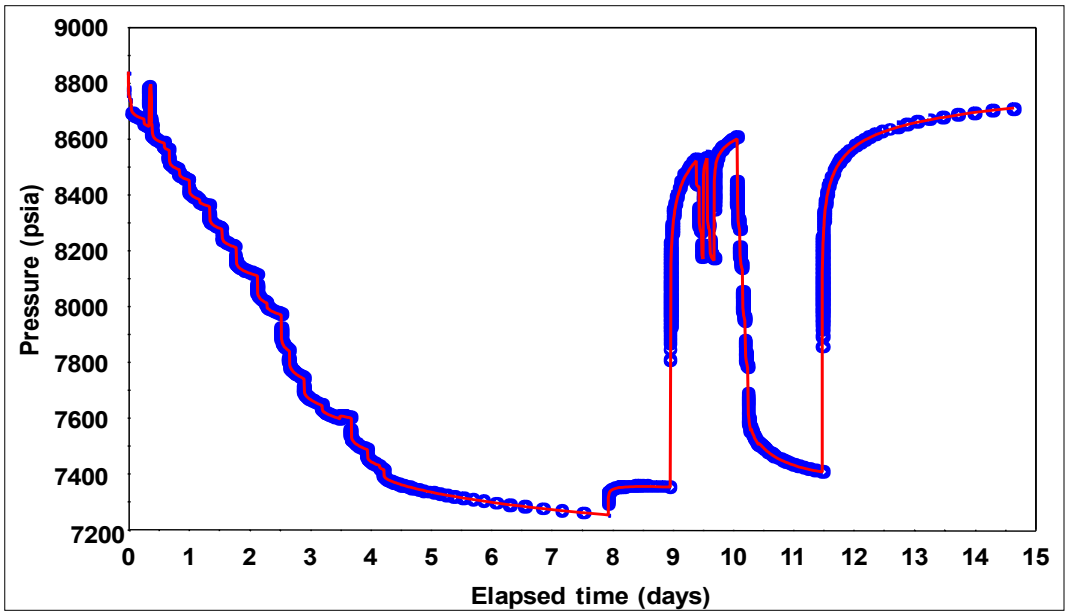


Figure 7- 9: Verification of the numerical model against the analytical solution

The measured DST data was analysed using pressure transient analysis package of Interpret, the main results of the analysis of both measured data and numerical model can be found in Table (*7-4*). As it can be seen, the calculated fracture and formation properties are similar in both models, which confirm robustness of the designed fracture model.

Parameters	Analytical	Numerical	Units
(pav)i	8836	8840	psia
P_{wf}	7400	7405	psia
kh	642	640	mD.ft
k	3	2.9	mD
C	0.012	0.0044	bbl/psi
X_f	70	65	ft
FcD	1.2	1.1	
$k_f.w_f$	260	240	mD.ft
S(w)	2.6	2.3	
S(t)	-1.2	-1.3	
r_i	1220	1217	ft

Table 7- 4: Comparison of well test interpretation results of analytical and numerical

The result of the numerical model is verified against the analytical solution in this field example as presented in the presented log-log plot below *(Figure 7-10*). The results indicate a good match with interpreted fracture half-length of 65 ft and *FcD* of 1.1 against fracture half-length of 70ft and *FcD* value of 1.2 from the analytical solution.

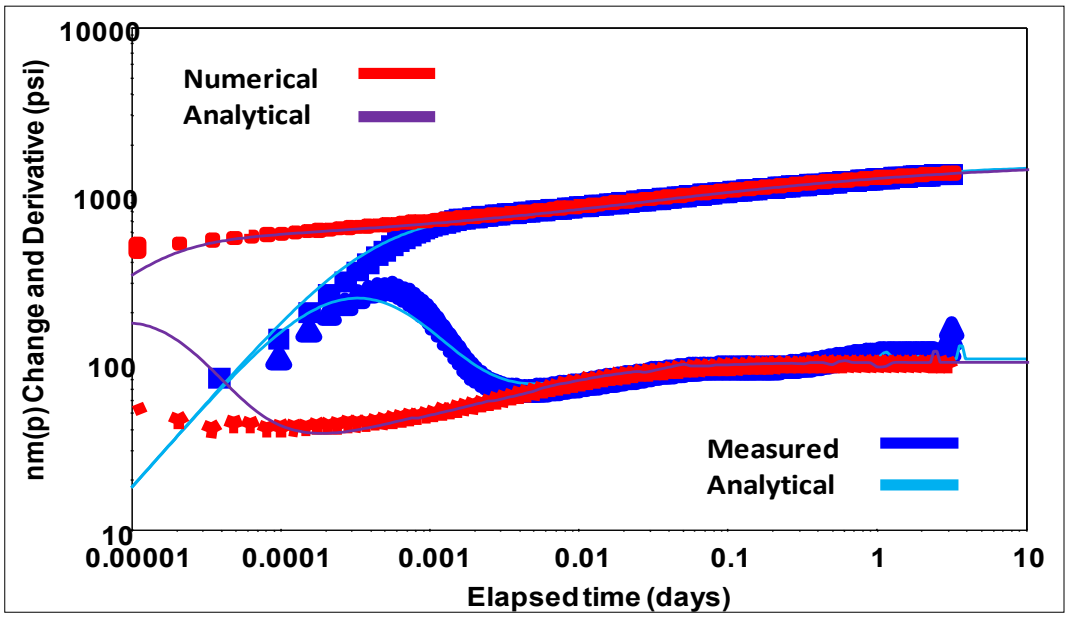


Figure 7- 10: Numerical model versus analytical solution results of the fractured well

7.3 Case (II): Fractured Gas Well_ (Low Fracture Conductivity)

The second studied example was taken from SPE 23630, a paper published by Azari *et al.* (1992). The gathered data from the paper is used with permission of the authors. Their study proposed that the investigated behaviour is likely to occur in fractured wells of low fracture conductivity typically *FcD <0.1* relative to the formation conductivity and short half-length (22ft in their case).

This field example is of a gas well initially experiencing difficulty in flowing naturally. The well was then propped fractured using 1430bbl of gel and 90.000 IBs of sand. Following the stimulation, the well was opened to flow back for 136.5 hours; however, about 800 bbl fracture fluid was not recovered. The gas rate was stabilised at 1.93 MMscf/D during flowing period before shut-in the well for 78.5 hour of post-frac pressure build-up period.

Table (*7-5*) below presents formation, fluid and fracture input parameters used for the investigated well with Figure (*7-11*) as presented in the paper and Figures (*7-12 and 7.13*) presenting the well test interpretation result, in which there is no indication of fracture flow behaviour at early time. Also, the interpreted fracture half-length in Figure (*7-14*) is relatively short, which clearly suggests that the problem is not likely associated with massive fractures.

Reservoir Properties	
Initial pressure, psia	2010
Formation permeability	4.2
Formation porosity, fraction	0.076
Rock compressibility, psi-1	3.356E-6
Well bore radius, ft	0.3
Sw	2
St	-1.3
Wellbore storage, bbl/psi	0.00446
Reservoir thickness, ft	21
drainage area, acres	40
Fluid Properties	
Gas Compressibility, psi-1	5.28E-6
Viscosity, cp	0.017
FVF, cf/scf	0.007277
Temperature, ^{o}F	155
Fracture Properties	
Fracture half-length, ft	22
Fracture width, ft	0.01
Fracture permeability, D	0.447

Table 7- 5: Fracture, formation and fluid input parameters used in the numerical model

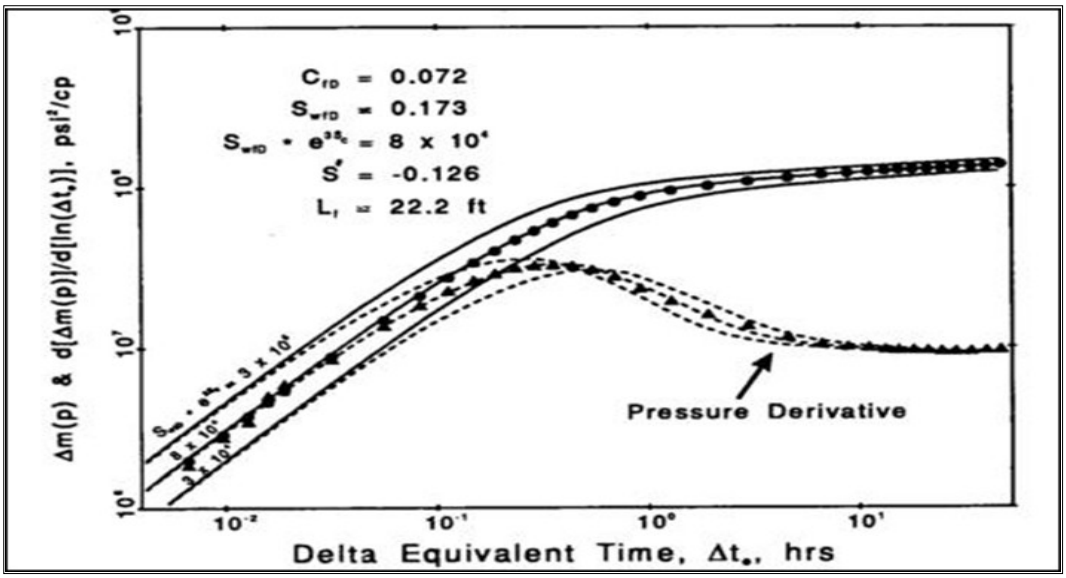


Figure 7- 11: Log-log diagnostic with WBS and radial flow features as presented in the paper

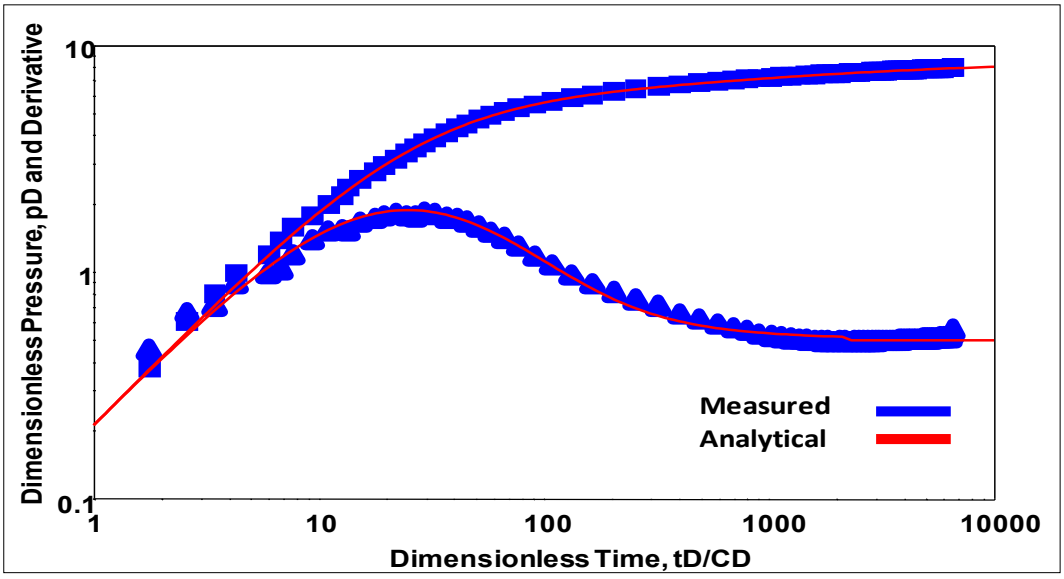


Figure 7- 12: Log-log plot of the measured data against analytical solution

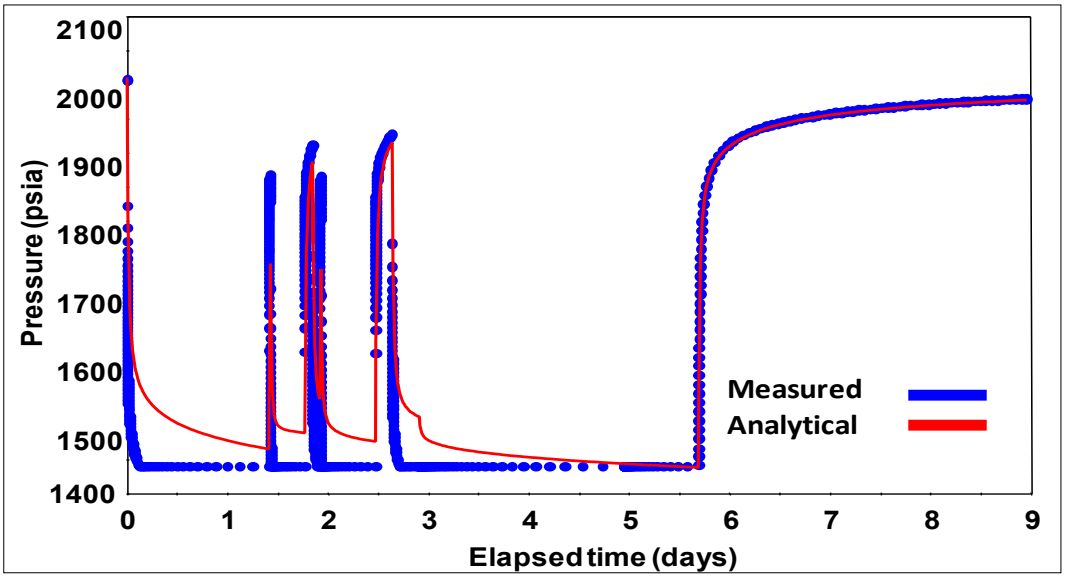


Figure 7- 13: Measured data versus analytical match for all flow periods

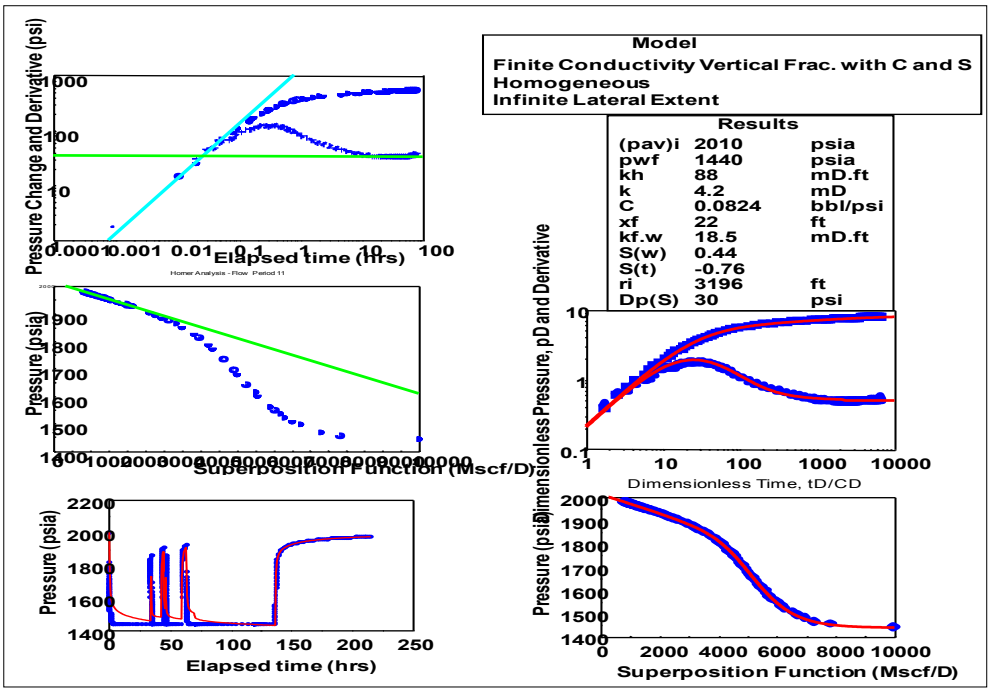


Figure 7- 14: Well test analysis results of the actual measured data

The well test analysis of the measured data result indicates wellbore storage effect and skin followed by radial flow, which is identical to the investigated unusual behaviour in the current study. The interpreted post-frac well test data indicates presence of relatively short fracture half-length of 22 ft and low *FcD* value. It is worth noting that the reported FcD of 0.2 in the table is higher than the value presented in the paper of (0.072) and this is because the minimum calculated *FcD* by the software is (0.2). To mimic the actual measured data in the paper, a single layer numerical model was constructed and the result of the synthetic model is presented below (*Figures 7-15 and 7-16*).

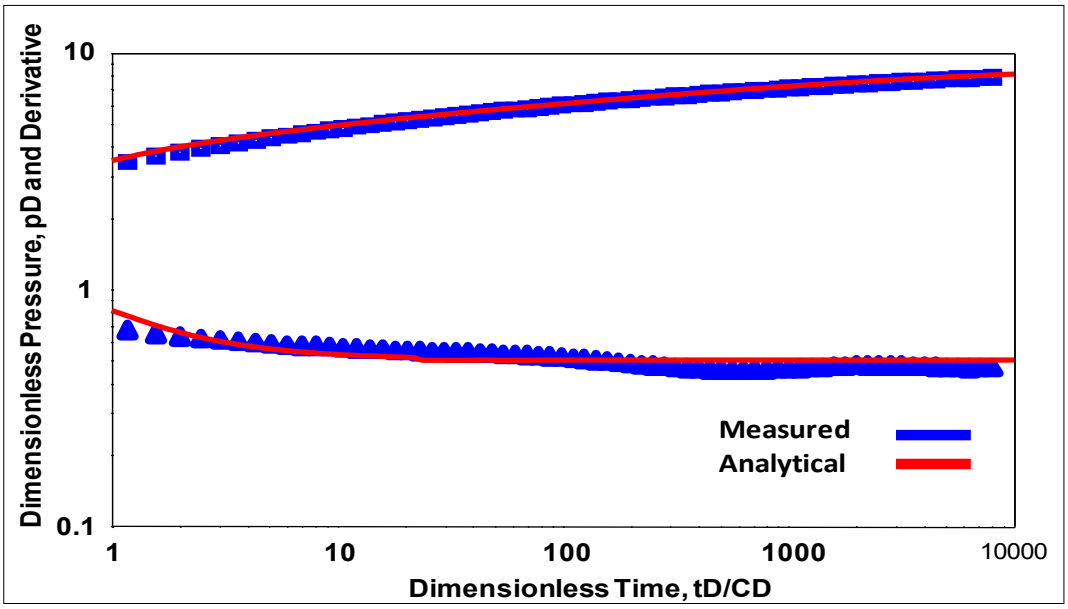


Figure 7- 15: Log-log pressure match for the main build-up of the numerical model

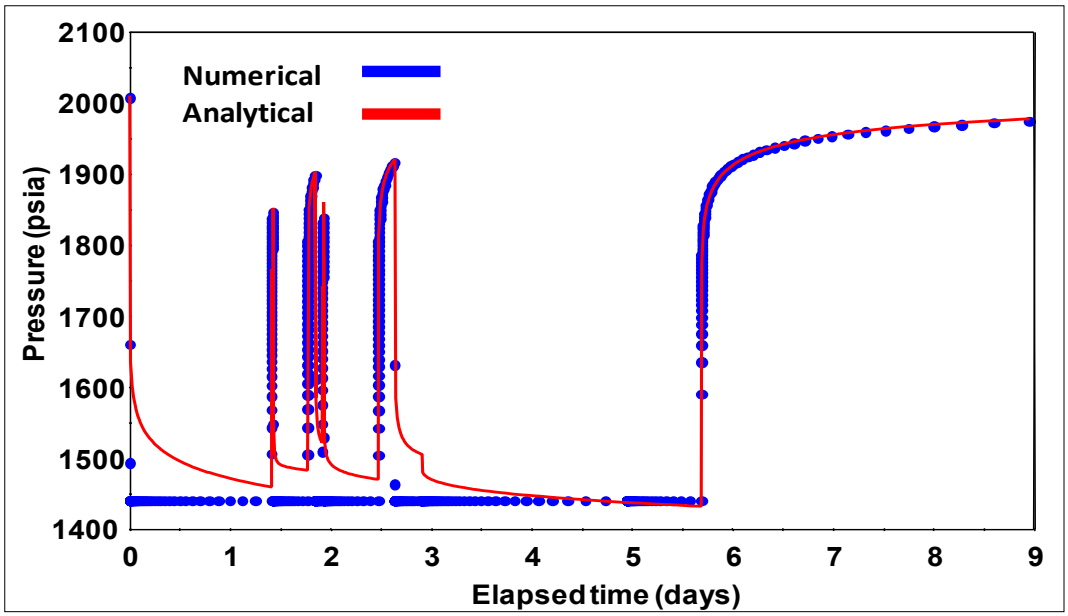


Figure 7- 16: Measured data versus analytical match for all flow periods

Pressure transient interpretation of the numerical model results demonstrate a good match with the measured data indicating short fracture half-length and low fracture conductivity relative to the formation and that is why the fracture flow behaviour not clearly observed at early time (*Figures 7-17 and 7-18*). The results also demonstrate the fact that the induced fracture half-length resultant from frac-skin process is likely to be short and of low conductivity, which can be good candidate for the unusual behaviour development.

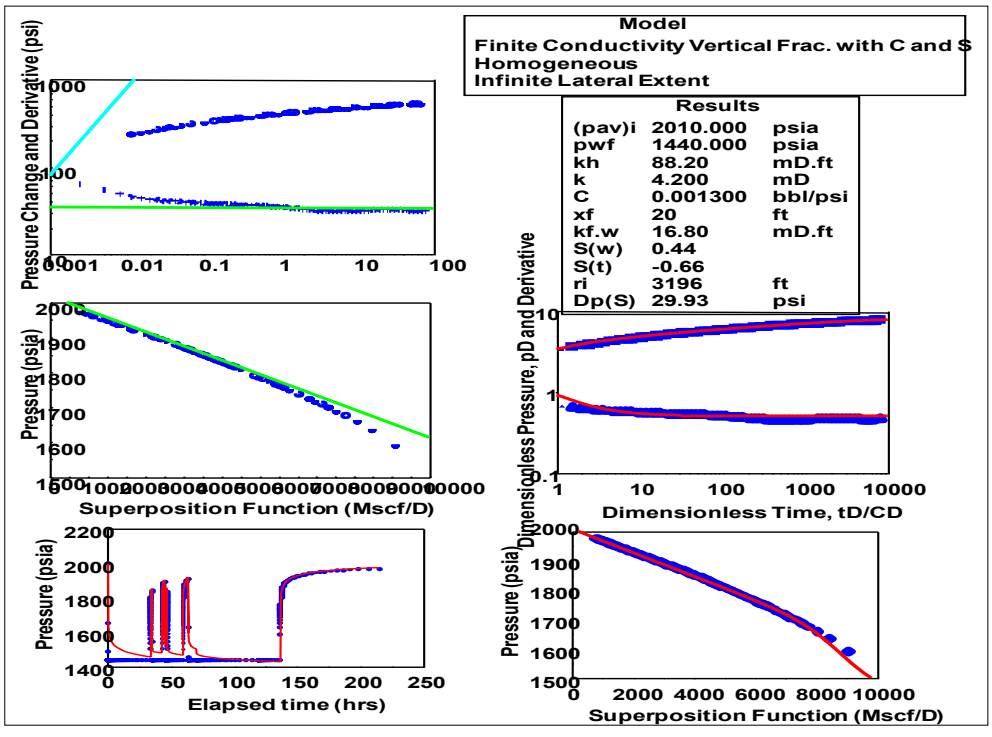


Figure 7- 17: Graphs showing well test analysis results of the numerical model

The numerical model results clearly indicate a good match with the actual measured data found in the paper (*Table 7-6*). It also confirms the conclusion that the investigated problem is likely to be associated with fractured wells of short half-lengths and low fracture conductivity (*Figure 7-18*). It is worth noting that this fracture configuration is usually obtained as a result of near wellbore skin removal through frac-skin or acid job. The results illustrate the impact of fracture damage on the development of unusual behaviour of fractured wells with fracture choke damage more effective in causing the behaviour and fracture face skin of less importance. This case represents a good example of a fractured well with no indication of fracture flow feature at early time due to fracture low conductivity or permeability.

Parameters	Analytical	Numerical	Units
(pav)i	2010	2010	psia
P_{wf}	1440	1440	psia
kh	86	88	mD.ft
k	4.4	4.2	mD
C	0.08	0.001	bbl/psi
X_f	22	20	ft
FcD	0.2	0.2	
$k_f.w_f$	18.6	16.8	mD.ft
S(w)	0.4	0.4	
S(t)	-0.8	-0.7	
r_i	3196	3198	ft
Dp(S)	30	29	psi

Table 7- 6: Shows results comparison between numerical against analytical solution

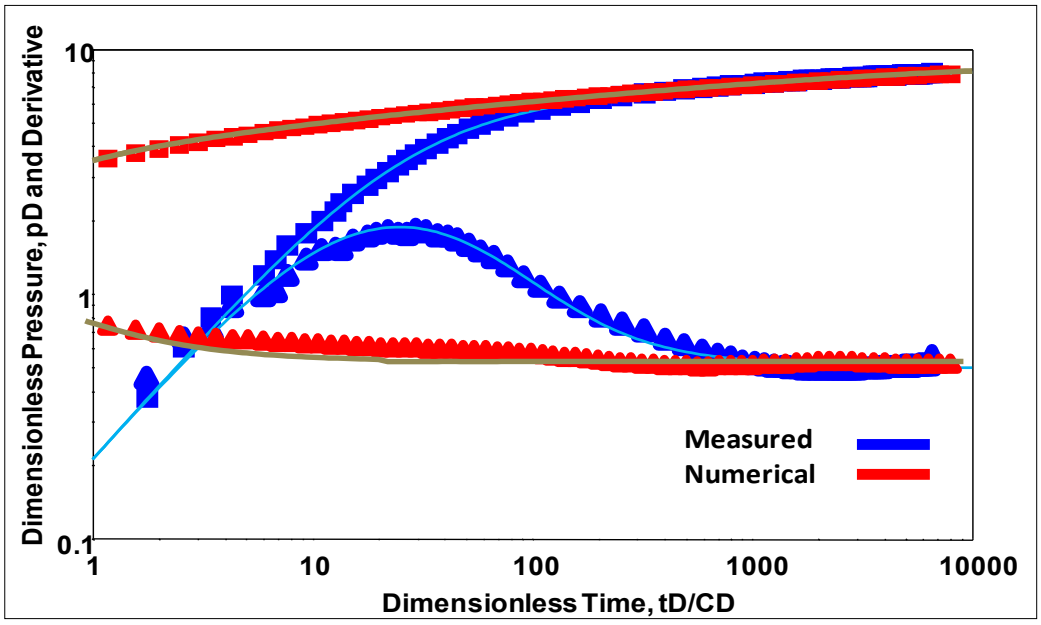


Figure 7- 18: Graph shows log-log plot of the numerical model with analytical solution

7.4 Case (III): Fractured Gas-Condensate Well

The third field example is a multi-layered commingled gas-condensate and volatile oil well from the North Sea. The well was drilled in March 2000 with first production in June 2000. Severe losses during drilling and cementing operations occurred and reported as a consequence of induced fractures while drilling. It is worth noting that this well was particularly prone to drilling induced fractures as it was drilled perpendicular to the direction of minimum stress. The well is penetrating three main reservoirs B, C and D from top to bottom consisting of 21 layers in total (Table 7-7) and this well is considered of complex structural and fluid characterisation.

No.	Zone	TOP MDBRT (m)	BASE MDBRT (m)	THICKNESS Measured (m)	TOP TVDSS (m)	TOP TVDBRT (m)	BASE TVDSS (m)	Pressure Measured (bara)
1	B1[a]	4612.50	4617.50	5.0	3787.8	3835.4	3791.97	572.96
2	B2b_1[a]	4657.50	4665.50	8.0	3825.4	3873.0	3832.20	575.15
3	B2b_2[a]	4700.50	4703.00	2.5	3861.9	3909.5	3864.27	515.16
4	B2b_3[a]	4734.50	4741.50	7.0	3891.4	3939.0	3897.46	543.71
5	B3_1[a]	4753.75	4760.25	6.5	3909.4	3957.0	3913.79	574.51
6	B3_2[a]	4795.50	4800.00	4.5	3945.0	3992.6	3949.03	510.00
7	B3_3[a]	4818.00	4830.50	12.5	3965.3	4012.9	3976.59	510.00
8	B3_3[b]	4839.75	4842.00	2.3	3984.9	4032.5	3986.97	n/a
9	B3_3[c]	4853.50	4856.50	3.0	3997.4	4045.0	4000.07	n/a
10	B3_3[d]	4860.50	4864.75	4.3	4003.7	4051.3	4007.52	510.00
11	C1_2[a]	4921.50	4925.00	3.5	4059.1	4106.7	4062.30	397.70
12	***C1_2[b]***	*4928.25*	*4935.50*	*7.3*	*4065.3*	*4112.9*	*4072.01*	*400.00*
13	C1_3[a]	4944.50	4950.50	6.0	4080.3	4127.9	4085.87	350.89
14	C1_3[b]	4953.00	4958.25	5.3	4088.2	4135.8	4093.03	522.82
15	C1_3[c]	4963.00	4969.75	6.8	4097.4	4145.0	4103.68	568.86
16	C2[a]	5004.00	5010.00	6.0	4135.7	4183.3	4141.33	n/a
17	***D1[a]***	*5054.50*	*5058.00*	*3.5*	*4183.2*	*4230.8*	*4186.56*	*357.69*
18	***D1[b]***	*5065.50*	*5074.50*	*9.0*	*4193.7*	*4241.3*	*4202.24*	*357.00*
19	***D2a[a]***	*5106.50*	*5111.00*	*4.5*	*4232.7*	*4280.3*	*4236.92*	*530.00*
20	***D2a[b]***	*5114.50*	*5121.25*	*6.8*	*4240.3*	*4287.9*	*4246.66*	*550.00*
21	D2b[a]	5132.50	5136.00	3.5	4257.4	4305.0	4260.78	n/a
22	D2b[b]	5151.00	5155.50	4.5	4275.2	4322.8	4279.48	n/a

Table 7- 7: Reservoirs B, C and D depths, thickness and initial pressure present in each layer

In addition, the fluid in Zones B and C of the reservoir is gas-condensate with volatile oil in the in the D zone. The dew point in the B and C formations is between 6500 and 7250 psia. This well was fully perforated in the D, C and B sands. The peak gas rate reached over 14 MMscf/d and 1500 bopd in July 2000 after a slow clean-up. However, the well productivity declined gradually over time with reservoir pressure plunged dramatically and in March 2001 a remedial hydraulic fracturing operation was carried out on the well, which resulted in skin reduction and improvement in the productivity index of the well.

All three reservoirs were targeted for hydraulic fracturing treatment (*Table 7-8*) to by-pass near wellbore damages as a result of drilling and completion operations. The designed fracture treatment lengths were short to remove skin and improve well productivity index.

Table 3	B2b_3[a]	B3_2[a]	B3_3[a]	B3_3[d]	C1_2[a]	C1_3[a]	C1_3[c]	C2[a]	D2a[b]
Frac. Length (m)	38	4	65	35	43	68	76	24	3
Frac Height (m)	21	10	33	17	21	37	37	16	10
Conductivity (md.ft)	689	346	1012	742	769	1106	977	767	261

Table 7- 8: Fracture length, height and conductivity of the induced fracture

An observation of the early time data of all build-ups before and after well stimulation illustrate a unit slope on the log-log derivative and pressure change plot indicating wellbore storage and skin followed by radial flow (*Figure 7-19*). However, the effect of the well stimulation is not apparent on the graph. The middle time data is represented by a stabilisations radial composite behaviour. An examination of the diagnostic plot of pre and post-frac below shows a first stabilization at the condensate bank and a second radial stabilization at the effective reservoir permeability.

The results show a slight improvement in the skin and the mobility in the bank after the propped fracture operation. Early time fractured well flow behaviour is not evident on the pressure or the derivative; therefore, fracture parameters cannot be calculated. In the graph below, pre-frac flow periods include FP15, FP28 and FP54 and post-frac flow periods FP59, FP66, FP70 and FP79.

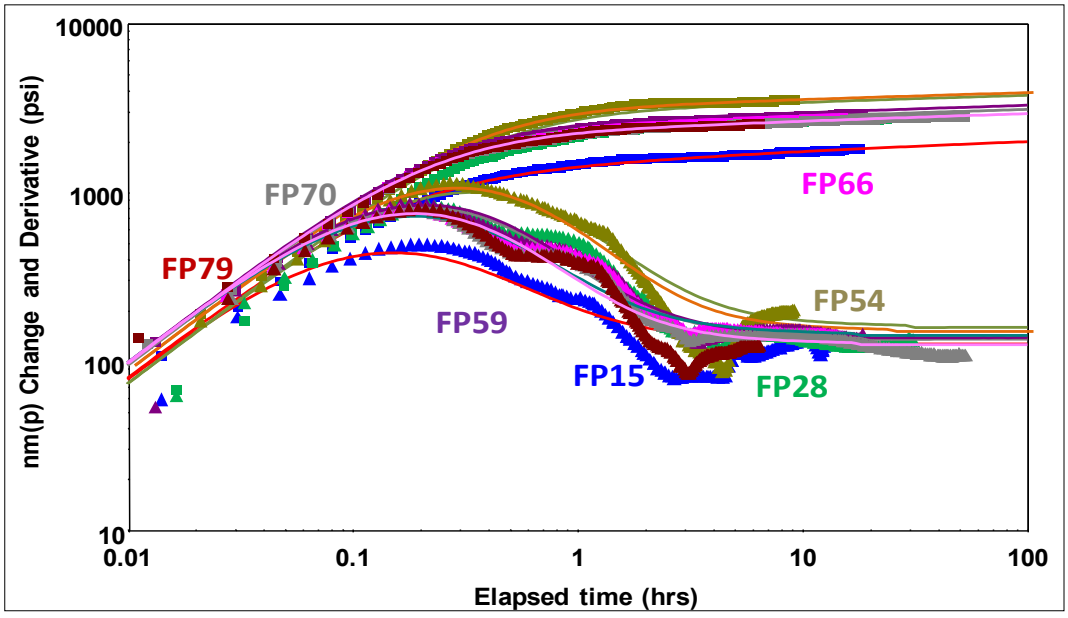


Figure 7- 19: Wellbore storage and skin with no indication of fractured flow in

Figure (*7-20*) shows well total history of the measured pressure and rate versus time. As it can be seen the initial pressure initially was about 7400 psia and after a few months production the reservoir pressure plunged dramatically about 2000 psia. To simulate the pressure history of this case with all flow periods for this well, a multi-layered numerical model was constructed using the fracture input parameters in the table above and the simulated production history includes pre and post-frac flow periods.

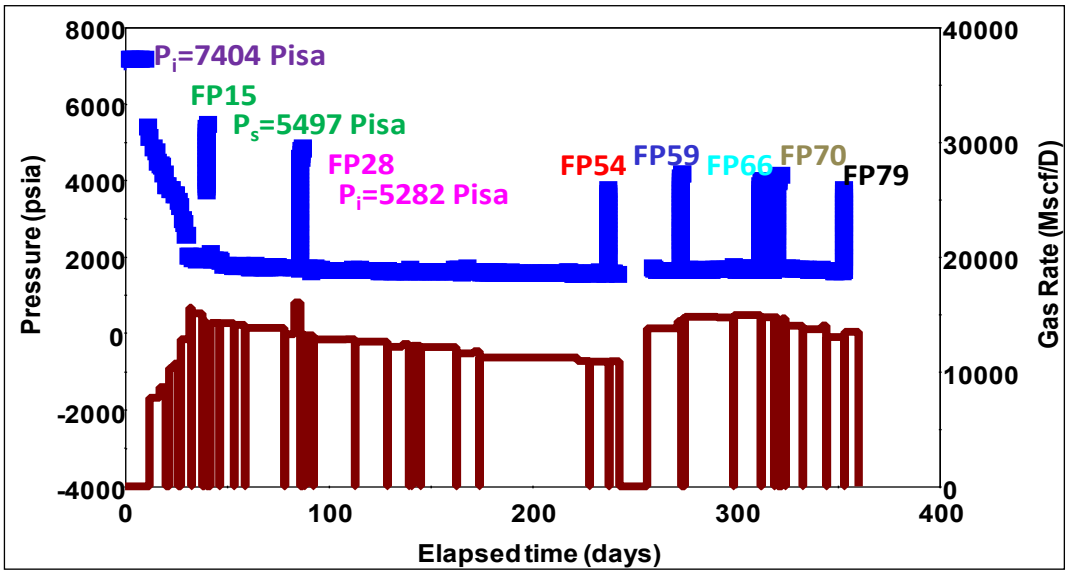


Figure 7- 20: Pre-frac flow periods (FP15, FP28 and FP54) and post-frac flow periods include (FP59, FP66, FP70 and FP79)

Figure (*7-21*) presents comparison of the actual measured pressure of flow period FP15 (pre-frac) together with the introduced pressure response from the numerical model with damaged induced fractures. The match is not perfect but acceptable taking into the account the complexity of the reservoir and fluid present in this well. The matching process was extremely time consuming exercise due to complexity of the model and fluid types present in the model.

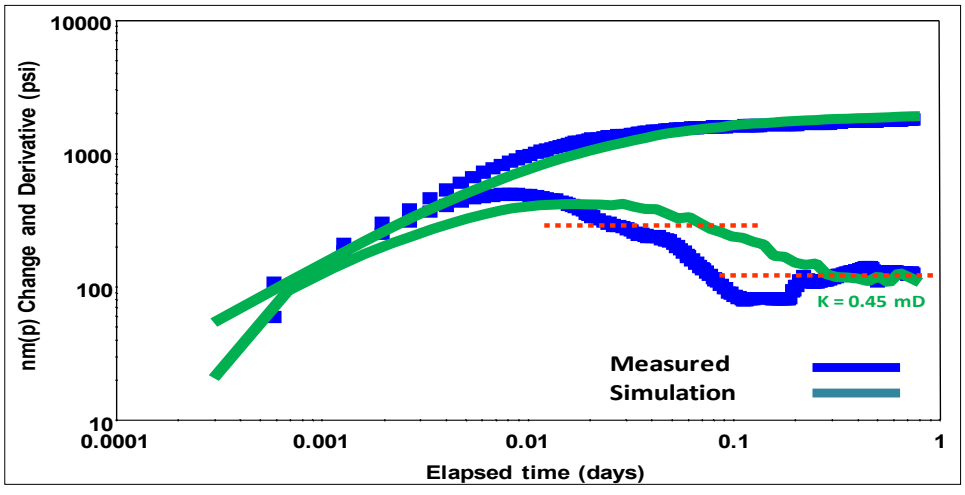


Figure 7- 21: Log-log plot of pre-frac FP#15indicating wellbore storage and skin

Figure (*7-22*) represents log-log plot of pre-frac flow period FP#28 in which WBS and skin can be seen at early time and two stabilization indicating condensate bank and effective reservoir permeability. Then all three reservoirs were propped fractured and plot below (*Figure 7-23*) shows post-frac flow period FP#59 with no indication of fractured well flow behaviour due to presence of choked fracture damage and low fracture flow conductivity. The results suggest that observing unusual fractured well flow behaviour in gas-condensate wells is not due to condensate bank effect. Also, the controlling parameters for the behaviour to develop are presence of low fracture conductivity (low *FcD*) and short damaged fracture half-length as found in this case.

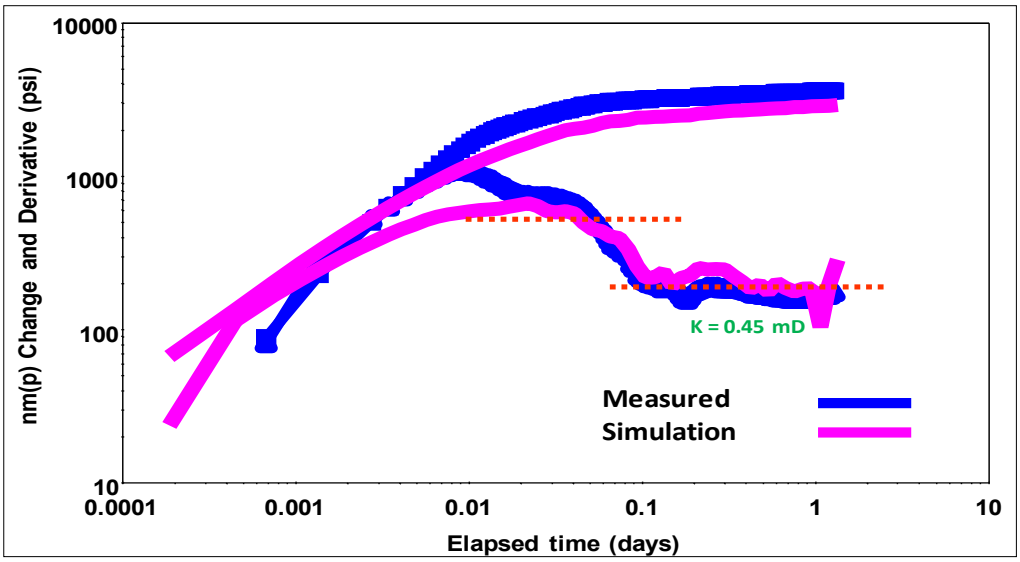


Figure 7- 22: Log-log plot of pre-frac FP#28 indicating wellbore storage and skin features

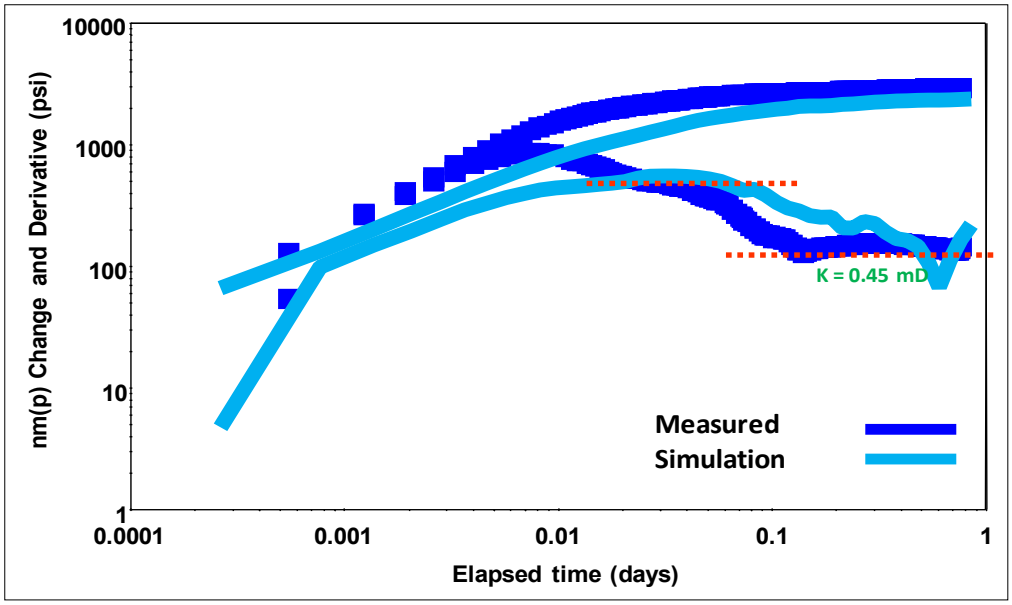


Figure 7- 23: Log-log plot of post-frac FP #59indicating wellbore storage and skin effects

7.5 Conclusions

The investigated fractured well flow behaviour in this study occurs periodically; therefore, it is difficult to find real field case examples where the behaviour problem is reported. In addition, obtaining case examples from service companies specialising in hydraulic fracturing is also considered as problematic and time consuming exercise. Most of these companies are not reporting bad frac jobs. As mentioned previously in this document, the investigated problem in the study might occur in any reservoir setting containing various fluids. However, three field case examples were investigated:

First real field case investigated in details was from onshore gas field in Canada of low permeability reservoir. The results of well test analysis of the pressure data indicate presence of damaged fracture of low fracture half-length (about 70 ft). The generated pressure behaviour from the numerical model is verified and compared against actual field data. A good match was achieved between the simulations and the actual measured data.

The second reported field case example taken from an SPE 23630, a paper published by Azari *et al*. (1992) The well test analysis of the numerical data indicate fracture half of over 75 ft and of low fracture conductivity ($FcD < 0.1$). The introduced fracture data from the constructed numerical model is matched against actual field measured data.

The third field case investigated in details in this study was a fractured well in commingled gas-condensate and volatile reservoirs in the North Sea. The well is extremely complex from geological and fluid characterisation point of view. For instance, the reservoir initial pressure was reported at 7,404 psia and after short period of production the reservoir pressure has dramatically dropped about 2,000 psia to reach 5,497 psia. Based on the results obtained from the numerical simulation runs, the behaviour problem is associated with this well is believed to be due to choked fracture effect. The actual calculated induced fracture lengths are relatively short (tens of metres).

Based on all the results obtained from running all above three cases, it can be concluded that the infrequent behaviour is most likely to occur in fractured wells of low fracture conductivity, short half-length, choked fracture damage in addition to non-Darcy effect in stimulated gas wells and fluid leak-off to certain degree in some occasions depending on the formation permeability.

CHAPTER VIII

CONCLUSIONS AND RECOMMENDATIONS

8.1 Summary

Observing infrequent pressure behaviour of fractured wells at early time had been referred to briefly in the literature without clear understanding of the causes. Current study indicates the unusual behaviour results from performing improper frac-jobs that yield fractures of low conductivity, short half-length with reduced skin and improved well productivity.

In this study, various numerical simulation models of fractured wells were considered to examine cases where the investigated behaviour occurs and what are possible causes for it. Cases of propped fractured wells in oil and gas reservoirs of single layer and multi-layered reservoirs were examined. Different fracture parameters were investigated in detail including fracture half-length, conductivity, width and formation permeability.

In addition, cases studied include fractures of finite conductivity penetrating low and high permeability reservoirs with choked fracture damage near the wellbore and fracture face skin due to fluid leak-off effect. Also, fracture configuration parameters including fracture length, conductivity and formation permeability contrast were among critical parameters explored.

Proppant agent type of Resin Coated Proppant (RCP) impact on the introduced pressure response was examined in this research work. However, this topic was not studied in much detail due to lack of sufficient resources to perform an actual frac job using *RCP* material. Non-Darcy effect in stimulated gas wells was also studied.

Reservoir heterogeneity due to multi-layering effect was studied through considering two and more layers to examine the impact of permeability contrast between layers on the introduced pressure behaviour. Cases of commingled and cross-flow multi-layered reservoirs containing different fluid types were examined.

Propped fractured wells penetrating naturally fractured reservoirs were investigated to study the pressure response of fractured wells in such reservoirs. Finally, fluid richness impact on pressure behaviour of fractured wells in gas condensate reservoirs was also explored as infrequent behaviour is reported to have occurred in such reservoirs due to liquid dropout effect near the wellbore.

8.2 Conclusions

In this study, a comprehensive understanding of fractured wells behaviour exhibiting unusual pressure features at early time was developed. The objective of the study is to investigate uncommon behaviour observed in post frac test of hydraulically fractured wells in oil and gas reservoirs. With this behaviour, fractured wells demonstrating pressure characteristics similar to the non-stimulated wells at early time is reported, which is on contrary to what is expected from stimulated wells behaviour.

Based on the literature review, the investigated unusual behaviour could happen in any reservoirs containing any fluid types. It is worth noting the fact that the examined topic in this research work has not been studied in detail in the literature. In this study, various models of stimulated wells were considered to examine cases in which the behaviour occurs and the main causes of it.

The study suggests that the investigated behaviour is associated with fractured wells penetrating low and high permeability reservoirs of low fracture conductivity; $k_f w_f$ and short fracture half-length; X_f. It is found Induced short fracture half-length of tens of feet and low conductivity in reservoirs of moderate to high permeability are candidates to experience the behaviour.

Damaged fracture due to fracture choke and less importantly fracture face skin is considered to be important factor causing the investigated behaviour. Non-Darcy effect in the case of stimulated gas wells and fluid leak-off effect in high permeability formations are considered as possible causes of the behaviour to develop based on the simulation run results.

Field examples of well tests data demonstrating the investigated behaviour in the study are presented. The examined cases indicate that fractures of low fracture conductivity, short fracture half-length and fracture damage are likely cases for the unusual flow behaviour to exist.

The study suggests that provided the frac job targeted the formation of interest, the investigated behaviour may occur occasionally as observed in some field cases and the main conclusions of the study are as follows:

- Fracture length is considered as the main controlling parameter for the behaviour to develop. It is found that the investigated behaviour is likely to exist in fractured wells of short lengths, usually 10s of feet.
- Fracture conductivity or permeability is critical in determining effectiveness of any frac job. The lower the fracture conductivity (< 0.1) the more likely for unusual behaviour to occur.
- Study suggests that fracture face skin has less impact than the choked fracture damage and that choked fracture causes development of the investigated behaviour.
- Fluid leak-off effect may impact the early time flow feature depending on the formation permeability and depth of fracture fluid filtrated into the formation.
- Non-Darcy effect in gas reservoirs will impact the behaviour to develop as it impacts the pressure response.
- Stimulating wells penetrating high permeability formations may result in fractures having conductivity less than the formation permeability, which causes the behaviour to develop.
- Un-equal fracture half lengths found to have a negligible impact on the pressure response at early time.
- Fracturing a well in naturally fractured reservoirs does not lead to development of infrequent features.
- Composite behaviour due to liquid drop out in gas condensate reservoirs appears not to cause the behaviour to develop and it is found that the induced fracture will improves well productivity depending on the fracture length in particular.
- Pressure matching of the actual well test data with numerical modelling results verifies the conclusions drawn from the study.

8.3 Recommendations

The investigated behaviour of fractured wells in this study concerns many operators and service companies. The reasons behind not observing typical early time behaviour of fractured wells characteristics in some post-frac well tests remained unsolved prior to this research work. The study suggests that performing improper frac jobs will result in the development of uncommon pressure behaviour. Based on the conclusions drawn from the study, it is recommended to:

- Properly perform propped frac jobs to prevent fracture choke damage effect in particular, which yields unusual fracture behaviour.
- Consider fractures of sufficient conductivities when designing Frac-Pack jobs to stimulate high permeability formations.
- Literature review indicates that using *RCP* as a proppant agent may cause uncommon pressure behaviour at early time; therefore, it is crucial to investigate post-frac well tests in cases where this proppant material is used in stimulating gas wells.
- Introduce fractures of sufficient conductivity and length prior to putting the well on stream in gas condensate wells to achieve optimum benefits from implementing propped fractured wells.
- Continue exploring field cases where unusual fracture flow behaviour is reported in post-frac well tests.

REFERENCES

Adegbola, K. and Boney, C.: "Effect of Fracture Face Damage on Well Productivity," SPE paper 73759 presented at the SPE International Symposium and Exhibition on Formation Damage Control, Lafayette, Louisiana, February, 20-21, 2002.

Agarwal, R.G., Al-Hussainy, R. and Ramey, H.J. Jr: "An Investigation of Wellbore Storage and Skin Effect in Unsteady Liquid Flow," I: Analytical Treatment, Soc. Pet. Eng. J., Sept., 1970, 279.

Agarwal, R.G., Carter, R.D. and Pollock, C.B.: "Evaluation and performance Prediction of Low-Permeability Gas Wells Stimulated by Massive Hydraulic Fracturing," J. Pet. Tech., March, 1979, 362-372.

Aguilera, R.: "Effect of Wellbore Storage, Skin and Outer Reservoir Boundaries on the Transient Behaviour of Naturally Fractured Reservoirs with Hydraulic Vertical Fractures," paper SPE 17023, 1987.

Aguilera, R.:"An Approximate Solution of Linear Flow in Naturally Fractured Reservoirs," paper SPE 16442, April, 1987.

Aguilera, R.: "Well Test Analysis of Naturally Fractured Reservoir," SPE Formation Evaluation, Sept., 1987, 239-252.

Aguilera, R.: "Well Test Analysis of Dual-Porosity Systems, Intercepted by Hydraulic Vertical Fractures of Finite Conductivity," paper SPE 18948, presented at the SPE Joint Rocky Mountain Regional/Low Permeability Reservoirs Symposium, Denver, Colorado, March 6-8, 1989.

Aguilera, R.:"Well Test Analysis of Multi-layered Naturally Fractured Reservoirs," Journal of Canadian Petroleum Technology, July, 2000, 39, 31-37.

Aguilera, R., and Aguilera, M.S.:"Well Test Analysis of Multi-layered Naturally Fractured Reservoirs with Variable Thickness and Variable Fracture Spacing," journal of Canadian Petroleum Technology, Dec., 2001, 40, 9-12.

Alagoa, A., Bourdet, D. and Ayoub, J. A.: "How to Simplify The Analysis of Fractured Well Tests," World Oil, Oct., 1985.

Al-Haddad, S., J.W., Arbaugh, R. E and McKnight, D.Y.: "Hydraulic Fracturing in High Permeability Wells," SPE paper 40008 presented at the SPE Gas Technology Symposium, Calgary, Alberta, March, 15-18, 1998.

Al-Ghurairi, F., Solares, R., Bartko, K. and Seirra, L.: "Results from a Field Trail Using New Additives for Fracture Conductivity Enhancement in a High Case Screen less Completion in the Jauf Reservoir, Saudi Arabia," SPE paper 98088 presented at the SPE International Symposium and Exhibition on Formation Damage Control, Lafayette, L.A., February, 15-17, 2006.

Al-Naimi, K., Al-Thawad, F., Bin Akresh, S., and Bartko, K.,:"Integrating Reservoir Characterisation and Fracturing Analysis to Understand the Pressure Transient Response of Frac Packed Wells," SPE 126079 presented at the SPE Saudi Arabia Section Technical Symposium and Exhibition, Alkhobar, May 09-11, 2009

Akram, A. H., and Samad, A.,:"Correcting Underestimation of Optimal Fracture Length by Modelling Proppant Conductivity Variations in Hydraulically Fractured Gas/Condensate Reservoirs," SPE 100321 presented at the SPE Gas Technology Symposium, Calgary, May, 15-17, 2006

Al-Hashim, H.S., and Hashmi, S.S.: "Long-Term Performance of Hydraulically Fractured Layered Rich Gas-condensate Reservoir," paper SPE 64774 presented at the 2000 SPE International Oil and Gas Conference and Exhibition, Beijing, 7 – 10 November.

Alvarez, C.H., Holditch, S.A, and McVay, D.A.:"Effects of Non-Darcy Flow on Pressure Build-up Analysis of Hydraulically Fractured Gas Reservoirs," paper SPE 77468 presented at the SPE Annual Technical Conference and Exhibition, San Antonio, Texas, 29 September-2 October, 2002.

Asar, H. and Handy, L.L.:"Influence of interfacial tension on gas-oil relative permeability in a gas-condensate system", SPE paper 11740, 1988.

Azari, M., Knight, J.W., Coble, L. E and Soliman, M.Y.: "Low-Conductivity and Short Fracture Half-Length Type Curves and Analysis for Hydraulically Fractured Wells Exhibiting Near Radial Flow Profile," paper SPE 23630 presented at the Second Latin America Petroleum Engineering SPE Conference, II LAPEC, Caracas, Venezuela, March, 08-11, 1992.

Azari, M., Soliman, M.Y., Wooden, W. O and Hunt, J.L.: "Performance Prediction for Finite Conductivity Vertical Fractures," paper SPE 22659 presented at the SPE Annual Technical Conference and Exhibition, Dallas, TX, October, 6-9, 1991.

Azari, M., Wooden, W., O., and Coble, L., E.,: "A Complete Set of Laplace Transforms for Finite Conductivity Vertical Fractures Under bilinear and Trilinear Flows," paper SPE 20556 presented at the 65th SPE Annual Technical Conferences and Exhibition, New Orleans, LA, Sept. 23-26, 1990.

Bardon, C. and Longeron, D.G.: "Influence of Very Low Interfacial Tensions on Relative Permeability," SPEJ, 1980, 391-400.

Barenblatt, G.I. and Zheltov, Y.P.:"Fundamental Equations of Filtration of Homogeneous Liquids in Fissured Rocks," Soviet Physics, Doklady, 1960, 5, 522.

Barker, B. and Ramey, H.J., Jr.:"Transient Flow to Finite Conductivity Vertical Fractures," paper SPE 7489 presented at the 53rd Annual Technical Conference and Exhibition of SPE of AIME, Houston, Texas, Oct. 1-3, 1978.

Barree, R.D., Cox, S.A., Gilbert, J.V., and Dobson, M.: "Closing the Gap: Fracture Half-length from Design, Build up, and Production Analysis," paper SPE 84491 presented at the SPE Annual Technical Conference and Exhibition, Denver, Colorado, 5-8 October, 2003.

Bennett, C.O., Reynolds, A.C. and Raghavan, R.:"Analysis of Finite Conductivity Fracture Intercepting Multilayer Commingled Reservoirs," SPEFE, June, 1986, 259-274.

Bennett, C.O., Rosato, N.D. Reynolds, A.C. and Raghavan, R.: "Influence of Fracture Heterogeneity and Wing Length on the Response of Vertically Fractured wells," SPE paper 9886-PA, April, 1983, 219-229.

Berthelot, J.M.:"Effects of Fracturing Fluid Recovery upon Well Performance and Ultimate Recovery of Hydraulically Fractured Gas Wells," MS Thesis, Texas A&M University, College Station, Texas, 1990.

Bertram, D.A., Van De Leemput, L.D.C., McDevitt, B. S. and AL-Harthy, N.M.A.: "Experiences in Gas-Condensate Well Test Analysis Using Compositional Simulation," SPE paper 37994 presented at the SPE Reservoir Simulation Symposium, Dallas, TX, June, 8-11, 1997

Bourdet, D.:"Well Test Analysis: The Use of Advanced Interpretation Models," Handbook of Petroleum Exploration and Production, 3, 2001

Bourdet, D. and Gringarten, A.C.: "Determination of Fissure Volume and Block Size in Fractured Reservoirs by Type-Curve Analysis," paper SPE 9293 presented at the SPE Annual Technical Conference and Exhibition, Dallas, Sept. 21-24, 1980.

Bourdet, D., Alagoa, A., Ayoub, J.A. and Pirard, Y.M.: "New Type Curves Aid Analysis of Fissured Zone Well Tests," World Oil, April, 1984, 111-124.

Bourdet, D., Ayoub, J.A., Whittle, T.M., Pirard, Y.M. and Kniazeff, V.:"Interpreting Well Tests in Fractured Reservoirs," World Oil, October, 1983, 77-87.

Brannon, H.D. and Pulsinelli, R.J.: "Evaluation of the Breaker Concentrations Required to Improved the Permeability of Proppant Packs Damaged by Hydraulic Fracturing Fluids," paper SPE 19402 presented at the SPE Formation Damage Control Symposium, Lafayette, Louisiana, 22-23 February, 1990.

Camacho-V., R.G., Raghavan, R., and Reynolds, A.C.: "Response of Wells Producing Layered Reservoirs, Unequal Fracture Length," SPE Formation Evaluation, March, 1987, 9-28.

Carlson, M.R., and Myer, J.W.G.: "The Effects of Retrograde Liquid Condensation on Single Well Productivity Determined via Direct (Compositional) Modelling of a Hydraulic Fracture in a Low-Permeability Reservoir," paper SPE 29561 presented at the SPE Rocky Mountain Regional/Low-Permeability Reservoirs Symposium, Denver, 20-22 March, 1995.

Cesar, H.A., Holditch, S.A., and McVay, D.A.: "Effects of Non-Darcy Flow on Pressure Transient Analysis of Hydraulically Fractured Gas Wells," paper SPE 77468 presented at the SPE Annual Technical Conference and Exhibition, San Antonio, Texas, 29 September-2 October, 2002.

Chen Chin-C., and Raghavan, R.:"Modelling a Fractured Well in a Composite Reservoir," SPEFE, December, 1995.

Chu, Wei-Chun: "Application of Pressure Transient Testing for Stimulation Decisions," SPE paper 36529 presented at the SPE Annual Technical Conference and Exhibition, Denver, TX, October, 6-9, 1996.

Chu, W. and Shank, D.: "A New Model for a Fractured Well in a Radial, Composite Reservoir," SPEFE, September, 1993.

Cinco-Ley, H.:"Evaluation of Hydraulic Fracturing by Transient Pressure Analysis Methods," paper SPE 10043 presented at Inter. Petrol. Exh. and Techn. Symp., Beijing, China, Mar 18-26, 1982.

Cinco-Ley, H., and Meng, H.Z.:"Pressure Transient Analysis of Wells with Finite Conductivity Vertical Fractures in Double Porosity Reservoirs," paper SPE 18172 presented at the 63rd Annual Technical Conference and Exhibition of the Society of Petroleum Engineers held in Houston, TX, October 2-5, 1988.

Cinco-Ley, H., and Samaniego, V.F.: "Effect of Well bore Storage and Damage on the Transient Pressure Behaviour of Vertically Fractured Wells," paper SPE 6752 presented at the SPE Annual Fall Meeting, Denver, Colorado, 9-12 Oct, 1977.

Cinco-Ley, H., and Samaniego, V.F.:"Pressure Transient Analysis for Naturally Fractured Reservoirs," paper SPE 11026 presented at the SPE Annual Technical Conference and Exhibition, New Orleans, Louisiana, 26-29 September, 1982.

Cinco-Ley, H., and Samaniego-V.F.: "Transient Pressure Analysis for Fracture Wells," J. Pet. Tech., Sept., 1981, 1749-1766.

Cinco-Ley, H., and Samaniego-V.F.: "Transient Pressure Analysis: Finite Conductivity Fracture Case Versus Damaged Fracture Case," paper SPE 10179 presented at 56th SPE Annual Technical Conference and Exhibitions, San Antonio., Oct 5-7, 1981.

Cinco-Ley, H., Samaniego-V., F. and Dominguez N.: "Transient Pressure Behaviour for Well with a Finite Conductivity vertical Fracture," Sot. Pet. Eng. J., Aug., 1978, 253-264.

Cinco-Ley, H., Samaniego-V.F. and Rodriguez, F.: "Application of The Pseudo Linear Flow Model to the Pressure Transient Analysis of Fractured Wells," paper SPE 13059 presented at the 59th Ann. Techn. Conf. and Exh. Of SPE, Houston, TX, Sept., 16-19. 1984.

Cipolla C. L. and Mayerhofer, M.: "Understanding Fracture Performance by Integrating Well Testing and Fracture Modelling," paper SPE 49044 presented at the SPE Annual Technical Conference and Exhibition, New Orleans, Louisiana, September, 27-30, 1998.

Clark, K.K.: "Transient pressure Testing of Fractured Water Injection Wells," J. Pet. Tech., June, 1968, 639-643; Trans. AIME 243.

Cramer, D.D.: “Fracture Skin: A Primary Cause of Stimulation ineffectiveness in Gas Wells,” SPE paper 96869 presented at the SPE Annual Technical Conference and Exhibition, Dallas, Texas, October, 9-12, 2005.

De Swan, O.A.: “Analytical Solutions for Determining Naturally Fractured Reservoir Properties by Well Testing,” SPEJ, June, 1976, 117-122.

Danesh, A., Henderson, G.D., Krinis, D., and Peden, J.M.: “Experimental investigation of retrograde condensation in porous media at reservoir conditions”, SPE paper18316, 1988.

Davidson, B.M., Saunders, B.F., and Holditch, S.A.:"Field Measurement of Hydraulic Fracture Fluids: Case Study," paper SPE 27694 presented at the SPE Permian Basin Oil and Gas Recovery Conference, Midland, Texas, 16-18 March, 1994.

Duvernay E., S., J., Garcia, R., Rivera, J., G. and Carrillo, A., B.: “Use of Conductivity Enhancement Material to Sustain Productivity in Hydraulic Fractured Wells: Northern Mexico Cases,” SPE paper 108697 presented at the SPE International Symposium and Exhibition, Veracruz, Mexico, June, 27-29, 2007.

Dyes, A.B., Kemp, C.E., and Caudle, B.H.: “Effect of Fractures on Sweep-out Pattern,” Trans., AIME (1958), Vol. 213, 245-249.

Earlougher, R.C., Jr. and Kersch, K.M.: Analysis of Short-Time Transient Test Data by Type Curve Matching, JPT 26(7), July 1974, 793-800

Earlougher, R. C., Jr.:“Advances in Well Test Analysis”, Monograph Series No 5, Society of Petroleum Engineers of AIME, Dallas, 1977.

Economides, J.M., Ehlig-Economides, A.C, and Tosic, S.: “Application of Pressure-Transient and Production Data Analysis for Hydraulic Fracture Treatment Evaluation,” SPE paper 106382 presented at the SPE Hydraulic Fracturing Technology Conference, College Station, Texas, January, 29-31, 2007.

El-Banbi, A.H., McCain, W.D. and Semmelbeck, M.E.:“Investigation of Well Productivity in Gas-Condensate Reservoirs,” paper SPE 59773 presented at the SPE/CERI Gas Technology Symposium, Calgary, 3 – 5 April, 2000.

Elbel, J. and Ayoub, J.:"Evaluation of Apparent Fracture Lengths Indicated from Transient Tests," JCPT, December 1992, 41-46.

Evans, G., John: “The Use of Pressure Build-up Information to Analyze Non-Respondent Vertically Fractured Oil Wells,” Paper SPE 3345 presented at the Rocky Mountain Regional Meeting of the Society of Petroleum Engineers of AIME, June 2-4, 1971.

Fevang, O. and C.H.Whitson,: “Modelling Gas-condensate Well Deliverability”, SPERE, November, 1996.

Forchhemier, P.: “Wasser Bewegung durch Boden,” ZVDI, 1901, 45, 1781.

Fox, L.T.: "The Effects of Damage in and Around a Fracture upon the Analysis of Pressure Data from Low Permeability Gas Wells," MS Thesis, Texas A&M University, College Station, Texas, 1980.

Garzon, F.O., Al-Marri, H.M., Solares, J. R., and Franco Giraldo, C.A., SPE, Saudi Aramco, and V. Ramanathan, SPE, Schlumberger,:“Long Term Evaluation of an Innovative Acid System for Fracture Stimulation of Carbonate Reservoirs in Saudi Arabia,” IPTC paper presented at the International Petroleum Technology Conference, 3-5 December 2008, Kuala Lumpur, Malaysia

Gdanski, R., Fulton, D. and Shen, C.: “Fracture Face Skin Evolution during Clean-up,” SPE paper 101083 presented at the SPE Annual Technical Conference and Exhibition, San Antonio, TX, October, 24-27, 2006.

Gidley, J. L.: “A Method for Correcting Dimensionless Fracture Conductivity for Non-Darcy Flow Effects,” SPEPE, Nov., 1991, 391-400.

Gil, J.A. and Ozkan, E.: “Fractured-Well-Test Design and Analysis in the Presence of Non-Darcy Flow,” paper SPE 71573 presented at the 2001 SPE Annual Technical Conference and Exhibition, New Orleans, Louisiana, 30 September - 03 Oct., 2001.

Goodin, B.:“Well Test Transient_ Analysing Production Improvements from Well Stimulation,” found in the link: http://www.nzpam.govt.nz/cms/pdf-library/petroleum-conferences-1/1991-petroleum-conference-proceedings/b-goodin-449-kb-pdf.

Gringarten, A.C.: "Well Test Analysis Notes", MSc Petroleum Engineering Course Note, Imperial College London, 2002.

Gringarten, A.C.: “Interpretation of Tests in Fissured and Multi-layered Reservoirs with Double-Porosity Behaviour, Theory and Practice,” J. Pet. Tech., April, 1984, 549-564.

Gringarten, A.C. and Ramey, Jr., H.J.: "The Use of Source and Green's Functions in Solving Unsteady Flaw Problems in Reservoirs," SPEJ, Oct., 1973, 285-296; Trans., AIME 255.

Gringarten, A.C. and Ramey, H.J., Jr.: "An Approximate Infinite Conductivity Solution for a Partially Penetrating Line-Source Well," SPEJ, Apr., 1975, 140-148; Trans., AIME 325.

Gringarten, A.C., Ramey, H.J., Jr., and Raghavan, R.:"Unsteady State Pressure Distribution Created by a Well with a Single Infinite-Conductivity Vertical Fracture," Society of petroleum Engineer Journal, August, 1974, 347-360.

Gringarten, A.C., Ramey, H.J., Jr., and Raghavan, R.: "Applied Pressure Analysis for Fractured Wells," J. Pet. Tech., July, 1975, 887-892; Trans., AIME 259.

Guppy, K.H., Cinco-Ley, H., and Ramey, H.J., Jr.: "Effect of Non-Darcy Flow on the Constant-Pressure Production of Fractured Wells," SPEJ, June, 1981, 390-400.

Guppy, K. H., Cinco-Ley, H., Ramey, Jr. H.J. and Samaniego-V, F.: "Non-Darcy Flow in Wells with Finite –Conductivity Vertical Fractures," SPEJ, Oct., 1982, 681-698.

Guppy, K. H., Cinco-Ley, H., and Ramey, H.J., Jr.: "Pressure Build-up Analysis of Fractured Wells Producing at High Flow Rates," JPT, Nov., 1982, 2656-2666.

Hawkins, M.,:"A Note on the Skin Effect," 207, Trans., AIME, 1956, 356-357.

Hegre, T.M.,:"Hydraulically Fractured Horizontal Well Simulation," SPE 35506, presented at the European 3-D Reservoir Modelling Conference, Stavanger, April 1996.

Henderson, G.D., Danesh, A., Tehrani, D. H., Al-Shaidi, S., Peden, J.M.,: "Measurement and Correlation of Gas-condensate Relative Permeability by the Steady-State Method," SPE 30770, presented at the 1995 SPE Annual Technical Conference and Exhibition, Dallas, 22-25 October, 1995.

Heydarabadi, R, F., Moghadasi, J. and Safian, GH., A.,:"Hydraulic Fracturing in Iran-Lessons from Four Case Histories," SPE 136103 presented at the SPE Production and Operations Conference and Exhibition, Tunisia, June, 08-10, 2010

Hinchman, S.B. and Barree, R.D.:"Productivity loss in gas-condensate reservoirs", SPE paper 14203, 1985.

Holditch, S. A.: "Factors Affecting Water Blocking and Gas Flow From Hydraulically Fractured Gas Wells," Journal of Petroleum Technology, Dec. 1979, 1515-1524.

Holditch, S.A. and Morse, R.A.: “The Effects of Non-Darcy Flow on the Behaviour of Hydraulically Fractured Gas Wells,” JPT, Oct., 1976, 1169-1179.

Homer, D. R.: “Pressure Build-ups in Wells”, Proc., Third World Pet. Cong., E. J. Brill, Leiden II, 1951, 503-521.

Houze, O.P., Home, R.N., and Ramey, H.J., Jr:“Pressure Transient Response of an Infinite Conductivity Vertical Fracture in a Reservoir with Double Porosity Behaviour,” SPE Formation Evaluation, Sept., 1988, 510-518.

Howard, G.C. and Fast, C.R.,:” Hydraulic Fracturing” Monograph Vol. 2 of the Henry L. Doherty Series, Society of Petroleum Engineers, New York, 1970.

Hunt J. L., Chen Chin-C. and Soliman, M.Y.: “Performance of Hydraulic Fractures in High Permeability Formations,” paper SPE 28530 presented at the SPE Annual Technical Conference and Exhibition, New Orleans, Louisiana, September, 25-28, 1994.

Hurst, W.,: "Establishment of the Skin Effect and its Impediment to Fluid Flow Into a Wellbore," Pet. Eng. J., Oct. 1953, B6 to B-16.

Indriati, S., Wang, X., and Economides, M.J.: “Adjustment of Hydraulic Fracture Design in Gas-Condensate Wells,” paper SPE 73751 presented at the 2002 SPE Annual Technical Conference and Exhibition, Lafayette, LA, 20-21 February.

Iqbal, G.M. and Civan, F.:“Simulation of Skin Effects and Liquid Clean-up in Hydraulically Fractured Wells,” SPE paper 25482 presented at the SPE Production Operations Symposium, Oklahoma City, OK, March, 21-23, 1993.

Jack, E. and Joseph, A.,:“Evaluation of Apparent Fracture Lengths Indicated from Transient Tests,” JCPT, December 1992, Volume 31, No. 10.

Johansen, A.T.: "The Effects of Fracture Fluid Clean-up Upon the Analysis of Pressure Build-up Tests in Tight Gas Reservoirs," MS Thesis, Texas A&M University, College Station, Texas, 1988.

Jones, J.R., Vo, D.T. and Raghavan, R.: “Interoperation of pressure build-up responses in gas-condensate wells,” SPE paper 15535, 1989.

Kabir, S.:"Wellbore Effects, "In M., Kamal (Ed.), Monograph series: Vol. 23. Transient well testing (1sted.) (pp.91–127), Dallas, Society of Petroleum Engineers.

Kazemi, H.: "Pressure Transient Analysis of Naturally Fractured Reservoir with Uniform Fracture Distributions," SPEJ, Dec. 1969, 451-462.

Kroemer, E., Abou-Sayed, I. S., Babu, D. K., Cohen, M. F.,:"Compositional Simulation of Well Performance for Fractured and Multiple Fractured Horizontal Wells in Stratified Gas-condensate Reservoirs," SPE 37995, presented at the SPE Reservoir Simulation Symposium, Dallas, June 1997.

Lancaster, D.E., and Gatens, J.M.:"Practical Well Test Analysis Methods for Hydraulically Fractured Wells in Dual-Porosity Reservoirs," paper SPE 15924 presented at the Eastern Regional Meeting held in Columbus, Ohio, November 12-14, 1986.

Lee, S.-T., and Brockenbrough, J, R: "A New Approximate Analytic Solution for Finite Conductivity Vertical Fractures," SPEFE, Feb., 1988, 75-88.

Lee, W.J Jr.:"Analysis of Hydraulic Fractured Wells with Pressure Build-up Tests," paper SPE 1820 presented at the SPE-AIME 42nd Annual Fall Meeting, Houston, Texas, Oct. 1-4, 1967.

Lee, W.J., and Holditch, S.A.: "Fracture Evaluation with Pressure Transient Testing in Low Permeability Gas Reservoirs. Part I: Theoretical Background" paper SPE 7929 presented at the. Symposium on Low Permeability Gas Reservoirs, Denver, Colorado, 20-22 May, 1979.

Lee, J. W., and Spivey, J.P,: "Numerical and analytical Well Test Analysis," SPE 50946 presented at the SPE Annual Technical Conferences and Exhibitions held in New Orleans, LA, 27-30 Sept., 1988

Lefkovits, H.C., Hazebroek, P., Allen, E.E. and Matthews, C.S.,:"A Study of the Behaviour of Bounded Reservoirs Composed of Stratified Layers," SPEJ, March, 1961, 43-58, Trans. AIME 222.

Liangyue, Liu, Jianming Deng, Yingwen, Ma, King Kwee Chong and Yong Wah Kee: "Single Trip, Multiple Zone Frac Packing Offshore Sand Control: Overview of 58 case histories," SPE paper 103779 presented at the SPE International Oil and Gas Conference and Exhibition, Beijing, Chine, December, 5-7, 2006.

Locke, G.l., and Sawyer, W.K.:"Constant Pressure Injection Test in a Fractured Reservoir-History Match Using Numerical Simulation and Type Curve Analysis," paper SPE 5594 presented at the 50th Annual Fall Technical Conference and Exhibition of SPE of AIME, Dallas, Texas, Sept. 28-Oct. 1975.

Lolon, R.E., McVay, A.D. and Schubarth, K.S.:"Effect of Fracture Conductivity on Effective Fracture Length," SPE paper 84311 presented at the SPE Annual Technical Conference and Exhibition, Denver, Colorado, October, 5-8, 2003.

Mathur, A.K., Ning, X. and Marcinew, R.B.: "Hydraulic Fracture Stimulation of Highly Permeable Formations: The Effect of Critical Fracture Parameters on Oil well Production and Pressure," SPE paper 30652 presented at the SPE Annual Technical Conference and Exhibition, Dallas, TX, October, 22-25, 1995.

Mavor, M.J. and Cinco-Ley, H.: "Transient Pressure Behaviour of Naturally Fractured Reservoirs," paper SPE 7977 presented at the California Regional Meeting held in Ventura, California, April 18-20, 1979.

Mayerhofer, M., Wolhart, S. L. and Rogers, J.D.: "Results of U. S. Department of Energy Deep Gas Well Stimulation Study," SPE paper 95639 presented at the SPE Annual Technical Conference and Exhibition, Dallas, Texas, October, 9-12, 2005.

McGuire, W.J. and Sikora, V.J.: "The Effect of Vertical Fractures on Well Productivity," JPT, 1960, 72-75.

Millheim, K.K. and Cichowicz, L.: "Testing and Analyzing Low-Permeability Fractured Gas Wells," JPT, Feb., 1968, 193-198; Trans., AIME 1.

Mott, R.:"Calculating Well Deliverability in Gas-condensate Reservoirs," 10th European Symposium on Improved Oil Recovery, Brighton, U.K., 18-20 August, 1999.

Mountford, Charles J. and Raghavan, R.: "Identification of near Wellbore Effects and Boundaries from Pressure Build-Up Tests," paper SPE 7162 presented at the Regional Gas Technology Symposium of the Society of Petroleum Engineers of AIME held in Omaha, Nebraska, June 7-9, 1978.

Muskat, N.: "Flow of Homogeneous Fluids through Porous Media," McGraw Hill Book Co. Inc., New York, 1937, 409.

Najurieta, H.L.:"A theory for Pressure Transient Analysis in Naturally Fractured Reservoirs," JPT, July, 1980, 1241-1250.

Narasimhan, T., N. and.Palen, W., A.: "A Purely Numerical Approach for Analyzing Fluid Flow to A Well Intercepting A Vertical Fracture," paper SPE 7983 Presented at the California Regional Meeting of the Society of Petroleum Engineers of AIME, Ventura, California, April18-20,1979.

Ning, X, Collins, J.L., Marcinew, R.P., Dumont, G.L. and Hogg, J.R.,:"Post Fracture Formation Evaluation in the Valhalla Field, Alberta," SPE 31132, presented at the SPE Formation Damage Control Symposium held in Lafayette, LA, USA, February, 14-15, 1996.

Okoye, C.U., Oshinuga, A.D., and Ghalambor, A.: "Pressure Transient Behaviour in Multilayer Vertical Fractured Gas Reservoir with Finite Conductivity," paper SPE 18960 presented at the SPE Joint Rocky Mountain Regional/Low Permeability Reservoirs Symposium, Denver, Colorado, 6-8 March, 1989.

Okoye, C.U., Oshinuga, A.D., and Ghalambor, A.: "Pressure Transient Behaviour of Vertically Fractured Wells in a Closed Square Multi-layered Reservoir," SPE paper 20136 presented at the Permian Basin oil and gas Recovery Conference, Midland, Texas, March, 8-9, 1990.

Olarewaju, J.S. and Lee, W.J.: "New Pressure Transient Analysis Model for Dual-Porosity Reservoirs," SPE Formation Evaluation, September, 1989, 384-390.

Olarewaju, J.S., and Lee, W.J.: "Pressure Behaviour of Layered and Dual-Porosity Reservoirs in the Presence of Wellbore Effects," SPE Formation Evaluation, Sept., 1989, 397-405.

Olivier H., Didier V. and Ole S. F.,: "The Theory and Practice of Pressure Transient and Production Analysis and The Use of data from Permanent Downhole Gauges in Dynamic Flow Analysis, Oct. 2008

Osman, M.E.:"Well Testing of Fractured Well in a Multi-layered Bounded Square," paper SPE 24533 presented at the Abu Dhabi Petroleum Conference, 18-20 May, 1992, 265-284.

Osman, M.E.:"Transient Pressure Analysis for Wells in Multi-layered Reservoir with Finite Conductivity Fractures," paper SPE 25665 presented at the SPE Middle East Oil Technical Conference and Exhibition held in Bahrain 3-6 Apr., 1993, 567-583.

Ozkan, E. and Raghavan, R.:"Some New Solution to Solve Problems in Well Test Analysis: Part I-Analytical Consideration," paper SPE18615 presented at the SPE Joint Rocky Mountain Regional / Low Permeability reservoirs Symposium and Exhibition, Denver, Colorado, March, 6-8, 1977.

Prats, M.: "Effect of Vertical Fractures on Reservoir Behaviour -Incompressible Fluid Case," Sot. Pet. Eng. Jour. presented at the 35th Annual Fall Meeting of SPE, Oct., 2-5, 1960, 105-118.

Prats, M., Hazelbreak, P, and Strickler, W. R.: "Effect of Vertical Fractures on Reservoir Behaviour - Compressible Fluid Case," Soc. Pet. Eng. Jour., June. 1962, 87-94.

Raghavan, R.: "Some Practical Considerations in the Analysis of Pressure Data," J. Pet. Tech., Oct., 1976, 1256-1268.

Raghavan, R., Cady, G.C. and Ramey, H.J., Jr.:"Well Test Analysis for Vertically Fractured Wells," J. Pet. Tech., Aug., 1972, 1014-1020; Trans., AIME 253.

Rahim, Z., Holditch, S.A., and Davidson, B.M.: "Quantitative Analysis of Production Loss Due to Fracture Fluid Degradation," paper SPE 29590 presented at the SPE Rocky Mountain Regional/Low-Permeability Reservoirs Symposium, Denver, Colorado, 20-21 March, 1995.

Ramey, H.J., Jr: "Short-Time Well Test Data Interpretation in the Presence of Skin Effect and Wellbore Storage," J. Pet, Tech., Jan., 1970, 97-104; Trans., AIME 249.

Ramey, H.J., Jr., and Gringarten, A.C.: "Effect of High-volume Vertical Fractures on Geothermal Steam Well Behaviour," presented at Second United Nations Symposium on Geothermal Energy, San Francisco, May, 20-29, 1975.

Berthelot, J.M.:"Effects of Fracturing Fluid Recovery upon Well Performance and Ultimate Recovery of Hydraulically Fractured Gas Wells," MS Thesis, Texas A&M University, College Station, Texas, 1990.

Robinson, J.C., Chu, W-C., Woods, M. E. and Hutchison, H.W.,: "Pressure Build-up Testing as an Aid in Well Stimulation: Case History," paper SPE 22750 presented at the SPE Annual Technical Conference and Exhibition, Dallas, TX, October, 6-9, 1991.

Romero, J.D., Valko, P.P, and Economides, J.M.: "The Optimization of the Productivity Index and the Fracture Geometry of a Stimulated Well with Fracture Face and Choke

Skins," SPE paper 73758 presented at the SPE International Symposium and Exhibition on Formation Damage Control, Lafayette, Louisiana, February, 20-21, 2002.

Russell, D.G. and Truitt, N.E.:"Transient Pressure Behaviour in Vertically Fractured Reservoirs", J. Pet. Tech., Oct 1964, 1159-1170.

Sanchez, R., Agut, R., Coulon, D., and Sentinelli, R., :"New Methodology of Effective Hydraulic Fracturing in High-Thickness Formation, " SPE 107392 presented at the Latin American and Caribbean petroleum Engineering conference, Buenos Aires, April, 15-18, 2007.

Sawyer, W.K., Locke, C.D. and Overbey, K. Jr.:"Simulation of a Finite-Capacity Vertical Fracture in a Gas Reservoir," paper SPE 4593 presented at the 48th Annual Fall Meeting of SPE of AIME, Las Vegas, Nevada, Sept. 30-Oct. 3, 1973.

Scott, J. O.: "Effect of Vertical Fractures on Transient Pressure Behaviour of Wells," J. Pet. Tech. (Dec. 1963) 1365-1369; Trans., AIME, Vol. 22S.

Scott, J.O.: "Application of A New Method for Determining Flow Characteristics of Fractured Gas Wells in Tight Sands," paper SPE 7931 presented at the SPE Symposium on Low-Permeability Gas Reservoirs, Denver, Colorado, May, 20-22, 1979.

Serra, K.V.: Reynolds, A.C. and Raghavan, R.,:"New Pressure Transient Analysis Methods for Naturally Fractured Reservoirs," JPT, Dec., 1983, 2271-2283.

Settari, A., Bachman, R.C., Hovem K., and Paulsen, S.G.: "Productivity of Fractured Gas-condensate Wells-A Case Study of the Smorbukk Field," paper SPE 35604 presented at the 1996 SPE Gas Technology Conference, Calgary, April 28-May 1.

Settari, A., Stark, A.J., and Jones, J.R.: "Analysis of Hydraulic Fracturing of High Permeability Gas Wells to Reduce Non-Darcy Skin Effects," JCPT, May, 2000, 39, No. 5, 56.

Schaible, D.F., Akpan, B. and Ayoub, J. A.,:"Identification, Evaluation and Treatment of Formation Damage, Offshore Louisiana", SPE 14820, presented at the SPE Symposium on Formation Damage Control of the SPE held in Lafayette, LA, February, 26-27, 19986.

Shaoul, J., Ross, M., Spitzer, W., Wheaton, S., Mayland, P. and Singh, A., P.: "Massive Hydraulic Fracturing Unlock Deep Tight Gas Reservoirs in India," SPE paper 107337 presented at the European Formation Damage Conference, Scheveningen, The Netherlands, 30th May- 1st June, 2007.

Siddiqui, M.A., Nasr-El-Din, H.A., Al-Anazi, M.S., and Bartko, K.M.: "Formation Damage in Gas Sandstone Formations by High-Temperature Borate Gels Due to Long Term Shut-In Periods," paper SPE 89476 presented at the 2004 SPE/DOE Fourteenth Symposium on Improved Oil Recovery, Tulsa, Oklahoma, 17-21 April.

Skaar, R.G., Walpot, K.S., Der Post, N.V.,:"Matching Production Rates from the Saih Rawl and Barik Gas-condensate Fields using State-of-the-art Single Well Reservoir Simulation Model," SPE 63163, presented at the 2000 SPE Annual Technical Conference and Exhibition held in Dallas, Texas, October, 1-4, 2000.

Smith, M.B., Bale, A., Britt, L.K., Cunningham, L.E., Jones, J.R., Klein, H.H., and Wiley, R.P.: "An Investigation of Non-Darcy Flow Effects on Hydraulic Fractured Oil and Gas Well Performance," paper SPE 90864 presented at the SPE Annual Technical Conference and Exhibition, Houston, Texas, 26-29 September, 2004.

Sognesand, S.:"Long-Term Testing of Vertically Fractured Gas-condensate Wells," paper SPE 21704 presented at the SPE Production Operations Symposium, Oklahoma City, OK, 7-9 April, 1991.

Streltsova, T.D.: "Well Pressure Behaviour of a Naturally Fractured Reservoir," SPEJ, October, 1983, 769-780.

Tannich, J.D.:"Liquid Removal from Hydraulically Fractured Gas Wells," JPT, November, 1975, 1309-1317.

Van Everdingen, A.F. and Hurst, W.: "The Application of the Laplace Transformation to Flow Problems in Reservoirs," Trans., AIME, 1949, 186, 305-324.

Valko, P., Oligney, R.E. and Economides, M.J. :"High Permeability Fracturing of Gas Wells," Harts Petroleum Engineer International, Jan. 1998, PP 75-88

Van Everdingen, A. F.: "The Skin Effect and its Influence on the Productive Capacity of a Well", Trans., AIME, 198, 1953, 171-176.

Van Poollen, H.K., Tinsley, J.M. and Saunders, C.D.,: "Hydraulic fracturing: Fracture Flow Capacity vs. Well Productivity," Trans., AIME, 1958, Vol. 213, 91.

Voneiff, G.W., Robinson, B.M. and Holditch, S.A.: "The Effect of Unbroken Fracture Fluid on Gas well Performance," SPE Production and Facilities paper 9886-PA, November, 1996, 223-229.

Umnuayponwiwat, S., Ozkan, E., Pearson, C. M., and Vincent, M.: "Effect of Non-Darcy Flow on the Interpretation of Transient Pressure Responses of Hydraulically Fractured Wells," paper SPE 63176 presented at the SPE Annual Technical Conference and Exhibition, Dallas, TX, Oct., 1-4, 2000.

Wang, X., Indriati, S, Valko, P.P. and Economides, J.M.: "Production Impairment and Pressure Built Design of Hydraulically Fractures in Gas-condensate Reservoirs," SPE paper 64749 presented at the SPE Annual Technical Conference and Exhibition, Beijing, Chine, November, 7-10, 2000.

Warren, J.E. and Root, P.J.: "Behaviour of Naturally Fractured Reservoirs," SPEJ, Sept., 1963, 245-255.

Wattenbarger, R.A. and Ramey, Jr., H.J.: "Well Test Interpretation of Vertically Fractured Gas Wells," JPT, May, 1969, 625-632.

Wong, D.W., Harrington, A.G. and Cinco-Ley, H.:"Application of the Pressure Derivative Function in the Pressure Transient Testing of Fractured Wells," SPEFE, October, 1986.

Xinghui, Liu and Civan, F.:"Formation Damage and Skin Factor due to Filter Cake Formation and Fines Migration in the Near Wellbore Region," paper SPE 27364 presented at the SPE International Symposium and Exhibition on Formation Damage Control, Lafayette, Louisiana, February, 7-10, 1994.

Xinghui, Liu, Cipolla C. L. and Mayerhofer, M.: "Case History of Hydraulic Fracture Performance in a Channel Reservoir," paper SPE 84396 presented at the SPE Annual Technical Conference and Exhibition, Denver, Colorado, October, 5-8, 2003.

Yadavalli, S.K. and Jones, R.J.:"Interpretation of Pressure Transient Data from Hydraulically Fractured Gas-condensate Wells," SPE paper 36556 presented at the SPE Annual Technical Conference and Exhibition, Denver, Colorado, October, 6-9, 1996.

Yatindra, B.:"Well test Analysis in a Lean Gas-condensate Reservoir," SPE 113121 presented at the Indian oil and gas Technical Conference and Exhibition, Mumbai, India, March. 4-6, 2008

Yizhu, Liao and Lee, W.J.: "Production Performance of Hydraulically Fractured Gas Wells," SPE paper 25465 presented at the SPE Production Operations Symposium, Oklahoma City, OK, March, 21-23, 1993.

Yizhu, Liao and Lee, W.J.: “New Solutions for Wells with Finite Conductivity Fractures Including Wellbore Storage and Fracture Face Skin,” SPE paper 26912 presented at the SPE Eastern Regional Conference and Exhibition, Pittsburgh, PA, November, 2-4, 1993.

Yizhu, Liao and Lee, W.J.: “New Solutions for Wells with Finite Conductivity Fractures Including Fracture Face Skin: Constant Well Pressure Cases,” SPE paper 28605 presented at the SPE Annual Technical Conference and Exhibition, New Orleans, LA, September, 25-28, 1994.

Zillur, R., and Ismail, B.,:”Integrating Pressure Transient Analysis in Hydraulic Fracturing,” SPE 106359 presented at the SPE Technical Symposium of Saudi Arabia Section, Dahran, May, 21-23, 2006.

APPENDIX A

I. Eclipse Black Oil Input File_ Single Layer Oil Model

```
-- Study: Single Layer Oil Well Test
-- Author: A. Amin
-- Simulator: Eclipse 100
-- Model: Finite Conductivity Vertical Fractured Oil Well
-- Fluid: Dead Oil and Water
--************************************************************
RUNSPEC
--************************************************************
TITLE
Fractured Oil Well Model

FIELD
OIL
WATER

LICENSES
'lgr'/
/
LGR
 1    31668 0 0 0 1000 'NOINTERP' 0 /

DIMENS
    27    19    1 /

EQLDIMS
5*  /
TABDIMS
  1 1 100 100 1 /
REGDIMS
 1  1    0     0 /
```

```
3
+VFPPDIMS
20 20 20 20 1* 1 /
WELLDIMS
1   10 /
NUPCOL
4/
NSTACK
24/
MESSAGES
 2*    1000     5* 100000   2*/

START
  1 'Aug' 2006 /

UNIFIN
UNIFOUT

--NOSIM
--************************************************************
GRID
--************************************************************
INIT
NOECHO
OLDTRAN
INCLUDE
'Include\Model_Geom.inc' /
INCLUDE
'Include\Model_GridProp.inc' /
--************************************************************
PROPS
--************************************************************
PROPS
-- THE PROPS SECTION DEFINES THE REL. PERMEABILITIES, CAPILLARY
```

```
-- PRESSURES, AND THE PVT PROPERTIES OF THE RESERVOIR FLUIDS
-- oil/water relative permeability and capillary pressure are tabulated as
-- function of water saturation
--    Sw        Krw             Kro             Pcow
SWOF
0.081          0               0.933           0
0.096          0.00018         0.8566          0
0.126          0.00167         0.714           0
0.166          0.00601         0.55337         0
0.206          0.01304         0.42237         0
0.266          0.02863         0.27249         0
0.336          0.05448         0.1538          0
0.406          0.08857         0.07986         0
0.476          0.1309          0.03707         0
0.546          0.18148         0.01469         0
0.616          0.2403          0.00457         0
0.686          0.30736         0.00094         0
0.84           0.5             0               0 /
/
-- SWITCH ON OUTPUT OF ALL PROPS DATA
RPTPROPS
 8*1 /

-- DENSITY created by PVTi
-- Units: lb /ft^3     lb /ft^3     lb /ft^3
DENSITY
-- Fluid Densities at Surface Conditions
       52.7896     62.4280      0.0572 /

-- PVT PROPERTIES OF WATER
--    REF.PRES.  FVF-WATER  COMPRESSIBILITY  VISCOSITY  VISCOSIBILITY
--    (PSIA)     (RB/STB)      (1/PSI)      (CP)        (1/PSI)
PVTW
      5021    0.99963     2.72e-006     0.4879      7.02305e-006 /
```

```
--     GOR     BUBBLE PT.
--             PRESSURE
--  (MSCF/STB)   (PSIA)
RSCONST
      1.0323   4228.6186  /

--    REF.PRES   ROCK-COMPRESSIBILITY
--     (PSIA)         (1/PSI)
ROCK
      5021         0.0000044 /

PVDO
      4228.6186     1.5148     0.3403
      4325.0000     1.5124     0.3445
      4426.0000     1.5099     0.3488
      4526.0000     1.5075     0.3531
      4626.0000     1.5052     0.3575
      4723.0000     1.5030     0.3616
      4821.0000     1.5008     0.3659
      5021.0000     1.4964     0.3745
/
--************************************************************
REGIONS
--************************************************************
--PVT and Saturation Functions regions
PVTNUM
  513*1 /
-- MAY NEED SATNUM data (allocate different saturation tables to different grid
blocks)

SATNUM
   513*1/
```

```
EQLNUM
   513*1/

REFINE
LGRFRAC /
BOX
    1    36     1     1     1     10 /

SATNUM
   360*1 /
ENDBOX
ENDFIN
--************************************************************
SOLUTION
--************************************************************
-- THE SOLUTION SECTION DEFINES THE INITIAL STATE OF THE SOLUTION
-- VARIABLES (PHASE PRESSURES, SATURATIONS AND GAS-OIL RATIOS)

RPTSOL
FIP=2 RS /
RPTRST
BASIC=2 FIP RS /

EQUIL
-- CONFIRM DATUM DEPTH AND PRESSURE
-- DATUM    PRESSURE    DEPTH    OWC    DEPTH    GOC    INIT    INIT    INTE
-- DEPTH    @ DATUM     OWC      CAP    GOC      CAP TYPE N
--                          PRESS          PRE LO   DO
  7765.5   5021   8050    0       8050      0       0   /

--************************************************************
SUMMARY
--************************************************************
SUMMARY
```

```
WBHP
/
WOPR
 /
WWPR
 /
WWCT
 /
WTHP
/
WBP9
/
WBP
/
RPTONLY
RUNSUM
PERFORMA
DATE
3/
TCPU
EXCEL

**********************************************************
SCHEDULE
--**********************************************************
SCHEDULE
MESSAGES
 2*15000 2*1000 2*100 4*30000 /

TUNINGL
   4.16667e-006   0.1  1.0E-9   1.0E-9   1.2 /
/
   8* 5   10 /
```

```
-- Specify performance of solver
-- Specify output of grid block pressures, oil saturations, water saturations,
-- and inter block flows to restart files

RPTSCHED
 'PRES' 'SWAT' 'RESTART=1' 'WELLS=2' 'SUMMARY=2'
 'CPU=2' 'WELSPECS' 'NEWTON=2' /
RPTSCHED
  FIP/
RPTRST
  BASIC=2 NORST=2 POT /
DRSDT
/
WELSPECL
'WELL' 1* 'LGRFRAC' 1 1 7765.8 'OIL' /
/
COMPDATL
'WELL' 'LGRFRAC' 1 1 1 10 'OPEN' 2* 0.1 3* 'Z' 1* /
/

WPIMULTL
'WELL' 0.25 5* /
/

INCLUDE
'Include\Model_VfPprod.inc'/


WCONPROD
'WELL'STOP 1* 1* 1* 1* 1* 1* /
/
TSTEP
 1*4.167e-006 /
```

```
-- 1DD
-- PRODUCTION WELL CONTROLS - OIL RATE IS SET TO 1000 BPD
--    WELL    OPEN/ CNTL   OIL  WATER   GAS   LIQU   RES   BHP
--    NAME    SHUT  MODE  RATE   RATE  RATE   RATE  RATE
WCONPROD
'WELL'  'OPEN'    'ORAT'   100   5*   2200   1  /
/

TSTEP
0.00001 49*1.83673469387755E-07 49*1.83673469387755E-06
49*0.000183673469387755 49*0.000183673469387755 49*0.00183673469387755
49*0.0183673469387755 49*0.0408161428571428/ 3days
--2BU
WCONPROD
-- NAME  STATUS  CONTMODE  OILT  WATT  GAST  LIQT  RESVT  BHPT
TOHT  PROVFP  ART
 'WELL'  'OPEN'    'ORAT'   0.0   5*   2200   1 /
/
TSTEP
0.00001 49*1.83673469387755E-07 49*1.83673469387755E-06
49*0.000183673469387755 49*0.000183673469387755 49*0.00183673469387755
49*0.0183673469387755 49*0.122448795918367 /7days
2days
END
```

II. Eclipse Compositional Input File_ Single Layer Gas-condensate Model

```
-- Study: Single Layer Oil Well Test
-- Author: A. Amin
-- Simulator: Eclipse 100
-- Model: Finite Conductivity Vertical Fractured Oil Well
-- Fluid: Gas-condensate
--************************************************************
RUNSPEC
--************************************************************
TITLE
Lean Gas-condensate
--Grid Dimensions
DIMENS
    24   12   1  /
--Units
FIELD
-- Grid Geometry
CART
AIM
-- Phases Present
OIL
WATER
GAS
-- Capillary Number Model
-- Model 1 for Oil Phase
-- Model 1 for Gas Phase
-- Default for Forchheimer Model for Oil Phase
-- Model 1 for Forchheimer Gas Phase
VELDEP
-- OCN GCN OFR GFR
  1  1  0  1  /
--Peng-Robinson equation of state
EOS
 PR /
ISGAS
--Number of Components
COMPS
 13 /
TABDIMS
 1  1 100 100 1 /
EQLDIMS
 5*  /
REGDIMS
```

```
 1 1   0    0 /
WELLDIMS
 1   10 /
VFPPDIMS
20 20  20  20  1*  1  /
NUPCOL
 4/
NSTACK
 24/
MESSAGES
  2*15000  2*1000  2*100  4*30000 /
--NOWARN
VECTABLE
 2000/
--fractured well
FWELLS
UNIFIN
UNIFOUT
UNIFSAVE
--NOSIM
START
  1 'Aug' 2006 /

--*************************************************************

GRID

--*************************************************************

INIT

ECHO
INCLUDE
'Include\Geom.inc' /
INCLUDE
'Include\GridProp_Frac.inc' /
 --*************************************************************

PROPS

--*************************************************************

INCLUDE
'Include\Run_0_example_PVT.inc' /
VDKRO
--    M     N1    N2    Ncb       a        b   c      d    Betad
      79.62      24.2 0     1.0E-6     0       0   0     0     1* /
VDKRG
--      M   N1    N2    Ncb       a        b   c     d     Betad
      23.89      6.23 1E-3       1.57E-3     5.5   5.5      1*
      0.5   1* /
-- Relative permeability and capillary pressure data
-- Water Relative Permeability
```

```
SWOF
--SW       KRW          KROW      PCWO
 0.251       0          0.897      0
0.276713   0.0000176    0.769065   0
0.302427   0.000141     0.653913   0
0.32814    0.000476     0.55087    0
0.353853   0.0011128    0.459264   0
0.379567   0.002203     0.378422   0
0.40528    0.003807     0.307671   0
0.430993   0.006045     0.246339   0
0.456707   0.009024     0.193752   0
0.48242    0.012849     0.149238   0
0.508133   0.017625     0.112125   0
0.533847   0.023459     0.081739   0
0.55956    0.030456     0.057408   0
0.585273   0.038722     0.038459   0
0.610987   0.048363     0.024219   0
0.6367     0.059484     0.014016   0
0.662414   0.072192     0.007176   0
0.688127   0.086592     0.003027   0
0.71384    0.102789     0.000897   0
0.739554   0.12089      0.000112   0
0.765267   0.141        0.0        0
1          1            0.0        0
/
SGOF
-- SG      KRg          KROG       PCGO
0.000      0.000000    0.8970000   0
0.03745    0.000113    0.711533    0
0.07490    0.000900    0.553574    0
0.11235    0.003038    0.420915    0
0.14980    0.007200    0.311348    0
0.18725    0.014062    0.222664    0
0.22470    0.024300    0.152656    0
0.26215    0.038587    0.099116    0
0.29960    0.057600    0.059834    0
0.33705    0.082013    0.032604    0
0.37450    0.112500    0.015216    0
0.41195    0.149738    0.005463    0
0.44940    0.194400    0.001137    0
0.48685    0.247162    0.000029    0
0.52430    0.308700    0.000000    0
0.56175    0.379687    0.000000    0
0.59920    0.460800    0.000000    0
0.63665    0.552713    0.000000    0
0.67410    0.656100    0.000000    0
0.71155    0.771638    0.000000    0
0.74900    0.897000    0.000000    0
/
RPTPROPS
SWFN  SGFN  SOF3  VDKRO VDKRG /
```

```
DENSITY
--        OIL           WATER          GAS
          40            63.0         0.001/
PVTW
--        WATER PROPERTIES -
--       Pref(psi)    Bwref      cw          uw
         2000         1.000   0.000003       0.42 /
ROCK
--          PREF          COMP
--          PSI          1/PSI
          3550          0.000004 /
--************************************************************
REGIONS
--************************************************************
--PVT and Saturation Functions regions
PVTNUM
  288*1 /
SATNUM
   288*1/
EQLNUM
   288*1/
REFINE
LGRFRAC /
BOX
     1    46     1     1     1     10 /
SATNUM
  460*1 /
ENDBOX
ENDFIN
--************************************************************
SOLUTION
--************************************************************
EQUIL
-- CONFIRM DATUM DEPTH AND PRESSURE
-- DATUM    PRESSURE    DEPTH    OWC    DEPTH    GOC    INIT    INIT    INTE
-- DEPTH    @ DATUM     OWC      CAP    GOC      CAP    TYPE    TYPE    N
--                              PRESS           PRE    LO      DO
   7865.8   5981    8000     0       7865.8     0     3*   1   1  /
FIELDSEP
 1  172.4    457    /
 2  60       14.5    /
```

```
/
OUTSOL
 PRES  SGAS  SOIL  SWAT   RESTART /
RPTSOL
 PRES  SGAS  SOIL  SWAT PSAT  STEN /
--************************************************************

SUMMARY
--************************************************************

WBHP
/
FGPR
FOPR
FWPR
FGOR
/
WTHP
/
WBP9
/
INCLUDE
'Include\blockproperties.inc' /
RPTONLY
RUNSUM
PERFORMA
EXTRAPMS
3/
TCPU
EXCEL
--************************************************************

SCHEDULE
--************************************************************

MESSAGES
 2*15000 2*1000 2*100 4*30000 /
RPTSCHED
  'CPU=2' /
RPTRST
 PRES  SGAS  SOIL  SWAT PSAT  RESTART /
RUNSUM
SEPCOND
 SEP1  FIELD   1   172.4   457   /
 SEP1  FIELD   2   60      14.5  /
/
-- Well Specifications
WELSPECL
'WELL' 1* 'LGRFRAC'   1    1    7865.8    'GAS' / --          0.0E+00        STD    3*
         AVG/
```

```
/
-- Well Completion Data
COMPDATL
'WELL' 'LGRFRAC'  1    1    1    10  'OPEN' 2*  0.01    1* 0.0  0.0000  'Z' /
/
WSEPCOND
 'WELL'  SEP1  /
/
INCLUDE
'Include\Run_0_example_VfPprod.inc'/

-- 1DD
-- PRODUCTION WELL CONTROLS - OIL RATE IS SET TO 1000 BPD
--    WELL    OPEN/ CNTL   OIL  WATER   GAS  LIQU   RES   BHP
--    NAME    SHUT   MODE RATE   RATE  RATE  RATE  RATE
WCONPROD
  'WELL'  'OPEN'     'GRAT'   2*   5000   2*   1*   1*   1 /
/
TSTEP
  1*4.167e-006 /
-- 1DD
-- PRODUCTION WELL CONTROLS - OIL RATE IS SET TO 1000 BPD
--    WELL    OPEN/ CNTL   OIL  WATER   GAS  LIQU   RES   BHP
--    NAME    SHUT   MODE RATE   RATE  RATE  RATE  RATE
WCONPROD
'WELL'  'OPEN'     'ORAT'   100    5*   2200    1  /
/
TSTEP
   0.00001   1.12236E-05 1.25968E-05 1.41381E-05  1.5868E-05
1.78096E-05 1.99887E-05 2.24344E-05 2.51794E-05 2.82602E-05
3.17181E-05
 3.5599E-05 3.99547E-05 4.48434E-05 5.03303E-05 5.64885E-05
6.34002E-05 7.11576E-05 7.98641E-05  8.9636E-05 0.000100604
0.000112913
0.000126729 0.000142235 0.000159638  0.00017917 0.000201093
0.000225698 0.000253314 0.000284308 0.000319095 0.000358138
0.000401958
 0.00045114  0.00050634 0.000568294 0.000637828  0.00071587
0.000803461  0.00090177 0.001012107 0.001135944 0.001274934
0.00143093
0.001606013 0.001802518 0.002023067 0.002270602 0.002548424
0.002860239 0.003210206 0.003602994 0.004043843 0.004538631
0.00509396
0.005717237 0.006416776 0.007201907 0.008083104 0.009072121
0.01018215 0.011427998 0.012826283 0.014395657 0.016157053
0.018133966
```

```
0.020352767 0.022843051 0.025638037 0.028775006 0.032295803
0.036247391 0.040682479 0.045660227 0.051247033 0.057517418
0.064555023
0.072453722 0.081318874 0.091268731 0.102436014 0.114969682
0.12903692  0.14482537 0.162545633 0.182434077 0.204755994
0.229809132
0.257927673 0.289486689 0.324907141 0.364661501 0.409280048
0.459357945 0.515563176 0.578645458 0.649446241 0.728909928
0.81809648
0.918195548 1.030542343 1.156635451 1.298156815 1.456994177
1.635266254
/ 15 days

--1BU
WCONPROD
-- NAME   STATUS    CONTMODE   OILT    WATT    GAST    LIQT
RESVT   BHPT TOHT   PROVFP   ART
  'WELL'  'STOP'      'GRAT'    2*    0    2*   1000   1*
1 /
/
TSTEP
   0.00001   1.12308E-05 1.26132E-05 1.41657E-05 1.59092E-05
1.78674E-05 2.00666E-05 2.25365E-05 2.53104E-05 2.84257E-05
3.19244E-05
3.58538E-05 4.02669E-05 4.52231E-05 5.07893E-05 5.70407E-05
6.40615E-05 7.19465E-05  8.0802E-05 9.07474E-05 0.000101917
0.000114461
 0.00012855 0.000144372 0.000162142 0.000182099 0.000204513
0.000229685 0.000257956 0.000289706 0.000325364 0.000365412
0.000410388
 0.0004609   0.00051763 0.000581342 0.000652896 0.000733257
0.000823509 0.00092487 0.001038707 0.001166556 0.001310141
0.001471398
0.001652504 0.001855901 0.002084333 0.002340882 0.002629008
0.002952597 0.003316015 0.003724164  0.00418255 0.004697356
0.005275527
0.005924861 0.006654118 0.007473135  0.00839296 0.009426001
0.010586193 0.011889187 0.013352558 0.014996048 0.016841825
0.018914788
 0.0212429  0.023857566 0.026794057 0.030091982 0.033795831
0.037955565 0.042627297 0.047874045 0.053766585 0.060384404
0.067816772
0.076163947 0.085538528 0.096066972 0.107891302  0.12117102
0.136085262 0.152835213 0.171646818 0.192773835 0.216501254
0.243149145
0.273076972 0.306688441 0.344436953 0.386831711 0.434444596
0.487917876 0.5479728741 / 5days
END
```

APPENDIX B

I. Oil Sample PVT Modelling

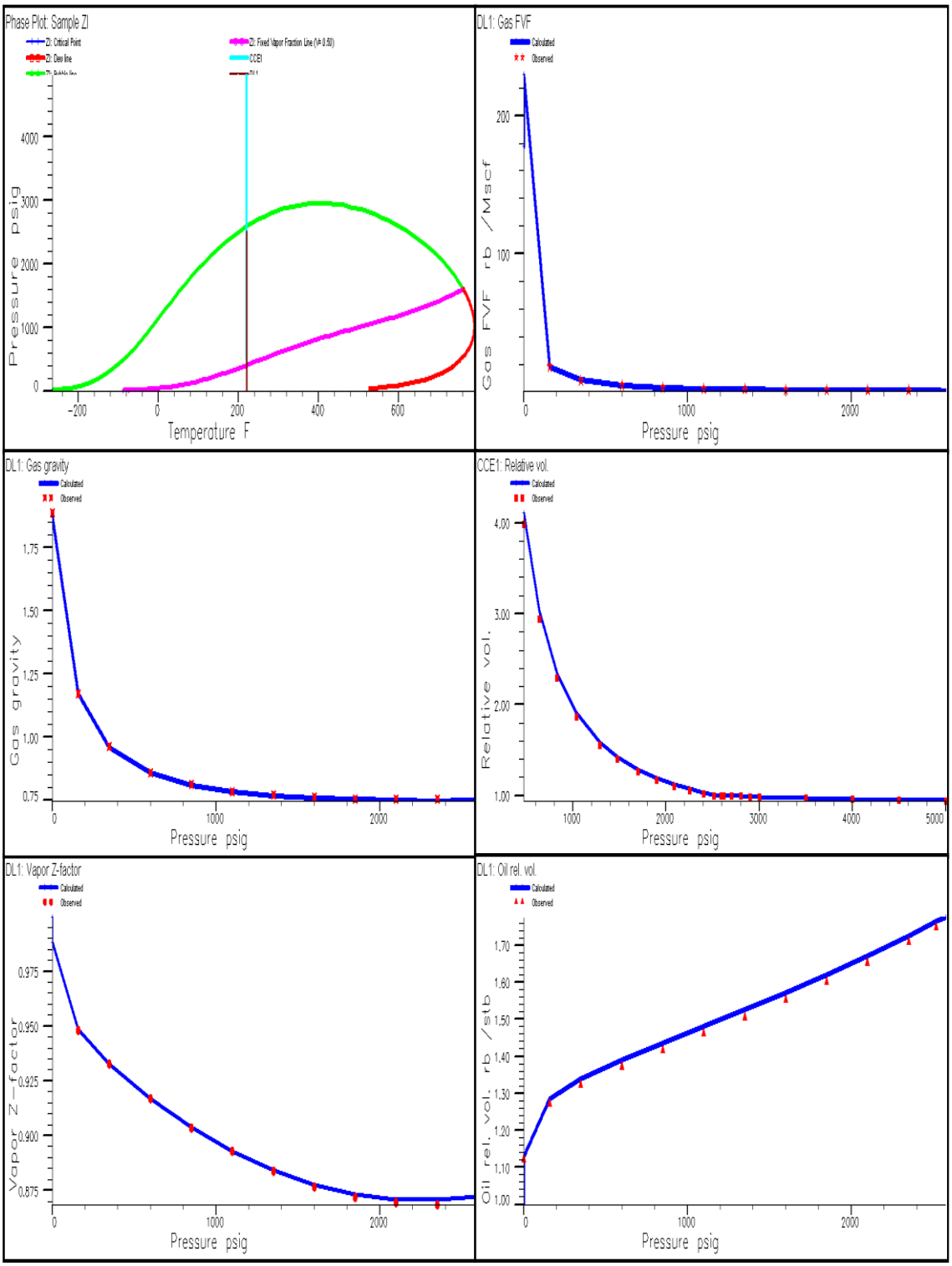


Figure B- 1: PVT properties analysed in PVTi for the used oil sample

II. Gas Sample PVT Modelling

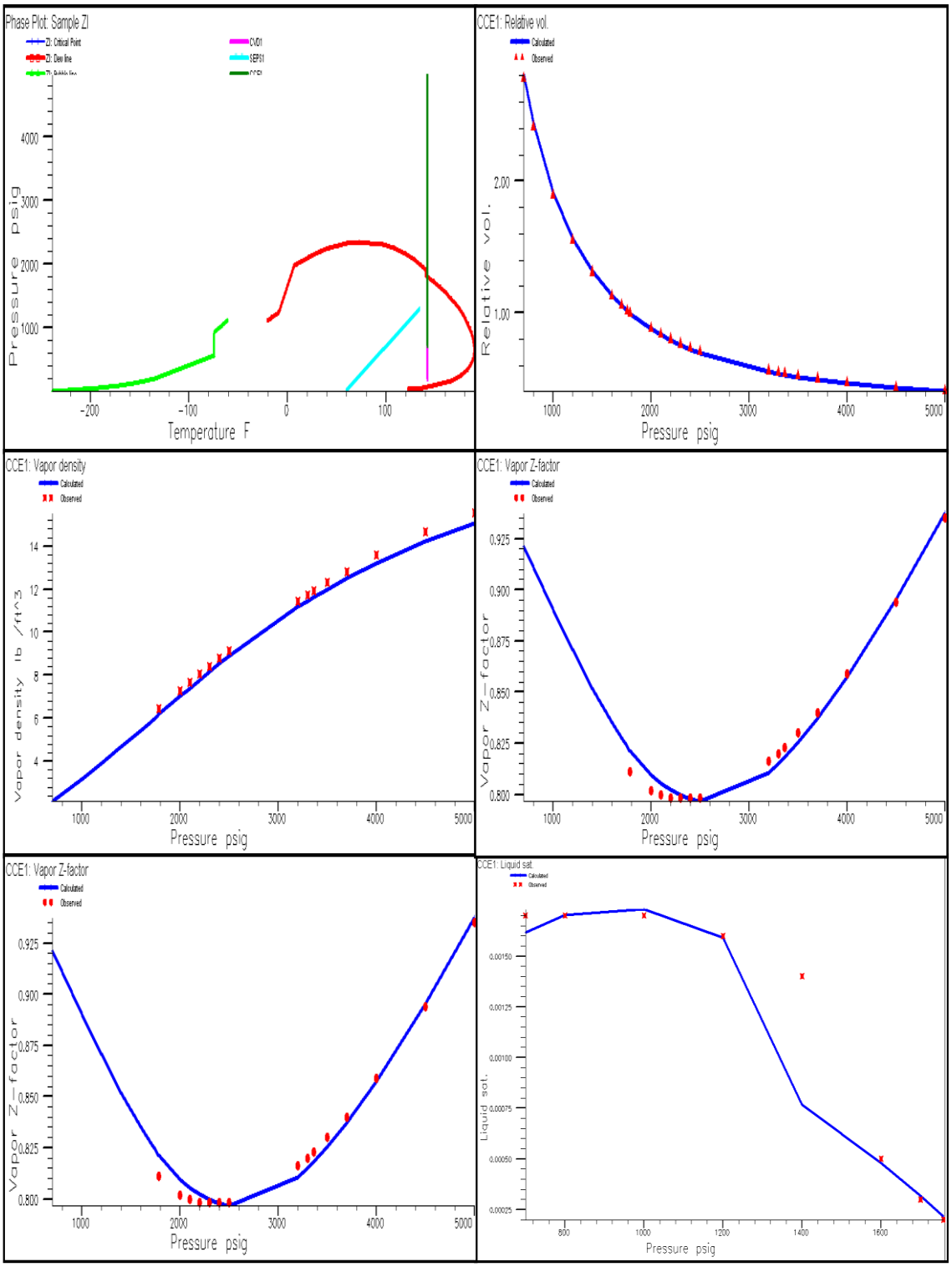


Figure B- 2: PVT properties analysed in PVTi for the used gas sample in the study

III. Lean Gas Condensate Sample PVT Modelling

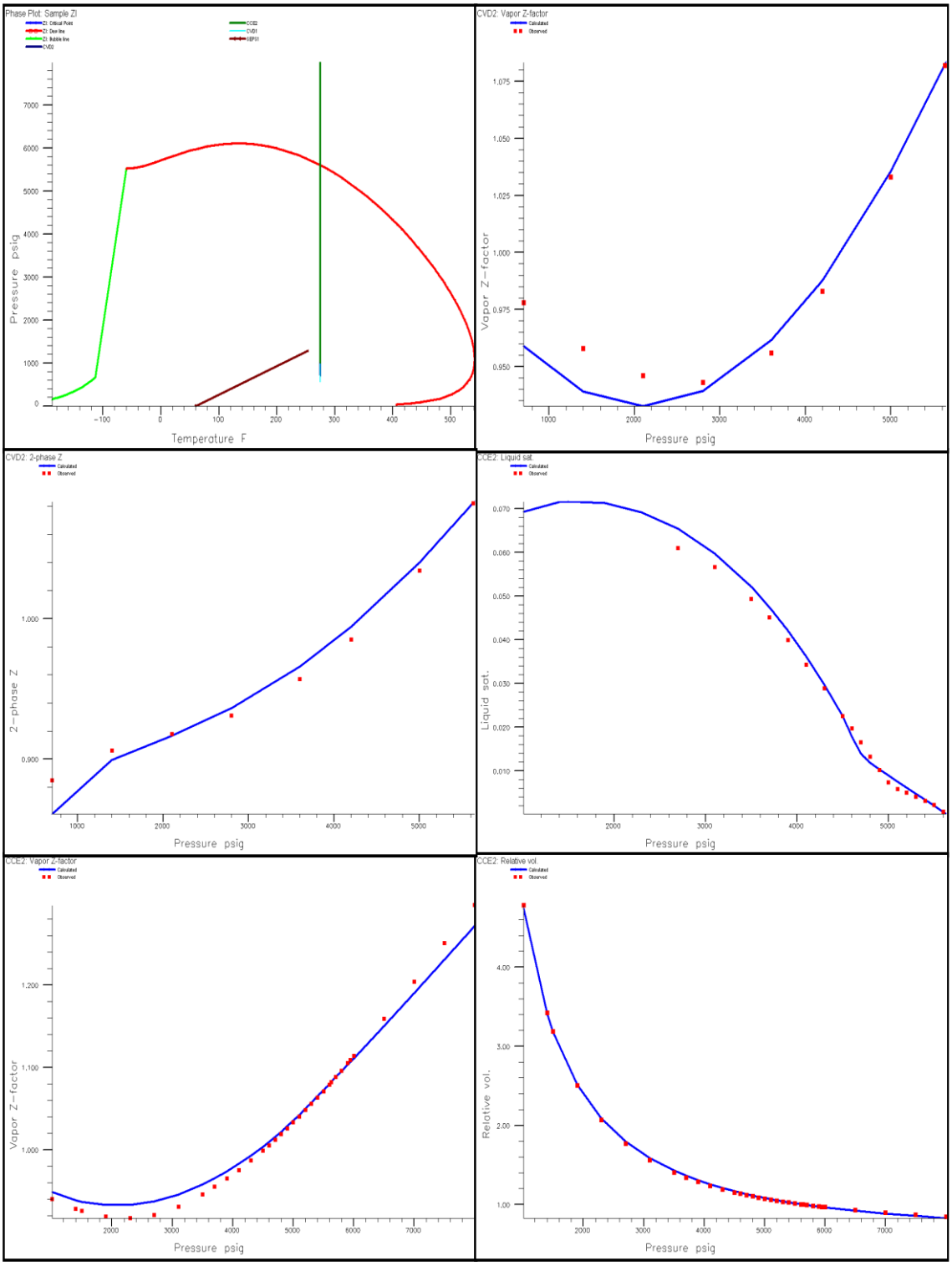


Figure B- 3: PVT properties analysed in PVTi for the lean gas condensate sample

IV. Moderate Gas Condensate Sample PVT Modelling

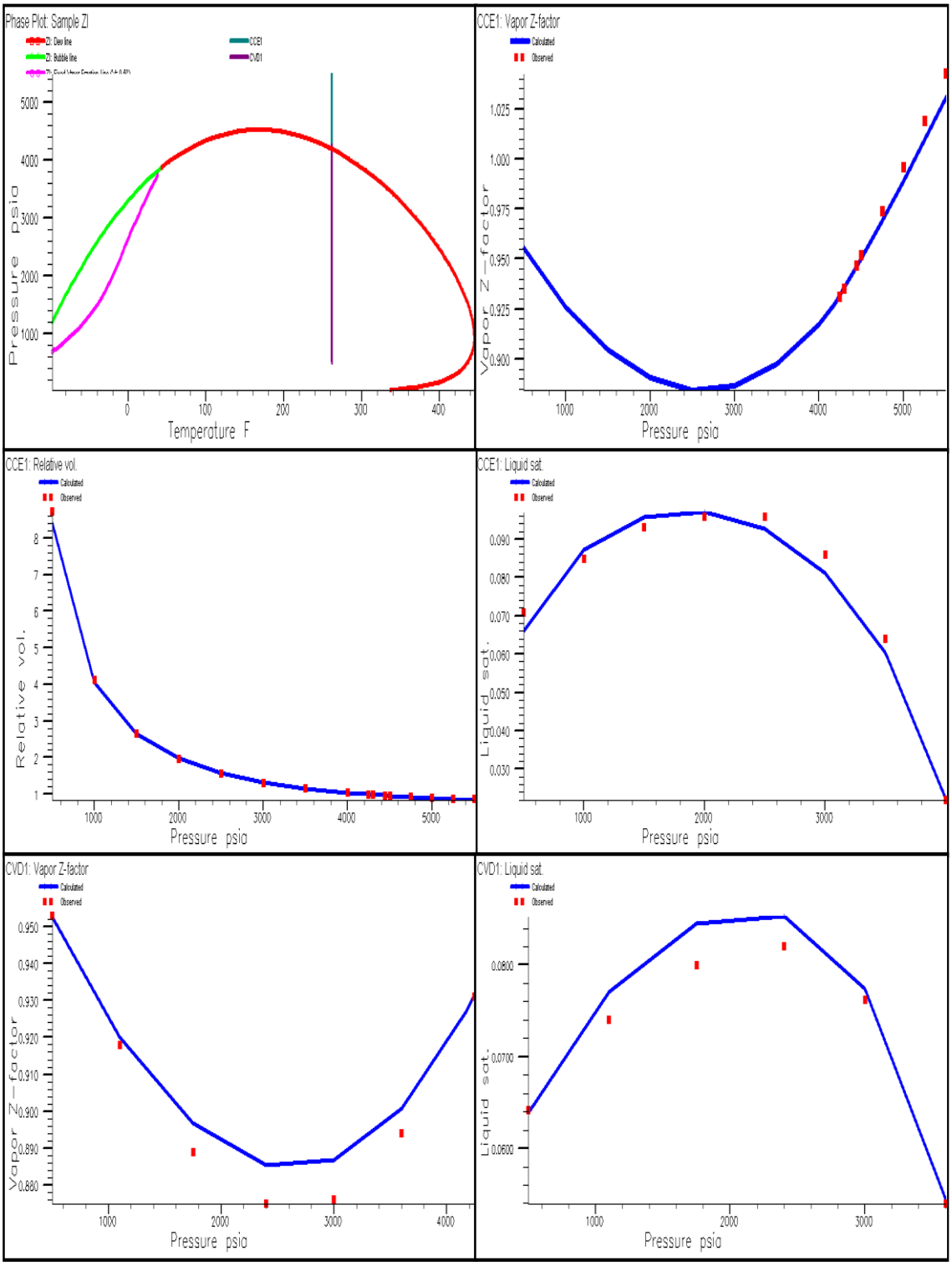


Figure B- 4: PVT properties analysed in PVTi for the moderate gas condensate sample

V. Rich Gas Condensate Sample PVT Modelling

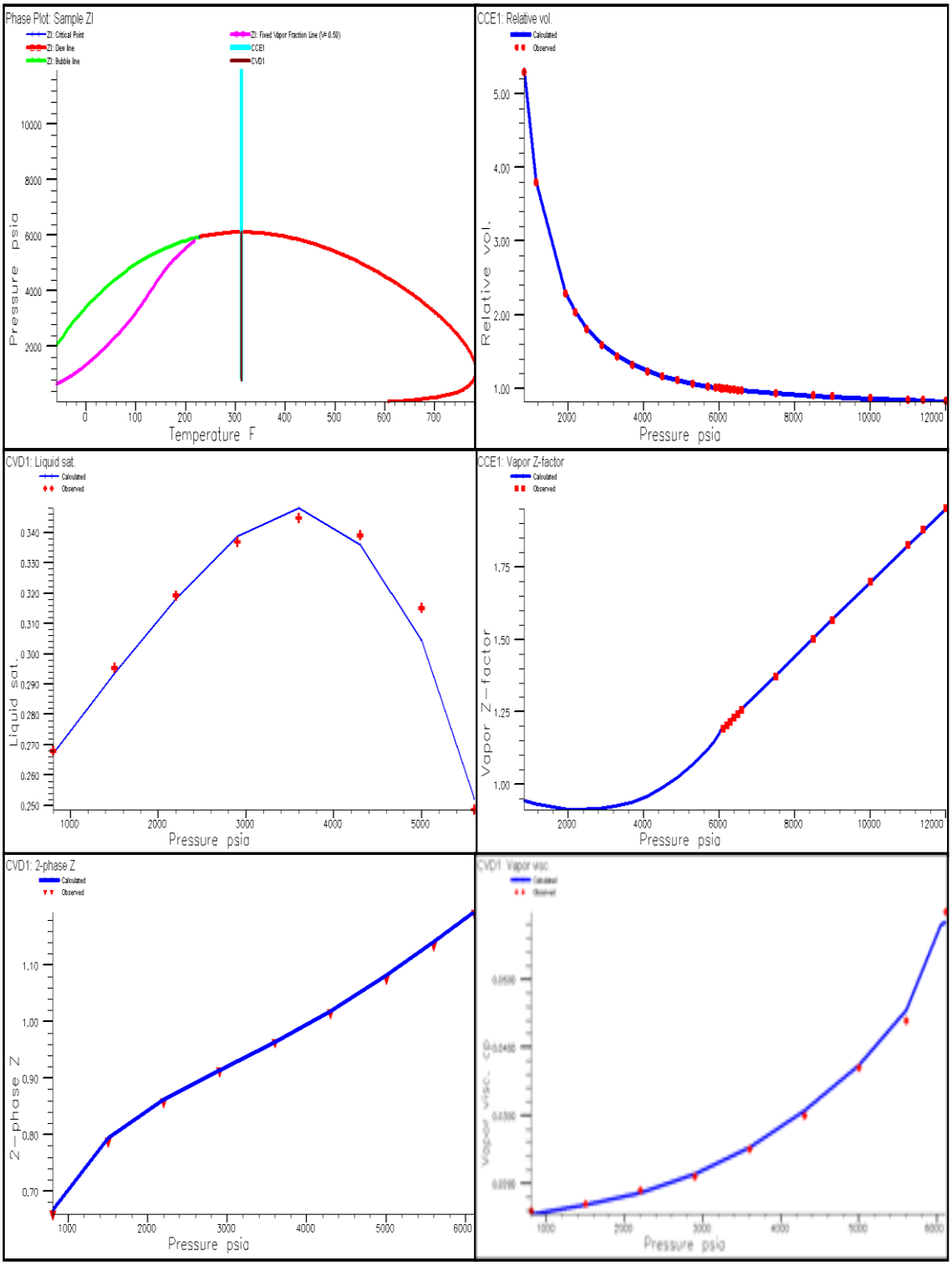


Figure B- 5: PVT properties analysed in PVTi for the rich gas condensate sample

APPENDIX C

I. Fractured Choke Effect

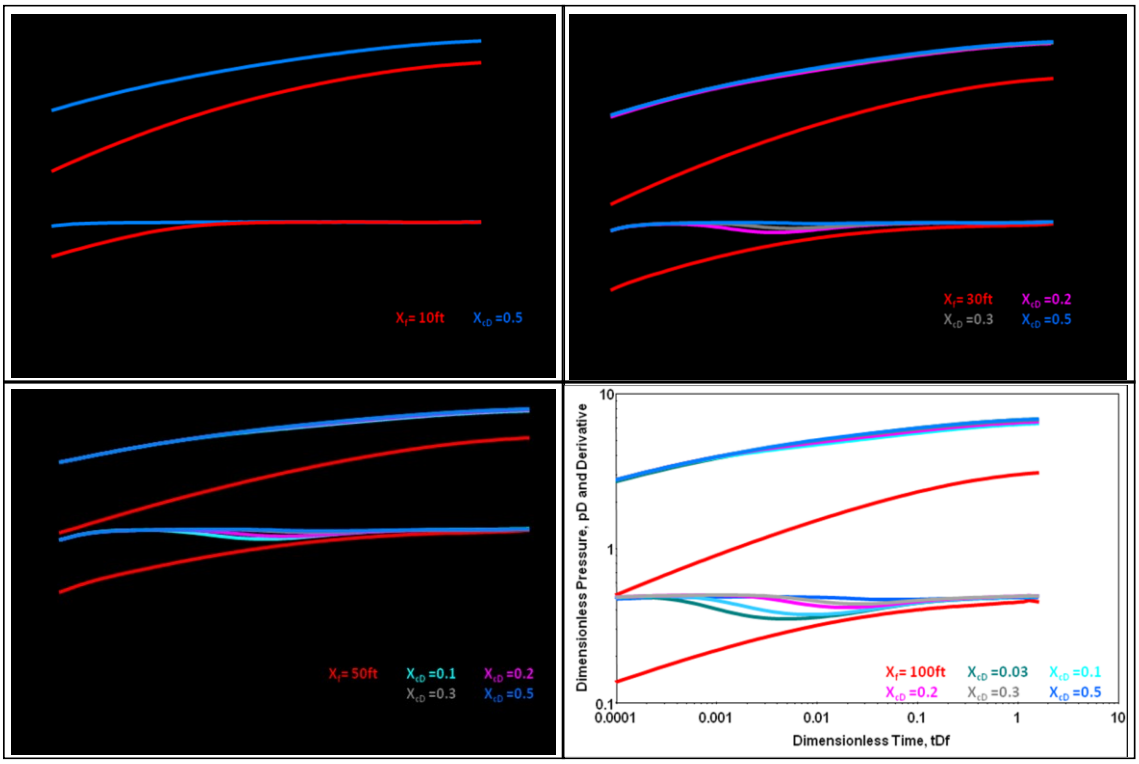


Figure C- 1: Fracture flow behaviour of 10, 30, 50 and 100ft with choked damage effect

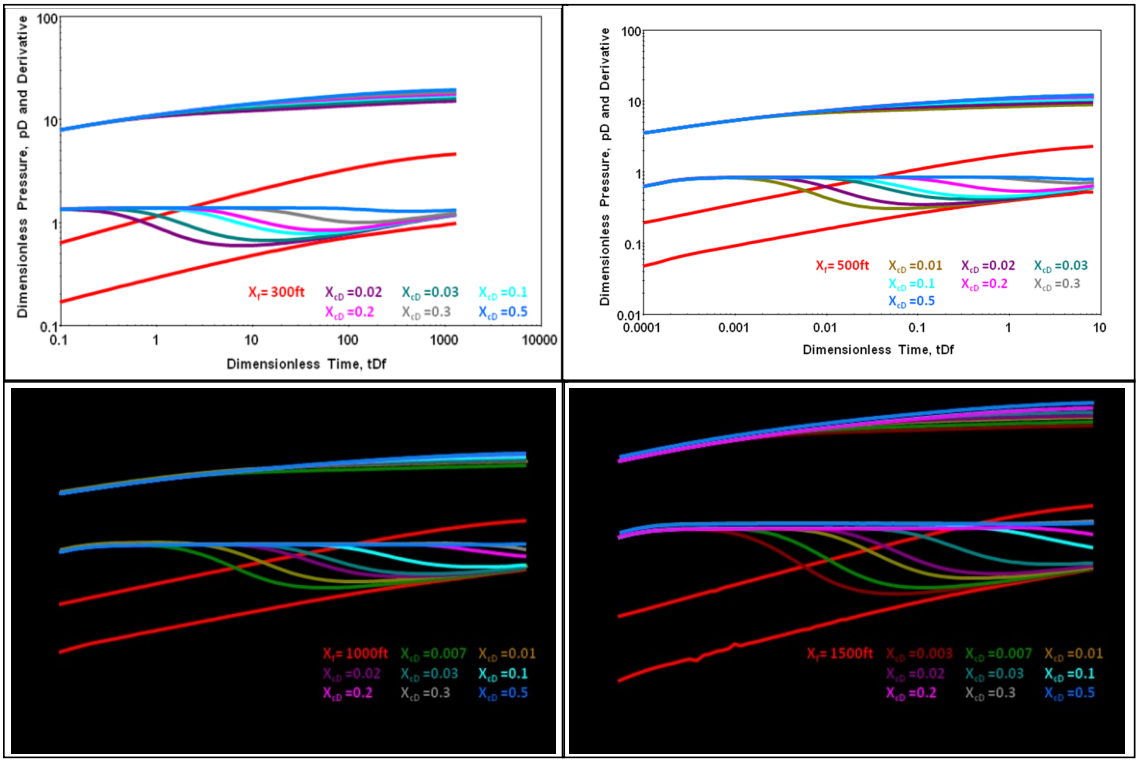


Figure C- 2: Fracture flow behaviour of 300, 500, 1000 and 1500ft with choked damage

II. Fractured Face Effect

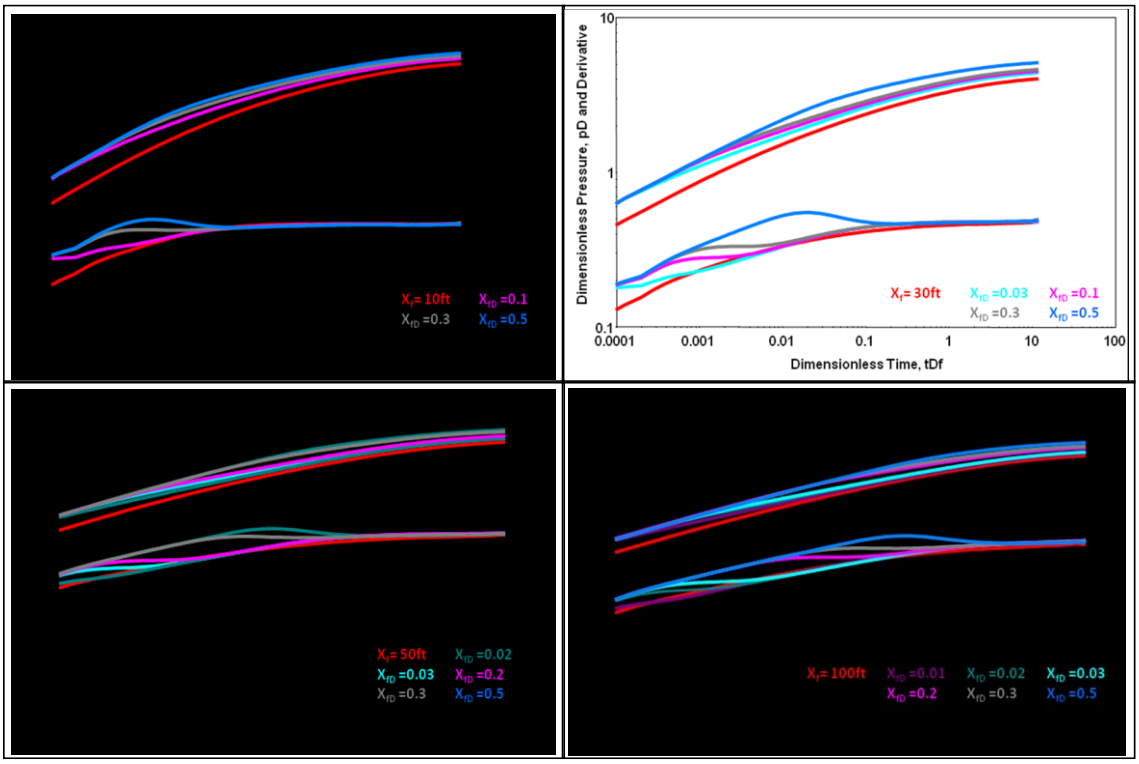


Figure C- 3: Fracture flow behaviour of 10, 30, 50 and 100ft with fracture face skin effect

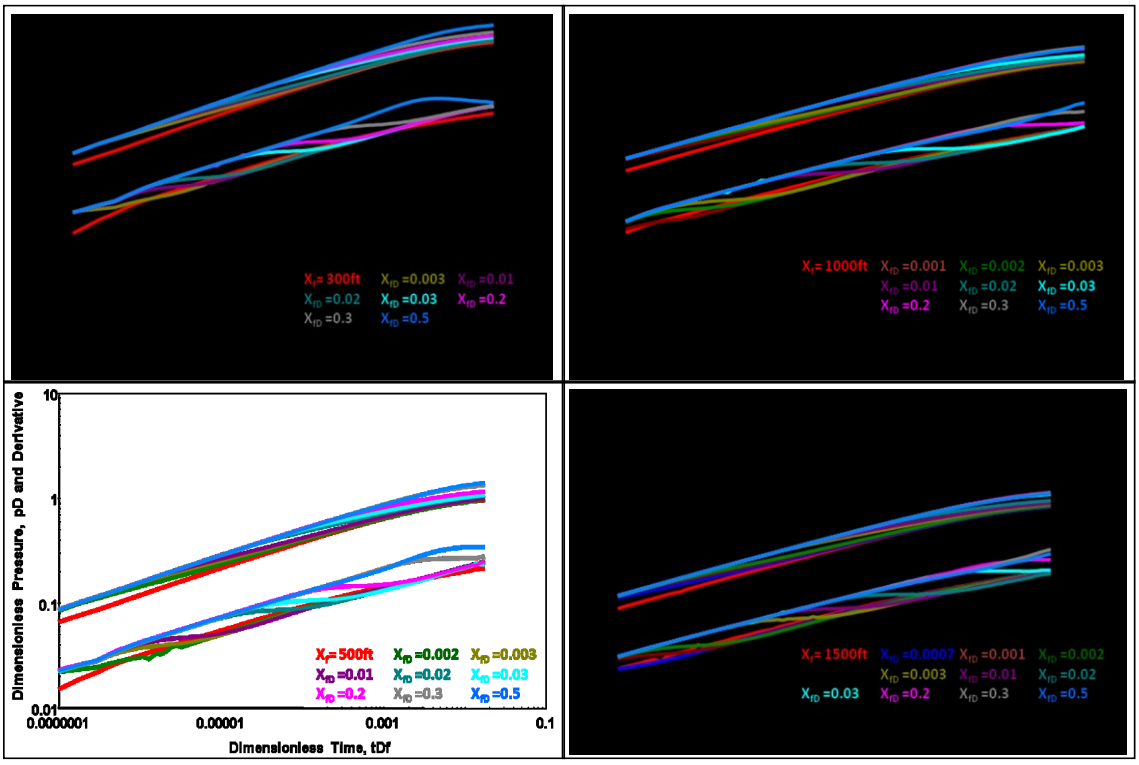


Figure C- 4: Fracture flow behaviour of 300, 500, 1000 and 1500ft with face skin effect

APPENDIX D

I - Gas-condensate Saturation Change Profiles

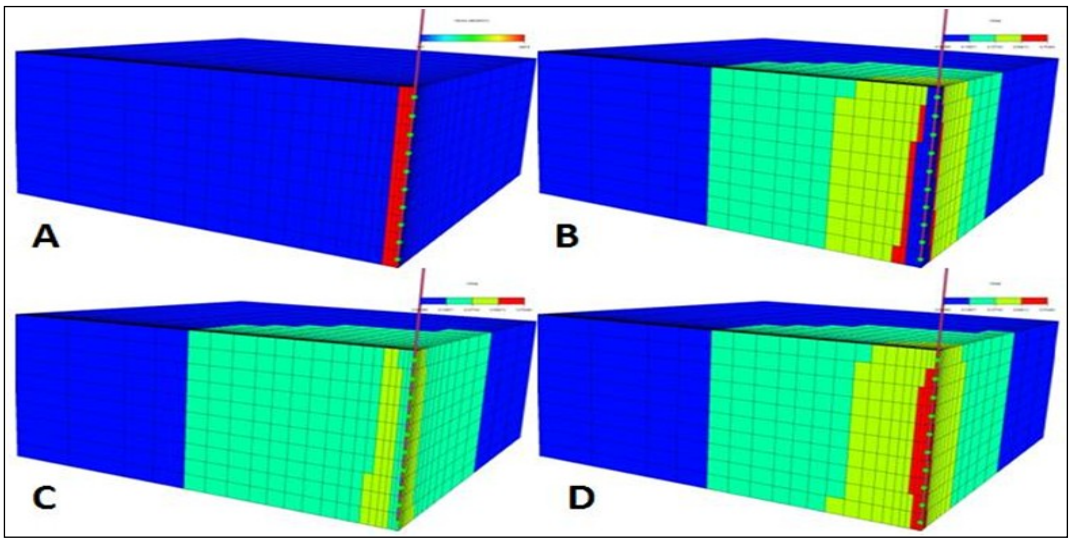


Figure D- 1: Graph A: shows 10ft fracture half-length before production
B: Liquid saturation at end of 5 days BU and 180 days of DD, fracture induced at this stage
C: Saturation end of 15 days of DD with fracture installed after 180days DD and 5 days BU
D: Saturation at end of 5days BU following 15days of DD following 180days DD & 5days BU

Results indicate that the fracture has removed liquid accumulated in the preceding DD and BU flow periods; however, some liquid remained at the and away from the tip of the fracture and liquid accumulated again at the end of the final 5 days BU flow period.

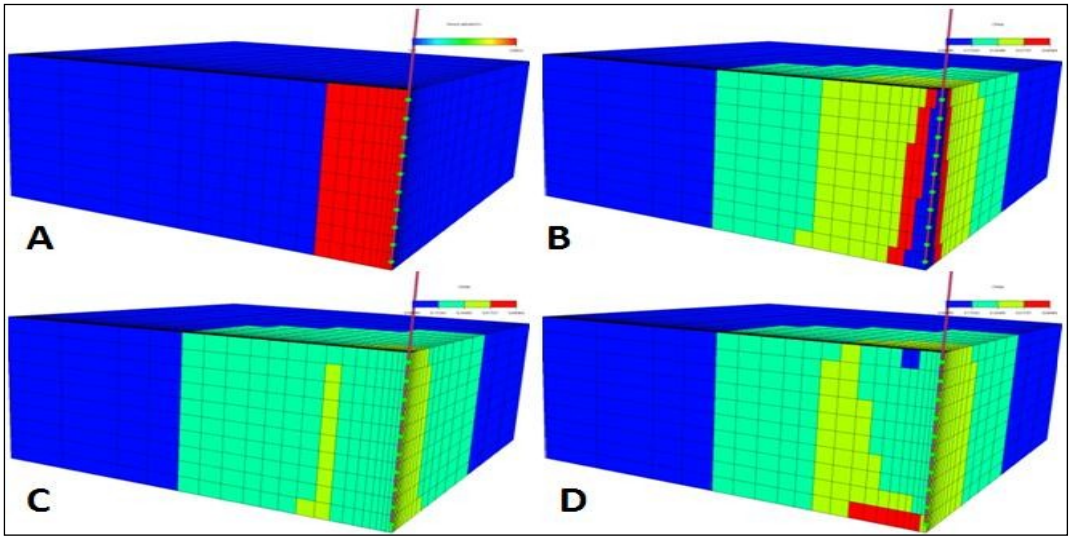


Figure D- 2: Graph A: shows 50ft fracture half-length before production
B: Liquid saturation at end of 5 days BU and 180 days of DD, fracture induced at this stage
C: Saturation end of 15 days of DD with fracture installed after 180days DD and 5 days BU
D: Saturation at end of 5days BU following 15days of DD following 180days DD & 5days BU

Results indicate that the fracture has removed liquid accumulated in the preceding DD and BU flow periods; however, some liquid remained at the and away from the tip of the fracture and liquid accumulated again at the end of the final 5 days BU flow period.

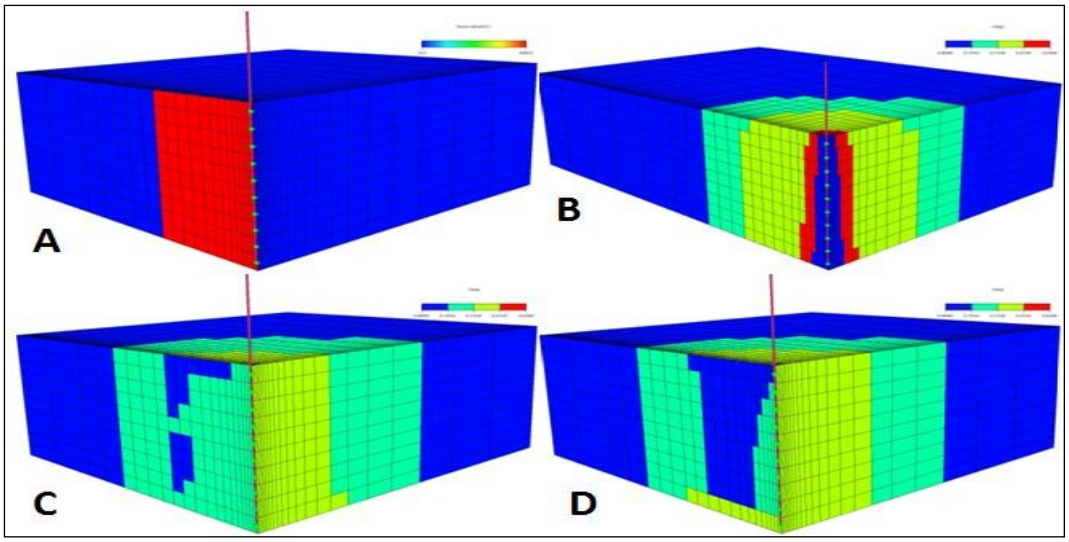


Figure D- 3: B: Graph A: shows 100ft fracture half-length before production
B: Liquid saturation at end of 5 days BU and 180 days of DD, fracture induced at this stage
C: Saturation end of 15 days of DD with fracture installed after 180days DD and 5 days BU
D: Saturation at end of 5days BU following 15days of DD following 180days DD & 5days BU

Results indicate that the fracture has removed more liquid accumulated in the preceding DD and BU flow periods; however, less liquid remained at the and away from the tip of the fracture compared to the 10ft and 50ft cases. The liquid accumulated again at the end of the final 5 days BU flow period.

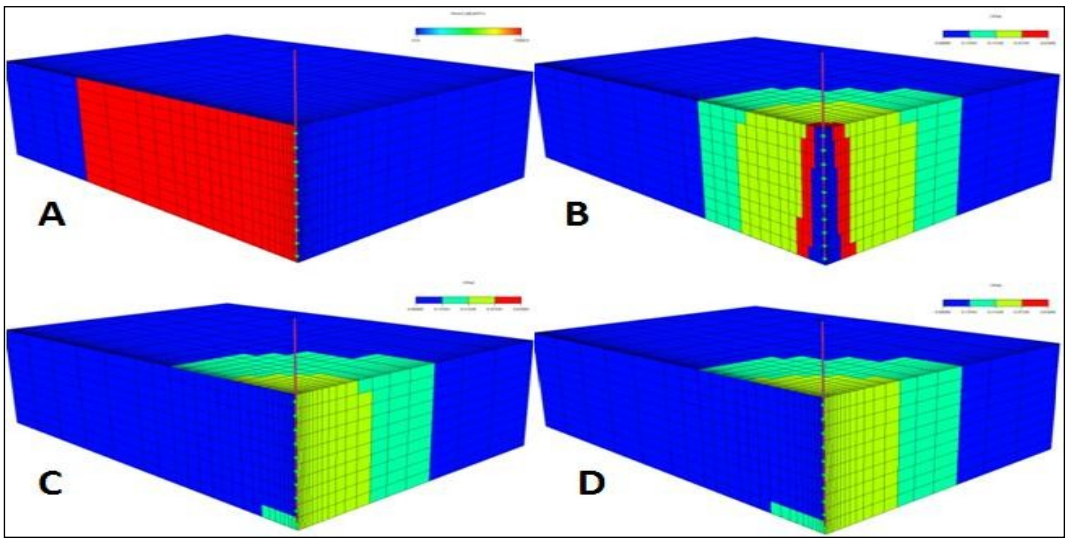


Figure D- 4: Graph A: shows 300ft fracture half-length before production
B: Liquid saturation at end of 5 days BU and 180 days of DD, fracture induced at this stage
C: Saturation end of 15 days of DD with fracture installed after 180days DD and 5 days BU
D: Saturation at end of 5days BU following 15days of DD following 180days DD & 5days BU

Results indicate that the fracture has removed all liquid accumulated in the preceding DD and BU flow periods in the fracture; however, liquid remained at the fracture face, which impacts fluid flow into the fracture. No liquid remained at the and away from the tip of the fracture compared to the 10ft, 50ft and 100ft cases. Also, liquid saturations at the end of 15days of DD and final 5 days of BU are of similar profiles. This suggests that long fractures are required to enhance productivity from gas-condensate wells.

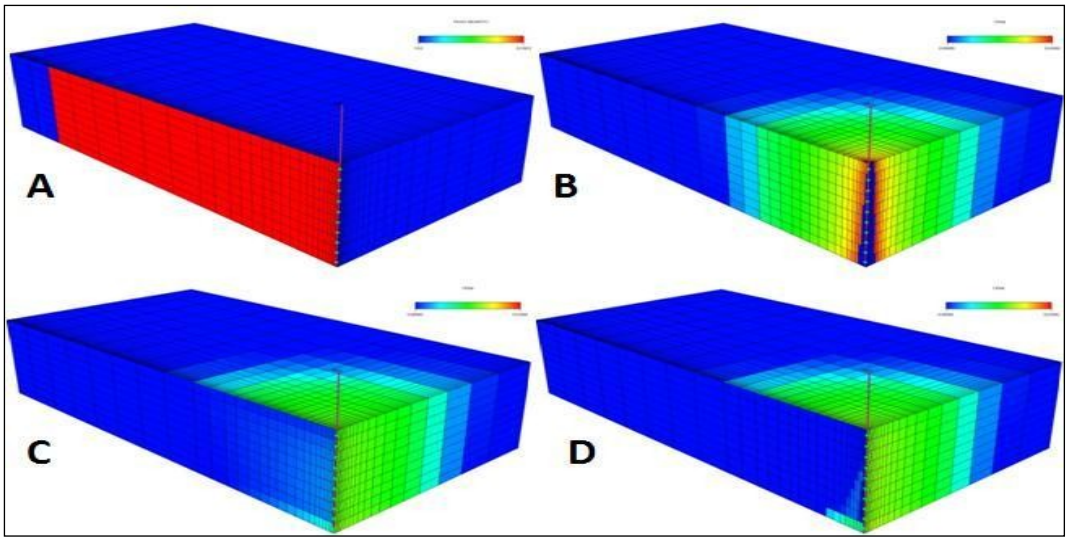


Figure D- 5: Graph A: shows 500ft fracture half-length before production
B: Liquid saturation at end of 5 days BU and 180 days of DD, fracture induced at this stage
C: Saturation end of 15 days of DD with fracture installed after 180days DD and 5 days BU
D: Saturation at end of 5days BU following 15days of DD following 180days DD & 5days BU

Results indicate that the fracture has removed all liquid accumulated in the preceding DD and BU flow periods in the fracture and less liquid remained at the fracture face. No liquid remained at the and away from the tip of the fracture compared to the previous cases. Also, liquid saturations at the end of 15days of DD and final 5 days of BU are of similar profiles. This indicates that fractures longer than 300ft-400ft in such reservoirs would not have significant impact reducing accumulated condensate bank. However, liquid remain at the fracture face in all these cases.

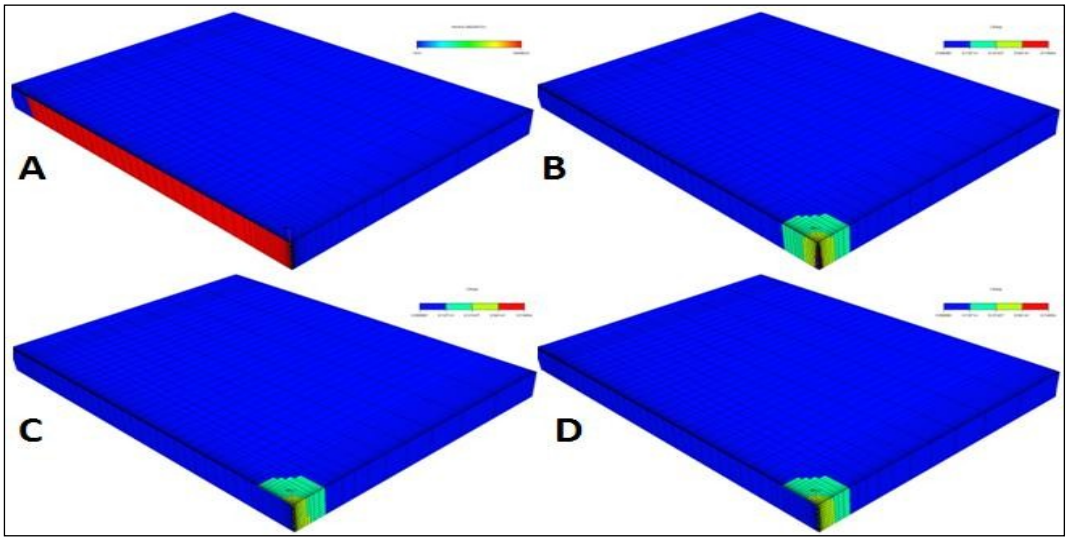


Figure D- 6: Graph A: shows 1000ft fracture half-length before production
B: Liquid saturation at end of 5 days BU and 180 days of DD, fracture induced at this stage
C: Saturation end of 15 days of DD with fracture installed after 180days DD and 5 days BU
D: Saturation at end of 5days BU following 15days of DD following 180days DD & 5days BU

Results indicate similar observation found in the case of 500ft fracture half-length. As can be seen from all the presented cases, the liquid accumulation at the fracture face can be reduced; however, it cannot be removed completely.

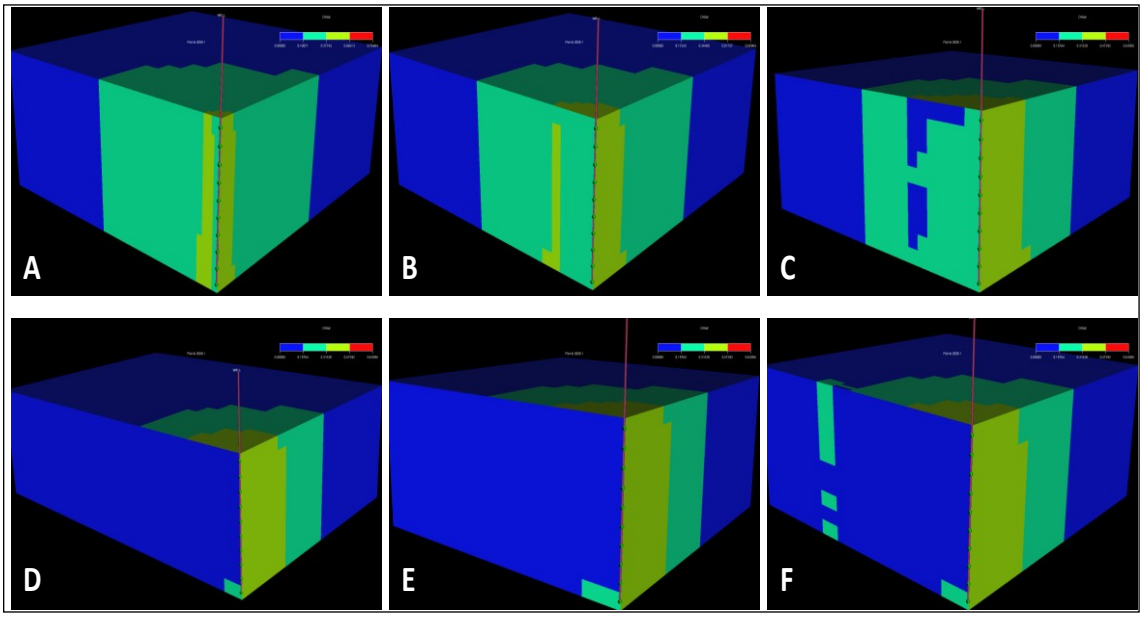


Figure D- 7: Liquid saturation distribution at the end of 30days DD for fracture half-length of 10 (A)-50(B)-100(C)-200(D)-300(E)-400ft(F)

Results indicate that fractures with half-length up to 100ft would not be effective in removing condensate deposited in the fracture; however, as fracture half-length increase less liquid can be observed within the fracture. It is worth noting optimum fracture half-length is considered to be 300ft to 400ft in the case of rich gas-condensate wells.

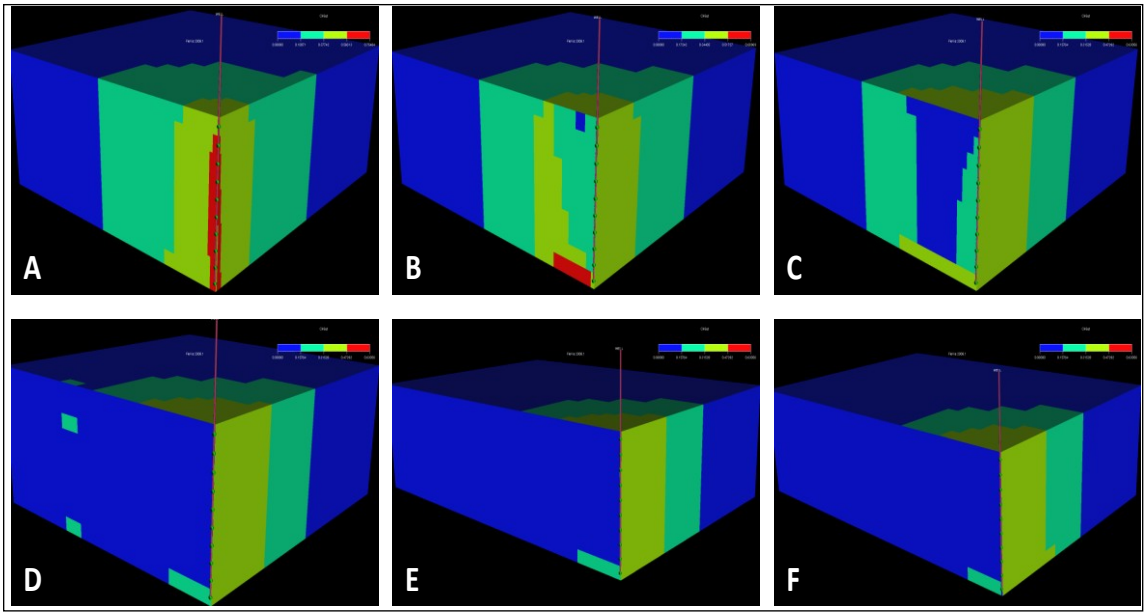


Figure D- 8: Liquid saturation distribution at the end of 5days BU following preceding 30days of DD for fracture half-length of 10 (A)-50(B)-100(C)-200(D)-300(E)-400ft(F)

Results indicate that in the case of short fracture half-lengths of 10 to 50ft and during the build-up period, some gas vaporizes from the liquid bank forming heavy components liquid in the vicinity of the wellbore, which impacts well productivity significantly causing more pressure drawdown compared to longer fracture half-lengths.

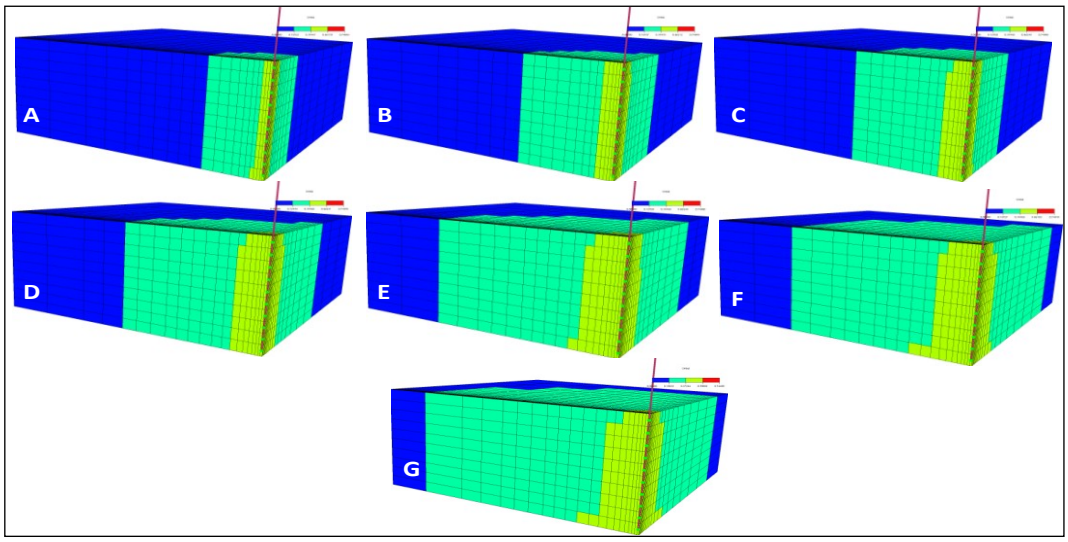


Figure D- 9: Liquid saturation distribution at the end of:
Graph A: 30 days DD
Graph B: 60 days DD
Graph C: 90 days DD
Graph D: 180 days DD
Graph E: 365 days DD
Graph F: 720 days DD
Graph G: 1095 days DD

Results indicate that condensate bank with different saturation despotised during the DD flow period with three zones of high liquid near wellbore and less condensate away from the well and initial gas saturation out in the reservoir. The extension of each saturation zone depends on the production time duration.

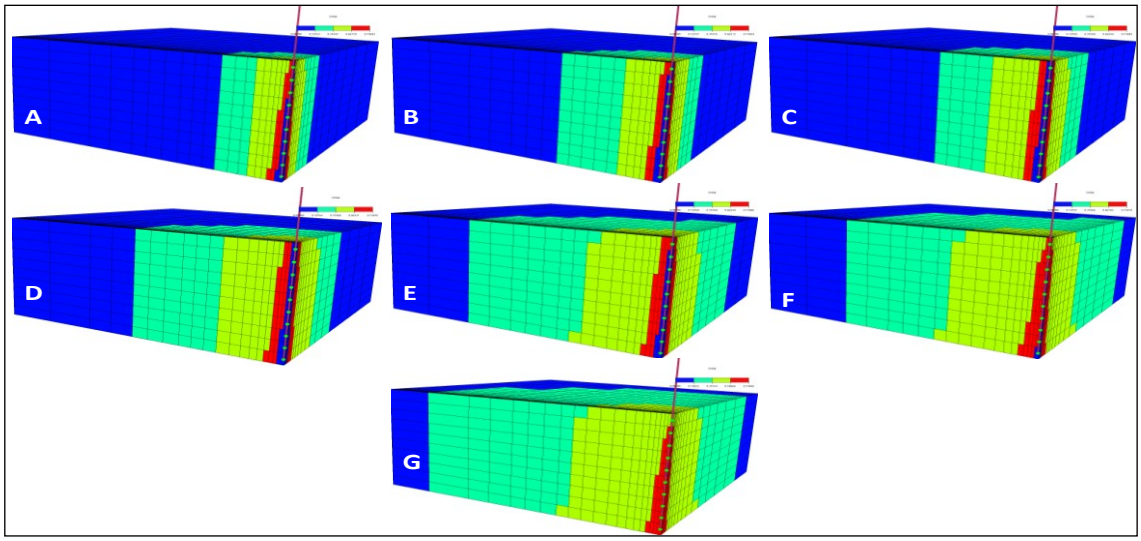


Figure D- 10: Liquid saturation distribution f at the end of 5 days BU following:
Graph A: 30 days DD
Graph B: 60 days DD
Graph C: 90 days DD
Graph D: 180 days DD
Graph E: 365 days DD
Graph F: 720 days DD
Graph G: 1095 days DD

Results suggest that during the build-up flow period some gas vaporizes near the wellbore compared to Figure D-9 forming high gas saturation thin zone in the vicinity of the well.

II Well Productivity in Lean and Rich Gas-condensate

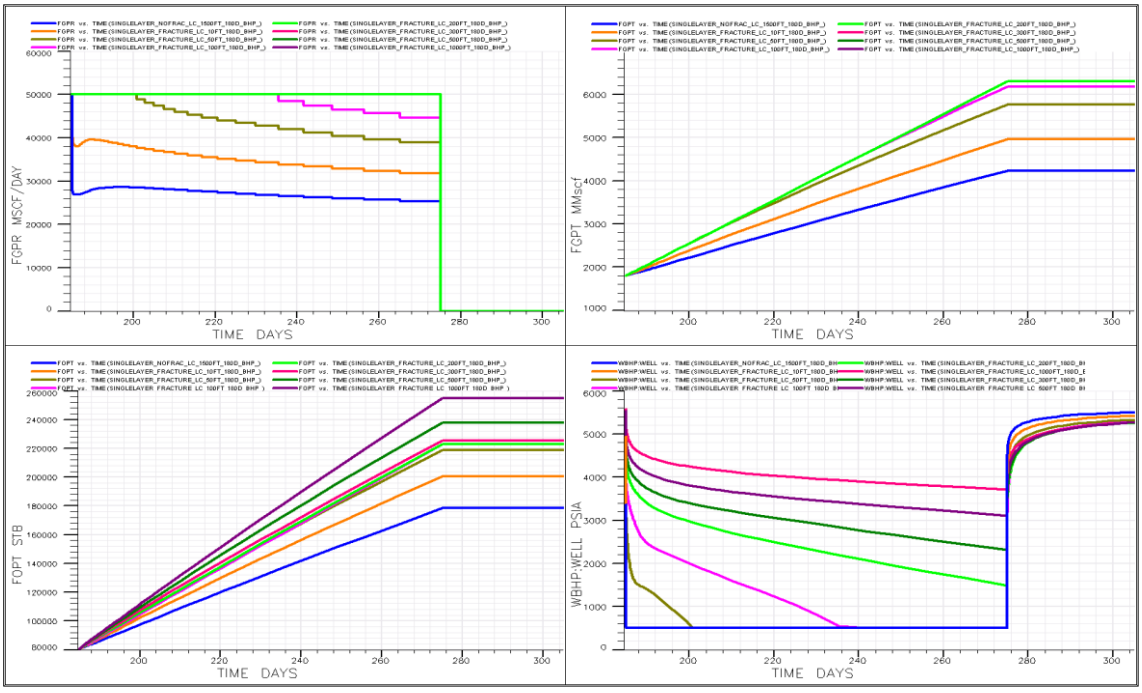


Figure D- 11: Production gas rate, cumulative gas and liquid plus WBHP comparison for fracture half-length of 10, 50, 100, 200, 300, 500, 1000 and No Frac in lean gas-condensate

Graphs shows that introducing a fracture in lean gas condensate well would improve productivity and cumulative volume recovered with less pressure drawdowns compared to non-stimulated well. Fracture half-length significantly determines benefits achieved.

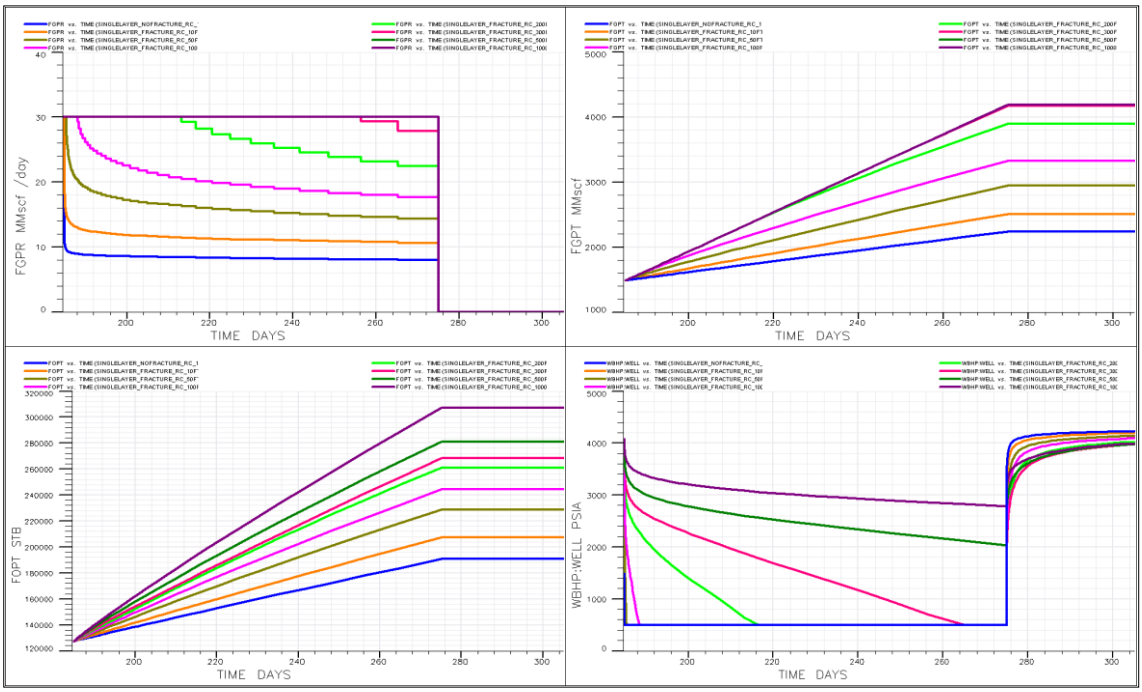


Figure D- 12: Production gas rate, cumulative gas and liquid plus WBHP comparison for fracture half-length of 10, 50, 100, 200, 300, 500, 1000 and No Frac in rich gas-condensate.

Similar conclusion can be drawn in the case of introducing a fracture into rich gas condensate well. However, condensate bank would impacts more derived benefits.